OPEN ACCESS

University of BRISTOL

This electronic thesis or dissertation has been downloaded from Explore Bristol Research, http://research-information.bristol.ac.uk

Author:
Michalopoulou, Eleni

Title:
Quantifying perfluorocarbon emissions and bridging discrepancies between top-down and bottom-up estimates

a sustainable development and systems thinking approach.

General rights
Access to the thesis is subject to the Creative Commons Attribution - NonCommercial-No Derivatives 4.0 International Public License. A copy of this may be found at https://creativecommons.org/licenses/by-nc-nd/4.0/legalcode This license sets out your rights and the restrictions that apply to your access to the thesis so it is important you read this before proceeding.

Take down policy
Some pages of this thesis may have been removed for copyright restrictions prior to having it been deposited in Explore Bristol Research. However, if you have discovered material within the thesis that you consider to be unlawful e.g. breaches of copyright (either yours or that of a third party) or any other law, including but not limited to those relating to patent, trademark, confidentiality, data protection, obscenity, defamation, libel, then please contact collections-metadata@bristol.ac.uk and include the following information in your message:

• Your contact details
• Bibliographic details for the item, including a URL
• An outline nature of the complaint

Your claim will be investigated and, where appropriate, the item in question will be removed from public view as soon as possible.

Quantifying perfluorocarbon emissions and bridging discrepancies between top-down and bottom-up estimates: a sustainable development and systems thinking approach

Eleni Michalopoulou

A dissertation submitted to the University of Bristol in accordance with the requirements for the degree of Doctor of Philosophy in the Faculty of Science School of Chemistry

October 2019

60,000 words

Abstract

Industrial activity, and namely the aluminium, semiconductor and rare earth smelting industries are reported to be the main emitters of the very potent, greenhouse gases (GHGs) CF_4 and C_2F_6. These GHGs belong to the larger group of GHG called perfluorocarbons (PFCs) and are gases monitored by the Kyoto Protocol. Previous studies demonstrated large discrepancies between the estimates inferred from atmospheric measurements in conjunction with modelling (top-down) and inventory-based estimates (bottom-up). Only ~50% of the global CF_4 and 20% of the global C_2F_6 emissions estimates could be explained by current emissions inventories. These studies also suggest that our understanding of PFC emissions was very poor. This work set out to bridge the gap between these top-down and bottom-up estimates and improve our understanding of current and historic emissions of these potent gases.

Using different methods, this work quantified emissions from each industry, produced updated, industry specific inventories and a global bottom-up inventory for both these gases (CF_4 and C_2F_6) for the period 1990-2017; a global spatial distribution of the PFC emitting facilities from all three industries are also presented. Additionally, the global bottom-up inventory produced through this work was used as a prior estimate field in two different Bayesian modelling techniques: the analytical and the hierarchical method. These methods combine high frequency atmospheric measurements from the AGAGE network and this prior knowledge field to produce regional emissions estimates. Three case studies were used to investigate PFC emissions through these modelling methods; the Australian, the East Asia and the South Korea case studies. Finally, this work uses systems and sustainable development to describe how PFC emissions are a wicked problem and introduces a different framework of understanding and describing these emissions. As part of this theoretical framework, a new impact factor was also developed, the De Minimis Scaling Impact Factor (DMSIF) that weighs the environmental burden of the PFC emissions against the socio-economic benefit of the industry emitting PFCs on a per country, per sector, over time basis.

While discrepancies and uncertainties remain, these bottom-up estimates compiled the most updated inventory of PFC emissions produced to this date. Equally, some of the modelling methods used have not been used in relation to PFC gases before. Finally, the theoretical frameworks and DM impact factor presented have never before been attempted and could play a critical role in future policy making and industrial emission reduction plans.

To my partner.

“March on, voidwards”.

Acknowledgements

I don’t think the list of acknowledgements would ever be complete to my satisfaction but here it goes!

First and foremost, I would like to thank my supervisor Simon O’Doherty and my advisors Mike Czerniak and Dudley Shallcross for their endless help and patience during the last 4 years. Special thanks are extended to Louisa Beer, Alison Redington, Tim Arnold, Alistair Manning, Matt Rigby, Jens Mühle, Jooil Kim.

Even more special thanks are extended to Hanno Vogel, David Wong, Pernelle Nunez, Jerry Marks, the International Aluminium Institute, the Semiconductor Industry Association, Laurie Beau, Chris Preist, Chris Willmore, Nick Norman, Neil Allan, Ed Atkins and the Cabot Institute for being an endless source of inspiration and always answering my seemingly never-ending list of questions.

Extra thanks go to my colleagues in the Atmospheric Chemistry Research Group for putting up with me, always being there for me with special mentions to Amy Foulds, Kieran Stanley, Luke Western and Rachel Tunnicliffe, Alecia Nickless. Also, to my non-chemist friends; Ash Tierney, Rebecca Saunders and Alex Birkett.

Massive thanks go to the owner and the employees of the pub The Gryphon. John, Howard, Joan I would not have made it without you! Equally, massive thanks go to the Woodes cafe and their staff that provided endless amounts of coffee throughout these 4 years!

To my partner Spiros, none of this would have been possible without our talks, discussions, your ideas and inquisitive mind. From the bottom of my heart, thank you.

To my mother Irini, and my late father Fanis, my grandparents and my siblings, I would never be where I am today without your support.

An ultra-special thank you to my uncle Kostas; I would not be here without you!

Finally, for the endless hours they kept my company while coding, writing, reading and trying to put my thoughts together a last bit of thank you needs to go to the following bands: Nightwish, Blind Guardian, Powerwolf, Rhapsody, Halestorm, Eluveitie, Ensiferum, Haggard, Turisas, Gamma Ray, Helloween, Wintersun, Within Temptation. Your songs kept me sane and awake when I needed it the \m/ost!

Declaration

I declare that the work in this dissertation was carried out in accordance with the requirements of the University's Regulations and Code of Practice for Research Degree Programmes and that it has not been submitted for any other academic award. Except where indicated by specific reference in the text, the work is the candidate's own work. Work done in collaboration with, or with the assistance of, others, is indicated as such. Any views expressed in the dissertation are those of the author.

SIGNED: ……MICHALOPOULOU ELENI…… DATE: ….07/10/2019….

Table of Contents

List of Figures

List of Tables

Frequently used abbreviations

List of Figures

List of Tables

Frequently used abbreviations

ABL: Atmospheric Boundary Layer

AE: Anode Effect

AES: Anode Effect Survey

AGAGE: Advanced Global Atmospheric Gases Experiment

AI: Aluminium Industry

COP: Conference of the Parties

CVD: Chamber vapour deposition

DMSIF: De Minimis Scaling Impact Factor

EITs: Economies in Transition

GDI: Gender Development Index (GDI)

GHG(s): Greenhouse gas(es)

GII: Gender Inequality Index (GII)

GWP: Global Warming Potential

HDI: Human Development Index

HDRs: Human Development Reports (HDRs)

HVAE: High Voltage Anode Effects

IAI: International Aluminium Institute

IHDI: Inequality-adjusted Human Development Index (IHDI)

IPCC: International Panel on Climate Change

IR: Infrared radiation

LLGHG: Long-lived greenhouse gases

LPDM: Lagrangian Particle Dispersion Model

LVAE: Low Voltage Anode Effects

MOZART: The Model for OZone And Related chemical Tracers

MPI: Multidimensional Poverty Index

NAME: The Numerical Atmospheric dispersion Modelling Environment

NIR(s): National Inventory Report(s)

PFC(s): Perfluorocarbon(s)

RCPs: Representative Concentration Pathway(s)

REE(s): Rare Earth Element(s)

REO(s): Rare Earth Oxide(s)

RESI: Rare Earth Smelting Industry

RF: Radiative Forcing

ROW countries: Rest of the World countries

SCI: Semiconductor Industry

SDG(s): Sustainable Development Goal(s)

SSPs: Shared Socio-Economic Pathways(s)

UM: Unified Model

UN: United Nations

UNDP: United Nations Development Program

UNEP: United Nations Environment Programme

UNFCCC: United Nations Framework Convention on Climate Change

USA EPA: United States of America Environmental Protection Agency

UV: Ultraviolet radiation

VNR: Voluntary National Review

WCED: World Commission on Environment and Development

WSC: World Semiconductor Council

Chapter 1

Context, motivation of the thesis, research aims and questions: Discrepancies between top-down estimates and bottom-up approaches

In 2010, in their work "Perfluorocarbons in the global atmosphere: tetrafluoromethane, hexafluoroethane, and octafluoropropane" Mühle et al., (2010a) presented the atmospheric trends of CF_4 and C_2F_6; These PFCs are among the longest-lived and most potent GHGs regulated under the Kyoto Protocol of the UNFCCC. They also presented discrepancies between top-down estimates, which are estimates produced through a combination of atmospheric observations and numerical modelling, and bottom-up approaches which are estimates produced either by industries (e.g. the International Aluminium Institute (IAI) or by countries reporting their greenhouse gas emissions to the UNFCCC. Emissions inferred from measurements from the AGAGE network show that only ~50% of global CF_4 and ~20% of global C_2F_6 emissions can be explained by current emissions inventories (AGAGE | MIT Center for Global Change Science, 2010; Mühle et al., 2010b; Kim et al., 2014).

Atmospheric measurements indicate pre-industrial concentrations of approximately 34 – 44 ppt and 0.1±0.02 for CF_4 and C_2F_6 respectively (Fabian and Gomer, 1984; Harnisch et al., 1996; Harnisch and Eisenhauer, 1998b; Khalil et al., 2003; Mühle et al., 2010b; Trudinger et al., 2016). Concentrations of these potent GHGs have been increasing significantly since the pre-industrial levels. In 2003, Khalil et al., measured concentrations of approximately 74 ±2 ppt and 2.9 ±0.1 ppt for CF_4 and C_2F_6 respectively (Khalil et al., 2003). Several studies suggest an increase a CF_4 specific growth rate for the years 1955-2003 of 0.8 ppt/yr, while a growth rate of 0.085 ppt/yr is reported for C_2F_6 for the years 1970-1990 (Harnisch et al., 1996; Khalil et al., 2003; Worton et al., 2007; Mühle et al., 2010b). Previous work (Figures 1.1 – 1.2) presented global estimates for both PFC gases for the years 1990-2010, discrepancies between top-down and bottom-up estimates and attempted to allocate the PFC emissions to industries (Mühle et al., 2010a; Kim et al., 2014).

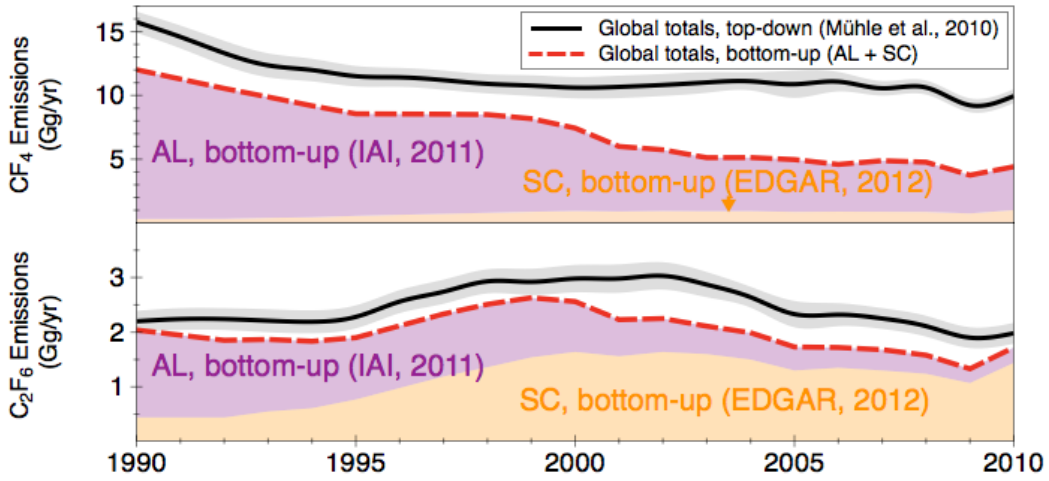

Figure 1.1: Global CF_4 and C_2F_6 emissions from the inversion of AGAGE atmospheric data with the AGAGE 2-D 12-box model. Updated from Mühle et al., 2010. The black line shows the global totals using the top-down method and the dotted red line shows the global bottom-up totals of the aluminium and semiconductor industry. The shaded purple area shows the bottom-up estimates of emissions related to the aluminium industry and the shaded orange area shows the bottom-up estimates related to the semiconductor industry. Figure courtesy of Kim.

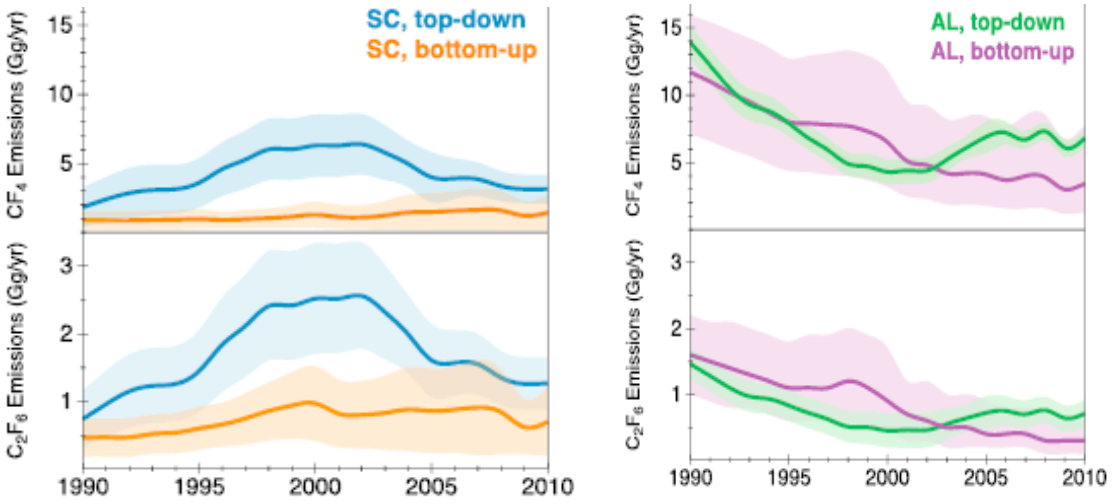

Figure 1.2: CF_4 and C_2F_6 bottom-up emissions estimates from the SCI (left) where the blue line shows the top-down estimates related to the SCI for CF_4 (above) and C_2F_6 (below) and the orange line shows the bottom-up estimates for the same gases respectively. Equally for the AI (right) compared against top-down emissions estimates inferred from atmospheric observations. Shaded areas represent uncertainties (Kim et al. 2014)

These descrepancies demonstrated that only ~50% of global CF_4 and 20% of global C_2F_6 emissions could be explained by current emissions inventories like the NIRs (Mühle et al., 2010b; Kim et al., 2014). The reasons why bridging this gap between top-down and bottom-up estimates are extremely important are:

- The volatility of those PFCs
- Their long atmospheric lifetime
- The absence of known sinks
- The fact that they are almost entirely anthropogenic (post-industrial revolution)
- The fact that they are gases monitored under the Kyoto protocol

In order to close this gap, this work explores three different approaches:

a) Bottom-up approach: In order to understand whether the discrepancies were originating from lack of information (or outdated information in the existing inventories) an updated bottom-up inventory was produced using existing and new information, existing and new methodologies. To produce this inventory all the sources of PFC emissions were investigated separately and updated as appropriate (Chapters 3,4 and 5). This bottom-up inventory is compared against the top-down estimates and against previous bottom-up inventories (Chapter 7) and it is also used as prior information for the inverse modelling (Chapter 6).
b) Top-down approach: Using high frequency atmospheric measurements from the AGAGE network, this works' updated bottom-up inventory, inverse modelling techniques, posterior emission estimates of the PFCs gases were also produced (Chapter 6).
c) Theoretical analysis of existing frameworks: To produce a holistic understanding of the PFC problem, this work explores the theory of wicked problems and simple problems, it gives a new definition of post-disciplinary work (Chapter 2). Using that definition, systems thinking, problem solving theory and the SDGs framework it presents a new theoretical framework of understanding PFC emissions (Chapter 2).

The original research question of this work was related exclusively to the discrepancies between bottom-up and top-down estimates. Originally this work set out to quantify and model PFC emissions in an attempt to "bridge the gap between top-down and bottom-up estimates of CF_4 and C_2F_6". However the original research question was expanded to include both questions of theoretical/qualitative nature (e.g. regarding frameworks specific to the SDGs) and industry specific quantitative questions. Given the GWP and lifetimes of both CF_4 and C_2F_6 but also, taking into consideration the extreme urgency of climate change as announced by the IPCC on

their special report on 1.5° C it is evident that these discrepancies are extremely significant. This work required a lot of collaboration and engagement with the industry especially as the limitation of these quantifications were explored. Through this interaction with different stakeholders it became obvious that there was perhaps a need for an altogether different, post-disciplinary approach regarding the quantification of the PFC emissions.

This thesis is suggesting, that because these GHGs are the products of specific anthropogenic activity, namely the AI, SCI and RESI, in order to fully understand and quantify the historic and current emissions it is required to engage with concepts like systems thinking, the SDGs and Earth Systems Science (Figure 1.3). This approach also helped broaden the understanding of the limitations of this work and allowed for future work and research suggestions.

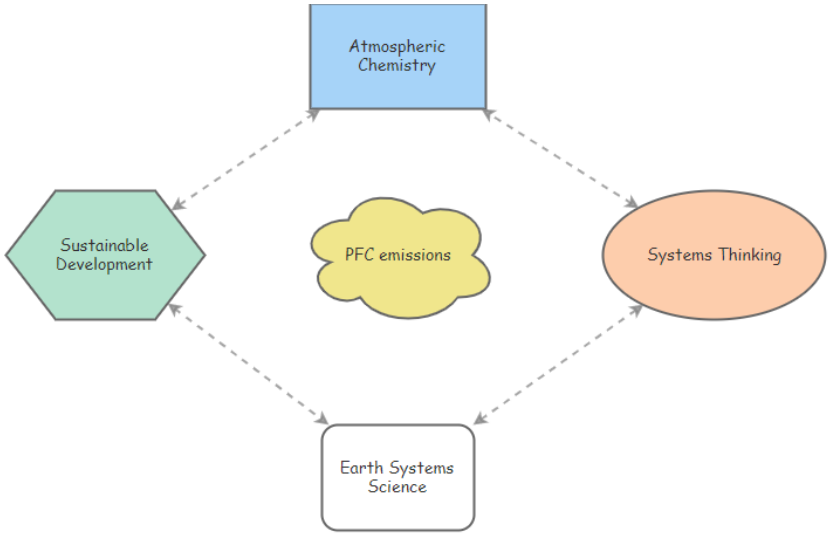

Figure 1.3: Schematic representation of systems thinking, sustainable development, atmospheric science and earth systems science in order to discuss the challenge of PFCs.

Consequently, the original research question was expanded from "bridging the gap between top-down and bottom-up estimates of CF_4 and C_2F_6" to "using systems thinking and sustainable development to quantify PFC emissions and bridge the gap between top-down and bottom-up discrepancies".

In order to bridge the gap using sustainable development and systems thinking, the PFC emitting industries were studied separately, and their emissions re-estimated using different methods. These updated, industry specific PFC emissions estimates formed the basis of a newly presented bottom-up inventory of global PFC emissions. This inventory was consecutively used as prior information as part of different modelling techniques. The aforementioned

discrepancies between top-down and bottom-up estimates have been greatly improved as a result of this work, however, uncertainties still remain.

Chapter Summaries

Chapter 1: Introduction

Chapter 1 gives background information and introduces the basic principles that will be used throughout this work. Additionally, it presents the research questions this thesis sets out to answer.

Chapter 2: PFCs, Simple and Wicked Problems: There and back again

Chapter 2 presents a new theoretical framework developed in this thesis. This framework combines systems thinking and sustainable development goals in relation to PFC emissions. It will demonstrate the role PFCs are playing within the SDGs framework and the role atmospheric chemistry has to play from a global challenges point of view. Chapter 2 also introduces a new impact factor developed in this work. This impact factor, namely the De Minimis Scaling Impact Factor (DMSIF) is a first attempt to quantify the atmospheric burden of PFC emissions weighed against socio-economic factors related to the PFC emitting industries. This approach is highly innovative and has not been attempted before. It is thought that this factor can play a critical role in high-level decision making with the PFC emitting industries.

This chapter will be answering the following research questions:

- Overall, with PFC gases having such large GWP and lifetimes and their emissions being almost entirely anthropogenic, what is their role as part of the sustainable development narrative?
- What roles can systems thinking and sustainable development goals play in understanding and interprenting historic emissions and discrepancies?
- What roles can sustainable development and systems thinking play in relation to PFCs mitigation?
- Are PFCs part of the Wicked Problems narrative?
- Considering that PFCs are emitted through the economic activity of specific industries, can the environmental impact of those gases be weighed against the industry specific socio-economic and environment gains?

- Can these assumptions be quantified using existing metrics and be compared against existing metrics?

Chapter 3: PFC Emissions from the Aluminium Industry (AI)

Chapter 3 provides an analysis of the aluminium industry, the perfluorocarbon emissions related to this industry (historical and current), it will present newly updated estimates of the PFC emissions from this industry for the gases CF_4 and C_2F_6 and an updated map showing the current spatial distribution of the industry. This Chapter will be answering the following research questions:

- Can an industry specific, updated bottom-up inventory be produced using newly developed methods?
- Was there significant contribution of the suspected low-voltage emissions?
- How large was the PFC emissions contribution from the emerging Chinese aluminium production?

Chapter 4: PFC emissions from the Semiconductor Industry (SCI)

Chapter 4 provides an analysis of the SCI and the PFC emissions related to this industry (historical and current). During this work, two new methods were developed to quantify bottom-up emissions from this industry for the gases CF_4 and C_2F_6; The combined Fab Method (CFM) and the Fab Specific Method (FSM). An updated map showing the current spatial distribution of the industry is also presented. This chapter will be answering the following research questions:

- Can an industry specific, updated bottom-up inventory be produced?
- How does the inventory developed in this chapter compare to previous work?
- Could an updated method for estimating PFC emissions from this industry brigde persisting discrepancies?

Chapter 5: PFC emissions from the Rare Earth Smelting Industry (RESI)

Chapter 5 provides an analysis of the RESI, the PFC emissions related to this industry and it will present updated PFC estimates specific to this industry. This is the first time PFC emissions from rare earth smelting are being considered as part of an inventory and the first

time the global emissions are estimated using both laboratory-based experiments and in-situ measurements. It should be noted that when this work started, the rare earth smelting industry was dismissed as a contributor of PFCs. However, after the joint efforts of Hanno Vogel (TRIMET Aluminium), the International Aluminium Institute (IAI), the U.S.A Environmental Protection Agency (EPA), EDWARDS Ltd and the author of this work rare earths are now considered as a potentially significant contributor of PFCs (IPCC, 2019a). This Chapter will be answering the following research questions:

- Are there electrolytical processes used in rare earth smelting have the potential to produce PFC emissions?
- Can PFC emissions from this industry using existing emission factors be quantified?
- What are the implications, related to sustainable development, if rare earth smelting is a significant contributor of PFCs?
- Can produce an industry specific, updated bottom-up inventory be produced?

Chapter 6: Modelling PFC emissions

Chapter 6 presents modelling work done using three different regional case studies (Australia, East Asia and South Korea). The purpose of this chapter was to test our bottom-up inventory as a prior knowledge field as part of Bayesian inversion methods. Two different modelling techniques were used; the analytical Bayesian approach and the hierarchical Bayesian approach. The latter has never been presented before in relation to PFC emissions and the former has only been presented using a very uncertain prior knowledge field. This Chapter will be answering the following research questions:

- Can inventories produced in this work be used as priors in inverse modelling?
- How do different modelling techniques using the same prior compare to each other?
- Can forward modelling combined with the newly developed prior from this work give new information regarding atmosperhic conenctrations of PFCs?

Chapter 7: Discrepancies and Conclusions

Chapter 7 presents in detail how this new bottom-up inventory has impacted the ‘gap’ between top-down and previous bottom-up estimates, and it will try to interpret were it was successful in decreasing the discrepancies, were it was not, and the reasons for this. It will also briefly present suggestions for future work. This Chapter will be answering the following

research questions:

- Combining the updated inventories estimated in this work, what happens to the discrepancies for both PFC gases?
- How does this updated inventory compare to previous work?

Introduction

1.1 The atmosphere

Atmospheric composition consists of ~78% diatomic nitrogen (N_2), ~21% diatomic oxygen (O_2), and other trace gases (e.g. CO_2 ~0.04%) (Baird, 1998). Varying amounts (0 to 4%) of water vapour are also present. The atmospheric stratification is broadly divided into five regions defined by their temperature gradients: the troposphere, stratosphere, mesosphere, thermosphere and the exosphere (Baird, 1998). The interfaces between these regions, where the temperature gradients change, are called pauses. This stratification is shown in Figure 1.4.

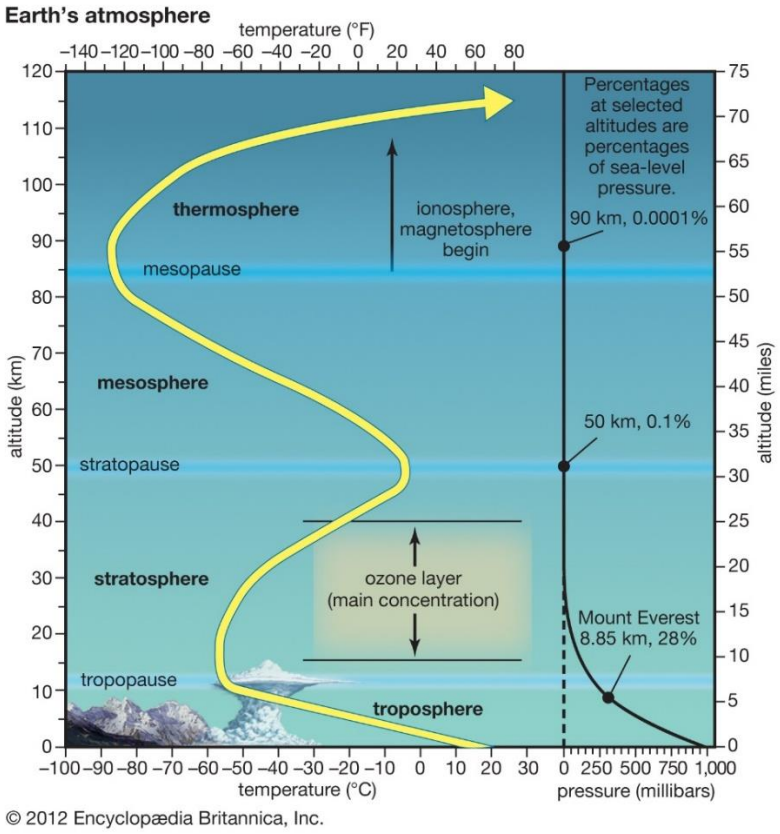

Figure 1.4: The atmospheric structure and the temperature change with altitude and pressure of the atmospheric layers (Encyclopaedia Britannica, 2012).

The function of the atmosphere is critical for the preservation of life on Earth. Indicatively, an Earth without atmosphere would experience mean surface temperatures of approximately -18 °C (NASA's Cosmos, 2015). Another important function of the atmosphere is to prevent excessive solar Ultraviolet (UV) radiation from reaching the Earth's surface.

The troposphere contains 80-90% of the atmospheric mass. This makes the troposphere the densest atmospheric layer which between 0 and ~15 km above sea levels. Characteristic of this layer is the temperature decrease as the altitude increases (Derwent, Powlson and Conrad, 1995). One of the lower layers of the troposphere is the Atmospheric Boundary Layer (ABL), the atmospheric layer closest to the Earth's surface. Most of the weather phenomena take place here. The ABL extends up to ~3 km above sea levels and it's that part of the atmosphere that is directly affected by human activities. This is the layer where air pollution and gas emissions are of concern.

Above the tropopause, the stratosphere is defined by temperature increase as altitude increases. This increase in the stratospheric temperature is driven by ozone (O_3) which absorbs near-UV and re-emits thermal infrared radiation (IR). The highest temperatures are observed at the highest stratospheric altitudes despite low O_3 concentrations in this region because this is where high energy UV wavelengths are absorbed. This large temperature inversion means that convention and/or mixing are minimal. This results in the stability of the stratospheric layers which in turn results into materials reaching the stratosphere often staying there for a long time.

The mesosphere temperatures decrease with increasing altitude for the same reason stated for the troposphere. It is the coldest part of the Earth's atmosphere and extends up to 85 km. The thermosphere then inverts this temperature gradient because O_2 and N_2 molecules present in this layer absorb far-UV at very short wavelengths.

1.2 Atmosphere dynamics

In order to understand what happens to a gas parcel (a theoretical body of air to which dynamic and thermodynamic properties are assigned) once it has been emitted from a source it is important to have a good understanding of how atmosphere air circulates. A three-cell model is commonly used to describe atmospheric circulation which maintains the global energy balance. This Earth's surface is heated unevenly resulting in warm air masses rise from the Equator and descend at ~30° north and south of the equator (Horse latitudes). Areas of high

pressure are thus created causing air masses to flow from these areas to the equator (trade winds). These circulation patterns around the tropics are called Hadley cells (Figure 1.).

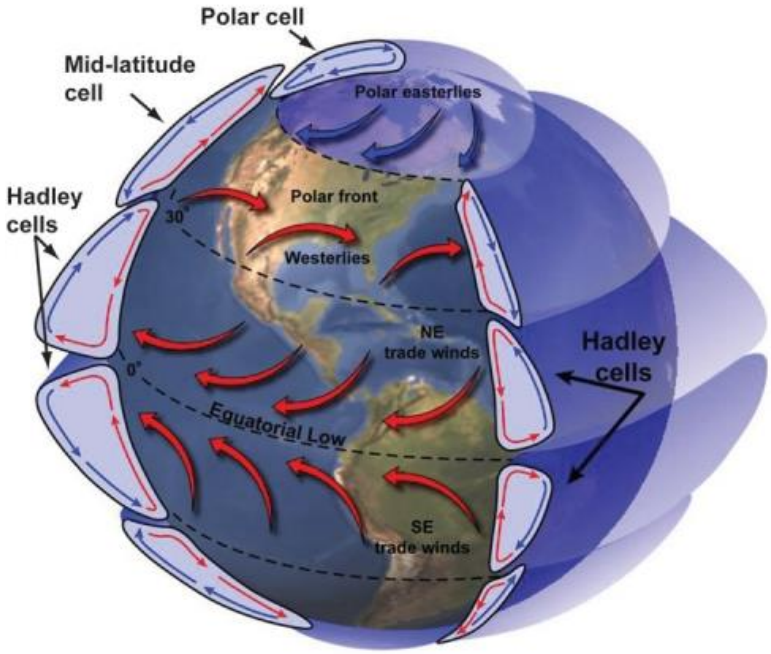

Figure 1.5: General circulation of the atmosphere (North Carolina Climate Office, 2019).

Heating at the equator and cooling at the poles combined with the Coriolis force (an effect generated by the Earth's rotation) are the mechanisms that control the circulation in these three cells (Phillips, 2000). These convection cells shown in Figure 1.2 (wind belts) allow air masses to flow from areas of high pressure to low pressure. This is called the global wind system and it consists of trade winds, westerlies and polar easterlies (Seinfeld, Pandis and Noone, 1998) and these processes make up the general circulation of the atmosphere.

Gases released at the Earth's surface need ~5 years to enter the stratosphere (Markandya and Dale 2001; Leedham et al. 2018). Between the emission of a gas and the gas mixing between hemispheres (interhemispheric mixing) the time is much shorter and it is ~6 months (Houghton 1994, 1997, 2002; Delmas, 2013). In addition to the large-scale processes described, there are smaller scale mixing processes (e.g. small-scale turbulence) taking place in smaller time scales. Small scale processes are of importance near the Earth's surface.

The ABL is the atmospheric layer directly affected by the processes that occur at the Earth's surface (e.g. heat exchange and friction). In this region, momentum, heat and matter are subject to turbulence, which mixes them within the boundary layer. The height of the ABL can vary

from a few metres to several kilometres (The Atmospheric Boundary Layer - Met Office; Garratt, 1994).

Turbulence in the ABL results in small to large scale eddies (from hundreds meters to millimetres) (Lauritzen et al., 2011). Convection, wind shear and the Earth's rotation are the main causes of this turbulence. All three of these processes are responsible for different types of mixing in the atmosphere. Convection causes mixing based on the temperature gradients within the ABL, wind shear causes mixing through wave-like motions (Figure 1.6) and the Coriolis force by redirecting the (ascending or descending) air masses (Wallace and Hobbs, 1977).

Figure 1.6: Representation of shear stress resulting in turbulence in the ABL.

1.3 The Greenhouse Effect (Natural VS Anthropogenic)

The energy equilibrium on the Earth's surface is driven by solar energy. The wavelengths of this solar energy consist of UV, visible and IR. Approximately 30% of the radiation arriving from the Sun is immediately reflected back into space while the remaining 70% is absorbed by the Earth's surface, the oceans and the atmosphere (Baird, 1998). Once the Earth absorbs the solar radiation it emits longwave radiation (IR, wavelengths ~4-50 μm) ~6% of which is emitted into space and the remaining percentage is absorbed by clouds and/or atmospheric molecules. This IR energy is reemitted by those molecules and, through dispersion mechanisms, will partly reach the Earth again and part of it will be remitted into space.

Greenhouse gases (GHGs) are defined as gases that absorb thermal IR and therefor contribute to global warming. While the same amount of solar energy is absorbed by the Earth's system, what these gases do is to prevent energy from escaping back into space and thus contribute to an increase in global temperature. This phenomenon is known as the Greenhouse Effect (Houghton 1994, 1997, 2002).

The natural greenhouse effect is caused by GHG concentrations that exist naturally in the

in the atmosphere. The enhanced (anthropogenic) greenhouse effect occurs when these natural atmospheric GHG concentrations are increased due to anthropogenic activities or the release of GHGs with no natural sources (e.g. C_2F_6). These increased (due to anthropogenic activity) GHG concentrations in the atmosphere increase the radiation absorbed by the atmosphere resulting in an overall increasing of the Earth's surface and lower atmosphere's temperatures.

Other factors that must be considered in relation to the Earth's radiation budget are cloud cover, water vapour concentrations, ice and snow cover. Changes in these factors could decrease or increase the warming effects of increased GHG concentrations. These are referred to as negative and positive feedbacks, respectively (Mitchell, 1989; Mitchell et al., 1990).

The atmospheric IR emission spectrum is shown in Figure 1.4. Regions where radiance is close to the blackbody radiance are regions where little IR is absorbed by GHGs and are called atmospheric windows. The absorption spectrum for CF_4, shown in Figure 1.7, indicates that CF_4 absorbs most strongly at ~8 μm.

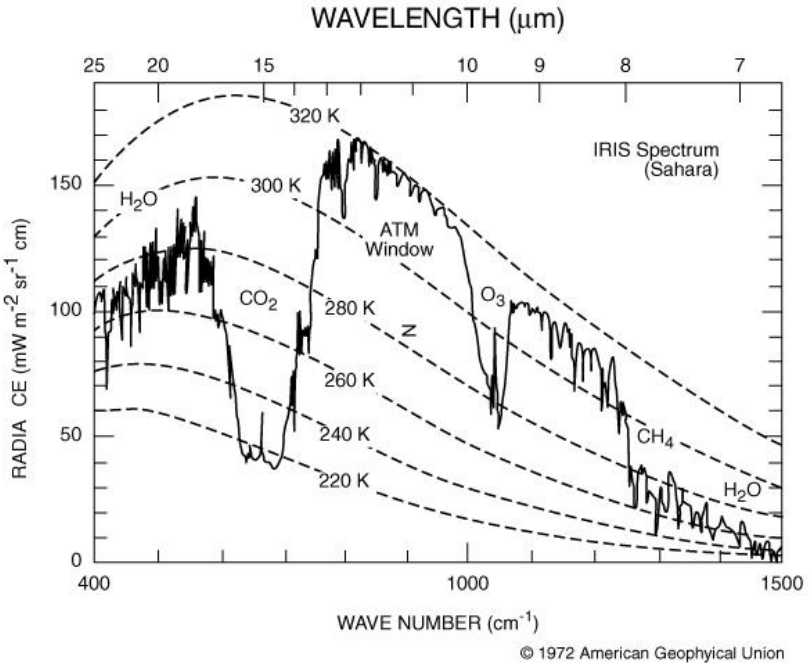

Figure 1.7: IR radiance and atmospheric window at ~10-13 μm (Hanel et al., 1972).

1.4 Global Warming Potential

The magnitude of the warming effect a GHG is described by its radiative forcing (RF). RF is the change in average radiation at the tropopause, due to imbalance between incoming solar radiation and outgoing thermal radiation (Houghton 1994, 1997, 2002).

The Global Warming Potential (GWP) is the relative measure of a chemical species' effectiveness in perturbing the radiative budget of the Earth's climate system. This perturbation (commonly referred to as RF) (Ramaswamy et al., 2001) is measured in relation to carbon dioxide which has a value of 1 over a given time period, usually 20 or 100 years allowing this way for comparison on different timescales. A mathematical definition of GWP is shown in Equation 1.1:

$$\mathrm{GWP(x)} = \frac{\int_0^{\mathrm{TH}} \mathrm{a(x)[x(t)]dt}}{\int_0^{\mathrm{TH}} \mathrm{a(CO2)[CO2(t)]dt}} \qquad (1.1)$$

Where:

a(x) = RF due to a unit increase in concentration of species x

[x(t)] = concentration of the species x, at time t after its release

TH = time horizon over which the calculation is performed (in years)

The corresponding values for carbon dioxide are found in the denominator.

The GWP of a chemical species is therefore depending on the species absorption features (a(x)) and lifetime (x(t)). Lifetime is defined as the global mean burden of a chemical species divided by the loss rate.

Each GHG has a GWP value associated with it. The GWP is a measure the amount of energy each GHGs will absorb over a given period (usually 100 years) in relation to CO_2 over the same period. This depends on the wavelength at which the molecules absorb, the strength of the relevant absorptions and the atmospheric lifetime of the molecules. Each atmospheric gas only absorbs at specific wavelengths, so each gas has a unique IR spectrum.

1.5 Fluorinated gases and Perfluorocarbons

The term fluorinated gases (or F-gases) describes a group of man-made gases used in a wide range of industrial applications. As these F-gases do not deplete the ozone layer are widely used as replacements for ozone-depleting gases. However, F-gases are powerful GHGs and their emissions are rising rapidly (European Union, 2018). The group of F-gases consists of hydrofluorocarbons (HFCs), perfluorocarbons (PFCs) and sulphur hexafluoride (SF_6) and nitrogen trifluoride (NF_3).

Perfluorocarbons (PFCs) are a group of manmade chemical compounds with the formula C_xF_y which means they only contain carbon and fluorine. This work, is focusing on CF_4, also known as carbon tetrafluoride (tetrafluoromethane) and C_2F_6 (hexafluoroethane); two of the compounds that belong to the broader F-gases group.

CF_4 is almost entirely anthropogenic with very few natural sources identified so far and in the case of C_2F_6 a very small natural contribution is suggested (Mühle et al., 2010a). This chapter presents a brief overview of natural and anthropogenic sources and sinks for CF_4 and C_2F_6. A detailed overview of the industrial processes that emit CF_4 and C_2F_6 in the aluminium, semiconductor and rare earth smelting industries is given in chapters 3, 4, and 5 respectively.

The GWPs and lifetimes of the gasses relevant to this thesis (CF_4 and C_2F_6) are given in Table 1.1. As indicated by Table 1.1 these PFCs have large GWPs. Large concentrations of PFCs could have a significant warming effect and therefore contribute towards climate change and global warming.

F- gas	GWP (100y) 4th assessment report	GWP (100y) 5th assessment report	Lifetime (yr)
CF_4	7,390	6,630	>50,000
C_2F_6	12,200	11,100	10,000
NF_3	17,200	16,100	740
SF_6*	22,800	23,500	800–3200

Table 1.1: Global Warming Potentials (GWPs) and lifetimes of F - gases.

Table 1.1 shows the lifetimes (Hartmann et al., 2013) and GWPs over a 100 year horizon from the 4th assessment report (Myhre et al., 1998) and the 5th assessment report (Myhre et al., 2013) of the International Panel on Climate Change (IPCC) (details regarding the IPCC are discussed in section 1.8.1) The GWPs from the 4th and 5th assessment reports are different because the 5th assessment report contains updated concentration and RF values compared to the 4th assessment report. Because of their long lifetimes these gases are also referred to as long-lived GHGs (LLGHG) (Myhre et al., 1998, 2013). It should be highlighted that this work uses the GWPs from the 4th assessment report and not the 5th assessment report. These values were used in order to be consistent with previous work and produce comparable results.

1.6 CF_4 and C_2F_6: an overview

CF_4 and C_2F_6 are non-ozone depleting substances. However, their extremely high GWPs (Table 1.1) suggest that even very small concentrations in the atmosphere can make significant contributions to climate change.

Both these gases are inert and stable due to the high energy of the C-F bond. The C-F bond is referred to as 'the strongest bond in organic chemistry'. The measure of the tendency of an atom to attract a bonding pair of atoms is called electronegativity. What happens in the case of the C-F bond is that because fluorine is much more electronegative than carbon (F = 4.0, C = 2.5 on the Pauling scale) means that fluorine attracts carbon very strongly. The bond strength in CF_4 and C_2F_6 is approximately 543 KJ mol^{-1} and 601 KJ mol^{-1} respectively compared to 439 KJ mol^{-1} in methane (CH_4). CF_4 is chemically inert and is the most abundant PFC in the atmosphere (Dixon et al., 1995; Mühle et al., 2010a). Figures 1.8 and 1.9 show the IR spectrum for CF_4 and C_2F_6, respectively. CF_4 absorbs most strongly at ~8 µm and this high frequency radiation falls within the atmospheric window at ~8-9 µm; this causes radiation that would otherwise be reemitted into space to remain trapped in the Earth's atmosphere (Warneck, 1999).

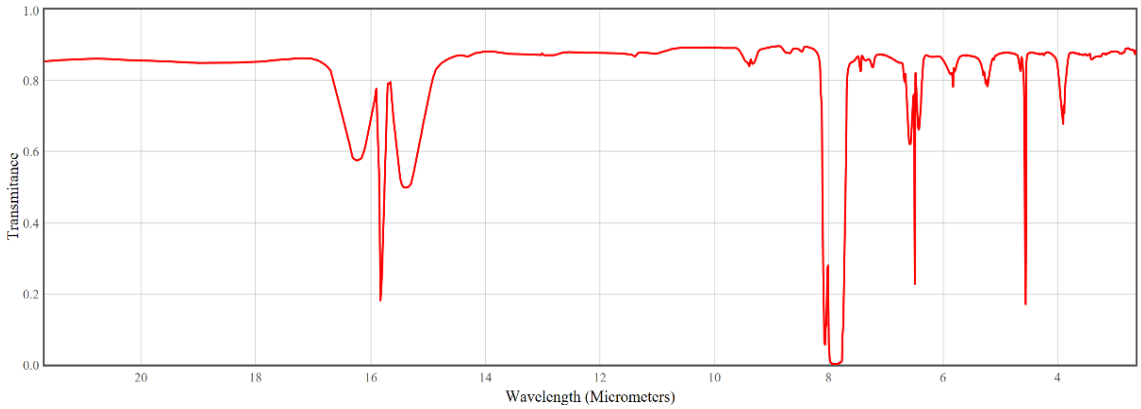

Figure 1.8: Infrared radiation spectrum of CF_4 (NIST workbook).

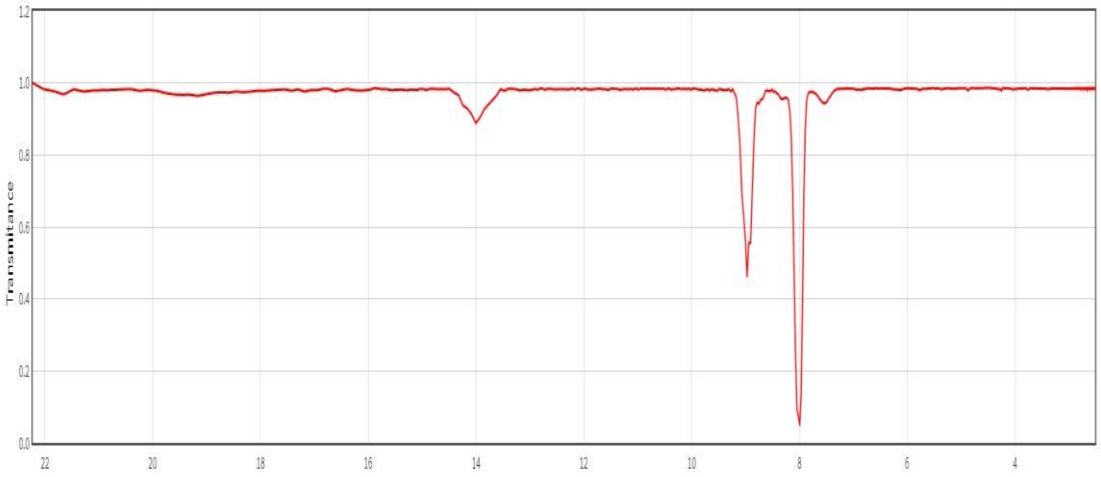

Figure 1.9: Infrared radiation spectrum of C_2F_6 (NIST workbook).

1.6.1 Sources

a) Natural

The first recorded and published observation of CF_4 was made in 1974 by Gassmann who, based on evidence from measurements of gases from fluorite minerals carried out by Kranz in 1966, carried out contaminant analysis of krypton samples and suggested a natural source of CF_4 (Gassmann, 1974) and in 1979 it was first detected in the troposphere (Rasmussen, Penkett and Prosser, 1979). Measurements by Gassmann over Europe and by Rasmussen and Penkett in both hemispheres indicated levels of tropospheric background concentrations in the 67 ± 10

ppt (parts per trillion) range and these were approximately the same worldwide (Gassmann, 1974; Rasmussen, Penkett and Prosser, 1979; Zander et al., 1996). The origins of a natural CF_4 source were unclear and at the time, one anthropogenic source was suggested to be the main contributor to emissions (Penkett et al., 1981). CF_4 emissions from volcanic gasses were originally suggested as a natural source of CF_4. Further work deemed the direct contributions to the CF_4 budget from volcanic gases unlikely and was eventually completely excluded as a possibility (Penkett et al. 1981a; Symonds, Rose, and Reed 1988; Harnisch and Eisenhauer 1998b).

A long series of studies has been carried out with the aim of estimating pre-industrial CF_4 levels which eventually confirmed the presence of a natural CF_4 emission source. An original estimate of ~40ppt was suggested, concentration which would account for half the global CF_4 budget. It was later suggested that a small contribution of natural CF_4 could occur from natural gas combustion, suggestion that was eventually confirmed (Harnisch and Eisenhauer 1998b; Harnisch et al. 1996; Worton et al. 2007; Mühle et al. 2010a; Trudinger et al. 2016).

Additionally, evidence suggested that CF_4 could be emitted due to radiochemical processes from fluorite minerals. In 1998, Harnisch and Eisenhauer reported the occurrence of CF_4 in natural fluorites and granite where fluorite is an accessory mineral, building on earlier work by Kranz in 1966 (Kranz, 1966; Harnisch and Eisenhauer, 1998a). It was demonstrated that CF_4 can be released from certain natural rocks and minerals by heating, crushing and dissolution in water. More recent studies have provided additional evidence that CF_4 can be released from fluorite minerals by tectonic activity and weathering (Deeds et al., 2008; Deeds, Mühle and Weiss, 2008; Mulder et al., 2013; Schmitt et al., 2013). The most recent CF_4 measurements used historical samples from firn, ice core, archived and in situ atmospheric measurements from both hemisphere by Trudinger et al., (2016). This work presents pre-industrial level for CF_4 of ~34.05 ± 0.33 ppt (Trudinger et al., 2016).

While C_2F_6 was thought to have negligible (or zero) natural abundance, Mühle et al, (2010) reported a concentration of 0.1±0.02 ppt from air extracted from firn samples. This finding could be evidence of very small natural background C_2F_6 concentration (Penkett et al., 1981; Harnisch et al., 2000; Khalil et al., 2003; Worton et al., 2007; Mühle et al., 2010a).

b) Anthropogenic

The major contributors to global CF_4 and C_2F_6 emissions are anthropogenic sources related with specific industrial activity (Rasmussen, Penkett and Prosser, 1979; Penkett et al., 1981; Ravishankara et al., 1993; Zander et al., 1996; Khalil et al., 2003; IPCC, 2006).

The Aluminium Industry (AI) is the oldest known anthropogenic source of PFCs. To extract primary aluminium from its ore (bauxite), a smelting process called the Hall-Héroult electrolytic process is used. It is during process upset conditions in the cell where the smelting takes place, known as the anode effects, when PFCs are emitted. These effects are referred to as high voltage anode effects (HVAE) while recently PFC emission from low voltage anode effects (LVAE) has been discovered (Tabereaux, 1994; Leber et al., 1998; Wong et al., 2014; Marks and Nunez, 2018). AI emissions have been recorded since 1990 and existing data is well documented by the International Aluminium Institute (IAI) (Holiday and Henry, 1959; Penkett et al., 1981; Tabereaux, 1994; International Aluminium Institute, 1990 - 2017). This industry, the processes and their respective PFC emissions will be discussed and presented in detail in Chapter 3.

In the Semiconductor Industry (SCI) PFCs are used during the process of etching and chemical vapour deposition (CVD) chamber cleaning. The main PFCs used for these processes are CF_4, C_2F_6, C_3F_8 and c-C_4F_8 (octafluorocyclobutane) (Cook, 1995; Tsai, Chen and Hsien, 2002; Khalil et al., 2003; WSC reports, 2000 - 2016). Etching is a process where PFCs are used to dril holes in the structure of a silicon wafer. The plasma can also interact with the semiconductor to form compound such as CF_4, C_2F_6, C_3F_8, CHF_3, CH_3F, HF and SF_6 (Mattrey, Sherer and Miller, 2000). During CVD, precursor gases are delivered into the reaction chamber. During the chamber cleaning step a portion of the gas flowing into the chamber does not react with the deposits being removed, and that unreacted portion flows through the chamber, and if no abatement technologies are used, eventually into the atmosphere (IPCC, 2006). This industry will be discussed in detail in Chapter 4.

The Rare Earth Smelting Industry (RESI) was just in 2019 included in the PFC emitting industries by the IPCC. This is reflected in the inclusion of GHG emissions from the RESI in the 2019 Refinement to the 2006 Guidelines, Chapter 4: Metal Industry Emissions where the author of this work appears as a co-author (IPCC, 2019a). During primary production of rare earth oxides an electrolytic process similar to the Hall- Héroult process used for aluminium smelting; it is during this process that PFCs are produced. Global estimates for PFC emissions are relatively low but are associated with large uncertainties due to additional illegal activity

on top of what is reported.(Vogel and Friedrich, 2017, 2018; Vogel et al., 2017). This industry will be discussed in detail in Chapter 5.

Minor sources of PFCs (e.g. manufacturing of F-gases fluorocarbons) are not considered in this work due to time constraints related to this project and these sources estimated low contributions to the global PFC budget.

1.6.2 Sinks

Most chemical compounds, when emitted in the atmosphere, are transformed in other species or are altogether removed from the atmosphere within a few years due to various mechanisms. The majority of atmospheric gases react with oxidants such as the hydroxyl radical (OH) or undergoes photolysis. However, due to the chemical inertness of PFCs, there are limited natural sinks and overall mechanisms that could remove these gases from the atmosphere.

Cicerone was the first (1979) to propose the existence of PFC destruction mechanisms in the atmosphere. For in and above the mesosphere it was suggested that the major loss process could be through high temperature combustion such as photolysis occurring by solar Lyman-α radiation at 121.6 nm. For stratospheric and higher altitudes, potential reactions with electronically excited oxygen and vibrationally excited OH were considered but were deemed unlikely to constitute a major loss mechanism (Cicerone, 1979).

Following Cicerone's work, five destruction mechanisms were investigated. Photolysis by Lyman-a radiation, reactions with O, OH and H and combustion at high temperatures (Ravishankara et al., 1993). It was concluded that reaction with H atoms was the most important destruction mechanism (Ravishankara et al., 1993), a conclusion that corroborates Cicerone's work (Cicerone, 1979). PFC lifetimes are depended on the existence and magnitude of these destruction mechanisms and any major loss process (Ravishankara et al., 1993).

1.6.3 Vertical Profiles

Concentrations of most GHGs demonstrate decreasing trends as the altitude increases, due to the various decay processes and destruction mechanisms present in the atmosphere. PFCs however demonstrate a very different vertical profile of their concentrations which represents this lack of destruction mechanisms described.

The uniform distribution of PFCs in both hemispheres is due to the horizontal and vertical mixing that takes place in the atmosphere. Vertical profiles presented in Figure 1.10 demonstrate how PFC concentrations remain relatively constant despite the increasing altitude (Fabian and Gomer 1984; Fabian et al. 1987).

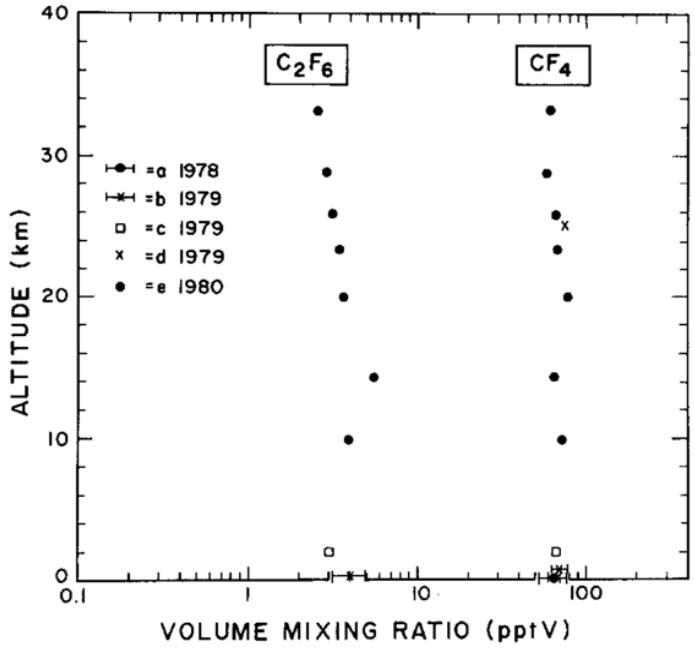

Figure 1.10: Vertical distribution of CF_4 and C_2F_6 (Fabian and Gomer, 1984) showing data collected during different measurement campaigns.

1.7 PFCs in perspective

While, as discussed, PFCs are very long-lived, volatile GHGs with no known sinks in the lower atmosphere, it is important to put their emissions in perspective and compare them with other GHG emissions. Overall, from all the GHG emitted annually, the F-gases group is only ~2% with carbon dioxide (CO_2) being ~76% and methane (CH_4) ~16%. Figure 1. shows the percentages of global anthropogenic GHGs for 2015.

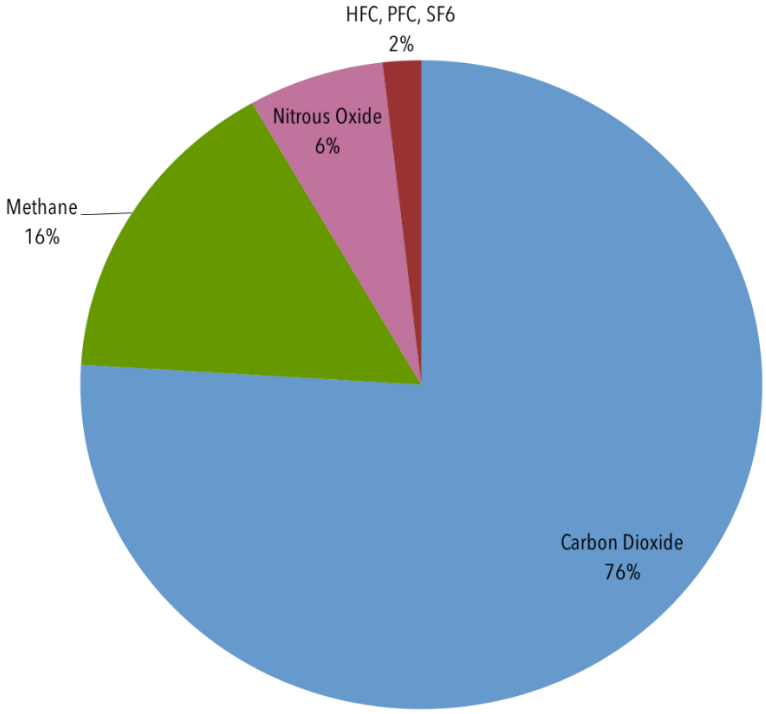

Figure 1.11: Global anthropogenic greenhouse gas emissions by gas, 2015 (Centre for Climate and Energy Solutions, 2015). Original figure adapted from EPA, 2015.

When comparing different GHG emissions an important metric (a tool) is what is referred to as 'carbon dioxide equivalent' or CO_2e (Equation 1.2). This is a term that allows to describe and compare GHG in a common unit. For any GHG CO_2e signifies the number of metric tons of CO_2 emissions with the same GWP as one metric ton of the other GHG. A quantity of GHG can be expressed as CO_2e by multiplying the mass of the GHG by its GWP as shown in Equation (EPA, 2013) below.

$$\text{Mass emissions x GWP} = \text{CO2e (metric tons)} \qquad (1.2)$$

1.8 Policy and International Response to GHG Emissions and Climate Change

1.8.1 The International Panel on Climate Change (IPCC)

The IPCC is the United Nations (UN) intergovernmental body for assessing the science related to climate change. It was created in 1988 by the World Meteorological Organization (WMO) and the United Nations Environment Program (UNEP). The IPCC has 195 members and it widely considered as the accepted leader on climate change. On October 2018, the IPCC published a special report on the impacts of global warming of 1.5^{o} C above pre-industrial levels and the related global GHG emission pathways in the context of strengthening the global response to the threat of climate change, sustainable development and efforts to eradicate poverty (Masson-Delmotte et al., 2018). The IPCC also produces documents called 'Good Practice Guidelines' that describe ways to measure, monitor and report GHG emissions for national inventories. The most recent update of these guidelines is the '2019 Refinement to the 2006 Guidelines'. These documents and summaries are agreed by representatives of all the governments that are members of the IPCC in order for those documents to be clear and concise for decision and/or policy makers.

Throughout this work industry specific methods, equations and uncertainties to calculate PFC emissions are used as described in the IPCC 2006 Good Practice Guidelines from Volume 3 (Industrial Processes and Product Use), Chapter 4 (Metal Industry Emissions) and Chapter 6 (Electronics Industry Emissions) (IPCC, 2006) and as described in the IPCC 2019 Refinement to the 2006 Guidelines, Volume 3, Chapter 4 (Metal Industry Emissions) and Chapter 6 (Electronics Industry Emissions) (IPCC, 2019b). These will be described in detail in the industry specific chapters 3,4 and 5.

1.8.2 The United Nations Framework Convention on Climate Change: Kyoto Protocol and the Paris Agreement

The United Nations Framework Convention on Climate Change (UNFCCC) is an international environmental treaty adopted on 9 May 1992. The UNFCCC entered into force on 21 March 1994 and currently, it has near-universal membership as 197 countries (called Parties to the Convention) have ratified the treaty (UNFCCC, 2007). One of the first goals set by the UNFCCC was for the Parties to the Convention to establish national GHG inventories of GHG emissions (UNFCCC, 2013).

Every year, the Parties to the Convention have an official meeting, referred to as Conference of the Parties (COP) (United Nations, 2019). The first COP took place in 1995 in Berlin and in 1997, COP 3 took place in Kyoto, Japan, where after intense negotiations, the Kyoto Protocol was adopted.

The Kyoto Protocol is an international agreement that commits the UNFCCC Parties by setting internationally binding emission reduction targets (UNFCCC, 2008). This protocol recognizes that the developed countries are primarily responsible for the high levels of GHG emission in the atmosphere as a direct result of more than 150 years of industrial activity (UNFCCC, 2008). Under the principle of "common but differentiated responsibilities" the Kyoto protocol places a bigger responsibility for moderation of GHG emissions to the developed countries (rather than the developing countries). This protocol was adopted in Japan, Kyoto on December 1997 but was entered into force on February 2005. Its first commitment period started in 2008 and was concluded in 2012 while the second commitment period started in January 2013 and will be concluded in December 2020 (UNFCCC, 2006, 2012).

The Parties to the UNFCCC fall under four main classifications (UNFCCC, 2007):

- Annex I: The 37 industrialised countries and economies in transition (EITs) and their commitments include regular reports on their climate change policies and measures and an annual inventory of their greenhouse gas emissions, including data for their base year (1990). These countries the European Union (all its members), Russia, Belarus, Croatia, Iceland, Kazakhstan, Norway, Switzerland, Ukraine, Japan, Australia New Zealand, Canada and the United States.
- Annex II: From the countries listed in Annex I, 24 are also listed in Annex II. These 24 countries are required to provide financial and technical support to the EITs and developing countries and help them reduce their GHG emissions (climate change mitigation) and manage the impacts of climate change (climate change adaptation). These countries are Australia, Austria, Belgium, Canada, Denmark, European Union, Finland, France, Germany, Greece, Iceland, Ireland, Italy, Japan, Liechtenstein, Luxembourg, Netherlands, New Zealand, Norway, Portugal, Spain, Sweden, Switzerland, Turkey, UK, and the USA.
- Annex B: Parties listed in Annex B of the Kyoto Protocol are Annex I Parties with first and/or second commitment period emission targets.
- Non-Annex I: Parties to the UNFCCC not listed in Annex I of the Convention are mostly developing countries.

1.9 Bottom-up estimates

The result of COP 21 was the adoption of the Paris Agreement under which every country is required to monitor and regularly report on its contribution to mitigate global change. Each Party to the Convention must submit national GHG inventories, called national inventory reports (NIRs) to the Climate Change secretariat. For the Annex I Parties the NIRs provide an annual report of the GHG emissions and for the non-Annex I Parties national communications and biennial update reports are submitted instead of the annual NIRs (UNFCCC, 2013). These types of inventories are also referred to as 'bottom-up' estimates. In this work GHG estimates from the Annex I NIRs are used as a comparison against the PFC estimates developed through this work (Chapter 7). COP 21 was held in Paris in 2015. This work presents a new, updated bottom-up estimate of global PFC emissions and will be presented in detail in chapter 7.

1.10 Sustainable Development and the United Nations

1.10.1 What is Sustainable Development

The most common definition of Sustainable Development is provided by a 1987 report by the World Commission on Environment and Development (WCED), which argued for the need of "Economic and social development that meets the needs of the current generation without undermining the ability of future generations to meet their own needs" (WCED, 1987).

This definition contains within it two key concepts:

1. The concepts of needs, the essential needs of the world's poor and vulnerable, to which overriding priority should be given
2. The idea of technological and societal limitations to meet present and future needs.

The 1987 report – commonly referred to as the 'Brundtland Report' after its primary author, the former Prime Minister of Norway, Gro Harlem Brundtland – was a landmark event in both coining and spreading the term 'Sustainable Development'. When policy makers and politicians often speak of this concept, they are often referring to this need to balance needs and limitations, arguing that economic development is likely to reach a metaphorical ceiling. The ceiling can come in a number of forms – limits in the technology available us, limits in how we – as a population – can be organised, and – most importantly – limits in the quantity and quality of natural resources available to us. The concept of Sustainable Development in relation to GHG (and specifically PFC) emissions is examined in Chapter 2.

1.10.2 Key moments in the formulation of sustainable development

Although the concept of 'Sustainable Development' could be mistakenly considered to be relatively recent, the discussion of human (in most cases) needs versus the inescapable natural limits has a long history in wider discussions of environmentalism (Creech, 2012; Hoornweg, 2015). Briefly, some of the key moments of the formulation of sustainable development are presented below:

- In his work, 'An Essay to the Principle of Population' (1798), Thomas Robert Malthus suggests that future population growth would be unsustainable with the natural world imposing limits on the process via a limited supply of food (Malthus, 1798). This essay was published at the beginning of the Industrial Revolution; a period characterised by numerous scientific and technological breakthroughs including sanitation, transport and manufacturing, which was also what proved the Malthusian theory wrong.
- In her work 'Silent Spring' (1962), Rachel Carlson documented the environmental impacts of the use of pesticides in agriculture (Carson, 2002).
- In his work 'The Tragedy of Commons' (1968), Garret Hardin considers the same problem as Malthus, the overuse of natural resources. The added argument in Hardin's case is that humans can no longer rely on technological advances, the same technological advances that had proven Malthus wrong and that a strong societal stance was needed in order to maintain shared publish resources (Hardin, 1968). These public resources included rivers, land and the atmosphere.
- In 1972, global leaders met at the United Nations (UNs) Conference on the Human Environment in Stockholm, Sweden where the United Nations set up the United National Environment Program (UNEP) (Creech, 2012; Handl, 2012).
- In 1980, the UNEP and the International Union for Conservation of Nature and World Wildlife Fund published the World Conservation Strategy: Living Resource Conservation for Sustainable Development. This international document calls for economic growth to consider its impacts on the environment and to ensure that ecosystems are preserved. It is this 1980 strategy that first used the language of 'development that is sustainable'.
- In 1987, the report 'Our Common Future' is published by the Brundtland Committee. The publication of the report provides a landmark moment in our history of Sustainable Development (Brundtland et al., 1987).

- In 1992, the UNCED is held in Rio de Janeiro and the Agenda 21 is adopted. Agenda 21 highlights the need for Sustainable Development to adopt a holistic and comprehensive approach to global challenges.
- In 2000 UN publishes the Millennium Development Goals. In the largest to date gathering of world leaders an agreement was reached to set measurable goals for combating poverty, hunger, disease, illiteracy and environmental degradation, to be achieved by 2015.
- In 2015, the UN publishes the 17 Sustainable Development Goals (SDGs) framework, a continuation of the Millennium Goals (Sachs, 2012; UN, 2015).

As PFCs are gases almost entirely anthropogenic, emitted by the aforementioned industries, the challenge of PFCs is inherently linked to sustainable development. However, the most frequently explored link is that between PFC emissions and climate change. Chapter 2 will explore links between PFC emissions and all of the 17 Sustainable Development Goals (SDGs) and it will introduce a new theoretical framework that links the SDGs to the challenge of PFC emissions. Chapter 2 will also discuss the three pillars of sustainable development, namely the social (relating to human needs, values and relationships), economic (concerning the allocation and distribution of resources) and environmental (addressing how the social and the economic have impacts on the environment and resources). Overall, it is only by addressing environmental, social and economic challenges simultaneously and holistically that 'sustainable development' can be achieved. To this end, Chapter 2 also presents a newly development impact factor that quantifies the environmental impact of PFC emissions against the socio-economic benefits of industries emitting them. This impact factor named the 'De Minimis Scaling Impact Factor', how it was developed through this work and a preliminary example will be shown in section 2.3.3.

1.11 Top-down estimates

Bottom-up estimates like the ones described section 1.9 do not, and cannot, consider actual atmospheric measurements. A top-down approach is an approach that can combine atmospheric measurements with output from chemical transport models in order to estimate emissions.

1.11.1 Atmospheric Dispersion Modelling

An atmospheric dispersion model is a mathematical tool that simulates the dispersion of gaseous species in the atmosphere using a range of equations and algorithms that simulate atmospheric processes and dynamics like those described in section 1.2. There are several kinds of models but they all broadly belong to either of two categories: the Lagrangian and Eulerian framework. The Lagrangian model (moving reference framework) follows a hypothetical particle of air as it moves through the atmosphere. The Eulerian framework (fixed reference framework) defines specific reference points within a gridded system. The models and modelling methods used in this work will be discussed in detail in Chapter 6.

1.11.2 Atmospheric Measurements

Necessary components of a top-down approach are accurate, and ideally, long-term atmospheric measurements. Estimates of global total emissions of PFCs can be made using long-term measurements of atmospheric mole fractions in the background atmosphere. The Advanced Global Atmospheric Gases Experiment (AGAGE) network (Figure 1.) was founded in 1978 in order to monitor the mole fractions of various greenhouse gases and was initially composed of five stations.

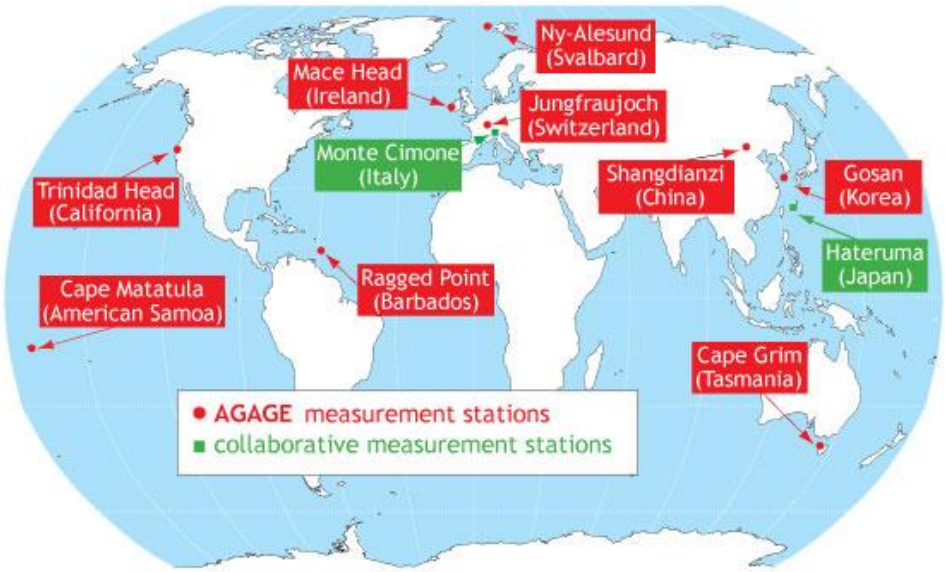

Figure 1.12: The Atmospheric Global Gases Experiment (AGAGE) network (MIT Center for Global Change Science, 2019).

The AGAGE stations that share common features (calibration and instrumentation) are the following (Prinn et al., 2000):

- Mace Head (53° N, 10° W; 25 m 1987 to present)
- Trinidad Head, California (41° N, 124° W; operational between 1995 to present)
- Ragged Point, Barbados (13° N, 59° W; operational between 1978 to present)
- Cape Matatula, American Samoa (14° S, 171° W; operational between 1978 to present)
- Cape Grim, Tasmania, Australia (41° S, 145° E; operational between 1978 to present)
- Jungfraujoch, Switzerland (47° N, 8° E; operational between 2000 to present)
- Zeppelin Mountain, Ny-Ålesund, Svalbard, Norway (79° N, 12° E; operational between 2001 to present)
- Gosan, Jeju Island, Korea (33° N, 126° E; operational between 2007 to present)
- Shangdianzi, China (41° N, 117° E; operational between 2010 to present with gap)
- Mt. Mugogo, Rwanda (1.6° S, 29.6° E; operational between 2015 to present).

Since 2004, the AGAGE network has been making high frequency measurements of over 50 largely synthetic gases including PFCs (Prinn et al., 2000) using a gas chromatography – mass spectrometry (GC-MS) Medusa instrument (Miller et al., 2008; Arnold et al., 2012) which is designed to measure gases which have mole fractions in the ppt range. The AGAGE network (Prinn et al., 2000) has 12 permanent stations all over the world. This network was originally set up to measure ozone depleting substances (CFCs etc.) and now measures the majority of GHGs covered by the Kyoto Protocol including CF_4 (Figure 1.13) and C_2F_6 (Figure 1.14).

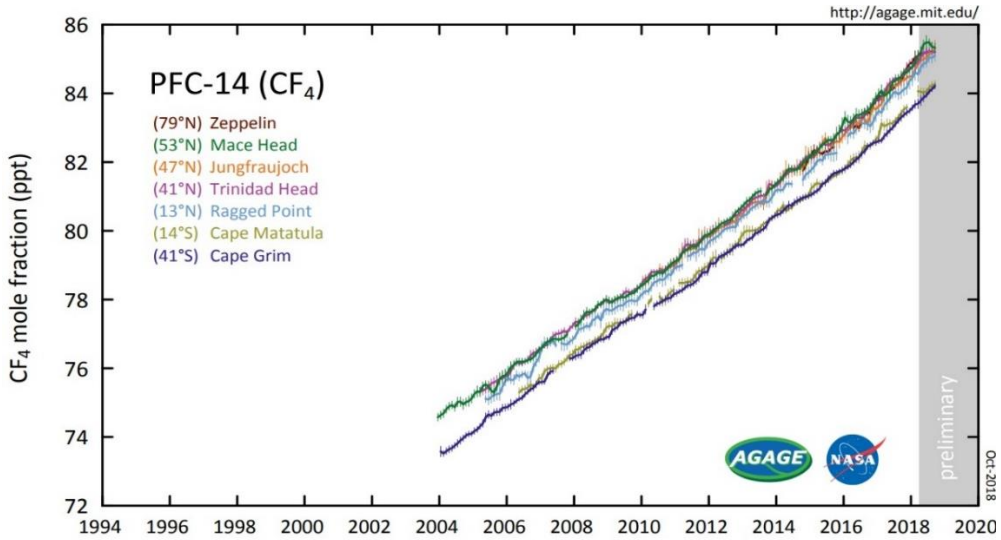

Figure 1.13: CF_4 mole fraction in parts per trillion (ppt) from seven AGAGE stations (Cape Grim, Tasmania; Mace Head, Ireland; Jungfraujoch, Switzerland; Trinidad Head, California; Ragged Point, Barbados; Cape Matatula, American Samoa) (MIT Center for Global Change Science, 2019).

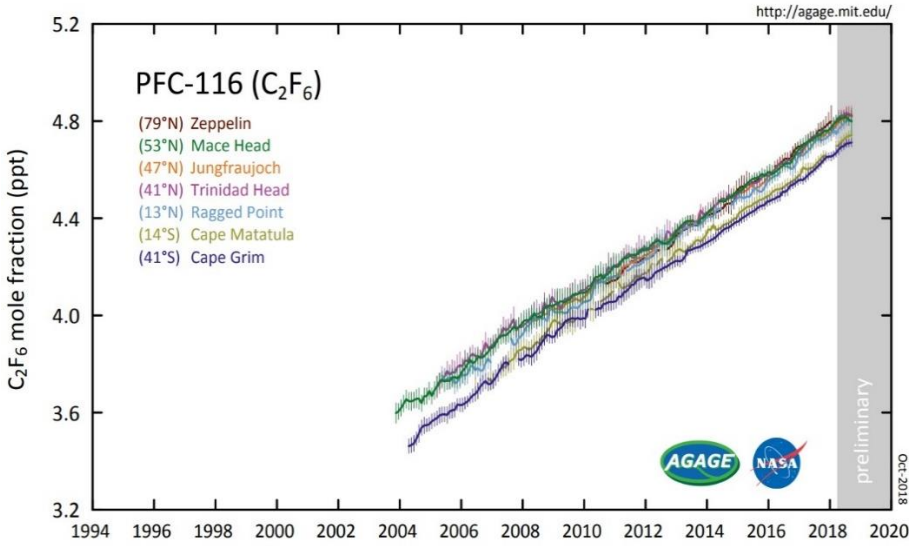

Figure 1.14: C_2F_6 concentrations in parts per trillion (ppt) from seven AGAGE stations in the Southern (Cape Grim) and Northern (Mace Head, Jungfraujoch, Trinidad Head, Ragged Point, Cape Matatula) Hemisphere (MIT Center for Global Change Science, 2019).

1.11.3 Principles of inverse modelling

To produce global total emissions estimates, high frequency atmospheric data is compared with simulated mole fractions of CF_4 and C_2F_6 atmospheric transport and chemistry models (Cunnold et al., 1983; Rigby et al., 2013). Emissions estimates are derived using the model and the data and a Bayesian inverse framework that will be discussed in detail in chapter 6. A Bayesian framework traditionally uses a set of prior estimates (a priori field) and updates our understanding of the emissions (posterior field) by using atmospheric data (observations). The Bayesian frameworks approach, the prior and posterior field and the emissions estimates will be discussed in detail in chapter 7.

Chapter 2

PFCs, simple and wicked problems: There and back again.

2.1 Aims

The purpose of this chapter is to discuss PFCs as part of the theory of sustainable development and the systems thinking narrative and to map these potent GHGs against specific sustainable development goals (SDGs). It is argued that PFC emissions are more than an issue related simply to climate change. PFC emissions are a sustainable development challenge which should be discussed and approached as such. A new definition of post-disciplinary approach is presented, and demonstrates how this type of approach, specific to the PFC emissions' helped develop some of the quantitative methods described in chapter 4, but also helped interpret the results presented in chapters 3, 4, 5 and 7. This chapter will also pose some fundamental questions regarding science; the role of atmospheric chemistry in the Anthropocene, the industries and PFCs, and it will explore PFCs as part of the wicked problems/wicked solutions narrative. Finally, it will propose a new theoretical framework and a newly developed PFC emissions impact factor. To my knowledge, this is the first time this type of analysis has been attempted.

Parts of this Chapter (sections 2.2.1-2.2.5) appear in "The End of Simple Problems: Re-positioning Chemistry in Higher Education and Society Using a Systems Thinking Approach and the United Nations' Sustainable Development Goals as a Framework" (Michalopoulou et al. 2019) a paper published in the Journal of Chemical Education. The original idea of this paper belongs to Michalopoulou E. and Shallcross D.E., which contributed with the mapping of sustainable development goals of the courses discussed in the paper. Atkins E., Preist C., Norman N., Tierney A., and O'Doherty S., contributed curriculum specific information and advise and Saunders R., Brirkett A., Willmore C., and Ninos I., contributed comments and information from their respective, different disciplines and backgrounds as well we comments regarding philosophy of science and history of science.

2.2 Introduction

2.2.1 Why is this discussion and this framework important?

In October 2018, the IPCC published a special report on the impacts of global warming of 1.5^{o} C above pre-industrial levels and the related GHG emission pathways in the context of strengthening the global response to the threat of climate change, sustainable development and efforts to eradicate poverty (Masson-Delmotte et al., 2018). This report unambiguously states that it will require "rapid, far-reaching and unprecedented changes in all aspects of society" in order to limit global warming to 1.5 ^{o} C (Summary for Policymakers of IPCC Special Report on Global Warming of 1.5^{o}C approved by governments, 2018).

PFCs are particularly unique in the role they play in global warming and climate change. As described in section 1.1, they are almost entirely anthropogenic and produced by specific industries (through different processes/circumstances for each industry), they have a very large GWP and atmospheric lifetime but most importantly, they have no known significant sinks (discussed in section 1.6.2). This implies that once these gases are emitted, they will forever (on any reasonable human timescale) remain in the atmosphere and that the atmospheric concentrations of these gases can only be regulated at the emission stage.

At the same time, it must be highlighted, that the industries responsible for emitting those gases are also facing limitations related to the extent of the emissions mitigation they can implement given current technological availability and innovation. During this work, apart from having to answer questions regarding the quantification of PFC emissions from these industries, it became apparent that other important questions regarding the challenge of PFC emissions were: 'Whose problem is this?', 'How can we solve it?', 'Why should we solve it?' as well as 'What level of emission reduction is good enough?'

In order to produce holistic, rounded answers regarding the problem of PFC emissions the scope of problem had to be considered and even go back to the very basic questions of the purpose of science and what kind of science is might be need for a particular problem. This chapter is going to attempt a preliminary socioeconomic analysis of PFC emissions.

2.2.2 Science and societal challenges

a) Science for whom?

As early as 1938 J.D. Bernal published an essay on 'The Social Function of Science' (Society and Journal, 2019) where he discusses the role of science as both an outcome of social forces but also as a social force itself:

> "Science, conscious of its purpose, can in the long run become a major force in social change. Because of the powers which it holds in reserve, it can ultimately dominate the other forces. But science unaware of its social significance becomes a helpless tool in the hands of forces driving it away from the directions of social advance, and, in the process, destroying its very essence, the spirit of free inquiry."

According to Bernal, science further to contributing to our understanding of the natural world, has a social role to play, which in essence, is applying this knowledge in order to make our lives better (Michalopoulou et al. 2019). The demand for greater 'social relevance' of science appears frequently in the literature ('The Credit Hour and Faculty Instructional Workload'; Bazzaz et al., 1998; Terborgh, 2004; Higgins, Chan and Porder, 2006; Matlin et al., 2016; The et al., 2019) (see Appendix A).

In the Dalhem Workshop Reports 'Earth System Analysis for Sustainability' (2005) (Schellnhuber et al., 2005) it is possible that an altogether new 'social contract between science and society' is needed. It becomes clear that the answer to the question 'what is the purpose of science' and the answer to the question 'science for whom' have both the same answer and that is 'society' (Michalopoulou et al. 2019).

b) What science?

Answering these questions, unavoidably raises the question 'which science' or 'what kind of science' is equipped to achieve one's goals? Over the last few centuries different disciplines have generally evolved in isolation from each other to the extent over-specialization in some areas is discussed (Mulder 2012; Michalopoulou et al. 2019) (See Appendix A). In 1959 C.P. Snow introduced the 'two cultures' theory, then in 1962 Kuhn suggested that devotion to a scientific paradigm can prevent absorption of new facts and knowledge to the work of MacKinnon, Hine and Barnard (2013), there are ample critiques in the literature that no one science discipline alone is equipped enough to solve every challenge humanity is faced with (Kuhn, 1962; Lecture, 1959; Mackinnon, Hine and Barnard, 2013).

The societal demand for greater 'relevance' of science and academic programs appears in the paper by Swora and Morrison (1974) 'Interdisciplinarity and higher education' while MacKinnon, Hine and Barnard (2013) reach an excellent conclusion where they describe

interdisciplinary work not as a means to an end, but a natural progression in the scientists' quest to answer a question and solve a problem (Mackinnon, Hine and Barnard, 2013; The et al., 2019).

> "The movement toward the interdisciplinary mode facilitates this restructuring in that disciplines are not demolished but are made to focus on their relationships with one another and with the problems of society."

Additionally, as described in 'Interdisciplinary science research and education' (MacKinnon, Hine & Barnard, 2013) p. 411:

> "For the scientists in our vignettes (case studies), interdisciplinarity was a natural progression in their scientific quest. They did not set out to engage in interdisciplinary science, rather they focused on solving a problem."

Earth systems science and the science of sustainable development are directly and indirectly trying to answer the question of 'which science' by introducing methods, approaches and frameworks which are deeply interdisciplinary, and use systems thinking in order to examine, as earlier defined, both the parts and the whole of the system. So far, some key interactions in the system this chapter attempts to describe have been presented (Michalopoulou et al., 2019) and apply those principles found in earth systems science and the science of sustainability to the challenge of PFCs. Any science (apart from advancing knowledge and understanding) needs to be able to address directly, or indirectly societal needs and problems and in its effort to do this it needs to be flexible enough to adopt either strong disciplinary-focused practices or strong interdisciplinary practices (Michalopoulou et al. 2019).

2.2.3 Systems thinking

The term 'systems thinking' is attributed to Barry Richmond (1987) and since then, the term has been defined several times (Richmond, 1993; Arnold and Wade, 2015).

For the purpose of this thesis parts of Senge's definition as well as Sweeney and Sterman's definition (Senge and Sterman, 1992; Sterman and Sweeney, 2000) are combined and systems thinking is defined as 'a holistic approach that enables simultaneous analysis of the parts as well as the whole itself, their evolution, overlaps and dynamic interactions' (Michalopoulou et al. 2019).

Using this definition and applying it to this work, it is very useful, before PFCs are examined from the point of view of atmospheric chemistry in isolation (Chapters 3, 4 and 5), to first examine it as part of a larger system. This chapter supports that global atmospheric trends and concentrations of PFCs cannot be discussed separately from the industrial processes that generate them, which in turn cannot be discussed separately from the economic activity that these industrial processes support.

2.2.4 Sustainable development and Sustainable Development Goals (SDGs)

As discussed in section 1.10, sustainable development has been defined by the Bruntland committee as "Economic and social development that meets the needs of the current generation without undermining the ability of future generations to meet their own needs" (WCED, 1987). However, even though this the most frequently used definition, other definitions appear in the literature including but not limited to:

- "Sustainable means using methods, systems and materials that won't deplete resources or harm natural cycles" (Rosenbaum, 1993).
- "Sustainability identifies a concept and attitude in development that looks at a site's natural land, water, and energy resources as integral aspects of the development" (Vieira, 1993)

It is important to note that the words 'sustainability' and 'sustainable development' are being used interchangeably and that defining sustainability is not a straightforward task which often in the word meaning different things to different people, including policy and decision makers as well as researchers. This work focuses on Sustainable Development' and not the theory of sustainability in general. One way of understanding sustainable development is by using what is described as 'the three pillars of sustainability'(Barbier, 1987) shown in Figure 2.1.

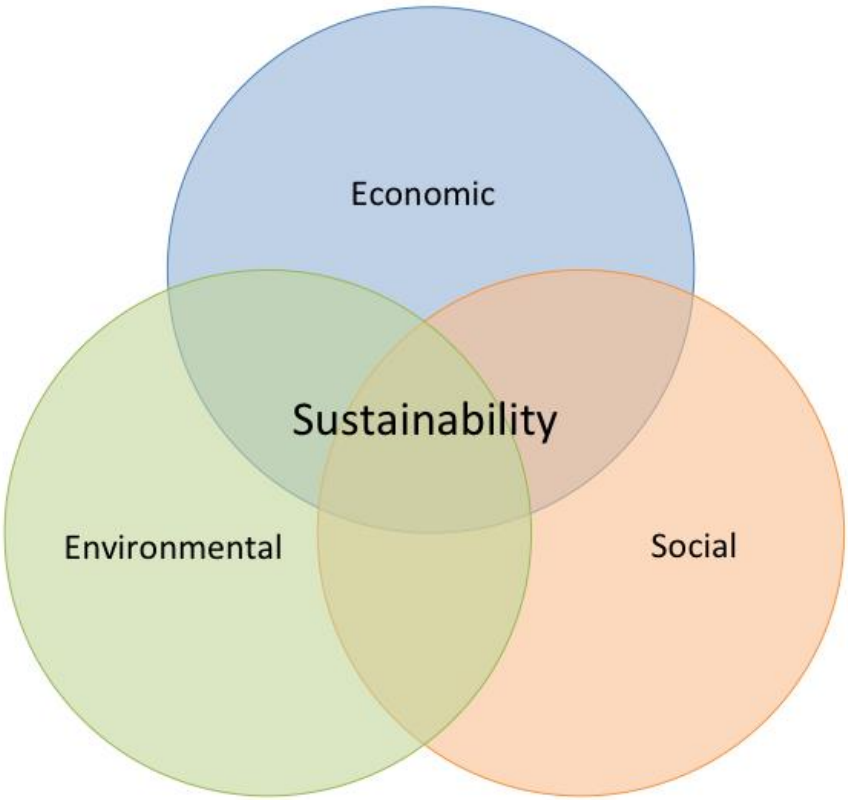

Figure 2.1: The three pillars of Sustainable Development: The Economic, Social and Environmental pillars (Barbier, 1987).

If one could speak of a 'topography' of sustainable development, it is the areas of interaction of the pillars that are of the biggest importance and complexity. This chapter argues that much like climate change, the emissions of gases like PFCs (and potentially other long-lived greenhouse gases (LLGHG) with the same characteristics as PFCs) are not just an issue related to climate change, but an issue related to sustainable development.

In September 2015 the UN General Assembly approved the "2030 Agenda for Sustainable Development". On 1st January 2016, the 17 Sustainable Development Goals (SDGs) (Figure 2.2) of the 2030 Agenda for Sustainable Development officially came into force. The goals that cover all three dimensions of sustainable development have a total of 169 targets, most of them overlapping and interacting (Sachs, 2012; United Nations, 2014, 2015).

The 17 SDGs are:

Goal 1: End poverty in all its forms everywhere

Goal 2: End hunger, achieve food security and improved nutrition and promote sustainable agriculture

Goal 3: Ensure healthy lives and promote well-being for all at all ages

Goal 4: Ensure inclusive and equitable quality education and promote lifelong learning opportunities for all

Goal 5: Achieve gender equality and empower all women and girls

Goal 6: Ensure availability and sustainable management of water and sanitation for all

Goal 7: Ensure access to affordable, reliable, sustainable and modern energy for all

Goal 8: Promote sustained, inclusive and sustainable economic growth, full and productive employment and decent work for all

Goal 9: Build resilient infrastructure, promote inclusive and sustainable industrialization and foster innovation

Goal 10: Reduce inequality within and among countries

Goal 11: Make cities and human settlements inclusive, safe, resilient and sustainable

Goal 12: Ensure sustainable consumption and production patterns

Goal 13: Take urgent action to combat climate change and its impacts

Goal 14: Conserve and sustainably use the oceans, seas and marine resources for sustainable development

Goal 15: Protect, restore and promote sustainable use of terrestrial ecosystems, sustainably manage forests, combat desertification, and halt and reverse land degradation and halt biodiversity loss

Goal 16: Promote peaceful and inclusive societies for sustainable development, provide access to justice for all and build effective, accountable and inclusive institutions at all levels

Goal 17: Strengthen the means of implementation and revitalize the global partnership for sustainable development

Figure 2.2: The 17 UN global goals for sustainable development (UN, 2015).

What the SDGs demonstrate, is broadly humanity's top priorities in terms of global challenges. It is argued that unlike problems and challenges humanity and sciences were facing 20 years ago, or even 10 years ago. This is demonstrated by the overlap and interconnection of the SDGs that proves that the human-environment interaction system is potentially more complex than originally thought. Complex challenges could require complex solutions (Michalopoulou et al., 2019). There are no simple, single solutions to climate change, much like there are no simple solutions to poverty; we are potentially witnessing the end of simple problems in science (Michalopoulou et al. 2019). A very interesting intellectual exercise that demonstrates the complexity of the human-environment interaction system in relation to the SDGs are the following questions: What is more important, lifting a portion of the population of a country from hunger and poverty (SDGs 1 and 2) or reducing the same country's emissions of a certain GHG and therefore its climate impact (SDG 13)? Are both achievable at the same time? If not, should one take priority over the other?

To keep track, share and record their priorities in relation to the SDGs, every member state to the UN SDG accord can produce a Voluntary National Review (VNR). The VNR facilitate sharing experiences, successes, challenges and lessons learned, with a view to accelerating the implementation of the 2030 Agenda (UN, 2019).

2.2.7 Representative Concentration Pathways (RCPs) and Shared Socio-Economic Pathways (SSPs)

Anthropogenic climate change is expected to impact both human and natural systems (IPCC, 2015). The consequences of climate change will differentiate between countries, economic sectors and time. The extent and magnitude of this impact doesn't just depend on the dynamics and physical properties of the earth system but also on socio-economic developments and the times that those will occur. These socio-economic factors include population dynamics, economic development, technological change, social, cultural and institutional changes, and policies (van Vuuren et al., 2014).

Since 2006, the scientific community, following extensive interdisciplinary discussion, begun pursuing an improved scenario-based climate change assessment process (Moss, 2008; Moss et al., 2010; van Vuuren et al., 2014). Scenario analysis is a tool that helps examine future climate and socio-economic developments and evaluate the uncertainties (Nakicenovic et al., 2000; Moss, 2008; Moss et al., 2010; Kriegler et al., 2012; van Vuuren et al., 2014).
This new scenario process described in Moss et al., (2010) has three phases:

1) In the first phase, the integrated assessment modelling (IAM) community developed the so called 'Representative Concentration Pathways' (RCPs) that are used by the earth system modelling (ESM) community to evaluate the extent and magnitude of climate change (van Vuuren et al., 2011, 2014; Taylor, Stouffer and Meehl, 2012; Kriegler et al., 2014). The purpose of these RCP-based models is to facilitate the creation of a set of climate model estimates.
2) In the second phase, the focus was on the development on a set of socioeconomic reference scenarios, the so called 'Shared Socioeconomic Pathways' (SSPs) (O'Neill et al., 2012, 2017; Kriegler et al., 2014; O'neill et al., 2014; van Vuuren et al., 2014).
3) The third phase is expected to combine the RCPs and the associated climate change projections with the SSPs for use by the climate change research community (van Vuuren et al., 2014).

This three-step process aims to inform and evaluate climate change policy but also, to evaluate the impact of these policies on a global and regional level (Kriegler et al., 2014;

O'Neill et al., 2014; O'Neill et al., 2017; van Vuuren et al., 2014). Informing policy using an integrated approach that includes both the RCPs and SSPs can, for example, help form strategies related to climate change mitigation (climate change mitigation includes those actions that help limit the magnitude and/or rate of long-term climate change). Climate change mitigation generally involves reductions in anthropogenic emissions of GHGs vs strategies related to climate change adaptation (climate change adaptation actions include those actions that improve the ability of the system – human or natural – to adjust to climate change impacts, moderate potential damages and to cope with the consequences). Finally, from a sustainable development point of view, this approach resonates well with the three pillars of sustainable development (social, economic and environmental).

2.2.8 SDGs, metrics and impact

In relation to SDG 13 specifically (climate action), one of the purposes of the climate change community in its entirety is to accurately quantify the impacts (also discussed as effects and/or consequences) of climate change on the human and natural system. Quantification of the impacts allows the formation of appropriate actions (policy) to decrease and/or prevent and/or offset these impacts.

To quantify but also, to compare, the various climate impacts of the different GHG emission, appropriate and common metrics are required. From emissions to climate change to impact various choices that need to be made, and its choice in this cause-effect chain, usually requires a modelling framework.

Parameters that allow us to quantify the impacts can be given in absolute terms (e.g.) radiative forcing (RF; described in chapter 1) or in relative terms by using a reference gas (e.g.) CO_2e (described in chapter 1). One of the most used metrics is GWP (described in chapter 1); this metric transfers emissions of the various GHGs to a common scale. The GWP (100 years) from the IPCC was adopted as a metric to implement the multi-gas approach embedded in the UNFCCC and made operational in the Kyoto Protocol (Myhre et al., 2013; UNFCCC, 2019). The 5^{th} assessment report, using these metrics, describes thoroughly the impact of climate change on the natural and human system (Myhre et al., 2013; Reis-Filho, Soares and Schmitt, 2014). Because this report describes the cause-effect chain after the gasses have been emitted, for the purpose of this chapter it will be referred to as a top-down approach. This will be explained in detail in the methods and results section.

Other SDGs can be discussed, analysed and quantified through different metrics and different parameters. The United Nations Development Programme (UNDP) (UNDP, 2019) produces the Human Development Reports (HDRs). These reports include a list of human development indices, namely the Human Development Index (HDI), the Inequality-adjusted Human Development Index (IHDI), the Gender Development Index (GDI), the Gender Inequality Index (GII) and the Multidimensional Poverty Index (MPI). Each of these indices includes different dimensions, indicators and measures (UNDP, 2018b). For example, poverty can be examined through the recently updated MPI index (UNDP, 2018a). The UNDP uses various sources to derive the required data in order to produce those indices (e.g. United Nations Children's Fund (UNICEF) Multiple Indicator Cluster Surveys and OECD, World Bank (2018), International Monetary Fund (IMF) and United Nations Statistics Division.

This analysis is of paramount importance as it gives an overview of the global and regional socioeconomic conditions over either a period of time or a specific year and allows a comparison between different countries and different socioeconomic conditions to be made.

2.2.9 Footprints and Handprints

The term 'carbon footprint' was derived by the term 'ecological footprint' coined by Professor William Rees (Rees, 1992). The term carbon footprint is used to describe the total amount of GHG emissions caused directly and indirectly by an individual, sector, country, product (etc) expressed as CO_2e. Carbon footprint is a quantitative expression of GHG emissions from an activity. However, quantifying the carbon footprint usually depends on the stakeholder. For example, a company trying to quantify their carbon footprint needs to consider both their direct and indirect emissions, which can be quite a complex process, depending on where they start the clock in terms of carbon accounting. If they assume that the clock starts when the receive all their raw materials, they will have carbon footprint A, but if they account for the whole process that led to the raw materials, they will have carbon footprint B, where B is $\geq$ A.

Despite the fact that carbon footprint is used more and more often by various stakeholders, its definitions and quantification methods vary significantly. There is little consensus as to what exactly constitutes a carbon footprint, which gases need to be included in this quantification, what are the direct and indirect activities that need to be included (Wiedmann and Minx, 2007; Pandey, Agrawal and Pandey, 2011). However, there is one

premise that remains unchanged throughout each estimate from any stakeholder: their carbon footprint needs to be as small as possible, ideally achieving carbon neutrality (carbon neutrality, or net zero carbon footprint, refers to either achieving net zero carbon emissions by balancing carbon emissions with carbon removal (offsetting) or by eliminating carbon emissions altogether).

On the flip side of the same coin of this analysis lies the term ‘handprint’. The concept of handprint emerged as a response to the demand for a quantification method of the positive impacts of a product (Biemer, Dixon and Blackburn, 2013; Norris, 2015; Grönman et al., 2019). The handprint is also introduced on the basis of a very simple principle found in the work by Noris (2015):

“While we can and must work to continually reduce them, we will never drive our footprints to zero. Sustaining a person and operating an organization inevitably causes harm, albeit unintended and regretted” (Norris, 2015).

2.2.10 The de minimis principle

The ‘De minimis’ term is an abbreviated form of the Latin phase ‘de minimis non curat lex’, that translates into "the law cares not for small things." This legal doctrine describes matters that are too small or unimportant to consider (West’s Encyclopedia of American Law, 2008). In the context of GHG emissions, some inventories use the de minimis principle in order to exclude emissions from sources that are below a certain threshold (Hess Corporation, 2017; Greenhouse Gas Protocol, 2019).

2.3 Methods and approaches

Drawing from the sustainable development and SDG framework, the systems thinking, problem solving and wicked problem theory, a new post-disciplinary framework is introduced. Through the three different systems examined, namely the micro, meso and macro system of PFC emissions, the dimension of where best to intervene in those systems in order to address the challenge of PFCs is also explored.

Additionally, drawing from this newly suggested theoretical and conceptual framework of the three different systems, the principles described sections 2.2.7 – 2.2.10 the newly developed ‘De Minimis Scaling Impact Factor (DMSIF)’ is presented; this factor aims to quantify both the climate change and socioeconomic impact of a gas emitted on a per country,

per sector, per time basis. This factor uses existing metrics developed by the UN (e.g. the Human Development Index (HDI) to quantify both the environmental but also the socio-economic dimensions of the PFC emitting industries.

It must be highlighted that throughout the methods and results, theories and concepts from different disciplines are used; law, economics, mathematics, atmospheric chemistry and physics and while this is both a particular strength and an innovative approach of this chapter it is, simultaneously, a limitation. This limitation relates to the time constraints tied to the completion of this project.

2.3.1 Why post-disciplinarity?

Defining post-disciplinarity is a far from simple task and it is usually achieved through examples or in some instances, by definitions (Wolmark and Gates-Stuart, 2004; Nyström, 2007; Biagioli, 2009; Lindley, 2016).

It was not for the sake of engaging with methodological pluralism that I turned to post-disciplinarity in order to explore the issue of PFCs. It was through the consistent interaction with the various industries discussed in this work (AI, SCI, RESI), as well as policy making bodies (namely the U.S.A Environmental Protection Agency, the PFC steering committee of the International Aluminium Institute, the IPCC) that I was forced to review my own preconceptions and biases regarding the limitations of a discipline specific approach.

Through those interactions it became evident that not only was information related to the PFC challenge ‘hiding’ in various disciplines (and therefore different understandings of the challenge of PFCs) but it was also ‘hidden’ in the different types of stakeholders involved in this project. Most of the obstacles this work was presented with (detailed in each chapter’s limitations section) were surpassed not because of information that existed in the published literature but information that existed in the years of practical experience, industrial or other, of these stakeholders.

Therefore, as part of this work, a new definition of post-disciplinarity is introduced and used throughout:

That practice that:

a) retains the knowledge and specificities of different disciplines and their histories
b) is able to operate well outside the limits of each discipline in a highly integrated manner

c) is able to incorporate expert knowledge from a variety of stakeholders (e.g. industries, communities)

I believe that this definition gives the concept of post-disciplinarity a two-dimensional approach: one dimension is dedicated to working across disciplines and one that can work across stakeholders incorporating in this way valuable knowledge which does not necessarily exist purely within academic circles.

2.3.2 An industry specific analysis

Before the SDGs linked to the micro, meso and macro system are discussed it is beneficial for this analysis to present some numbers related to the industries emitting PFCs. For the purpose of this chapter this analysis is focused on four main characteristics of every industry, namely, the revenues, products, geospatial distribution and workforce of each industry; these parameters were chosen as they are defined as key industry characteristics (Dufour, 2019). Chapters 3, 4 and 5 will further discuss and take into consideration specific annual production numbers and GHG emissions.

2.3.2.1 The Aluminium Industry (AI)

The AI has a long history that is explored in detail in Chapter 3. Briefly, the use of aluminium goes back to the Chinese and Roman Empires and is very different from the aluminium used today. Currently, the global picture of the aluminium industry is the following:

- **Revenue:** In 2015 the global aluminium market was valued at $133 billion and is projected to reach $167, 277 million by 2022 (Sinha, 2015).
- **Products:** Aluminium is used in a huge variety of products (e.g. cans, foils and aeroplane parts). The aluminium market is segmented on the basis of end user and processing methods. From an end-user perspective the aluminium market is categorised into transport, building and construction, electrical engineering, consumer goods, foil and packaging, machinery and equipment. Development in those areas (e.g. transport or building) is what drives growth in this industry. Rise in global economic growth rate but also emerging economies of the developing countries (e.g. China and India) drive demand for more aluminium in order to cover their needs in technological and infrastructural expansion. In 2019 China became the biggest global producer of primary aluminium, producing more than 52% of the global primary aluminium (see chapter 3).

- **Geospatial distribution:** The locations where the aluminium smelters are physically present play a big part in this analysis. The IAI categorises countries under specific geographical areas using the following categorisation (IAI, 2008):

    - Africa: Cameroon, Egypt, Ghana, Mozambique, Nigeria, South Africa
    - Asia (excluding China): Azerbaijan, Bahrain, India, Indonesia, Iran, Japan, Kazakhstan, Malaysia, North Korea, Oman, Qatar, South Korea, Tadzhikistan, Taiwan, Turkey, United Arab Emirates.
    - China: China
    - Gulf Cooperation Council (GCC): Bahrain, Oman, Qatar, Saudi Arabia, United Arab Emirates
    - North America: Canada, United States of America
    - South America: Argentina, Brazil, Mexico, Suriname, Venezuela
    - West Europe: Austria, France, Germany, Greece, Iceland, Italy, Netherlands, Norway, Spain, Sweden, Switzerland, United Kingdom
    - East & Central Europe: Bosnia, Croatia, German Democratic Republic, Hungary, Montenegro, Poland, Romania, Russian Federation, Serbia and Montenegro, Serbia, Slovakia, Ukraine
    - Oceania: Australia, New Zealand
    - Rest of the World (ROW): As ROW countries are defined the countries that do not belong on the above geographical categorisation.

The IAI has available information on primary aluminium smelters from 1973 to 2019 (IAI statistics, 2019). According to this information the geospatial distribution of the aluminium smelters has changed drastically over the years. In 1973 the leaders in primary aluminium production were North America (~5,713 kt) West Europe (~3,226 kt), Asia – excluding China (~1,500 kt) and South America and Africa (~200 kt each) while there is no data available for East and Central Europe. In 2019 the global picture of aluminium production is very different (Figure 2.3).

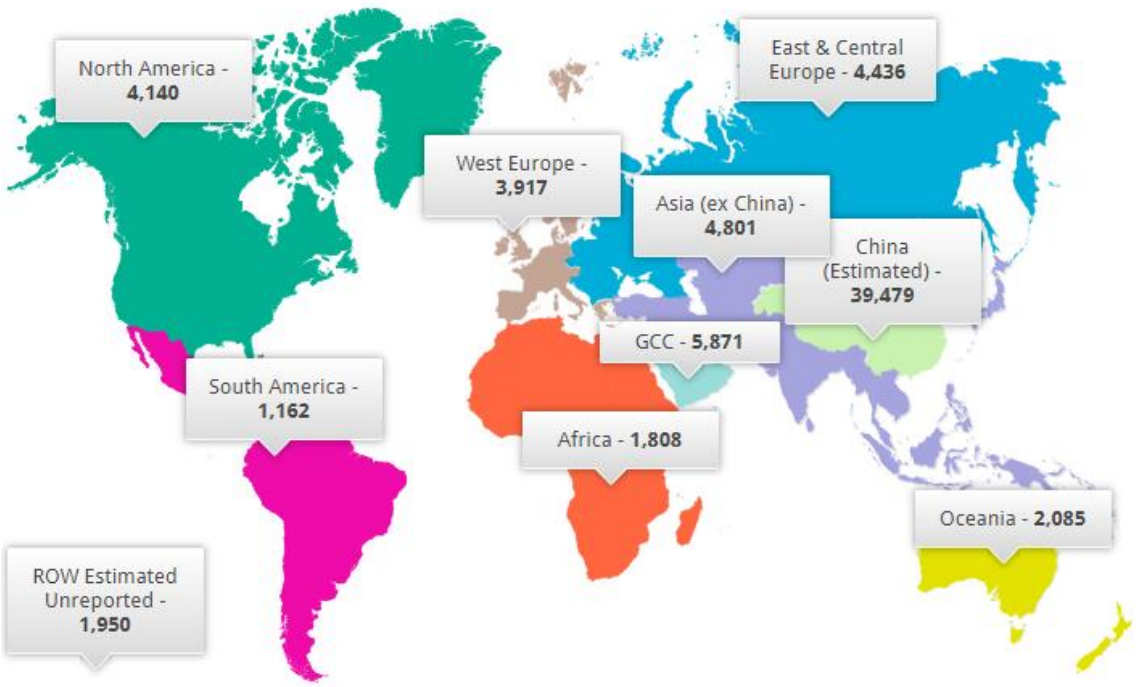

Figure 2.3: Global geospatial distribution of primary aluminium production (in kt) for the years 2018 to 2019. Geographical categorisation as described by the International Aluminium Institute (IAI) (http://www.world-aluminium.org/statistics/)

Figure 2.3 shows the global geospatial distribution of primary aluminium production for the years 2018 to 2019 (IAI, 2019). China, as discussed, is now leading the global aluminium production with an estimated ~39,500 kt of primary aluminium, followed by North America (~4,100 kt) and East and Central Europe (~4,400 kt). It is important to highlight that several of the countries present in this geographical classification belong to the developing countries, least developed countries (LDC) and economies in transition (EITs) (UN, 2014).

- **Workforce:** This industry supports a large number of workers. While data on the number of employees for the global aluminium industry are extremely difficult to find and validate against publicly available sources even the indicative numbers show the size of this industry's workforce. The U.S.A aluminium industry alone employs directly 162,000 workers and indirectly supports 530,000 workers (The Aluminium Association, 2019). The United Company RUSAL employs ~64,000 workers, the Aluminium Corporation of China Limited – only one of the Chinese aluminium corporations - (Chalco) employs ~ 65,000 workers (Financial Times, 2019).

2.3.2.2 The Semiconductor Industry (SCI)

The SC industry is discussed in detail in Chapter 4. Briefly, the SI part of the wider electronics industry that consists of the semiconductor, thin-film-transistor flat panel display (TFT-FPD), and photovoltaic (PV) manufacturing industries (Agostinelli et al., 2006). This work is only examining the SI and not the broader electronics industry. In parallel with the AI, the global picture of the SI is currently the following:

- **Revenue**: In 2017 the semiconductor industry was valued at ~$400 billion (Statista, 2019).
- **Products:** Much like the AI, this industry produces a wide variety of products that include personal computers, smartphones, audio equipment, televisions, calculators, GPS automotive electronics, digital cameras, players, recorders, cars.
- **Geospatial distribution:** The geospatial distribution of this industry has not changed in the same drastic way that it has for the AI. Between 1980 and 1996 the key produces of semiconductors have historically been the USA, Europe, and Japan (Macwilliams, 2014). After 1996, more Asian countries begin to produce semiconductors and between 1996 and early 2000, the global production of semiconductors is split between USA, Europe, Japan, and the Asia-Pacific region, which includes countries like Taiwan, Malaysia and South Korea. From 2003 and onwards, China ramps up semiconductor manufacturing and is now producing ~20% of the semiconductors globally (Macwilliams, 2014; Chitkara and Pausa, 2016). It is again important to highlight that China and Taiwan are both developing economies according to the UN classification (UN, 2014).
- **Workforce:** According to the International Labour Organization, there are globally ~18 million people employed by the electronics industry (International Labour Organisation, 2019) and while there are no publicly available numbers specific to the SI (instead of the broader electronics industry) the U.S.A Semiconductor Industry Association (SIA) reports a total of 1.2 million direct and indirect jobs supported by the SI (SIA, 2019).

2.3.2.3 The Rare Earth Smelting Industry (RESI)

PFC emissions from the Rare Earth Smelting Industry (RESI) are discussed in detail in Chapter 5.

- **Revenue**: In 2018 the RESI was valued at approximately $8 million and is projected to reach approximately $14million in 2025 (Zion Market Research, 2019).
- **Products:** Much like the AI and SCI this industry produces a wide variety of products, for example, in rechargeable batteries, hybrid vehicles, renewable energy (such as wind turbines), mobile phones, flat screen display panels, laptops, glass staining, conductors and amplifiers and the car industry (Becker, Olsson and Simpson, 1999; Hammond, 2000; DePaolo, 2012; Zepf, 2013). Approximately 60% is mainly used in permanent magnets used for power generators in wind turbines, that are increasingly becoming an important source of renewable energy, and electric motors (Goodenough, Wall and Merriman, 2018). Other uses include flint for lighters, added to glass to remove the green colour caused by iron contaminants.
- **Geospatial distribution:** Production of rare earth oxides begun in early 1965 in the USA and until 1985 the USA was the major producer of rare earth element oxides. After 1990, the global production is dominated by China. In 2015, about 170 kt of rare earth oxides were produced globally with a high uncertainty due to illegal mining and black-market trading (Zepf, 2013; Castilloux, 2014; Vogel and Friedrich, 2018) with China having produced approximately 110 kt out of 130 kt of global rare earth oxides (Rare Earths Statistics and Information, USGS, 2015).
- **Workforce:** A specific number of this industry's workforce does not appear to be readily available in the literature or the internet however, following a series of websites, a rough estimate is ~1 million people (Asian Metalpedia, 2012; The Chinese Society of Rare Earths, 2019).

2.3.3 Economic Activity

For the purpose of this chapter the definition of economic activity used is the one given by Raich (2004) "Economic activity is defined as the production, distribution and consumption of commodities" (Raich, 2004). The concept of commodity and that of product are key concepts in this analysis.

2.4 Results and discussion

2.4.1 A three level post-disciplinary analysis of the challenge of PFCs

2.4.1.1 The micro-system

Literature discussions regarding anthropogenic GHGs traditionally focus on the rising concentrations of these gases in the atmosphere and consequently the role they will play in global warming. This system defined by the relationship "PFCs => Atmosphere => Climate Change (global warming)" will be referred to as 'micro-system' (Figure 2.4).

Effectively, this approach is focusing and limiting discussions of the impacts of these emissions only to the domain of SDG 13: Action for Climate change. As discussed, PFCs, are strong IR absorbers and increasing concentrations will contribute towards the anthropogenic GHG effect and to the rise of temperature. However, this approach is only considering one of the three pillars of sustainability, the environmental pillar, a premise which itself, reduces the issue to a "simple" problem. Of course, any impact on SDG 13 will have a knock-on effect on several other SDGs but this still means that any indirect impact of these emissions only through the lens of SDG 13.

Thinking and understanding PFCs emissions only through SDG 13 is particularly limiting in terms of potential solutions and does not fully consider the complexity of the bigger system.

When considering the micro-system, it is easy to conclude that "if atmospheric PFC concentrations are increasing resulting in an increase of the global mean temperature, in order to avoid the global mean temperature increase, the PFC emissions must decrease'. And while this sentence is logically true, it doesn't give us an unknown for which to solve for. Simply put it provides no solution to the problem.

Finally, this micro-system approach leaves the problem vulnerable to questions with dangerous connotations: 'Whose problem is it?', 'Who are the stakeholders involved?' with the worst kind of question being 'Is this really a problem?'

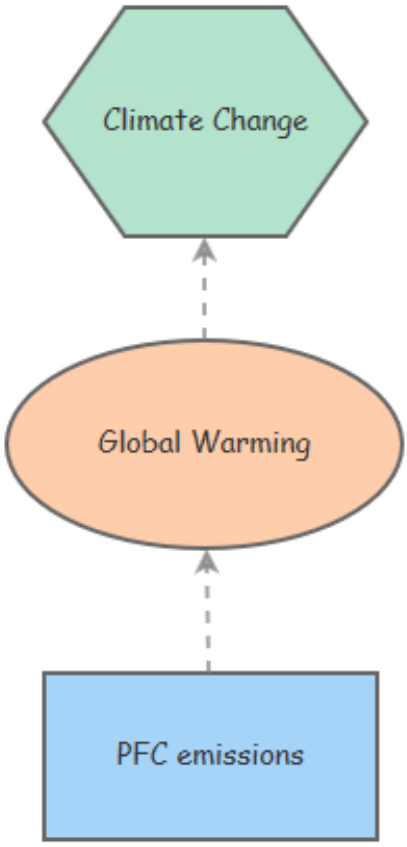

Figure 2.4: Schematic representation of the micro-system.

Within the boundaries of this micro-system the only sources of information are atmospheric observations (e.g. observations from the AGAGE network) and while these observations show, beyond doubt, that concentrations of these gases are increasing over time, this information in itself is not enough to inform policy.

2.4.2.2 The meso-system

If the complexity of the micro-system is increased and the boundaries of the system examined are also increased, PFC emissions can now be considered from a different perspective.

In the case of PFCs like CF_4 and C_2F_6, that are both almost exclusively the results of industrial processes, the next logical step is to increase the boundaries of the previous system is to consider the meso-system "industrial process => PFCs => Atmosphere => Climate change (global warming)" which will be referred to as 'the meso-system' (Figure 2.5).

As described in chapter one, PFC emissions are a result of different types of processes from different industries. To reiterate: in the case of the aluminium industry PFC emissions occur during Low Voltage Anode Effects (LVAE) and High Voltage Anode Effects (HVAE), in the case of the semiconductor industry PFCs are used as part of the chamber cleaning and etching processes and in the rare earth smelting industry PFC emissions are a result of the electrolytical process used, a process similar to the one used for aluminium smelting.

By considering this system, the impact of PFC emissions on more SDGs than just SDG 13 can be observed but also two-way interactions between those industrial processes that generate PFCs and SDGs that were not obvious before; in the case of the AI and the RESI, the electrolytic process that produces PFCs and is referred to as the Hall-Héroult process and the case of the SCI, PFCs used by the industry for the purposes of etch and CVD that were described in section 1.6.1.

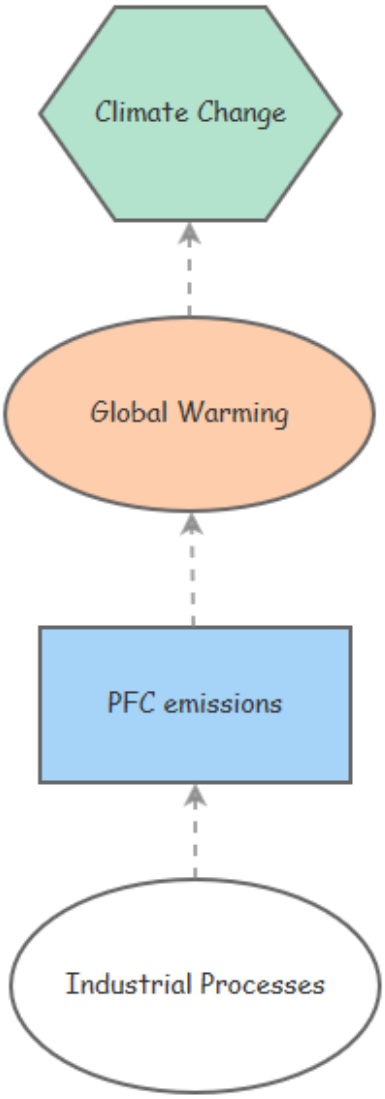

Figure 2.5: Schematic representation of the meso-system.

For example, two of the targets of goal 9 (Build resilient infrastructure, promote inclusive and sustainable industrialization and foster innovation), targets 9.4 and 9.B state:

- Target 9.4: “By 2030, upgrade infrastructure and retrofit industries to make them sustainable, with increased resource-use efficiency and greater adoption of clean and environmentally sound technologies and industrial processes, with all countries taking action in accordance with their respective capabilities” (UN, 2015e).

- Target 9.B: “Support domestic technology development, research and innovation in developing countries, including by ensuring a conducive policy environment for, inter alia, industrial diversification and value addition to commodities” (UN, 2015e).

Equally, two of the targets of goal 12 (Ensure sustainable consumption and production patterns), targets 12.6 and 12.A state:

- Target 12.6: “Encourage companies, especially large and transnational companies, to adopt sustainable practices and to integrate sustainability information into their reporting cycle” (UN, 2015c).
- Target 12.A: “Support developing countries to strengthen their scientific and technological capacity to move towards more sustainable patterns of consumption and production” (UN, 2015c).

The combination of these goals and targets with the meso-system provides the PFC emissions (and therefore PFC atmospheric concentrations) problem with an unknown that can be solved for. This unknown can be expressed in the following question ‘can the processes that produce PFCs be improved in a way that they no longer emit PFCs?’.

Industrial processes are, broadly speaking, the result of technological innovation. In the case of the aluminium industry, for instance, the electrolytic process responsible for primary aluminium production (the Hall-Héroult process) was developed as early as 1880 and is the process used for primary aluminium production to this date.

Considering that by improving the industrial processes, the industry specific PFC emissions will respectively decrease raises the next logical question. The question of limits to technological innovation.

- Is there the possibility for further improvement of the industrial processes?
- Is there always the possibility for further improvement of the industrial processes?
- Is this true for all the industries?

One issue with this approach is that it implies a linear relationship between “amount of commodity produced” and “concentrations of PFCs in the atmosphere”. One could come to the conclusion that since “the more aluminium/semiconductors/rare earths are produced the more PFCs are emitted, therefore the less aluminium/semiconductors/rare earths produced the less PFCs will be emitted” and while this is a logical assumption, it is untrue. For instance, in the case of the SCI, the industry has introduced gas abatement methods, which are broadly methods

that don't allow these potent gases to be released into the environment once they are used on a factory level. This will be discussed this in detail in chapter 4.

Finally, and most importantly, this approach does allow for consideration of the social and economic benefits of the output of the industries when compared with the environmental burden.

2.4.2.3 The macro-system

Taking a high-level view of the problem of PFC emissions allows to consider not just the processes that produce those gases but the economic activity those processes support "economic activity => PFCs=> Atmosphere". This system will be referred to as 'the macro-system'. Therefore, this sections suggests that, since CF_4 and C_2F_6 are the direct result of industrial processes that facilitate and support economic activity, this is the 'complete', big-picture system that should be examined and this is how the problem of PFCs becomes in fact, a wicked problem.

Figure 2.6 explores the components and links of the macro-system. The industrial processes shown in Figure 2.6 are not industry specific, they represent the various processes that emit GHGs. However, every industrial process is linked, physically to the industrial facility, regardless of the industry specific characteristics of this facility. As briefly discussed in section 2.3.2 global economic growth is what drives the industries but equally, these industries can help local economies grow. What in the Figure 2.6 appears with the general term 'society' relates to what was briefly described in section 2.3.2 under both the products and product uses of the outputs of every industry but also the workforce that each industry consists of. There are of course, additionally to the interactions described in Figure 2.6, closed loops of interactions between society and economy, but this chapter will not be addressing those in detail.

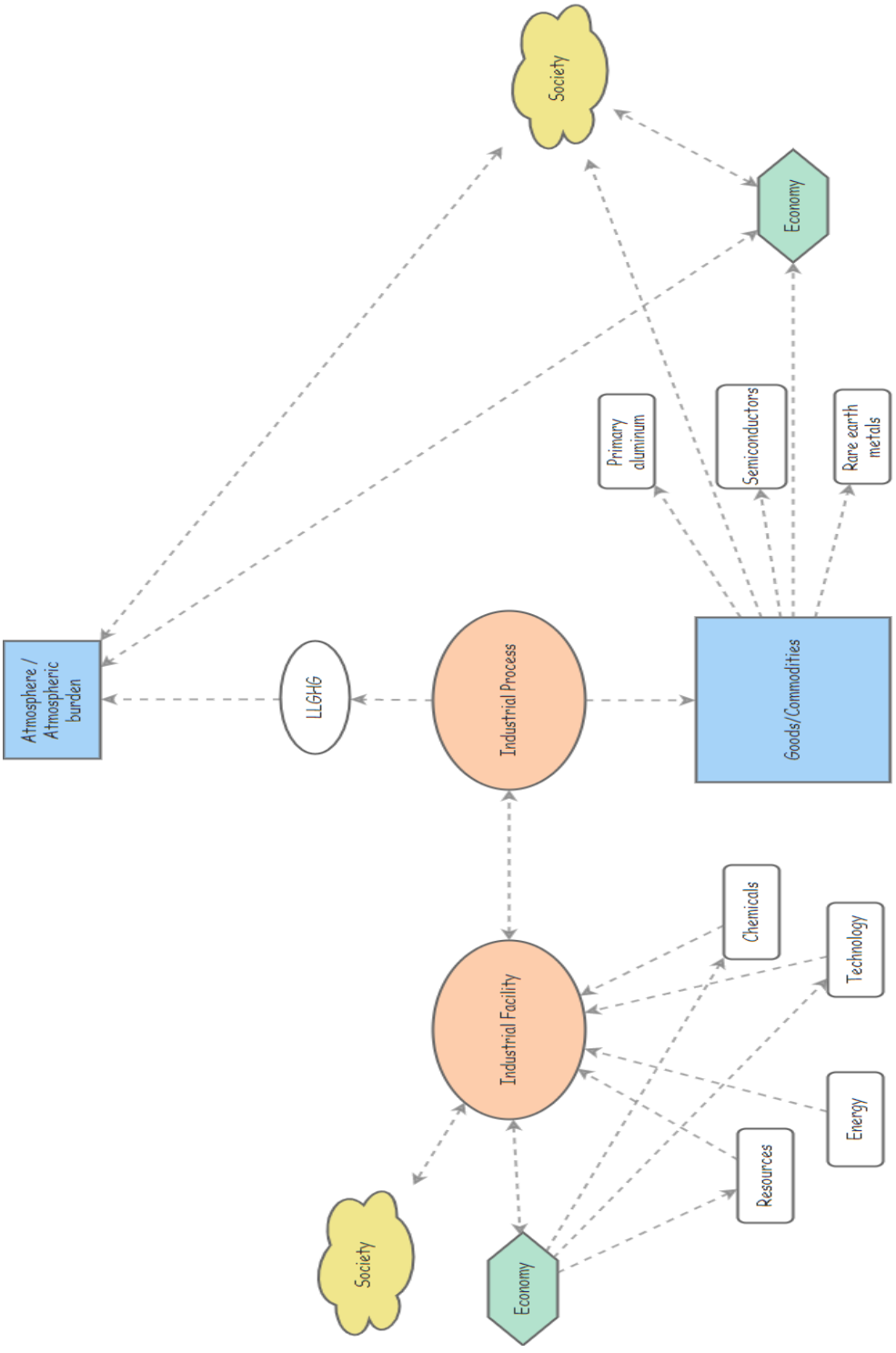

Figure 2.6: Representation of the macro-system.

In section 2.3.2, the geospatial distribution was described, and a particular focus was placed in the developing countries, the LDCs and the EITs. Now, having defined the macro-system, and having grounded the original problem to the concepts of society and economy different implications with regards to the SDGs can be seen.

For example, two of the targets of SDG 1 (No poverty) state:

- Target 1.1: "By 2030, eradicate extreme poverty for all people everywhere, currently measured as people living on less than $1.25 a day" (UN, 2015b).
- Target 1.2: "By 2030, reduce at least by half the proportion of men, women and children of all ages living in poverty in all its dimensions according to national definitions" (UN, 2015b).

Another example, is one of the targets of SDG 5 (Gender Equality) which states:

- Target 5.B: "Enhance the use of enabling technology, in particular, information and communications technology, to promote the empowerment of women" (UN, 2015d)

Table 2.1 presents the SDG targets that this analysis helps address when taking the high-level, macro-system view, on an SDG case basis according to the targets and indicators presented in the 2030 Agenda for Sustainable Development (UN, 2015f).

Sustainable Development Goal (SDG)	**Targets**
Goal 1: End poverty in all its forms everywhere	1.1, 1.2, 1.4, 1.A, 1.B
Goal 2: End hunger, achieve food security and improved nutrition and promote sustainable agriculture.	2.1, 2.4, 2.A
Goal 3: Ensure healthy lives and promote well-being for all at all ages	3.2, 3.3, 3.9, 3.B, 3.C
Goal 4: Ensure inclusive and equitable quality education and promote lifelong learning opportunities for all	4.B.
Goal 5: Achieve gender equality and empower all women and girls	5.5, 5.B
Goal 6: Ensure availability and sustainable management of water and sanitation for all	6.3, 6.A
Goal 7: Ensure access to affordable, reliable, sustainable and modern energy for all	7.A, 7.B

Goal 8: Promote sustained, inclusive and sustainable economic growth, full and productive employment and decent work for all	8.1, 8.2, 8.3, 8.6
Goal 9: Build resilient infrastructure, promote inclusive and sustainable industrialization and foster innovation	9.1 – 9.5, 9.A – 9.C
Goal 10: Reduce inequality within and among countries	10.1, 10.6, 10.C
Goal 11: Make cities and human settlements inclusive, safe, resilient and sustainable	11.2, 11.3, 11.A, 11.C
Goal 12: Ensure sustainable consumption and production patterns	12.4, 12.5, 12.6, 12.A
Goal 13: Take urgent action to combat climate change and its impacts	13.1-13.3, 13.A., 13.B
Goal 14: Conserve and sustainably use the oceans, seas and marine resources for sustainable development	14.A
Goal 15: Protect, restore and promote sustainable use of the terrestrial ecosystems, sustainably manage forests, combat desertification and halt and reverse land degradation and halt biodiversity loss	15.6
Goal 16: Promote peaceful and inclusive societies for sustainable development, provide access to justice for all and build effective, accountable and inclusive institutions at all levels	16.8
Goal 17: Strengthen the means of implementation and revitalize the Global Partnership for Sustainable Development	17.2, 17.5

Table 2.1: SDG targets that this analysis helps address when taking the high-level, macro-system view, on an SDG case basis according to the targets and indicators as they are presented in the 2030 Agenda for Sustainable Development (UN, 2015f)

2.4.3 The De Minimis Scaling Impact Factor (DMSIF)

2.4.3.1 Context

What is very interesting and should be highlighted at this stage is that this work never set out to produce this impact factor. Before any of these concepts, ideas and frameworks were considered, during an industrial conference a very important question was raised as a comment on my PFC estimates presentation: 'How much CF_4 can an industry emit based on what it has to offer to the country it's based and the world?". It was at the end of this work that I had to work my way through the concepts described in section 2.1 in order to conclude that there was no known way to respond to this question; and there was no known way to quantify this answer. Pulling the concepts described in section 2.1 together was an extremely intense and complex task. Because of the increased complexity but also the newly framed ideas described here, the possibility exists that mistakes have been made during the combination of this information and this section will be thoroughly investigated further in future work.

The series of questions that led to the development of the DMSIF were the following:

- Is there a way to quantify the atmospheric impact of a GHG weighted against the socioeconomic benefits of the industry (actor or stakeholder) emitting the GHG?
- Can the country specific priorities in terms of the SDGs as an extra weighting parameter in this equation be quantified?
- Can the global dependency of a specific industry (or economic activity) on a regional scale be quantified?
- Can the goals mentioned be achieved using existing metrics, indices and/or parameters?
- Can such a factor be used in a similar way as other metrics and/or scenarios (such as the RF, GWP, RCP and SSP)?

Perhaps, the most important aim of the DMSIF is to discuss whether such a factor is needed, is useful and necessary.

DMSIF is defined in its general form as:

$$\mathrm{GHGimpact}_{\text{on Climate Change}}(\text{country}, \text{sector}, \text{time}) = \frac{\mathrm{E} * \mathrm{GWP} * \mathrm{ODP}^{*}}{\mathrm{x} * \mathrm{y} * \mathrm{z}} \times \mathrm{a} \times \frac{1}{\mathrm{k}}$$

Where:

E = the normalised emission rate over a suggested timeframe

GWP = the Global Warming Potential of a GHG

ODP* = Ozone Depleting Potential (where applicable) that is rescaled to allow very short-lived species that have low ODPs to be included. Here, species that do not depleted stratospheric ozone would have a factor of unity.

x = people employed by this sector in the specific country

y = types of products produced by the specific sector including any offsetting attributes

z = a parameter estimating any additional offsetting factors

α = country specific SDG priorities weighting factor

k = global dependency on the products of the specific sector

The parameters will be thoroughly discussed in section 2.4.3.2. The PFC specific form of the DMSIF is given by Equation 2.1:

$$\mathrm{PFCimpact}_{\text{on Climate Change}}(\text{country}, \text{sector}, \text{time}) = \frac{\mathrm{E} * \mathrm{GWP}}{\mathrm{x} * \mathrm{y} * \mathrm{z}} \times \mathrm{a} \times \frac{1}{\mathrm{k}} \qquad (2.1)$$

The name of the factor was chosen based on the de minimis principle described in section 2.1.10. However, it must be highlighted that this work does not advocate for exclusion of any GHG emissions from any country, any sector in any inventory. It is merely suggesting that this scaling factor could be used alongside the quantified GHG emissions as a form of bottom-up quantification approach that uses both atmospheric and climate change related parameters as well as socio-economic parameters.

2.4.3.2 Fantastic parameters and where to find them

It needs to be highlighted again that this work is at a very early stage. There are some limitations and gaps that could not be overcome but will be mapped and explained. It will require the joint efforts of several disciplines in order to thoroughly analyze and quantify the suggested parameters. Equation 2.2 presents the basic principle of the opportunity cost equation which is the basis on which the DMSIF has been built on.

$$\text{Opportunity Cost} = \frac{\text{What one is sacrificing}}{\text{What one is gaining}} \qquad (2.2)$$

I. Why a per country, per sector, per time analysis?

Several inventories use a per country, per sector, per time analysis to quantify GHG emissions; the UNFCCC requires from the reporting countries to report the GHG monitored under the Kyoto protocol under five sectors (energy, industrial processes and product use; agriculture; land use, land-use change and forestry (LULUCF) and waste) (UNFCCC, 2013a, 2013b). Therefore, it was deemed that this choice requires further explanation. The added factor of time is added to facilitate aggregation over specific periods of time.

II. Normalized emission rate (over the studied period): E

The normalized emission rate is defined as (Equation 2.3):

$$\mathrm{E} = 1 - \frac{\text{Emission Rate (year n)}}{\text{Emission Rate (year m)}} \tag{2.3}$$

Where year n > year m.

Alternatively, the emission intensity could be used. Emission intensity is defined as the level of GHG emissions per unit of economic output (Herzog, Parshing and Baumert, 2005). However, this parameter includes the GDP which for the moment, is best avoided.

III. Why GWP?

GWP is (as described in section 2.2.8) one of the most used metrics that allows a comparison between GHGs. Since the DMSIF aims to allow a comparison between GHGs (and/or countries, and/or sectors) it is a good choice. However, depending on the gas, it could potentially be preferable to use different time horizons of GWPs instead of the 100-year horizon; for instance, the 20-year horizon.

IV. What is x?

The purpose of parameter x is to provide an estimate of the number of people employed by this sector in the specific country (for example number of people employed by the semiconductor industry in South Korea) over the same period of time the GHG emissions are studied. Therefore, x, is a function of the country, the sector and the time itself (Equation 2.4).

$$\mathrm{x} = \mathrm{x}\,(\text{country}, \text{sector}, \mathrm{t}) \tag{2.4}$$

There are several existing metrics, parameters and indices that could be used to represent x including the UNDP indices described in section 2.2.8. This function could also be the absolute value of people employed by the specific sector projected on a scale (for instance 1 – 5) with discreet, different bands of numbers employed per band. However, even in this case, the

function could and perhaps should be expanded to include some measure of the sector and country specific development stage as explored by the HDI (described in section 2.2.8). For example, if the function of x were to be the absolute value of people employed per sector per country projected on a 1 – 5 scale, then x could be expanded to include the UNDP indicators: employment to population ratio and/or the labor force participation rate. This process can be repeated to include more than one HD indicators. Therefore, x would be described by Equation 2.5:

$$x = x\left(\text{country}, \text{sector}, t, HD_{\text{indicator1}}, HD_{\text{indicator2,}}, \dots, HD_{\text{indicatorn}}\right) \quad (2.5)$$

V. What is y?

The purpose of the parameter y is to provide an estimate of the types of products produced by the specific sector in the specific country of the period studied. It is important to have a factor that considers the output of the specific economic activity but also that allows differentiation between products, their attributes and shares between different product categories (Equation 2.6).

$$y_i = y_i\left(\text{country}, \text{sector}, t, A_1, A_{2,}, \dots, A_n, m\right) \quad (2.6)$$

Where

y_i = the estimate y for every product i.

A_1, A_2,…,A_n = the desired product attributes

m = the market share for the product.

This function follows the basic principles of the demand equations as described in economics and is based on the principle that differentiation between products is possible on the basis of their different attributes (Teach, 1990; Kim, Allenby and Rossi, 2005; Norris, 2015).

For the purpose of this work and the DMSIF the product attributes that is logical to focus on are those attributes related to green uses and offsetting technologies. For example, aluminium is a highly recyclable material with nearly 75% of all aluminium ever produced is still in use today (The Aluminium Association, 2019). Additionally, it is a material primarily used in green technologies such as electric vehicles.

VI. What is z?

The parameter z will provide an estimate of any other offsetting factors, specific to climate change, relevant to the country, sector and timeframe studied, not covered by function y.

VII. What is α?

The parameter α will be used to weigh climate change against other SDGs based on country specific priorities. The purpose of this parameter is to provide some estimate of where action against climate change is within country specific agendas and boundaries. Currently the VNR are used as an indicator of how high climate change is in each country's SDG priorities and this priority is then projected on a 1-5 scoring band (1 being lowest, 5 being the highest).

VIII. What is k?

The parameter k will be used to describe the global technological dependency of the different sectors on the products produced by country, by sector, over the period studied. For example, while the RESI is now recorded to emit PFCs (emissions which will be discussed at length in chapter 5), there is a large technological dependency on the products of the RESI. Rare earth metals are used in wind turbines and electric vehicles (discussed in detail in chapter 5). This parameter will therefore be a function of the country, the sector, the timeframe studied but also exports, local use and market share (Equation 2.7):

$$k_{j,h} = k_{j,h}(\text{country}, \text{sector}, t, \text{export}, \text{local use}, m) \qquad (2.7)$$

Where

$k_{j,s}$ = the dependency (k) of the global sector (j) on the country specific sector (s) studied

export = annual exports to the global sector (j) from the country and sector (s) studied

local use = regional (country specific) use of the products produced by sector (s)

m = normalized market share of sector (s) defined as:

$m = \text{size of the sector on a global scale} / \text{size of the sector on a regional scale}$

It is expected that this function, when fully developed, will have the form of a non-linear dynamic equation.

This work and the suggestions described in this chapter need thorough and extensive investigation. For this investigation to be fruitful, it will require the collaboration of more than one disciplines. The DMSIF is the outcome of post-disciplinary discussions between industry,

policy makers and academia and between different disciplines. Future work will engage further with colleagues from law, economics, mathematics, climate science, and data science in order to investigate each parameter and produce a spectrum of DMSIF factors.

I strongly believe that this factor has potential to be used alongside the RCPs, SSPs, RF and could perhaps give valuable insight into what happens when you weigh directly, the atmospheric cost and the socio-economic benefit of the process (sector) that produces the GHG in question. The DMSIF could also be used as a heuristic tool that can examine a series of metrics, parameters, functions and indices using the basic principle of the opportunity cost function (Equation 2.2).

2.4.3.3 Preliminary results

To test these hypotheses and the DSMIF the following well-studied gas, country and sector were chosen.CF_4 emissions in China from the RESI for the years 2010 to 2015. The general Equation 2.8:

$$\mathrm{PFCimpact}_{\text{on Climate Change}}(\text{country}, \text{sector}, \text{time}) = \frac{\mathrm{E} * \mathrm{GWP}}{\mathrm{x} * \mathrm{y} * \mathrm{z}} \times \mathrm{a} \times \frac{1}{\mathrm{k}} \qquad (2.8)$$

Becomes (Equation 2.9):

$$\mathrm{CF4}_{\mathrm{impact}}(\mathrm{China}, \mathrm{RESI}, 2010 - 2015) = \frac{\mathrm{E} * \mathrm{GWP}}{\mathrm{x} * \mathrm{y} * \mathrm{z}} \times \mathrm{a} \times \frac{1}{\mathrm{k}} \qquad (2.9)$$

Where:

E = 1.3

This number was estimated through Equation 2.3 using CF_4 emissions from the RESI in 2015 (~ 4 Gg/yr) and in 2010 (~2.3 Gg/yr). These estimates will be discussed in detail in chapter 5.

GWP = 6630

For the purpose of this example, and until such time as the remaining factors of Equation 2.9 can be fully quantified with their uncertainties, it was decided to use scoring bands of 1-5 for each factor (with 1 being low and 5 being high). These scores are still based on the sources discussed in the methods sections (UN, 2015a).

x = 3 (Based on estimates from UNHD index (UN, 2015a))

y = considering a very rough estimate of % being used in electric vehicles and the remaining % being used in wind turbines and multiplying both percentages by 5.

z = 1 (no other offsetting attributes)

α = 3 (Country's prioritization of climate change above average; based on China's VNR (NDRC, 2008))

k = 5 (high global technological dependency based on Chinese exports vs ROW production of REO (USGS, 2018))

The DMSIF for this example is estimated to be 430. What this broadly means is that once all these offsetting factors and sector specific, regional and global socioeconomic dependencies are taken into consideration, the impact of this gas (per country, sector and time) decreases from 6630 (that was the original impact of the gas related to the GWP) to 430.

It is expected that the DMSIF will range between a maximum value equal to the existing GWP of each GHG studied (upper boundary) but the minimum value (lower boundary) this factor can take has not been explored.

As already mentioned, further and detailed analysis and quantification of this factor is required before any further assumptions can be made. However, and having recognized this, I believe that this factor can give extremely valuable insight for those gases that are entirely anthropogenic (as is the case with PFCs) and are emitted from industries that the current technology heavily relies on.

2.5 Conclusion

Writing a conclusion for the specific chapter is particularly challenging as its function was to introduce a series of frameworks and ideas that have not been introduced before in relation to PFC emissions.

This world is rapidly changing. Although the function of science has always been to help interpret the natural world and to improve our lives using this knowledge, humanity is now facing urgent challenges on a global scale. These challenges have been mapped according to the UN under the SDGs.

This chapter discusses the challenge of PFC emissions through the lens of systems thinking and sustainable development as part of the global challenges narrative. This resulted

in a new definition for post-disciplinary work, a new theoretical framework to understand PFC emissions and eventually in incorporating PFC emissions as part of the wicked problems narrative. While PFC emissions are often considered a simple problem, this chapter argues that this is not the case. Examining the challenge of PFCs strictly through a disciplinary less may prove an inefficient strategy especially in terms of policy making and emission reduction policies.

An industry specific analysis was presented in conjunction with the post-disciplinary three-tiered understanding of PFCs. Further engagement with concepts and ideas from law, economics, mathematics, physics, chemistry and modelling, resulted in quantifying all of the elements presented in the chapter. Much like sustainable development set out to discuss the need for development versus the limitations of the natural systems, this chapter presents PFCs as part of the larger system of 'needs' and grounds PFC emissions to the economic activities the industries producing PFCs are supporting.

This led to the creation of the De Minimis Scaling Impact Factor; the DMSIF is a newly introduced factor developed in this work and its function is to way the environmental impact of specific anthropogenic gases against the socioeconomic contribution of the GHG emitting sectors, per country, per sector, per time period. It is thought that this highly innovative analysis could become critically important in terms of high-level decision making within the industries and it could potentially play a role as a policy making tool. However, this factor needs further work and development that is planned to be carried out in the future by a post-disciplinary group of experts.

Chapter 3

PFC emissions from the Aluminium Industry (AI)

3.1 Aims

The aims of this chapter are to quantify and discuss PFC emissions from the aluminium smelting process, aluminium production over time, discrepancies between top-down and bottom-up estimates specific to this industry and present an updated bottom-up inventory for

global aluminium PFC emissions. As discussed in chapter 1 the following research questions will be answered:

- Can an industry specific, updated bottom-up inventory be produced?
- Is there a significant contribution from suspected low-voltage emissions?
- How large are PFC emission contributions from emerging Chinese aluminium production?

Parts of this chapter appear in the paper 'Challenges in estimating CF_4 and C_2F_6 emissions' written by the author of this thesis, Michalopoulou E. (Eleni Michalopoulou, 2018). This paper was a single author paper and all data analysis and writing was done by Michalopoulou E.

Quantifying and understanding PFC emissions from the AI is not a straightforward task. Primary aluminium production has been historically reported as potentially the largest anthropogenic source of both CF_4 and C_2F_6 (Harnisch et al., 1996; Mühle et al., 2010a; Kim et al., 2014; Mahieu et al., 2014). It was generally perceived, and to some extent it was presented in the literature that PFC emissions were approximately a linear function of the aluminium produced and a gas specific emission factor as shown in Equation 3.1:

$$E_{PFC} \propto EF_{PFC} \times MP \qquad (3.1)$$

Where:

E_{PFC} are the emissions from the different PFC,

EF_{PFC} the emission factor specific to each PFC gas,

MP is the metal production per year.

This chapter will be examining both these factors (EF_{PFC}, MP) and it discuss the role each factor plays in PFC emissions. Also presented are critical aspects of current and historic literature and updated, recent findings that demonstrate that PFC emissions are a function of more factors than the two described in Equation 3.1. Constructing this function allows for better understanding, not only of the PFC emissions from the AI and their fluctuations over time but provides the inventory maker with a better understanding and interpretation of the discrepancies specific to the PFC emissions from this industry.

3.2 Introduction

3.2.1 Aluminium Production and the International Aluminium Institute (IAI)

There is great abundance of the metallic element of aluminium in the Earth's crust, but aluminium is not found in isolation. It is present in clays and aluminosilicate minerals, but commercially the most valuable aluminium source is bauxite. Bauxite is a complex mixture of aluminium hydroxide and aluminium oxide (alumina) (Peacor et al., 2003).

In 1825 Hans Christian Oersted produced an aluminium alloy for the first time (The history of aluminium industry). Since then, the AI has gone through several changes, ranging from technological to geographical (Nappi, 2013). In 1972 the International Primary Aluminium Institute (IPAI) was founded; a global forum for aluminium producers and the name of the Institute was changed in 2000 in order to reflect a more inclusive agenda, focusing on sustainability and the Institute became the International Aluminium Institute (IAI) (Nappi, 2013). Current IAI membership represents over 60% of global bauxite, alumina and aluminium production; this will be discussed in detail further in this section. The purpose of the IAI is to promote both a wider understanding of its industrial and manufacturing activities but also its commitment to enhance corporate responsibility through sustainable development (World Aluminium — The Institute).

From 1973 until 2019 the global aluminium industry has produced 1,284,773 kt of aluminium (World Aluminium — The Institute). The global primary aluminium production has gone through several shifts and changes throughout its history. Figure 3.1 shows how the industry has evolved and how the geographic distribution of the primary aluminium industry has changed over time.

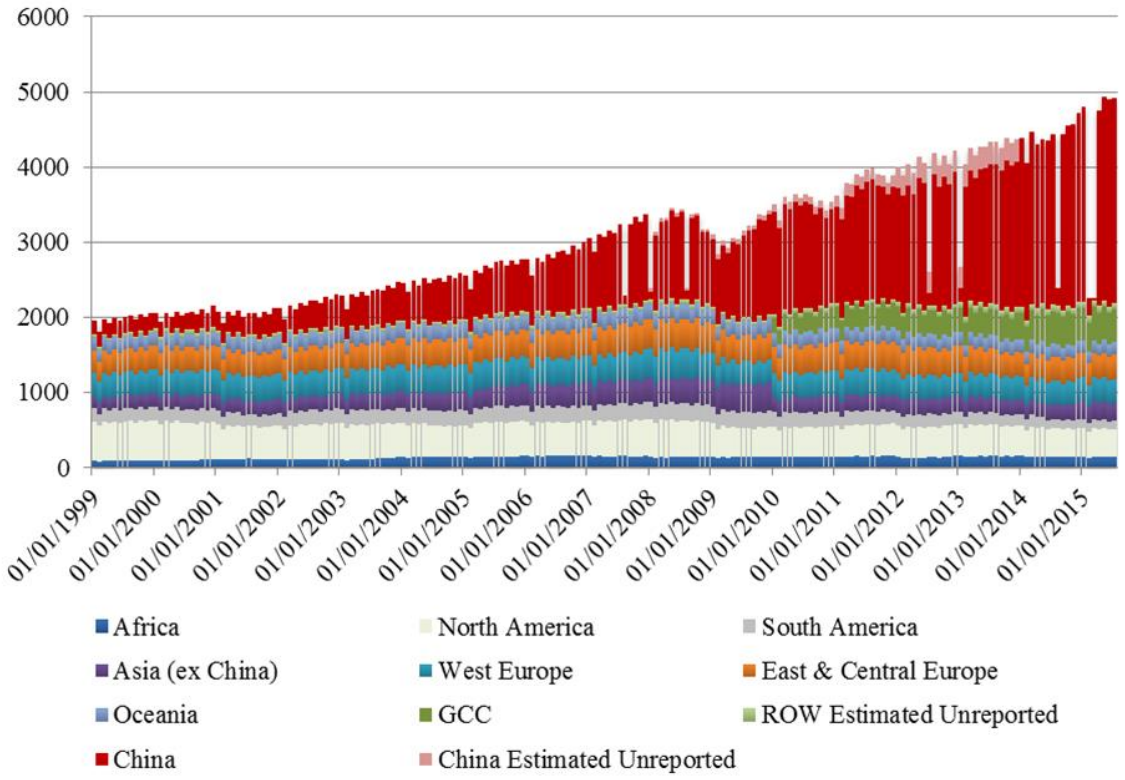

Figure 3.1: Geographical split of world aluminium production (in kt) from 1999 to 2016 (China Consumes Too Much Coal to Produce Aluminium | ALUWATCH).

Figure 3.1 shows a production of ~2,500 kt for 2016 and China is still dominating the global aluminium production with an estimated production of 2,900 kt in April 2019 when in total the global aluminium production was 5,200 kt meaning that China produced more than 55% of the global primary aluminium (World Aluminium — The Institute). According to James King, these geographical shifts in production reflect several trends in the industry, most them being economic growth, global and local financial crises and political instability (King, 2001). The role the geospatial distribution plays in quantifying PFC emissions will be elaborated in section 3.2.2.

3.2.2 PFC emissions from the smelting process

Primary aluminium production from bauxite consists of two main processes. Bauxite is refined to alumina (Al_2O_3) during the Bayer process and alumina is converted to aluminium during the Hall–Héroult process (Hind, Bhargava and Grocott, 1999; Thonstad et al., 2001;

Norgate, Jahanshahi and Rankin, 2007; Haupin, 2009; Gu and Wu, 2012). During the Hall–Héroult process alumina is electrolysed in molten cryolite (Na_3AlF_6). Figure 3.2 shows the structure of the electrolytic cell where the Hall–Héroult process takes place.

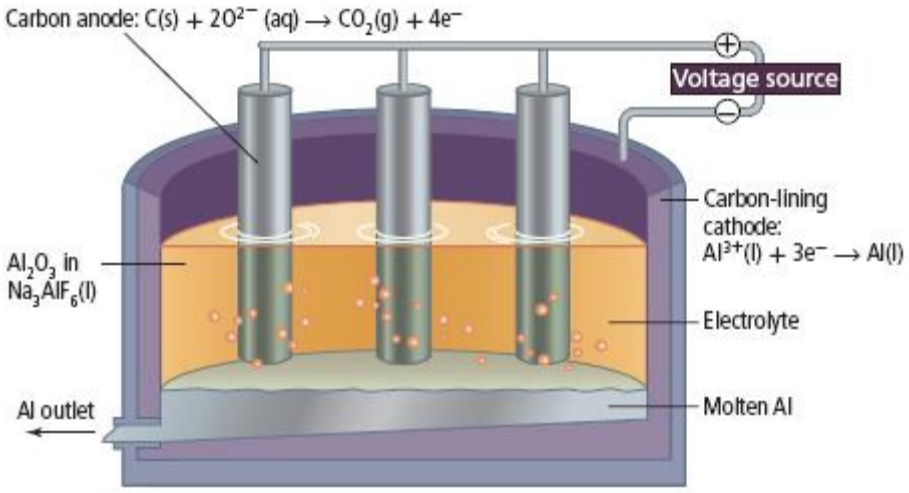

Figure 3.2: Hall–Héroult electrolytic cell (McGraw Hill Education, 2017).

Equation 3.2 shows Al^{3+} reduced to aluminium metal at the cathode.

$$AlF_6^{3-} + 3e^- \rightarrow Al + 6F^- \quad (3.2)$$

Carbon oxidation occurs at the anode as carbon interacts with oxygen, shown in Equations 3.3 to 3.4 (Haupin, 2009).

$$Al_2O_2F_4^{2-} + 2AlF_6^{3-} + C \rightarrow 4AlF_4^- + CO_2 + 4e^- \quad (3.3)$$

$$2Al_2OF_6^{2-} + 2AlF_6^{3-} + C \rightarrow 6AlF_4^- + CO_2 + 4e^- \quad (3.4)$$

$$C + 2O^{2-} - 4e^- \rightarrow CO_2 \quad (3.5)$$

During this process CO_2 and CO are the two main gases produced. However, CF_4 and C_2F_6 are also produced under certain conditions. Emissions of CF_4 and C_2F_6 during the primary aluminium smelting process can occur primarily during what is referred to as "anode effects" (Tabereaux, 1994). The term anode effect (AE) is used to describe a particular working state of the cell which is characterised by: a) high voltage, b) interruption of the aluminium production and c) production of the PFCs CF_4 and C_2F_6. This particular cell state (henceforth referred to as a high voltage anode effect (HVAE)) is usually triggered by a deficiency in the

alumina concentration (< 0.5-2 wt%) in the electrolyte bath as shown above (Figure 3.2). To restore normal cell operation and stop the emission of PFCs the alumina concentration must be restores to normal levels and the layers of gas must be removed (The Anode Effect - The Aluminum Smelting Process; Thonstad et al., 2001).

HVAE occur when alumina concentration is low and there is an insufficient supply of oxygen. For the current in the cell to be maintained the reactions shown in Equations 3.6 to 3.8 occur (Kjos et al., 2012). These reactions consume the electrolyte and allow for an accumulation of fluoride ions near the anode; the result of these reactions is PFC emission during these high voltage conditions of the cell.

$$2Na_3AlF_6 + Al_2O_3 + 3C \rightarrow 4Al + 6NaF + 3COF_2 \quad (3.6)$$

$$4Na_3AlF_6 + 3C \rightarrow 4Al + 12NaF + 3CF_4 \quad (3.7)$$

$$2Na_3AlF_6 + 2C \rightarrow 2Al + 6NaF + C_2F_6 \quad (3.8)$$

It was assumed that these reactions and subsequent PFC emissions would only occur when the cell was in that state and a specific indicator of that state was the operation voltage of the cell. Overall it was assumed that it was only once the cell exceeded the voltage of 8 V for more than 3 seconds it would enter that working state and therefore emit PFCs (Alton T Tabereaux, 1994; Thonstad et al., 2001; Tabereaux, 2004). However, threshold voltages used across the industry vary from 6 V to 10 V and from 1 to 90 seconds (Marks and Bayliss, 2012; Wong et al., 2014).

3.2.3 Industrial reporting of PFC emissions

In 1990, the IAI introduced a voluntary survey that enabled and allowed for the collection of information in order to calculate PFC emissions from AE. Prior to 1990, there were no consistent and official inventories for the aluminium industry. This survey is ongoing and is referred to as the Anode Effect Survey (AES) (‘Perfluorocarbon emissions reduction programme 1990-2000’, 2000; Results of the 2016 Anode Effect Survey Report on the Aluminium Industry’s Global Perfluorocarbon Gases Emissions, 2017; Results of the 2012 Anode Effect Survey Report on the Aluminium Industry’s Global Perfluorocarbon Gases Emissions Reduction Programme; International Aluminium Institute, 2009, 2011)The IAI members that participate in this voluntary effort report primary aluminium production, anode effect frequency, duration and overvoltage.

These reported parameters form the basis for AE performance statistics used in the global AI to account for total PFC emissions (IPCC, 2006). Overall, the IAI derives the PFC emissions by using the IPCC Guidelines for National Greenhouse Gas Inventories (Chapter 4: Metal Industry Emissions, 2006). According to these guidelines there are three different methods for estimating individual plant CF_4 and C_2F_6 emissions: Tier 1, Tier 2 and Tier 3 (IPCC, 2006; IPCC, 2019a). Tier 1 methods are applied to those smelters that do not participate in the AES and those smelters are referred to as 'non-reporting entities' and this method will be discussed below.

The methods Tier 2 and Tier 3 are based on facility-specific process data which are regularly collected as part of the voluntary, annual reports and are both based on the relationship between anode effect and cell performance; the smelters participating in the AES are referred to as 'reporting entities' (Marks, 2006; IAI, 2009, 2011). These methods use the slope and overvoltage coefficient equations (Equations 3.9 – 3.12). Throughout these methods, it is assumed that the same process mechanisms that produce CF_4 are similar for C_2F_6 and so the two gases are considered together.

The slope coefficient is a metric that estimates the mass of CF_4 emitted per tonne of aluminium produced taking into consideration the amount of time the cell was in an AE mode every day. It also includes the amperage and current efficiency as these are key factors that could affect the quantity of PFCs emitted. (IPCC, 2006).

$$E_{CF4} = S_{CF4} \times AEM \times MP \quad (3.9)$$

$$E_{C2F6} = E_{CF4} \times F_{C2F6/CF4} \quad (3.10)$$

Where:

E_{CF4} = CF_4 emissions from aluminium production

E_{C2F6} = C_2F_6 emissions from aluminium production

S_{CF4} = the slope coefficient for CF_4

AEM = the anode effect minutes per cell-day

MP = the metal production

$F_{C2F6/CF4}$ = the weight fraction of C_2F_6/CF_4

Another metric is what is referred to as the 'overvoltage' method. In this case what is

taken into consideration the voltage levels above the target operating voltage level of a cell. This extra cell voltage has been shown to be a good predictor of PFC emissions when recorded by the process control systems and forms the bases of the Anode Effect Overvoltage (AEO) statistic. AEO is calculated by summing how long the overvoltage lasted as well as its magnitude.

$$E_{CF4} = \text{OVC x AEO}/(\text{CE}/100) \text{ x MP} \quad (3.11)$$

$$E_{C2F6} = E_{CF4} \text{ x } F_{\frac{C2F6}{CF4}} \quad (3.12)$$

Where:

E_{CF4} = CF_4 emissions from aluminium production

E_{C2F6} = C_2F_6 emissions from aluminium production

OVC = the overvoltage coefficient for CF_4

AEO = the anode effect overvoltage

CE = the aluminium production process current efficiency expressed

MP = the metal production

$F_{C2F6/CF4}$ = the weight fraction of C_2F_6/CF_4

Both types of coefficients are based on direct measurements of PFCs at different sites. Tier 2 uses an average coefficient from measurements at numerous facilities while Tier 3 is based on measurements at the individual facility (IPCC, 2006). However, as discussed above, not every smelter participates in the voluntary survey. This chapter will refer to those smelters reporting their PFC emissions as ‘reporting entities’ and to the smelters that do not participate in this survey and therefore, do not report their emissions as ‘non-reporting entities’, as they are discussed in the literature.

In order to account for the PFC emissions related to the non-reporting entities, the IAI uses the Tier 1 method. The Tier 1 approach is an estimate of PFC emissions that uses activity data (aluminium production) and technology specific emission factors derived as a result of the Tier 2 and 3 facility specific information. The Tier 1 method can be applied according to Equations 3.13 and 3.14:

$$E_{CF4} = \sum_i (EF_{CF4} \times MP_i) \quad (3.13)$$

$$E_{C2F6} = \sum_i (EF_{C2F6} \times MP_i) \quad (3.14)$$

The cells used during the Hall–Héroult use different anodes and different methods to feed the alumina into the cell depending on the smelter. Depending on the type of anodes used and the method to feed alumina in the cell, cells can be broadly categorised under five different types: Bar Broken Centre Worked Prebake (CWPB), Point Feed Prebake (PFPB), Side Worked Prebake (SWPB), Vertical Stud Søderberg (VSS) and Horizontal Stud Søderberg (HSS) (Haupin, 2009). Each technology is linked with a different emission factor for Tiers 1, 2 and 3 as shown in Table 3.1 for CF_4 and Table 3.2 for C_2F_6. Also shown is the different percentage of uncertainty associated with each emission factor and technology.

Technology type	**Emission Factor by Technology Type (kg CF_4 / t Al)**	**Tier1 Uncertainty Range (%)**	**Tier2 (Slope) Uncertainty Range (%)**	**Tier2 (Overvoltage) Uncertainty Range (%)**	**Updated emission factors (including LVAE)**	**Uncertainty Range (%)**
CWPB	0.02	-99/+380	6	24	0.048	-93/+438
SWPB	0.278	-40/+150	15	43	0.391	-76/+116
PFPB	0.025	-99/+380	6	24	0.048	-93/+438
VSS	0.127	-70/+260	17	n/a	0.210	-95/+447
HSS	0.187	-80/+180	44	n/a	0.503	-79/+112

Table 3.1: CF_4 emission factors from the 2015 AES for the five different technology types of cells. N/a represent data that are not publicly available. Uncertainties associated with every Tier method as presented in the IPCC good practice guidelines 2006 (IPCC, 2006).

Technology type	Emission Factor by Technology (kg C_2F_6 / t Al)	Tier1 Uncertainty Range (%)	Tier2 (Slope) Uncertainty Range (%)	Tier2 (Overvoltage) Uncertainty Range (%)
CWPB	0.04	-99/+380	6	24
SWPB	0.4	-40/+150	15	43
PFPB	0.025	-99/+380	6	24
VSS	0.4	-70/+260	17	n/a
HSS	0.03	-80/+180	44	n/a

Table 3.2: C_2F_6 emission factors from the 2015 AES for the five different technology types of cells. N/a represent data that are not publicly available. Uncertainties associated with every Tier method as presented in the IPCC good practice guidelines 2006 (IPCC, 2006).

This description shows that the emission factor is a function of smelting technology and therefore the emission of PFCs is a function of the different types of technologies which leads to Equations 3.15 and 3.16.

$$EF_{PFC} \propto EF_{PFC}(\text{technology}) \quad (3.15)$$

$$E_{PFC} \propto E_{PFC}(\text{technology}) \quad (3.16)$$

Furthermore, a key factor of uncertainty is whether the smelter takes part in the voluntary survey launched by the IAI (reporting entity), and therefore has PFC emissions that were estimated using facility specific data or whether it is a non-reporting entity whose PFC emissions were estimated using the Tier 1 method.

In addition to the anode effects (and their different threshold voltages) where PFC emission has been observed, recent work shows that PFCs can be emitted from a cell during normal operation as well.

It is reported that this phenomenon was first recorded by the late Warren Haupin of Alcoa in an internal Alcoa report in 1995 (Thonstad and Rolseth, 2017). Now, several studies verify the discovery of PFC emissions in absence of any detected or officially declared AEs

(Al Zarouni and Al Zarouni, 2011; Li et al., 2011; Marks and Bayliss, 2012; Wangxing et al., 2012; Wong et al., 2014, 2015; Thonstad and Rolseth, 2017). According to these studies the PFCs generated in such scenarios are not declared by smelter control systems as "anode effects" as they are either:

- Low voltage effects with PFC emission signatures similar to conventional AEs but with overall peak cell voltages under the threshold cell voltage (e.g. <8 V) that controls the systems (Wong et al., 2014).
- Continuous background emissions of PFCs that do not have the same discrete voltage and emission characteristics as conventional (>8V) and low-voltage (<8 v) AEs (Wong et al., 2014).

The IAI uses the terms "high voltage anode effects" (HVAE) to describe PFC emission during the state of a cell into overvoltage and "low voltage anode effects" (LVAE) to describe PFC emission during normal operation of the cell (Marks and Nunez, 2018).

Therefore, as the emission factor is now a function of both the LVAE and HAVE Equation 3.15 becomes:

$$\mathrm{EF_{PFC}} \propto \mathrm{EF_{PFC}}\,(\mathrm{LVAE}, \mathrm{HVAE}) \qquad (3.17)$$

the emission of PFCs becomes a function of both the LVAE and the HAVE (Equation 3.18):

$$\mathrm{E_{PFC}} \propto \mathrm{E_{PFC}}(\mathrm{LVAE}, \mathrm{HVAE}) \qquad (3.18)$$

And combined with Equations 3.1, 3.15, 3.16, 3.17, 3.18:

$$\mathrm{E_{PFC}} \propto \mathrm{E_{PFC}}\,(\mathrm{MP}, \mathrm{LVAE}, \mathrm{HVAE}, \mathrm{technology}) \qquad (3.19)$$

Equation 3.19 will be used to interpret and discuss the results and PFC emissions in the conclusion section 3.5 and in conclusions chapter 7.

It must be noted at this point that, as demonstrated in Tables 3.1 and 3.2 and as shown in Figure 3.3 in section 3.4.1, while the contribution to CF_4 emissions from LVAE could be substantial based on updated emission factors (Marks and Nunez, 2018) this is likely not the case for C_2F_6 with LVAE emissions reported below detection levels and is only detected during HVAE (Åsheim et al., 2014; Dion et al., 2016; Dion, Gaboury, et al., 2018; Dion, Nunez, et al., 2018). As PFC emissions from HVAE decrease (Figures 3.3 - 3.4 in section 3.4.1), more research is carried out on emissions during normal function of the cells.

Several methods that could help minimise PFC emissions from the AI are being investigated, such as, the use of an inert anodes that could eliminate PFC emissions. Currently, RUSAL is investigating inert anodes and reports published by the Russian smelters state that

the inert anode technology would be ready for extensive use in 2012 (Rusal targets 2021 to roll out carbon-free aluminium | Financial Times, 2019; Research and technological development, RUSAL, 2015). There is currently no standardised method to predict the optimum feed rate and amount of alumina as alumina itself varies in properties much like each cell's properties also vary. This means that aluminium production facilities are currently unable to completely eradicate local or full cell anode events while significant improvements in technology have been made and a substantial decrease in PFC emissions has been noted.

3.3 Methods

3.3.1 Limitations and challenges in producing a bottom-up inventory

The main limitation of this study relates to the lack of publicly available smelter specific data. Activity data that provide facility specific information regarding annual aluminium production are, in most cases, commercially sensitive, incomplete or unavailable in the public domain. Equally, in order to compile a bottom-up inventory that will also be used for modelling purposes the location of the smelters was required (Michalopoulou, 2018). However, information regarding the locations of smelters, is in some cases extremely difficult to find.

Additionally, for the inventory compiler who does not have access to the information necessary to reproduce a Tier 2 or Tier 3 method, the uncertainty is significant as the only method that the IPCC Good Practice Guidelines advise to use is the Tier 1 (IPCC, 2006). This is a limitation that could not be resolved for the time being. This chapter uses data available from the IAI (World Aluminium — The Institute) and it will present PFC emissions and their uncertainties in the results sections.

Originally, this work set out to collect facility specific activity data (such as aluminium production per year, changes in technology and potlines over time) as well as locate the coordinates of aluminium smelters (Michalopoulou, 2018). In some cases, this endeavour was successful, and a database with this information has been complied, but due to the limitations and uncertainties described in this section this chapter does not use information from this database. However, this database can be made available upon request.

3.3.2 Methods to estimate PFC emissions

As described in section 3.2, since 1990, the IAI has collected industrial activity data though an annual voluntary survey program, the AES, and the data collected during this survey form the basis for AE performance statistics used in the global AI to estimate total PFC emissions (IAI, 1990). According to the IPCC guidelines there are three different methods for estimating individual plant CF_4 emissions: Tier 1, Tier 2 and Tier 3. These three calculations suggested by the IPCC come with different uncertainties (IPCC, 2006). Tables 3.1 and 3.2 present the uncertainties associated with every Tier and type of technology. As discussed, the smelters that participate in the AES collect facility specific information on specific parameters and then use the Tier 2 or Tier 3 method to calculate CF_4 emissions. The IAI uses the PFC estimates calculated by the reporting entities to derive a median emission factor that they then apply to the non-reporting entities using the T1 methodology (IAI, 2014). The alumina reduction cells, and in general, the aluminium smelters, can be divided into two categories depending on how their anodic system is arranged: the pre-bake cell and the Søderberg cell.

To estimate global CF_4 and C_2F_6 emissions from aluminium production in this study, aluminium production data, median emission factors, CF_4 and C_2F_6 emissions and uncertainties reported in the IAI surveys from 1990 to 2017 (IAI, 2017) were combined with newly published information on CF_4 and C_2F_6 emissions from LVAE (Marks and Nunez, 2018), as well as the good practice guide presented in IPCC (2006). Uncertainties used throughout this chapter are discussed and presented in Tables 3.1 and 3.2.

Different emission factors (Kg of PFCs per tonne of Al produced) were used as suggested by the IAI, to calculate CF_4 (Table 3.3) and C_2F_6 (Table 3.4) emissions from each technology (International Aluminium Institute: The International Aluminium Institute Report On The Aluminium Industry's Global Perfluorocarbon Gas Emissions Reduction Programme,1990, 2006, 2008; Results of the 2017 Anode Effect Survey Report on the Aluminium Industry's Global Perfluorocarbon Gases Emissions, 2018; Results of the Anode Effect Survey Report on the Aluminium Industry's Global Perfluorocarbon Gases Emissions Reduction Programme, International Aluminium Institute, 2000, 2001, 2002, 2003, 2004, 2005, 2006, 2007, 2008, 2009,, 2010, 2011, 2012, 2013, 2014, 2015, 2016, 2017, 2018; IAI, 2011; Gases and Reduction, 2013, Marks and Nunez, 2018).

Four equations are used to produce four estimates of CF_4 and C_2F_6 emissions respectively.

Global emissions specific to HVAE are estimated using Equation 3.20:

$$\mathrm{EGlobal_i(t)} = \mathrm{Global\ AP(t)} \times \mathrm{EF_{HVAE,i}(t)} \qquad (3.20)$$

Where

$EGlobal_i(t)$ = Global emissions of gas i (CF_4 and C_2F_6) over time

Global AP(t) = Global aluminium production as estimated from the IAI over time

$EF_i(t)$ = Year specific emission factors for each PFC studied (CF_4 and C_2F_6) over time

Emission factor specific uncertainties were used as described in Tables 3.1 and 3.2.

Global emissions including both HVAE and LVAE are estimated using Equation 3.21:

$$\mathrm{EGlobal_i(t)} = \mathrm{Global\ AP(t)} \times \mathrm{EF_{HVAE,LVAE,i}(t)} \qquad (3.21)$$

Where

$EGlobal_i(t)$ = Global emissions of gas i (CF_4 and C_2F_6) over time

Global AP(t) = Global aluminium production over time

$EF_i(t)$ = Year specific emission factor for each PFC studied (CF_4 and C_2F_6) over time

Emission factor specific uncertainties were used as described in Tables 3.1 and 3.2.

Chinese emissions are estimated using China specific aluminium production values and China specific emission factors through Equation 3.22:

$$\mathrm{EChina_i(t)} = \mathrm{Chinese\ AP(t)} \times \mathrm{EF_{China,i}(t)} \qquad (3.22)$$

Where

$EChina_i(t)$ = Chinese emissions of gas i (CF_4 and C_2F_6) over time

Chinese AP(t) = Chinese aluminium production over time

$EF_{China,i}(t)$= Year specific emission factors specific to each PFC studied (CF_4 and C_2F_6) over time

Emission factor specific uncertainties were used as described in Tables 3.1 and 3.2.

ROW emissions are estimated using ROW specific aluminium production values and ROW specific emission factors through Equation 3.23:

$$\mathrm{EROW_i(t)} = \mathrm{ROWAP(t)} \times \mathrm{EF_{ROW,i}(t)} \qquad (3.23)$$

Where

$EROW_i(t)$ = ROW emissions of gas i (CF_4 and C_2F_6) over time

ROW AP(t) = ROW aluminium production over time

$EF_{ROW,i}$ (t)= Year specific emission factors specific to each PFC studied (CF_4 and C_2F_6) over time.

Emission factor specific uncertainties were used as described in Tables 3.1 and 3.2.

CF_4	Emission factors per technology type over time (EF in kg CF_4/ t Al)					
Year	**CWPB**	**PFPB (ROW)**	**PFPB (China)**	**SWPB**	**VSS**	**HSS**
1990	0.36	0.37	n/a	1.88	0.7	0.38
1991	0.28	n/a	n/a	1.6	0.57	0.42
1992	0.28	n/a	n/a	1.71	0.54	0.4
1993	0.22	n/a	n/a	1.61	0.56	0.39
1994	0.18	n/a	n/a	1.34	0.49	0.41
1995	0.16	0.12	0.09	1.34	0.48	0.43
1996	0.16	n/a	n/a	1.58	0.48	0.47
1997	0.15	n/a	n/a	1.34	0.45	0.46
1998	0.24	0.13	0.1	1.45	0.37	0.57
1999	0.24	0.11	0.09	1.37	0.37	0.49
2000	0.21	0.11	0.1	1.06	0.36	0.51
2001	0.09	0.08	0.1	1.12	0.37	0.24
2002	0.15	0.07	0.1	1.27	0.33	0.21
2003	0.1	0.06	0.1	0.94	0.29	0.17
2004	0.06	0.04	0.1	1.39	0.23	0.7
2005	0.06	0.03	0.1	0.92	0.16	0.68
2006	0.09	0.04	0.1	0.81	0.22	0.22
2007	0.1	0.04	0.09	0.78	0.19	0.21
2008	0.12	0.04	0.1	0.6	0.18	0.19
2009	0.08	0.03	0.09	0.5	0.14	0.18
2010	0.08	0.37	0.1	0.51	0.14	0.15
2011	0.08	0.03	0.1	0.51	0.15	0.22
2012	0.02	0.03	0.09	0.43	0.14	0.24
2013	0.02	0.02	0.1	0.36	0.15	0.28
2014	0.02	0.02	0.1	0.47	0.13	0.33
2015	0.01	0.02	0.1	0.31	0.19	0.15
2016	0.01	0.02	0.1	0.31	0.16	0.15
2017	0.01	0.01	0.1	0.25	0.1	0.13
2018*	0.04	0.04	0.16	0.4	0.5	0.2

Table 3.3: CF_4 emission factors (in kg of CF_4/ t of Al) for the years 1990 to 2018 and the five different cell technology types. N/a represents not publicly available data. Note: The years 1990 - 2017 are only demonstrating emission factors related to HVAE and not LVAE. Only 2018 is showing emission factors including HVAE and LVAE.

C_2F_6	Emission factors per technology type over time (EF in Kg C_2F_6/ t Al)					
Year	**CWPB**	**PFPB (ROW)**	**PFPB (China)**	**SWPB**	**VSS**	**HSS**
1990	0.05	0.05	0.00	0.13	0.02	0.05
1991	n/a	n/a	n/a	n/a	n/a	n/a
1992	n/a	n/a	n/a	n/a	n/a	n/a
1993	n/a	n/a	n/a	n/a	n/a	n/a
1994	n/a	n/a	n/a	n/a	n/a	n/a
1995	0.03	0.01	0.00	0.4	0.03	0.02
1996	n/a	n/a	n/a	n/a	n/a	n/a
1997	n/a	n/a	n/a	n/a	n/a	n/a
1998	0.02	0.01	0.004	0.42	0.02	0.02
1999	0.02	0.01	0.004	0.39	0.02	0.02
2000	0.02	0.01	0.004	0.10	0.01	0.05
2001	0.02	0.01	0.004	0.10	0.01	0.05
2002	0.01	0.009	0.004	0.32	0.01	0.01
2003	0.01	0.008	0.004	0.23	0.01	0.01
2004	0.01	0.007	0.004	0.29	0.01	0.01
2005	0.009	0.007	0.004	0.21	0.01	0.01
2006	0.01	0.005	0.004	0.19	0.01	0.01
2007	0.01	0.005	0.004	0.18	0.01	0.01
2008	0.02	0.004	0.004	0.13	0.01	0.01
2009	0.01	0.004	0.004	0.12	0.008	0.01
2010	0.01	0.004	0.004	0.12	0.009	0.01
2011	0.01	0.003	0.004	0.12	0.01	0.01
2012	0.003	0.003	0.004	0.10	0.008	0.02
2013	0.002	0.003	0.004	0.08	0.008	0.02
2014	0.002	0.003	0.004	0.11	0.01	0.02
2015	0.001	0.003	0.004	0.08	0.007	0.01
2016	0.001	0.002	0.004	0.09	0.008	0.01
2017	0.002	0.001	0.004	0.08	0.006	0.01
2018	0.002	0.001	0.004	0.08	0.006	0.01

Table 3.4: C_2F_6 emission factors (in kg of CF_4/ t of Al) for the years 1990 to 2018 from the five different cell technology types. N/a represents not publicly available data. Note: For C_2F_6 no contribution from LVAE is considered.

By using existing data and newly published information (International Aluminium Institute: The International Aluminium Institute Report On The Aluminium Industry's Global Perfluorocarbon Gas Emissions Reduction Programme,1990, 2006, 2008; Results of the 2017 Anode Effect Survey Report on the Aluminium Industry's Global Perfluorocarbon Gases Emissions, 2018; Results of the Anode Effect Survey Report on the Aluminium Industry's Global Perfluorocarbon Gases Emissions Reduction Programme, International Aluminium Institute, 2000, 2001, 2002, 2003, 2004, 2005, 2006, 2007, 2008, 2009,, 2010, 2011, 2012, 2013, 2014, 2015, 2016, 2017, 2018; IAI, 2011; Gases and Reduction, 2013, Marks and Nunez, 2018; IPCC, 2006, Dion et al, 2016; Dion, Gaboury, et al., 2018; Dion, Nunez, et al., 2018) the updated global aluminium production and global PFC emissions in different scenarios are presented. The different uncertainties between reporting and non-reporting entities and how those impact the quantification and subsequent interpretation of PFC emissions are also shown and discussed.

3.3.3 Method to produce industry specific spatial distribution of emissions

To produce the map demonstrating the current spatial distribution of the AI previously collected information (personal communication with Jens Mühle, personal communication with industrial representatives) and unstructured web data mining were used. Web data mining was very labour intensive and time consuming, and it was mostly successful for smelters located in developed countries where facility specific information was available on the internet and mostly unsuccessful in developing countries where there was either a complete lack of information, the information available was incomplete or the quality and/or correctness of the information could not be verified (Madria et al., 1999; Feldman and Sanger, 2007; Aggarwal and Zhai, 2012).

3.4 Results and discussion

Globally, aluminium productions fluctuate (Figure 3.3) and a major driver of that are the global and local economies. Significant drops in production are due to global economic crises like the 2008-2009 when global production dropped from 3466 kt to 2833 kt. Overall, global production has increased from 1,000 kt in 1973 to 5,000 kt in 2018 (Facing new crisis,

can aluminum industry learn from past crisis? Andy Home - Reuters, 2016; What Caused the Aluminum Industry's Crisis?, 2013; Nappi, 2013; Central Bank, 2017).

With the latest significant change being the shift of production from Rest of the World (ROW) countries (IAI, 2014) to China emissions from ROW and China are presented separately (Figure 3.3) especially as China's share of global aluminium production is increasing (IAI, 2017). In 2018 the Chinese production was estimated to be 3120 kt representing more than 50% of the global production for 2018. Chinese production was zero from 1990 until 1998, then rising linearly from194 kt in 1999 to 1208 kt in 2008 before it dropped to 929 kt in 2009.

Global aluminium production (Figure 3.3) is shown for the period between 1990 and 2017 using updated data from the IAI (IAI, 2017).

Figure 3.3: The primary aluminium production (in kt) from China (blue) and the countries referred to collectively as ROW (orange) countries. The total global (grey) primary aluminium production is also presented (IAI, 2017).

Changes in the geographical distribution of the smelters are often associated with uses of different smelting technologies from one country to another, or even within the same country and, as shown in Table 3.3 and 3.4, this can result in different emissions factors. Additionally,

smelting capacity can greatly vary from one smelter to another. These differences can cause fluctuations both in the aluminium production and/or CF_4 emissions. Figure 3.3 demonstrates the geographical shift of aluminium production to China. In 2000, ROW aluminium production was ~2000 kt of primary aluminium while China produced ~200 kt of aluminium. In 2013, ROW countries and China produced approximately the same amount of aluminium, ~2150 kt and in 2017 China produced ~3200 kt of aluminium while ROW countries produced ~2200 kt.

The AES generates data from approximately 200 reporting entities (smelters and potlines) representing ~2100 kt of primary aluminium production (IAI, 2016). It should be highlighted that China largely does not participate in this survey.

3.4.1 CF_4

Using Equations 3.20 – 3.23, Table 3.3 and the aluminium production presented in Figure 3.3, CF_4 estimates are presented. Figure 3.4 shows four different estimates of CF_4 emissions for ROW related production, China specific production and the overall contribution from HVAE and LVAE (Equations 3.20 – 3.23).

Previous estimates did not include the contribution from LVAE effects but recent published work (Marks and Nunez, 2018) presents new emission factors that include the emissions contribution from both HVAE and LVAE as well as new, China specific emission factors.

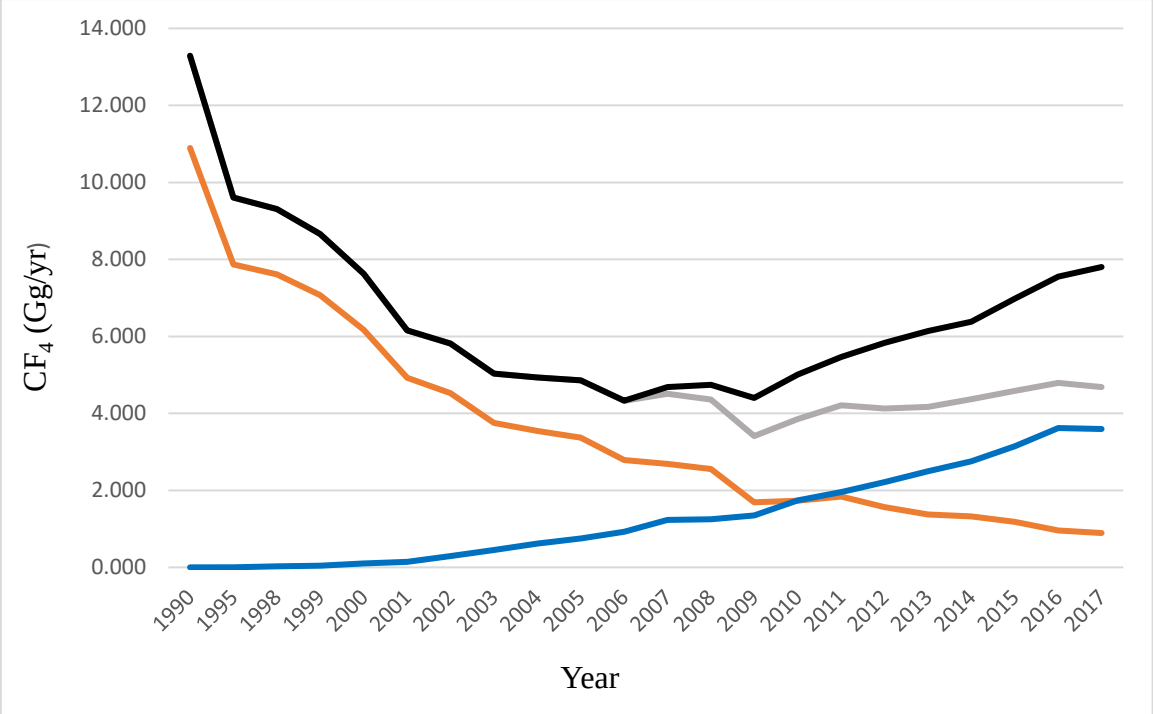

Figure 3.4: CF_4 emissions (Gg/yr) coming from the countries defined as ROW countries (orange), China (blue) and the global total of CF_4 emissions (grey) using previous emission factors and the emissions estimates using the newly updated emission factors that include HVAE and LVAE (black).

CF_4 emissions of ~13 Gg/yr are estimated for the year 1990. There is no estimate of the CF_4 emissions for the years prior to 1990 as discussed in section 3.1. During the years 1990 to 2000 China was a minor contributor of CF_4 as their primary aluminium production was still in early stages. However, Figure 3.4 does show a discrepancy between ROW and global estimates. This could indicate that there was some production in China earlier than 1990 as some reports show but no data regarding these production numbers are available (Hunt, 2004; Nappi, 2013).

Additionally, the contribution from LVAE is assumed to be a minimum as it is only the more modern (post 1995) smelters that are suspected to be contributing to the LVAE emissions as these smelters are driven by higher amperage and larger anodes (Marks and Nunez, 2018; IPCC, 2019a). Due to consistent efforts from the AI and subsequent implementation of the Kyoto protocol emissions from the ROW countries, CF_4 emissions have significantly decreased in the last 27 years from ~11 Gg/yr in 1990, to ~2 Gg/yr in 2009 and <1 Gg/yr in 2016. However, the China specific emissions of CF_4 have been increasing over time, matching the increase in their production and expansion of smelters.

While the overall emissions coming from the aluminium industry and the ROW smelters have been significantly reduced especially for the period 2010-2015, this has been offset by emissions from the Chinese facilities that seem to be a major driver of the CF_4 trend for the period of 2010-2015. Measurements in China are limited and there is very large uncertainty associated with those measurements.

Emission estimates that include both HVAE and LVAE seem to increase the post 2006 estimates significantly (from ~4.6 Gg to ~8 Gg in 2017) when compared with those that include HVAE only.

Figures 3.5 and 3.6 show the different uncertainties related to the CF_4 emissions from the reporting and non-reporting entities. The emissions of CF_4 related to the reporting entities have been steadily decreasing from 8 Gg/yr in 1990 to 1.5 Gg/yr in 2015. A similar decrease is noted regarding the uncertainties related to these CF_4 emissions, meaning that for those smelters that do participate in the AES there is a high level of accuracy related to the CF_4 emissions. Between 1990 and 2000, the uncertainties and CF_4 emissions presented in Figure 3.6 are associated with those ROW smelters that did not participate in the AES; China's aluminium production only starts to reach significant numbers after 2000. After 2000, Chinese smelters are broadly not participating in the AES. However, as their production increases so do the uncertainties related to the PFC emitting non-reporting entities which are particularly significant after 2010. CF_4 emissions from this industry currently appear to be returning to pre-2000 levels with an approximate estimate of 4 Gg/yr in 2016.

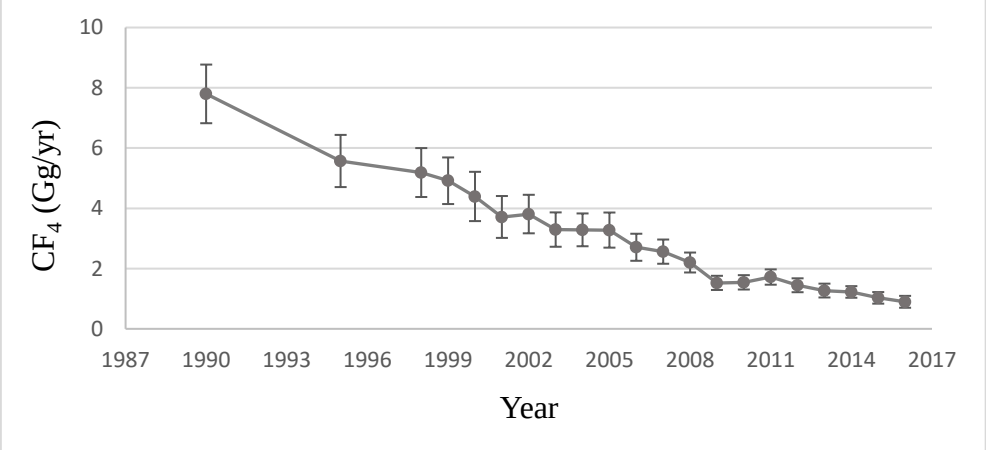

Figure 3.5: CF_4 emissions (Gg/yr) and uncertainties associated with reporting entities participating to the IAI through the AES.

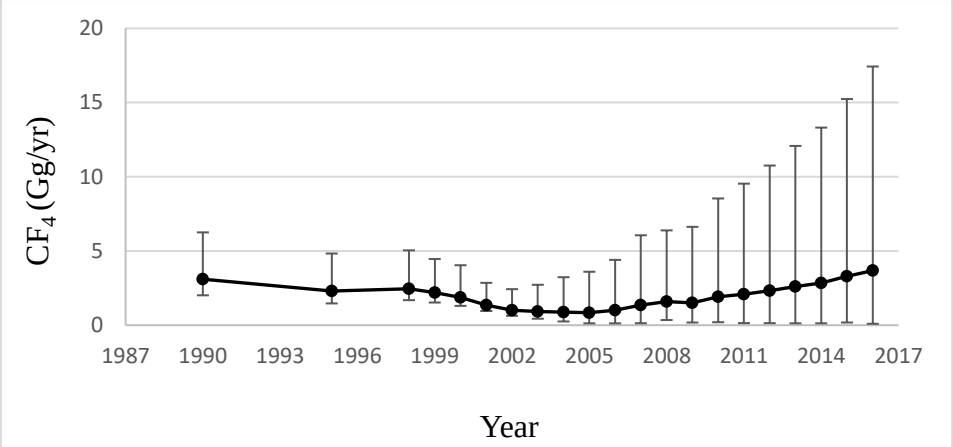

Figure 3.6: CF_4 emissions (Gg/yr) and uncertainties of the non-reporting entities.

Figure 3.7 shows the CF_4 emissions associated with the global aluminium industry and their uncertainties. The uncertainties associated with the emissions are mostly related to the non-reporting entities. Between 1990 and 2000 a decrease in CF_4 emissions from approximately 11 Gg/yr to 6 Gg/yr is observed. Equally there is an equivalent decrease in the uncertainties as during this time the smelters that participated in the survey increased. After 2000 both the emissions and the uncertainties appear to be increasing with the increase of the uncertainties being very noticeable especially for the years after 2009. This is attributed to the very significant increase in Chinese aluminium production and therefore emissions coming from the Chinese smelters.

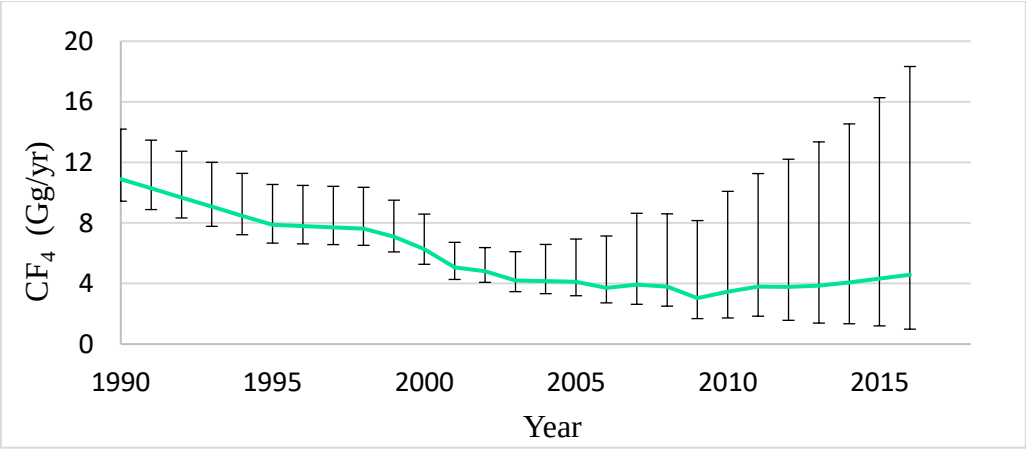

Figure 3.7: Global (reporting and non-reporting) entities CF_4 emissions (Gg/yr) from the aluminium industry and their associated uncertainties.

	CF_4 emissions (Gg/yr)			
Year	**Global (HVAE only)**	**ROW**	**China**	**Global (HVAE, LVAE)**
1990	13.29	10.89	0.00	13.29
1995	9.60	7.86	0.00	9.60
1998	9.31	7.61	0.02	9.31
1999	8.66	7.06	0.04	8.66

Table 3.5: Summary of CF_4 (Gg/yr) emissions from the countries defined as ROW countries, China and the global total of CF_4 emissions using HVAE and LVAE factors.

Overall, as demonstrated in Table 3.5 emissions from the countries under the ROW classification have been steadily decreasing from ~11 Gg/yr in 1990 to 0.93 Gg/yr in 2018. However, this decrease in CF_4 emissions has been offset by emissions coming from the Chinese smelters where CF_4 estimates where 0 in 1990 and increased to 3.7 Gg/yr in 2018. An emission estimate of the order of 3.7 Gg/yr for China means that Chinese aluminium production contributed approximately 78% in the global CF_4 emissions. Additionally, while global estimates using HVAE specific emissions factors show a decrease in emissions from 13.29 Gg/yr in 1990 to 4.71 Gg/yr in 2018, global estimates using HVAE and LVAE emission factors (post - 2006) show global estimates of 7.98 Gg/yr for 2018, a discrepancy of approximately 3.2 Gg/y.

3.4.2 C_2F_6

Using Equations 3.20 – 3.23, Table 3.4 and the aluminium production presented in Figure 3.3, C_2F_6 estimates are presented.

Despite CF_4 and C_2F_6 being emitted from the same processes during primary aluminium smelting (Equations 3.7 and 3.8), newly published work demonstrates that in the case of LVAE, C_2F_6 behaves differently as in most cases it is below the detectable level and therefore, no new emission factor to include emissions from LVAE has been allocated to them (Dion et al., 2016; Dion, Gaboury, et al., 2018; Dion, Nunez, et al., 2018). For this reason, C_2F_6 is considered separately. C_2F_6 emissions coming from the countries defined as ROW countries, China and the global total of C_2F_6 emissions are presented (Figure 3.8).

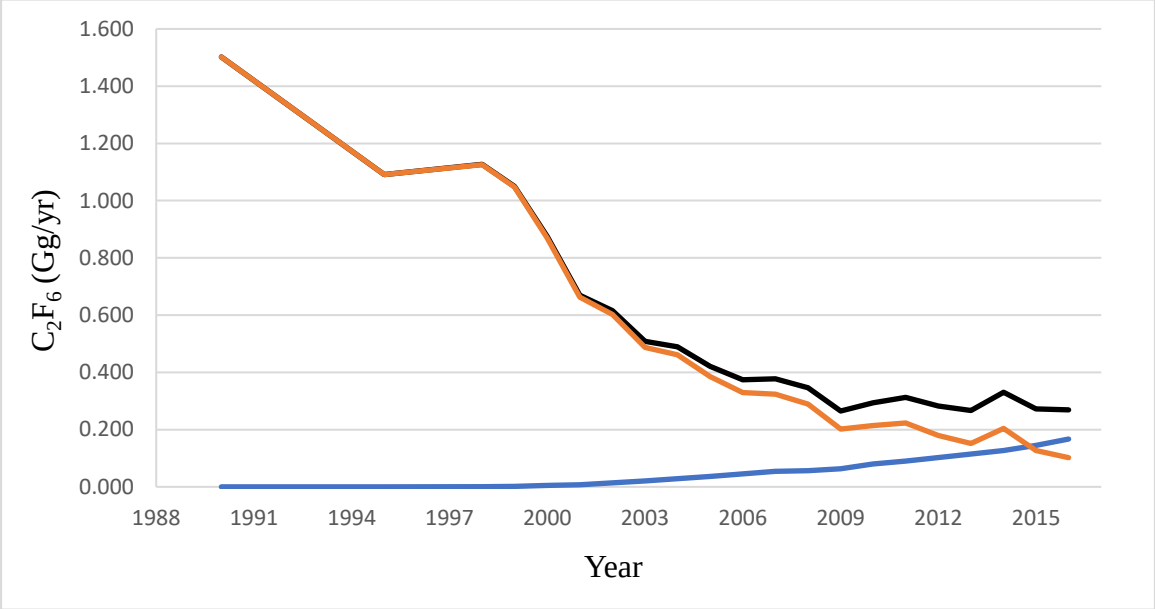

Figure 3.8: C_2F_6 emissions coming from the countries defined as ROW countries (orange), China (blue) and the global total of C_2F_6 emissions (black).

Figure 3.8 shown global, ROW and Chinese C_2F_6 emissions estimates. In 1990, ROW emissions are estimated at ~1.5 Gg/yr which decrease to ~0.2 Gg/yr in 2010. During 2010-2014 C_2F_6 emissions from ROW countries have remained relatively stable at the same levels as 2010 and in 2017 a further decreased estimate of ~0.1 Gg/yr is estimated. PFC estimates from the Chinese primary aluminium production are zero (or negligible) for the years 1990 – 2000. After 2003 Chinese emissions increase from ~0.02 in 2003 to ~0.16 in 2017. As discussed, currently the assumption is that LVAE either do not emit C_2F_6 or that the concentrations emitted are below the detectable level. Therefore, only HVAE estimates have been produced for the case of C_2F_6. Figures 3.9 and 3.10 demonstrate the uncertainty associated with C_2F_6 emissions coming from reporting and non-reporting entities. Much like CF_4, it is also

the case for C_2F_6 that global estimates are made more uncertain by those countries that do not participate in the AES (Figures 3.9, 3.10, 3.11).

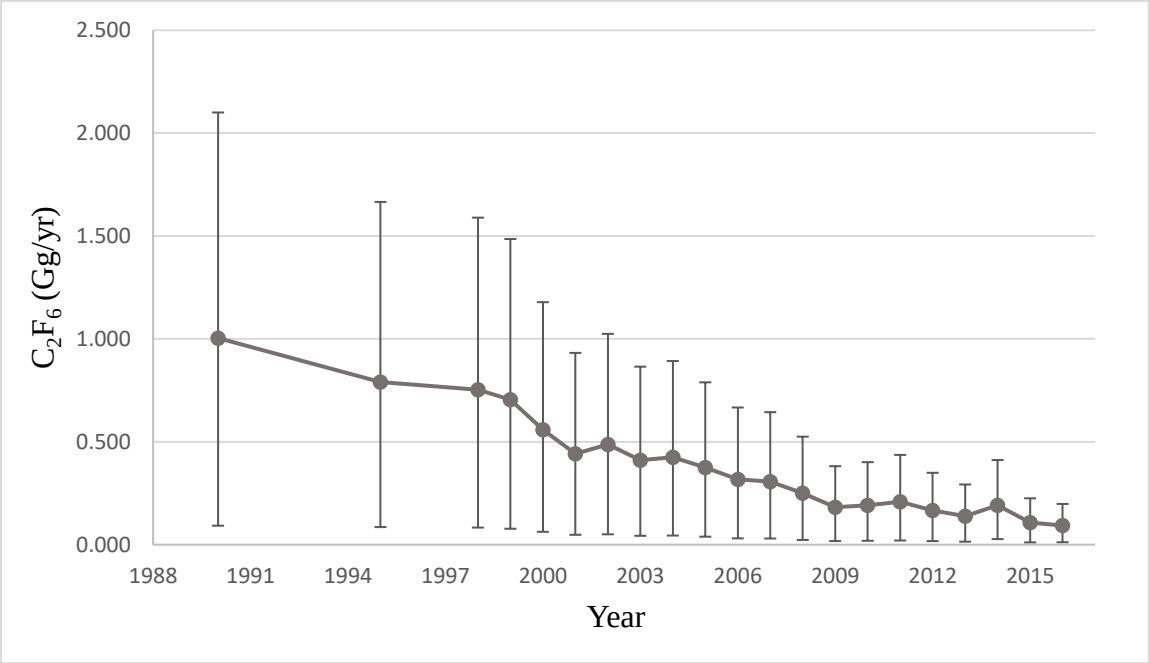

Figure 3.9: C_2F_6 emissions and uncertainties associated with reporting entities participating to the IAI through the AES.

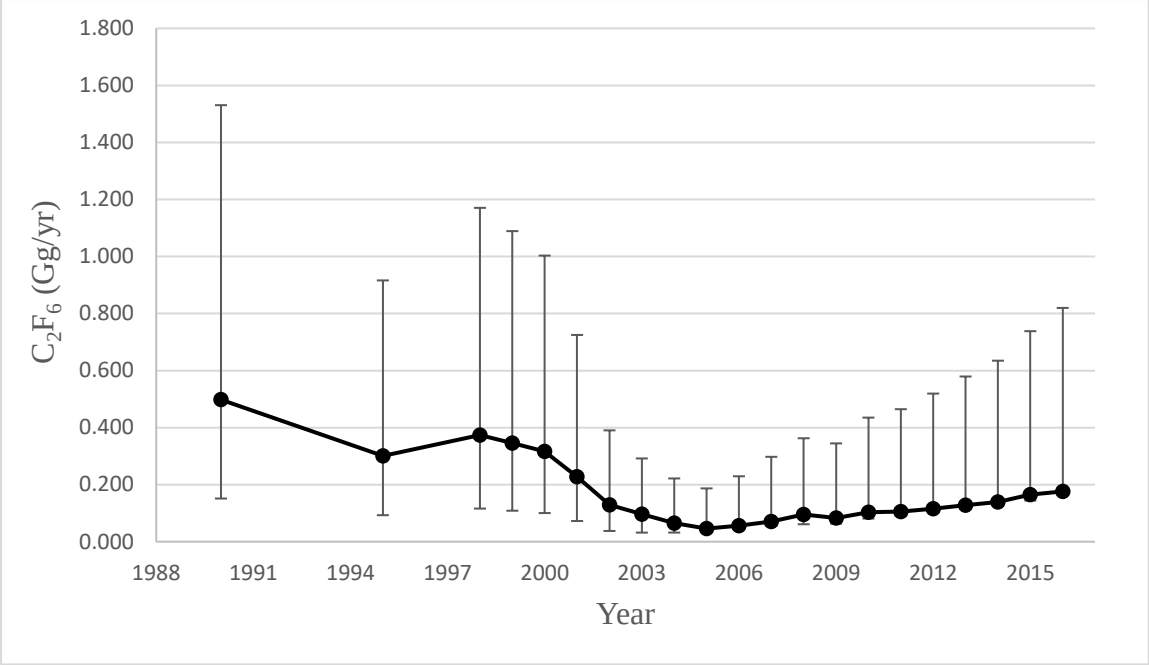

Figure 3.10: C_2F_6 emissions and uncertainties associated only with non-reporting entities.

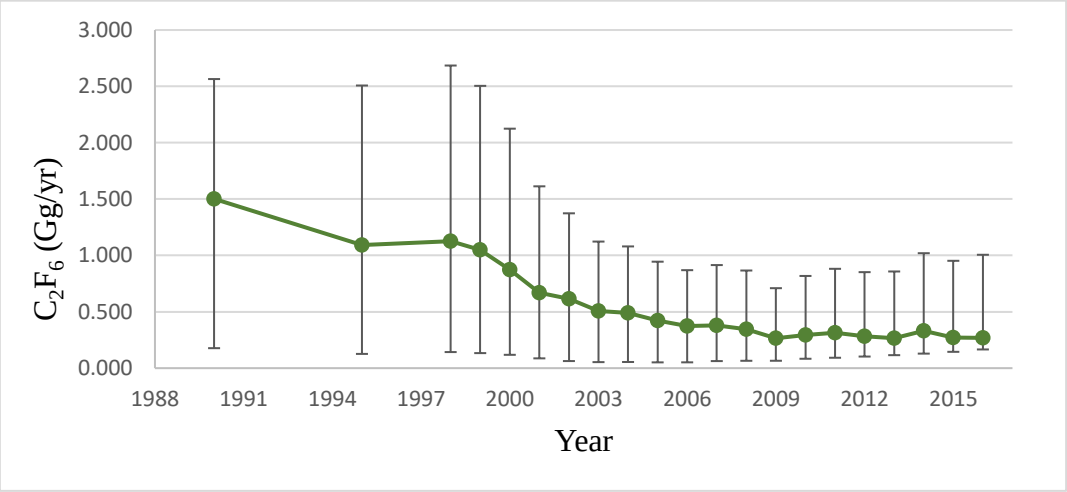

Figure 3.11: Global (reporting and non-reporting) C_2F_6 emissions from the aluminium industry and their associated uncertainties.

As demonstrated for CF_4, C_2F_6 emissions are following a similar trend. While ROW countries have decreased emissions from ~1.5 Gg/yr in 1990 to 0.17 Gg in 2018, emissions from China have been increasing from approximately 0 in 1990 to approximately 0.3 Gg in 2018. Overall, the results of the bottom-up estimates for C_2F_6 are summarized in Table 3.6:

	C_2F_6 emissions (Gg/yr)		
Year	**Global**	**ROW**	**China**
1990	1.50	1.50	0
1995	1.09	1.09	0
1998	1.12	1.12	0.001
1999	1.05	1.04	0.002
2000	0.87	0.87	0.005

Table 3.6: Summary of C_2F_6 (Gg/yr) emissions from the countries defined as ROW countries, China and the global total of CF_6 emissions using HVAE factors.

3.4.3 Spatial Distribution

Using the methods described in section 3.3 the locations of the aluminium smelters globally are presented (Figure 3.12).

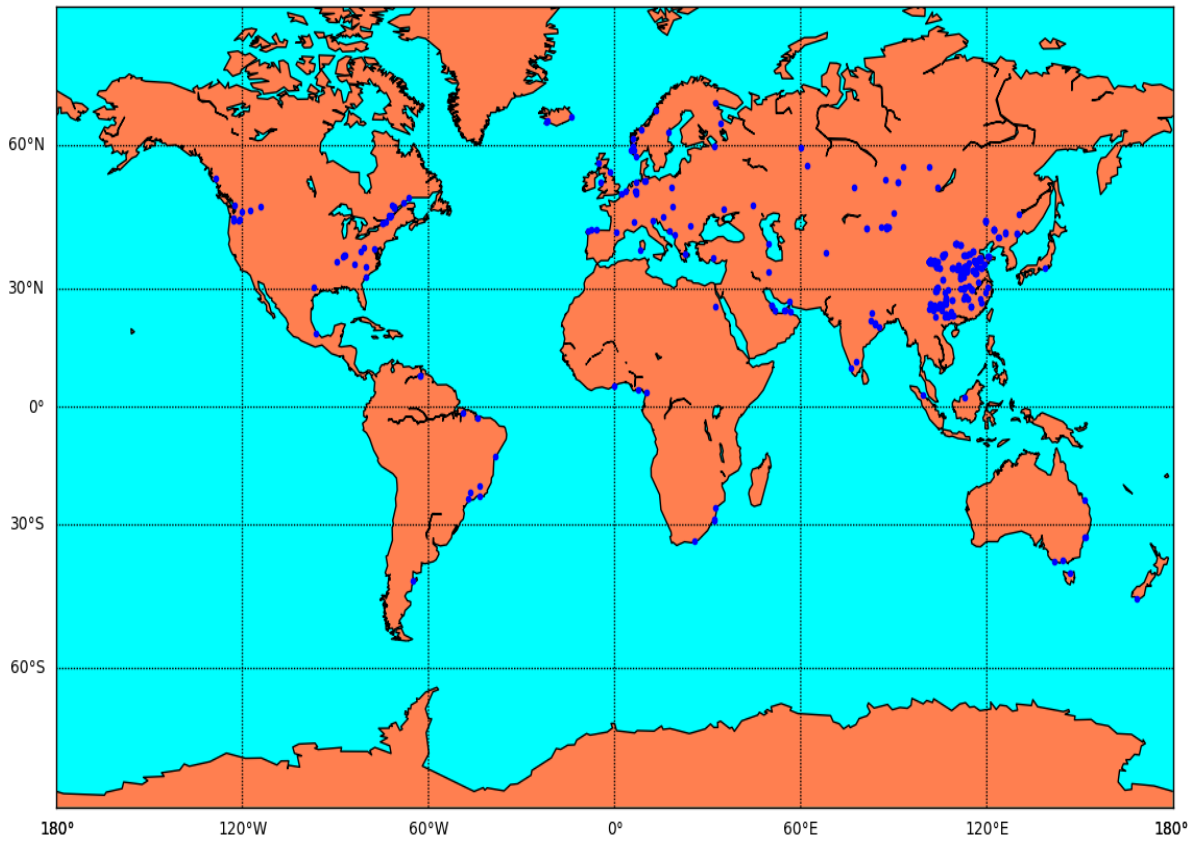

Figure 3.12: Locations of aluminium smelters globally (black dots) in 2019.

To my knowledge this is the most complete and up-to-date list of the geographical distribution of aluminium smelters. The most interesting location is China, where more than 200 hundred smelters have been found. Of particular interest are the smelters on the North East coast of China and the Northeast province of China specifically close to the North Korean borders. These locations will be used further in the discussions of the modelling chapter (Chapter 6).

3.5 Conclusion

New estimates for global CF_4 and C_2F_6 emissions from the AI have been presented. As demonstrated by Equation 3.19 in section 3.1, PFC emissions are a function of several parameters, namely annual metal production, LVAE, HVAE and technology (expressed through the different emission factors for CWPB, PFPB, SWPB, VSS and HSS technologies). Table 3.7 summarizes these emissions estimates over specific timeframes and the contribution of the parameters is presented.

For the years 1990 - 1995 both for CF_4 and C_2F_6, the main contributor of PFC emissions were the ROW countries and HVAE, as neither China had started production at a significant scale, nor was there contribution from LVAE. Time averaged CF_4 emissions estimates for this period ~1.4 Gg/yr and for C_2F_6 ~ 1.7 Gg/yr.

For the years 1995 – 2000 PFC emissions are as described above, however while there is indication that the China specific values are not zero, there is not enough information in the literature to quantify these emissions. Time averaged CF_4 emissions estimates for this period are ~7.85 Gg/yr and for C_2F_6 ~0.98 Gg/yr demonstrating that the aluminium industry was decreasing emissions as early as 1995.

Time period	**Averaged bottom-up estimates (Gg/yr)**		**HVAE contributions (ROW, Gg/yr)**		**HVAE (China, Gg/yr)**		**LVAE contribution (ROW, Gg/yr)**		**LVAE (China, Gg/yr)**	
	CF_4	**C_2F_6**	**CF_4**	**$C2F_6$**	**CF_4**	**C_2F_6**	**CF_4**	**C_2F_6**	**CF_4**	**C_2F_6**
1990-1995	11.4	1.7	9.3	1.7	0	0	0	0	0	0
1995-2000	7.85	0.98	7.01	0.98	< 0	<0	0	0	0	0
2000-2005	6.23	0.625	4.77	0.645	0.5	0.0205	<0	0	0	0
2005-2010	4.93	0.3575	2.5	0.2995	1.25	0.058	0.8	0	0	0
2010-2017	4.6	0.295	2.5	0.158	2.15	0.137	1.6	0	0	0

Table 3.7: Summary of time averaged CF_4 and C_2F_6 (Gg/yr) emissions for the periods of 1990-1995, 1995-2000, 2000-2005, 2005-2010 and 2010-2017 and separated in HVAE contributions from ROW countries (Gg/yr), HVAE from Chinese aluminium smelters (Gg/yr), LVAE contributions from ROW countries (Gg/yr) and LVAE from Chinese aluminium smelters in (Gg/yr).

For the years 2000 – 2005, time averaged emissions for CF_4 are ~6.23 Gg/yr of which 4.77 Gg/yr belong to ROW countries and ~0.5 Gg/yr to Chinese smelters. For C_2F_6, time averaged emissions are ~0.625 Gg/yr with 0.645 Gg coming from ROW countries and 0.02 Gg/yr from Chinese smelters. There is still either minimum (non-zero) contribution from LVAE or (especially in the case of C_2F_6) zero contribution.

During 2005- 2010, time averaged emissions for CF_4 are ~4.93 Gg/yr of which ~2.5 Gg/yr are attributed to HVAE from ROW countries, ~0.8 Gg/yr to LVAE from ROW countries

and ~1.25 Gg/yr to Chinese aluminium emissions (HVAE only). For C_2F_6, averaged emissions are ~0.35 Gg/yr of which ~0.29 Gg/yr are attributed to HVAE ROW emissions, and ~0.05 Gg/yr to HVAE Chinese emissions. No contributions from LVAE have been considered.

Finally, for the years 2010 – 2017, time averaged emissions for CF_4 are ~4.6 Gg/yr, of which ~0.15 Gg/yr are attributed to HVAE ROW emissions, 1.6 Gg/yr are attributed to LVAE ROW emissions and ~2.15 Gg/yr are attributed to Chinese specific emissions. For C_2F_6, ~0.295 Gg/yr are estimated for this time period with ~0.15 Gg/yr attributed to HVAE ROW emissions and ~0.137 Gg/y to HVAE Chinese emissions. No contribution from LVAE is considered.

This chapter set out to answer the following questions:

- Can an industry specific, updated bottom-up inventory be produced?
- Was there significant contribution of the suspected low-voltage emissions?
- How large was the PFC emissions contribution from the emerging Chinese aluminium production?

In conclusion, despite several difficulties and limitations, the compilation of an industry specific bottom-up inventory was successful. Overall, the AI appears to have been successful in substantially reducing HVAE ROW emissions for both CF_4 and C_2F_6 gases, however, this decrease has been offset either by an increase in HVAE China specific emissions or an increase in LVAE ROW emissions (in the case of CF_4), or both. Further investigation is required to fully explore the range of LVAE related emissions.

Chapter 4

PFC emissions from the Semiconductor Industry (SCI)

4.1 Aims

The aims of this chapter are to quantify and discuss PFC emissions from the SCI, present new methods that were developed in order to quantify PFC emissions, discrepancies between

top-down and bottom-up estimates specific to this industry and present an updated bottom-up inventory for the global SCI PFC emissions. This chapter aims to address the following questions:

- Can an industry specific, updated bottom-up inventory be produced?
- How does this inventory compare to previous work?
- What is the current spatial distribution of the semiconductor industry?

Parts of this chapter appear in the paper 'Challenges in estimating CF_4 and C_2F_6 emissions' written by the author of this thesis, Michalopoulou Eleni (Michalopoulou, 2018) [this paper was a single author paper and the idea, data analysis and discussion were only conducted by Michalopoulou E.] and the paper 'Perfluorocyclobutane (PFC-318, c-C4F8) in the global atmosphere' where the author of this work appears as a co-author (Mühle et al., 2019). For this paper the contribution of Michalopoulou E., was providing a map with the location of the semiconductor factories (globally and in the UK particularly). Parts of the data analysis were conducted in collaboration with Louisa Beer, a Master's student within the Atmospheric Chemistry Research Group (ACRG) and Dr. Mike Czerniak, industrial expert from Edwards LTD.

4.2 Introduction

The SCI is a part of the wider electronics industry that consists of the semiconductor, thin-film-transistor flat panel display (TFT-FPD), and photovoltaic (PV) manufacturing industries (Agostinelli et al., 2006). Due to time restrictions this work is only focusing on the SCI and not the broader electronics industry. Semiconductor fabrication plants (commonly referred to as 'fabs') are separated into two kinds based on the size of the semiconductor wafer fabrication capacity, 300 mm fabs and <300 mm fabs. The latter kind consists of the 200 mm, 150 mm, 125mm. 100mm. 75mm and 50mm plants. Prior to 1990 approximately only 180 fabs exist globally (compared to <600 in 2016) and their production rates appear to be limited. Growth for this industry begins after 1990, which is also the time when the industry recovered from the severe recession of 1985-86 (Worth, Duffin and Modrey, 1998; Modrey, 2005; Global Semiconductor Market Trends, 2018, Analysis of Semiconductor Market Data, 2014).

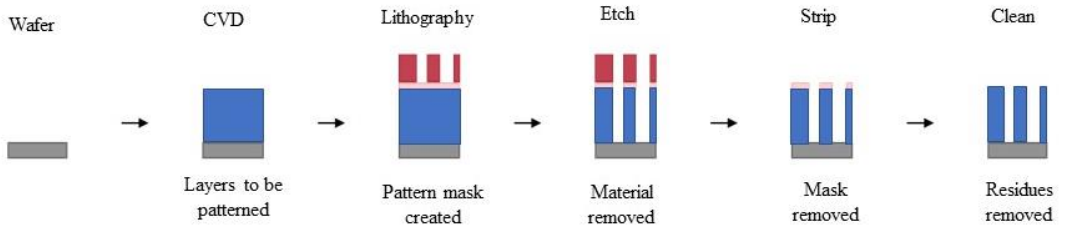

Figure 4.1: The multi-step process used to fabricate integrated circuits on the Si wafer.

Semiconductor chips are widely used in electronic devices. An estimated 70% of all semiconductor components are used in consumer related products (e.g. smartphones, laptops, electric vehicles etc). During the last decade (2000-2010) and as demand for electronic devices increases this industry has been expanding rapidly (Global Semiconductor Market Trends, 2018). The group of circuit elements on a small piece of conducting material, usually silicon (Si), are referred to as an integrated circuit (IC) chip (Integrated Circuit (IC) | JEDEC). ICs are critical elements in the production of electronic equipment and are manufactured in fabs. Circular wafers are produced from large Si cylinders by specialist suppliers, and every fab produces wafers of a specific diameter (e.g. 150mm, 200mm and 300mm). The multi-step process required to build electronic circuits onto the wafer is shown in Figure 4.1. Once the structure is created through this process, the wafer is sliced into small IC chips (Ceric, 2010; Walkey, 2018). The growth of the SCI was followed by the establishment of larger diameter wafer fabs that were introduced to accommodate the increasing demand of ICs(Global Semiconductor Market, 2018).

4.2.1 Etching

Etching is a process that removes material from an exposed surface. This is a very common process that, in order to be carried out, areas of the silicon wafer must be covered with a photoresist mask. The unmasked surface is then exposed to atom bombardment and then the patter can be etched. The most modern etching process is that of dry etching and there are three main types of this type of etching: Physical Dry Etching (PDE), Chemical Dry Etching (CDE) and Reactive Ion Etching (RIE) (Lee and Chen, 1983; Modrey, 2005).

In PDE, the wafer is bombarded high energy beam of inert ions which targets the surface vertically thus removing atoms that eventually evaporate (Modrey, 2005; Illuzzi and Thewissen, 2010a).

CDE involves the Si surface chemically reacting with etchant gases. Reactive species (e.g. radicals) are generated in plasma and react with surface atoms. The result of this interaction is the creation of volatile products.

$$4F + Si \longrightarrow SiF_4(g) \quad (4.1)$$

CF_4 can break into radicals (e.g. F, CF, CF_2, CF_3) which react with Si and produce a gas that can be pumped away (Equation 4.1). Similarly, C_2F_6 by-product emissions have been detected as a result of the decomposition of C_4F_6 molecules (Agostinelli et al., 2006; Illuzzi and Thewissen, 2010).

RIE is the method most used in the industry. The combination of the physical properties of PDE with the chemical properties of CDE making it the most efficient process.

4.2.2 CVD Chamber Cleaning

Chemical Vapour Deposition (CVD) is a process where a precursor gas is used to deposit a thin film of different materials on the wafer surface. This is another critical step in the IC production process (Agostinelli et al., 2006; Modrey, 2005; Illuzzi and Thewissen, 2010). After this step, PFCs are used for chamber cleaning purposes. To remove the residual material, chemical etching is used during which volatile materials are produced that can then be pumped away. This ensures elimination of any contaminants on the chamber walls or process tools (Agostinelli et al., 2006; Modrey, 2005; Illuzzi and Thewissen, 2010).

4.2.3 PFC emissions and emission reduction by the semiconductor industry

As discussed in section 1.8.2, due to increased recognition of the global warming challenge the UNFCCC was adopted in 1992 and in 1997 the Kyoto Protocol was agreed (Kyoto Protocol - Targets for the first commitment period | UNFCCC, 1995; KyotoProtocol - Toward Climate Stability, 1998).

The Semiconductor Council was created by a joint agreement between the Electronic Industries Association of Japan (EIAJ) and the Semiconductor Industry Association (SIA) that

signed an agreement on “International Cooperation regarding Semiconductors” signed on August 2, 1996 in Vancouver, Canada and in April 11, 1997 the name “World Semiconductor Council (WSC)” was established (History | World Semiconductor Council).

In 1999, through a voluntary agreement, WSC members agreed on PFC reduction goals of 10% below the baseline levels set for each Semiconductor Industry Association (SIA) by 2010 (Modrey, 2005; Overview, 2010). As shown in Figure 4.2, the WSC estimated that PFC emissions would increase due to the growing industry, unless action was taken (Modrey, 2005). The 10% emissions reduction goal was decided based on the 2006 IPCC Guidelines and the 4th assessment report GWP values (Agostinelli et al., 2006; Myhre et al., 1998). The PFC reduction target was achieved through the development and implementation of four key activities, following what is referred to as ‘the hierarchy in PFC emission reduction technology’: process optimization, alternative methods, gas capture and abatement, described below (Agostinelli et al., 2006; Worth, Duffin and Modrey, 1998; Modrey, 2005; Illuzzi and Thewissen, 2010).

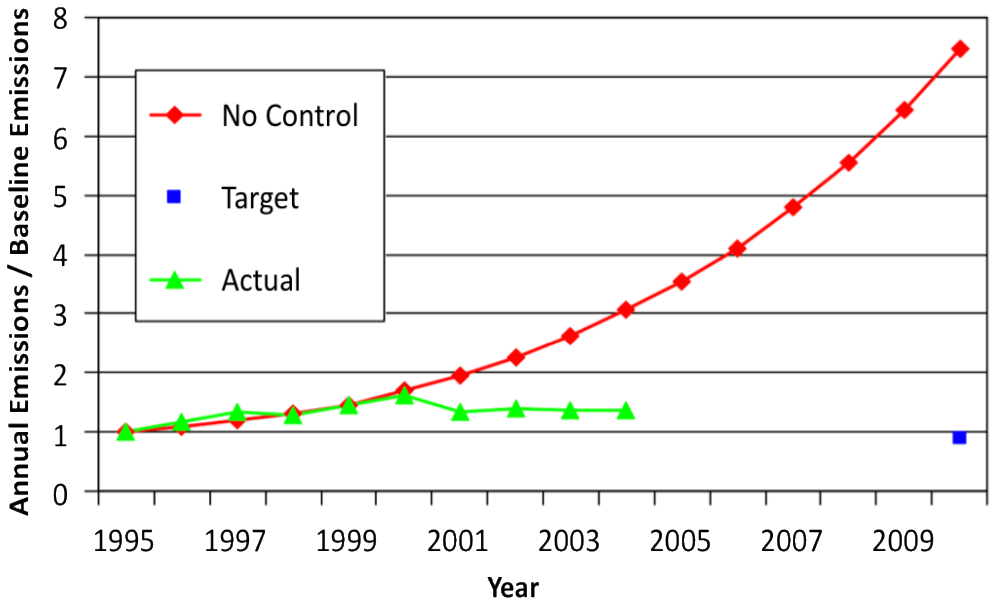

Figure 4.2: Figure presented by the WSC in 2005 highlighting the success of control technologies on PFC emissions (WSC, 2005).

4.2.4 Process Optimization

With many chamber cleaning and etching processes using ~30-40% of the PFCs delivered to this process, the aim of process optimisation in chip manufacturing is to reduce the amount of PFCs emitted (Fthenakis, 2001). Variables such as the temperature, pressure and gas flow are adjusted for this to be achieved. The process is monitored through endpoint detection systems (e.g. mass spectrometry) (Agostinelli et al., 2006; Modrey, 2005; Illuzzi and Thewissen, 2010). There is ongoing research into use of GWP-free gases in CVD chamber cleaning and progress has been made by switching to NF_3. While this GHG still has a very high GWP of 17,200 (Forster et al., 2007) it dissociates to radicals more efficiently in plasma during chamber cleaning and therefore reduces overall GHG emissions (Agostinelli et al., 2006; Modrey, 2005; Illuzzi and Thewissen, 2010). The vast majority of new fabs that were opened from the year 2000 use NF_3 in CVD chamber cleaning. 300mm fabs were first built around the same time, hence are assumed to all use this technology. Information about the number of smaller fabs operating with NF_3 is not publicly available (Illuzzi and Thewissen, 2010a).

4.2.5 Alternative Methods

The process during which ion bombardment is used to chemically etch residual materials inside a chamber is referred to as in-situ CVD. In-situ CVD cleans only those areas of the chamber that are directly exposed to the bombardment which can, however, eventually result in erosion (IPCC, 2006). NF_3 is used in conjunction to new, remote cleaning technology is used (Worth, Duffin and Modrey, 1998; Modrey, 2005; Illuzzi and Thewissen, 2010b). A plasma generating unit is held separate from the CVD chamber which allows for NF_3 to be converted into radicals before it is directed into the CVD chamber. No ion bombardment-induced reactions are involved in this process and the rate of dissociation of NF_3 is enhanced, resulting in a 99% conversion. It is reported that this type of remote cleaning technology has a high conversion efficiency and therefore, emits significantly less PFCs than the in-situ CVD process (IPCC, 2006; Illuzzi and Thewissen, 2010b; WSC, 2012; Annex III: Revision of 2013 World Semiconductor Council (WSC) PFC data, 2014). Other PFC reducing techniques that have been investigated (e.g. membrane separation, cryogenic recovery) but are not discussed further in this work (Worth, Duffin and Modrey, 1998; Modrey, 2005).

4.2.6 Abatement

Abatement systems were introduced in early 1990s (approximately in 1995) but they were not widely used by industry until the early 2000s (2001-2004). Since then, abatement related research continued to be carried out and the efficiency of the abatement technology has increased up to 90% in 2010 (Worth, Duffin and Modrey, 1998; Modrey, 2005; IPCC, 2006; Illuzzi and Thewissen, 2010c; WSC, 2010). Abatement technology can be applied to both etching and chamber cleaning processes.

During thermal abatement, PFCs are combusted at temperatures ~1200°C, energy that is required to break the strong C-F bonds. Natural gas (e.g. CH_4) is frequently used to fuel this process. Early developments in this technology did not successfully abate CF_4, and the process today is still less than 100% efficient.

Replacing the PFC gases previously used in chamber cleaning with NF_3 was critical to reducing emissions as NF_3 is almost entirely converted into radicals and very little escapes. However, when NF_3 is abated there is the possibility that fluorine radicals could react with the combustion fuel resulting in PFC production. Equation 4.2 shows an example of CF_4 being created as a result of the methane-fluorine reaction.

$$8\,F + CH_4 \longrightarrow CF_4 + 4\,HF \qquad (4.2)$$

To prevent PFCs being emitted as a result of the NF_3-combustion fuel interaction special equipment has been developed (Fthenakis, 2001; Czerniak, Tang and Li, 2010) where input fuel and exhaust gas are kept separate. By implementing this equipment instead of Equation 4.2, only the reaction shown in Equation 4.3 occurs.

$$4\,F + 2\,H_2O \longrightarrow 4\,HF + O_2 \qquad (4.3)$$

Point of use (POU) technology is widely used because of its efficiency. This technology involves abatement close to the source, as opposed to end of pipe (EOP) abatement which is centralised within the fab for all processes (Fthenakis, 2001; Modrey, 2005). The reason why abatement has been a very effective PFC reduction method is its ability to be both built into the older fabs and be included in the development of the newer ones (Modrey, 2005).

Finally, it should be noted that both the IPCC and the US Environmental Protection Agency are highlighting the possibility of PFC emissions from the semiconductor industry as a result of by-product emissions during some processes (IPCC, 2006; US EPA, 2017).

Overall, unlike the aluminium industry that only emits PFCs during specific states of operation of the smelting cell, the semiconductor industry uses PFC gases for the purpose of the processes described above. As discussed, there are four distinct 'phases' in the history of the semiconductor industry in relation to their PFC emissions:

a) Older 150 and 200 mm fabs (pre-1995)
b) Roll out of abatement (post-1995)
c) New generation 200mm fabs (post 2000)
d) 300mm fabs (post-2000)

The reason why these phases are important is, as described above, their correlation to different consumption, emission and abatement levels of both CF_4 and C_2F_6. We will describe below in section 4.2 'Methods and limitations' how these different phases can help us understand PFC emission from this industry and will discussed further in chapter 7 'Discrepancies'.

4.3 Methods

To estimate PFC emissions from the SCI and to compile the part of the bottom-up inventory related to this industry two new methods were developed; The Combined Fab Method (CFM) and the Fab Specific Method (FSM).

4.3.1 The Combined Fab Method (CFM)

As discussed in section 4.2, the main source of semiconductor production and PFC emission data for this industry is the WSC, which is comprised of the SIAs. Since 1997, when the first WSC meeting took place, until 2013, all the emissions were reported as a mix of fluorinated compounds in tonnes of CO_2 equivalent emissions (WSC, 1999, 2005, 2008, 2009, 2011, 2012, 2013, 2017, Annex III: Revision of 2013 World Semiconductor Council (WSC) PFC data, 2014; Taipei, Manufacturing and Corporation, 2015).

Since 2013, emissions of individual compounds are reported separately. According to the 2017 Joint Statement of WSC in Kyoto, out of 13.9 Gg of fluorinated gaseous compounds consumed by the semiconductor industry, 1.5 Gg is CF_4 and CF_4 emitted by the semiconductor industry is 0.16 Gg/yr. (World Semiconductor Council Best Practice Guidance for Semiconductor PFC Emission Reduction, 2017). Much like the methods to compile PFC estimates by the aluminium industry the IPCC (2006) guidelines provide a set of methods for estimating SCI emissions, Tier 1, Tier 2a, Tier 2b and Tier 3 (IPCC, 2006). These three equations (described in detail in this section) are used to quantify PFC emissions according to the IPCC guidelines for both methods developed in this work (2006). Different equations have different uncertainties and equation choice depends on information availability.

For most inventory compilers (the ones with no access to industrial information), some of the parameters related to the Tier equations are not publicly available as the information is considered commercially sensitive. In this section a newly developed method is presented (CFM) to estimate the, otherwise unknown, values for C_d, C_u and FC_i used in the IPCC equations. This method was co-developed with industrial experts from Edwards LTD, a gas abatement company. This collaboration allowed for quantification of some of the parameters (C_d, C_u and FC_i and a_i) that would otherwise be impossible to quantify unless access to facility specific measurements was provided. It should be noted that due to confidentiality issues and commercially sensitive information some of the original sources cannot be included in this section, the references and bibliography, however this information can be made available upon request to the author of this work after agreement with Edwards LTD.

a) Tier 1

The Tier 1 equation uses an emission factor multiplication formula shown in Equation 4.4. The IPCC good practice guide indicates that this Equation (4.4) should only be used when company specific data is unavailable because of the high uncertainty related to this method.

$$\mathrm{E_i\ (kg\ y^{-1})} = \mathrm{EF_i\ (kg\ m^{-2} y^{-1})} * \mathrm{C_d (m^2)} * \mathrm{C_u} \qquad (4.4)$$

Where:

E_i Amount of gas i produced annually

EF_i Emission factor for gas i (IPCC, 2006)

C_d Annual capacity of substrate (Si wafer) processed (Akkermans and Van Wassenhove, 2013)

C_u Fraction of production capacity utilised on average (Akkermans and Van Wassenhove, 2013; Semiconductor Capacity Utilization Rising – Semiwiki, 2014)

The annual capacity (C_d) is estimated using information that the Semiconductor Equipment and Materials International (SEMI) provided upon request; the data provided included total area of silicon bought annually by semiconductor manufacturers and fab specific demand of the different wafer sizes studied. Equation 4.5 shows how C_d was calculated by dividing total silicon area purchased by the SCI between the 300 mm and ≤200 mm wafer fabs according to the % demand for each size domain (150mm, 200mm and 300mm), as shown in Equation 4.5.

$$C_d = \text{Area Shipments of Si} * \%\ \text{Demand} \quad (4.5)$$

One assumption that Equation 4.5 makes is total area of silicon purchased per facility was equal to the total wafer area produced per facility. This is considered a good approximation based on industrial experts (Private Communication with Edwards LTD).

Annual calculations were carried out using the data provided by SEMI. The calculated C_d values were substituted into Equation 4.4 to quantify emissions. Uncertainties were calculated for each year using the IPCC guidelines uncertainty range for Tier 1 equation (IPCC, 2006). Tier 1 PFC emissions estimated using Equation 4.4 do not consider the use of abatement systems or account for the separate processes (etch and CVD) that emit CF_4. With abatement not accounted for in this Equation 4.5 a de-facto overestimation of the emissions was expected. However according to literature a good approximation of the application of abatement in the Tier 1 scenario is to consider the linear increase of abatement from 0 in 1990 to 90% in 2010 (Worth, Duffin and Modrey, 1998; Modrey, 2005; WSC, 2005, 2010; IPCC, 2006; Illuzzi and Thewissen, 2010b; Taipei, Manufacturing and Corporation, 2015; World Semiconductor Council Best Practice Guidance for Semiconductor PFC Emission Reduction, 2017). PFCs emissions using Equation 4.5 were estimated without differences for CF_4 and C_2F_6.

b) Tier 2A

Tier 2A uses gas consumption information instead of wafer output data. It also accounts for abatement, as shown in Equation 4.6.

$$E_i\ (kg) = (1 - h) * FC_i\ (kg) * (1 - U_i) * (1 - a_i d_i) \quad (4.6)$$

Where:

E_i Amount of gas i produced

h Fraction of gas i obtained but not used (Assumed all gas obtained was used: h = 0)

FC_i Annual consumption of gas i (Baird, 1998; Personal Communication with Edwards LTD)

U_i Fraction of gas i used up in the process (IPCC, 2019a)

a_i Fraction of gas i used up in processes with abatement technologies (Personal communication, Edwards LTD)

d_i Fraction of gas i destroyed by the abatement process (Martinelli and Worth, 1994)

For emissions estimated using Equation 4.6 there are important differences in the assumptions made for CF_4 and C_2F_6. To estimate annual gas consumption, FCi, a linear increase was assumed between two known values of 10 t used in 1980 and 1000 t used in 2016 for CF_4 and ~10 t used in 1980 and 650 t used in 2016 for C_2F_6 (Baird, 1998; Personal Communication with Edwards LTD).

For the years prior to 1995 (before abatement was implemented) it was assumed that the amount PFCs consumed by a fab was equal to the amount of PFCs emitted. This was considered a good approximation for the years 1980 to early 1990. After 1995 the WSC provides some numbers of the PFCs consumed by the industry (e.g. ~1.5 Gg/yr in 2016) (WSC, 2016). Although the shift to NF_3 after 2000 reduced the need for CF_4 in CVD chamber cleaning, this reduction has been offset by the significant increase in semiconductor chip production as the industry has grown. Between the years 1980 and 1990, a linear increase of PFC consumption by the industry for the 150mm and 200mm fabs and to calculate the amount of gas used for the different processes was assumed (Etch and CVD) after consulting industrial experts in Edwards LTD. Between the years 1980 and 1995 there were no 300mm fabs

(Personal communication with Edwards LTD; Worth, Duffin and Modrey, 1998; Modrey, 2005). For the years 1995 to 2000 first generation 200mm used predominantly PFCs for CVD and by 2000, 200mm fabs were dominating the market (Worth, Duffin and Modrey, 1998; Modrey, 2005). After 2001 (and predominantly between 2001 and 2004) the industry moves towards new generation 200mm and 300mm fabs. The new generation fabs use NF_3 for CVD (Worth, Duffin and Modrey, 1998; WSC, 2005). This description is demonstrated in Figure 4.3.

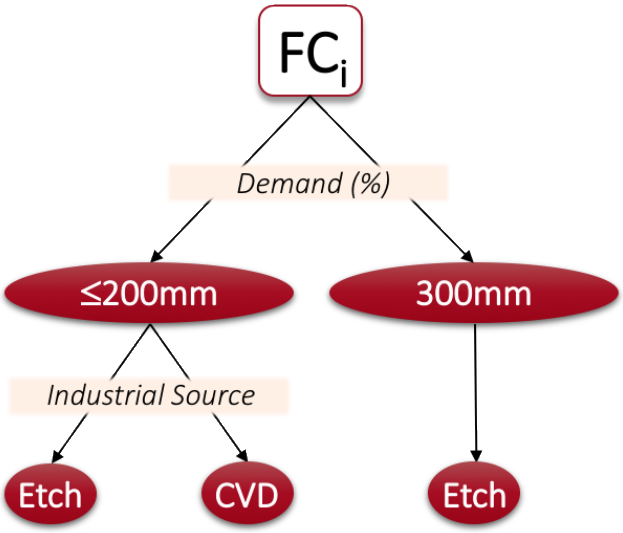

Figure 4.3: Gas consumption split between <200 mm and 300 mm fabs and the processes for the CFM.

It was assumed that no abatement took place before 1995 and so d_i was set to zero for these years (Personal Communication with Edwards LTD; Martinelli and Worth, 1994). The systems rolled out in 1995 had recorded efficiency of approximately 90% which has been maintained to the current time, but the proportion of abatement systems has steadily increased from zero before 1995 to approximately 90% of the industry's exhaust lines (Personal Communication with Edwards; Modrey, 2005). In this instance a_i was estimated to be approximately 0.8 after consultation with Edwards LTD (Personal Communication with Edwards LTD).

The global average for abatement destruction removal efficiency (DRE) was determined by the IPCC to be 90% in 2006 (IPCC, 2006). From 2006 onwards to estimate abatement, di was estimated using effective abatement (overall industry emission reduction) $d_i = D_i$ = DRE (95% of gas destroyed) x N_i (% abatement). The parameter N_i was used as a scaling

factor to reflect the increase in abatement from 0 to 90%. This linear increase in d_i was assumed to be a good approximation for the years studied (post-1995) (WSC 2005, 2010; Taipei, Manufacturing, and Corporation 2015). The IPCC suggested value of 0.9 was used in calculations. An error for 1-U_i of 15% was used as per the IPCC guidelines, and it was used to calculate an uncertainty for Tier 2A annual CF_4 emissions (IPCC, 2006).

c) Tier 2B

Tier 2B uses gas consumption. It accounts for abatement systems and it differentiates between the different processes (CVD and etch) as shown in Equation 4.7.

$$\begin{aligned} E_i\ (kg) = &\left[(1-h) * FC_{i,etch}\ (kg) * \left(1-U_{i,etch}\right) * \left(1-a_{i,etch}d_{i,etch}\right)\right]_{etch} \\ &+ \left[(1-h) * FC_{i,CVD}\ (kg) * \left(1-U_{i,CVD}\right) * \left(1-a_{i,CVD}d_{i,CVD}\right)\right]_{CVD} \end{aligned} \quad (4.7)$$

Constants involved in 2B are defined as per 2A (Equation 4.6), but in this case they are process specific.

IPCC guidelines provide relative errors for 1-U_i, etch and 1-U_i, CVD of 60% and 10%, respectively for CF_4 and for C_2F_6 a value of 100% and 30% are described in the IPCC guidelines for the respective values of etc and CVD. These were used to calculate an uncertainty for Tier 2B annual PFC emissions. In this instance $a_{i,etch}$ and $a_{i,CVD}$ were estimated to be approximately 0.8 after consultation with Edwards LTD (Personal Communication with Edwards LTD).

The separation of processes described in Equation 4.7 resulted in the annual gas consumption being divided between the processes of etch and CVD. Two groups of fabs were considered: the 300mm fabs and the <300mm fabs. This grouping was based on the fact that most 300mm fabs use NF_3 in their CVD chamber cleaning process and therefore only use PFCs in etching. Therefore, it was assumed that all post-2000, 300 mm fabs used NF_3 in their CVD as shown in Equation 4.8 where all the CVD processes were assumed to be zero. In this instance $a_{i,etch}$ was estimated to be 1 after consultation with Edwards LTD (Personal Communication with Edwards LTD).

$$E_{i,300mm}\ (kg) = \left[(1-h) * FC_{i,etch}\ (kg) * \left(1-U_{i,etch}\right) * \left(1-a_{i,etch}d_{i,etch}\right)\right]_{etch} \quad (4.8)$$

Gas consumption was split per the 300mm and <300mm grouping using the SEMI data and additionally between processes (etch and CVD). For the ≤200 mm fabs It was assumed that 10% of gas is used in etching and 90% is used CVD chamber cleaning for CF_4 and 25% of the gas is used in etching and 85% is used in CVD chamber cleaning for C_2F_6 (Personal Communication with Edwards LTD).

This work could not replicate the equivalent of the Tier 3 equation used by the IPCC as none of the parameters could be quantified using publicly available information.

4.3.2 The Fab Specific Method (FSM)

This method uses a database provided by an industrial source which includes fab locations and activity data and some publicly available information to calculate C_d and FC_i from the IPCC equations. This method allows for PFC emission estimates per facility, per year, per country. PFC emissions were estimated for 7 different domains, namely the USA, South Korea, Japan, Taiwan, Europe, China and Asia. Due to commercially sensitive information contained in the database will not be made public and the bulk of the original sources of information will remain confidential. However, there is the ability share some of this information upon request to the author of this work. To estimate PFC emissions using the Tier 1, Tier 2A and Tier 2B approaches, Equations 4.4, 4.6 and 4.7 were used respectively.

a) Tier 1

To estimate wafer area per facility, the total number of wafers that each facility produced per year and Equation 4.9 were used (where r is the radius of the wafer produced).

$$C_d = \text{No. of Wafers} * \pi r^2 \quad (4.9)$$

C_d values were estimated per year per facility before they were used in Equation 4.4 to quantify PFC emissions per facility. To produce the global total, emissions of every fab operating within the estimated year were summed; to produce the country specific totals this step was repeated for every country and domain studied.

b) Tier 2A

To estimate annual gas consumption, FCi, the same method described for the Tier 2A CFD estimates was applied. Using the same linear increase between the known values of PFC production in 1980 and 2016. Gas was split according to the same grouping of fabs (300 mm and ≤200 mm) per year. Information about the number of process tools that use PFCs was made available by Edwards Vacuum. It was assumed that 300 mm fabs use approximately 6 times less CF_4 than ≤200 mm fabs. To allocate gas consumption per facility, Equation 4.10 was used for every year studied.

$$(N_{\leq 200} * 6\mathrm{G}) + (N_{300}G) = \mathrm{FC_i} \quad (4.10)$$

$N_{\leq 200}$ Number of ≤200 mm fabs

N_{300} Number of 300 mm fabs

G Gas consumed per 300 mm fab

FC_i Total annual gas consumption

The per facility gas allocation using Equation 4.10 was considered a good approximation by industry experts. The same amount of gas was allocated to fabs of the same wafer size. Gas consumption estimates were then substituted into Equation 4.6, and PFC annual global and domain emissions estimates were produced.

c) Tier 2B

To estimate annual gas consumption for Tier 2B gas consumption had to be divided between the two processes; etching and CVD chamber cleaning. 100% of PFC usage in the 300 mm fabs for etching processes was assumed. For ≤200 mm fabs, 94% consumption from the CVD chamber cleaning process and only 6% from the etching processes was assumed. Facility and process specific values for gas consumption were then substituted into Equation 4.7, and PFC emissions were summed over all fabs operating per year to produce the global and domain total. For completion, the results produced through the CFM were compared against the results produced through the FSM.

4.4 Results and Discussion

4.4.1 Estimating global PFC emissions using the CFM

PFC emissions from the SCI were estimated (Gg/yr) for the period between 1980 and 2017 (Equations 4.4 – 4.8). Emissions estimated for every Tier method were summed and averaged and these averaged estimates are presented for CF_4 and C_2F_6 in Figures 4.4 and 4.5 respectively.

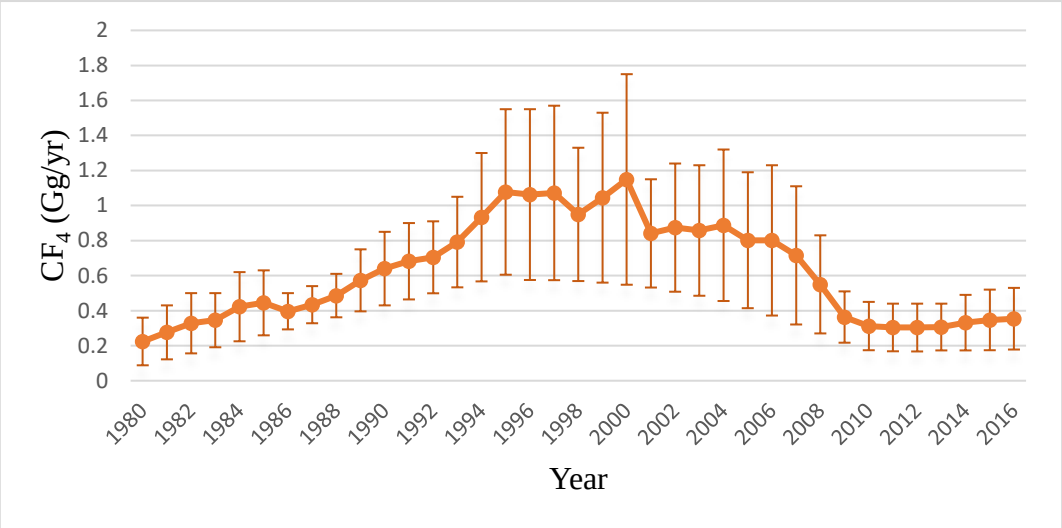

Figure 4.4: Global CF_4 emissions (in Gg/yr) from the SCI for 1980 to 2017

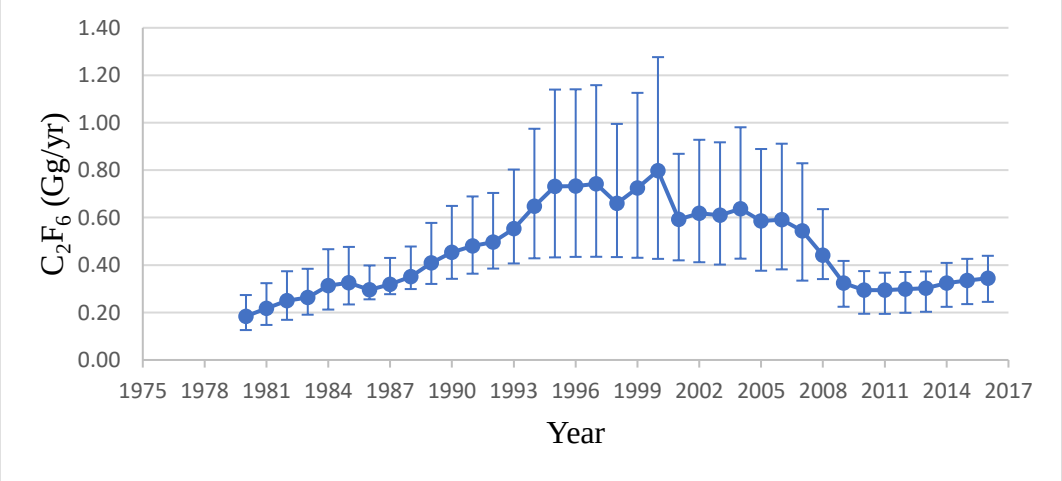

Figure 4.5: Global C_2F_6 emissions (in Gg/yr) from the SCI for 1980 to 2017

For cleaning CVD chambers and dry etching in the SCI, the primary chamber clean gas prior to 2000 was predominantly CF_4 and only in some cases C_2F_6. Emissions from the SCI were rising significantly (up to ~1.2 Gg/yr for CF_4 and 0.8Gg/yr for C_2F_6) in early 2000. The SCI undertook efforts to reduce fluorine related emissions following the pollution prevention hierarchy. The abatement and the replacement of PFCs with NF_3 after 2000 (Modrey, 2005) appear to have contributed to the decrease of PFC emissions steadily. In 1980 ~0.22 Gg/yr of CF_4 and 0.18 Gg/yr C_2F_6 respectively were estimated. Emissions for both gases increased to 1.07 Gg/yr and 0.8 Gg/yr of CF_4 and C_2F_6 respectively for the year 2000 and then followed a steady decrease until 2010 when 0.31 and 0.29 Gg/yr of CF_4 and C_2F_6 were emitted. After 2010 emissions appear to be slightly increasing for both gases reaching 0.35 Gg/yr and 0.34 Gg/yr for CF_4 and C_2F_6 for the year 2016.

As discussed in section 4.1 and 4.2 bottom-up estimates of this work are compared with previous bottom-up estimates and against previously published top-down estimates (Kim et al., 2014). For ease, Figure 4.6 shows the emission estimates produced by every scenario instead of comparing with the averaged emissions of the scenarios only.

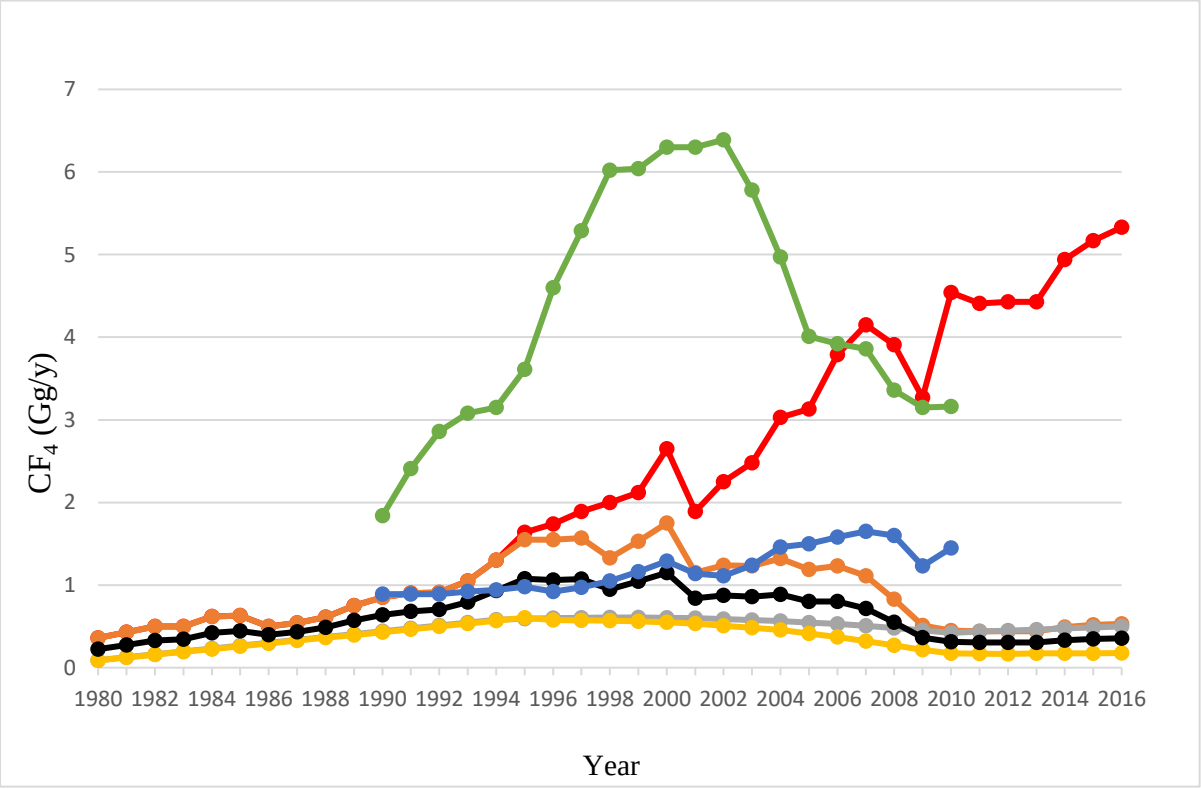

Figure 4.6: Comparing the bottom-up estimates for CF_4 emissions (Gg/yr) from the semiconductor derived from the scenarios described above. Tier 1 scenario without abatement (hypothetical scenario) in red, Tier 1 with abatement scenario in orange, Tier 2A and Tier 2B

in grey and yellow, respectively and the averaged emissions scenario in black. These results are also compared with the top-down (green) and bottom-up (blue) estimates as presented in Kim et al. (2014).

Figure 4.6 shows the different CF_4 estimates that were derived using the different Tier methods described in section 4.2. The emission estimates occurring from the use of Tier 1 Equation (4.4) with no abatement are shown in red. As the CF_4 estimates associated with the Tier 1 equation does not include abatement, they could be described as a 'worst case' scenario of emissions coming from the SC industry. In orange, the estimates from the use of Tier 1 Equation (4.4) with a linear increase in abatement are shown. In grey the estimates as a result of the Tier 2a Equation (4.5) and in yellow the estimates from the Tier 2b Equation (4.6) are presented. The averaged emissions estimates are demonstrated in black (as shown in Figure 4.4). In green the top-down estimates presented in Kim et al. (2014) is shown and in blue the bottom-up estimates presented in the same work (Kim et al., 2014) All values used in Figure 4.6 are presented in Table 4.1.

Comparing the hypothetical, Tier 1 without abatement scenario with the Tier 1 with abatement but also with T2a and T2b it is obvious that abatement has played a significant role in reducing CF_4 emissions from the SCI. In the event that no abatement was rolled out by the industry the emissions from CF_4 would be ~5.1 Gg/yr in 2016 while with abatement only an estimated 0.35 Gg/yr were emitted in 2016.

The bottom-up estimates from Kim et al. (2014) are presented in the figure by a blue line. Compared with the newly developed bottom-up inventory these estimates seem to be in good agreement especially between the period 1993 to 2003.

It is interesting to note that the top-down estimates presented in Kim et al. (2004) are significantly higher than the Tier 1 without abatement scenario which is believed to be an overestimate of the emissions from the SCI. According to very few published information and industrial experts between 1990 and 2005, CF_4 production (for industrial, semiconductor use) did not surpass 500 tons of gas per year (personal communication with Edwards; Manahan, 2005).

	CF_4 emissions (Gg/yr)				
Year	**Tier 1 (no abatement)**	**Tier 1 (with abatement)**	**Tier 2a**	**Tier 2b**	**Averaged total**
1980	0.36	0.36	0.09	0.08	0.22
1981	0.43	0.43	0.12	0.12	0.27
1982	0.5	0.5	0.16	0.15	0.32
1983	0.5	0.5	0.19	0.19	0.34
1984	0.62	0.62	0.23	0.22	0.42
1985	0.63	0.63	0.26	0.25	0.44
1986	0.5	0.5	0.3	0.29	0.39
1987	0.54	0.54	0.33	0.32	0.43
1988	0.61	0.61	0.37	0.36	0.48
1989	0.75	0.75	0.40	0.39	0.57
1990	0.85	0.85	0.44	0.43	0.64
1991	0.9	0.9	0.47	0.46	0.68
1992	0.91	0.91	0.51	0.49	0.70
1993	1.05	1.05	0.54	0.53	0.79
1994	1.3	1.3	0.58	0.56	0.93
1995	1.64	1.55	0.59	0.60	1.07
1996	1.74	1.55	0.59	0.57	1.06
1997	1.89	1.57	0.60	0.57	1.07
1998	2	1.33	0.60	0.56	0.94
1999	2.12	1.53	0.60	0.56	1.04
2000	2.65	1.75	0.63	0.54	1.14
2001	1.89	1.15	0.59	0.53	0.84
2002	2.25	1.24	0.58	0.50	0.87
2003	2.48	1.23	0.57	0.48	0.85
2004	3.03	1.32	0.56	0.45	0.88
2005	3.13	1.19	0.54	0.41	0.80
2006	3.79	1.23	0.52	0.37	0.80

2007	4.15	1.11	0.50	0.32	0.71
2008	3.91	0.83	0.48	0.27	0.55
2009	3.27	0.51	0.45	0.21	0.36
2010	4.54	0.45	0.42	0.17	0.31
2011	4.41	0.44	0.43	0.16	0.30
2012	4.43	0.44	0.44	0.16	0.30
2013	4.43	0.44	0.46	0.17	0.30
2014	4.94	0.49	0.47	0.17	0.33
2015	5.17	0.52	0.48	0.17	0.34
2016	5.33	0.53	0.5	0.17	0.35

Table 4.1: This table summarises the values used in Figure 4.6 presenting the bottom-up estimates for CF_4 emissions from the SCI derived from the scenarios described in section 4.2. Tier 1 scenario without abatement (hypothetical scenario), Tier 1 with abatement, Tier 2A, Tier 2B and the averaged emissions scenario. The values for the top-down and bottom-up estimates from Kim et al., 2014 are not presented here as they can be found in the supplementary material of that work (Kim et al., 2014).

Additionally, estimates for the years 2010-2016 using the Tier 2b method appear to be in agreement with estimates presented in the WSC joint statements (WSC, 2005 - 2010; Illuzzi and Thewissen, 2010) as shown in Table 4.2.

Year	**CF_4 emissions (Gg/yr)**
2010	0.15
2011	0.15
2012	0.13
2013	0.15
2014	0.15
2015	0.14
2016	0.16

Table 4.2: CF_4 emissions (in Gg/yr) between the years 2010 and 2016 inferred from WSC published data (WSC, 2010 - 2016).

Finally, it should be highlighted highlight that using this method (CFM) emissions estimates regarding by-product emissions of CF_4 appear to be negligible for the years 1980 – 2017 and for this reason these emissions are not included in the updated bottom-up inventory this work has compiled nor are they considered further.

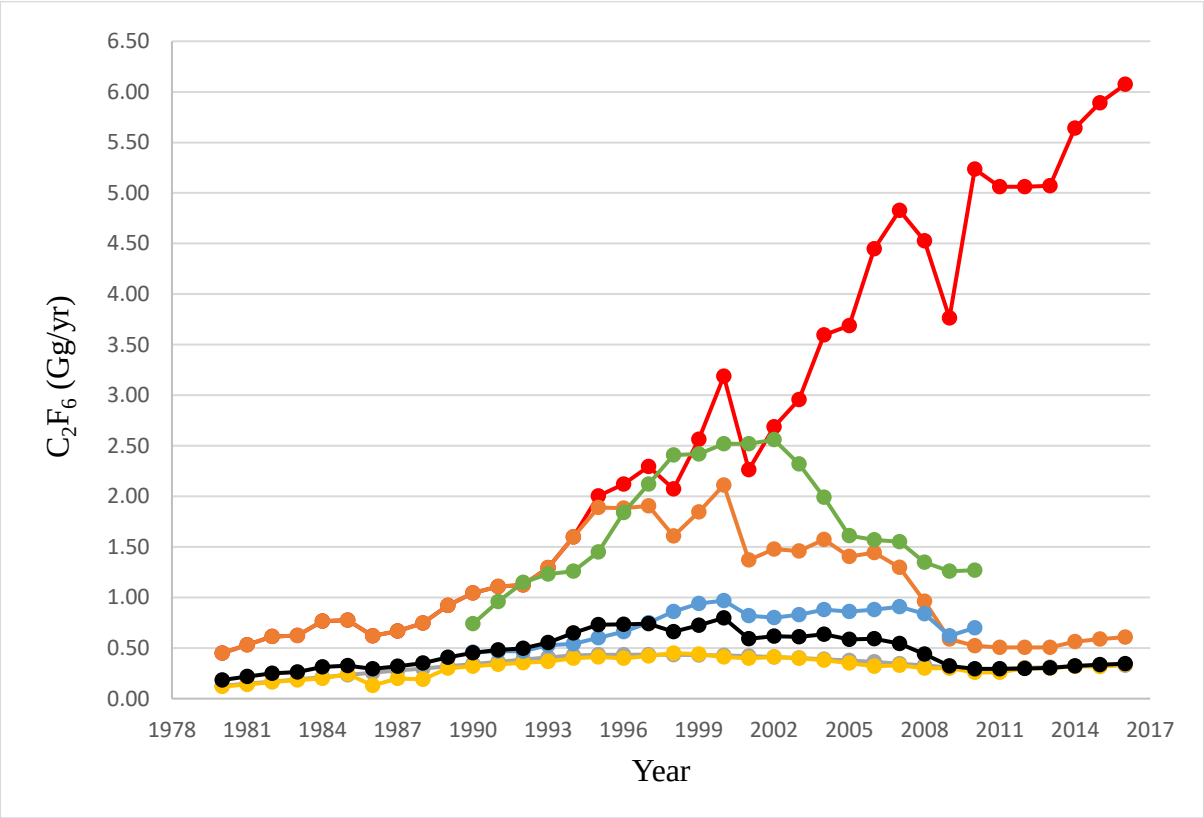

Figure 4.7: Comparing the bottom-up estimates for C_2F_6 emissions from the semiconductor derived from the scenarios described above. Tier 1 scenario without abatement (hypothetical scenario) in red, Tier 1 with abatement scenario in orange, Tier 2A and Tier 2B in grey and yellow, respectively and the averaged emissions scenario in black. These results are also compared with the top-down (green) and bottom-up (blue) estimates as presented in Kim et al. (2014).

Figure 4.7 shows the different C_2F_6 estimates that were derived using the different Tiers described in section 4.2. The emission estimates occurring from the use of Tier 1 Equation (4.4) with no abatement are shown in red. Like the CF_4 estimates, the C_2F_6 estimates associated with the Tier 1 equation that does not include abatement, could be described as a hypothetical 'worst case' scenario of emissions coming from the SC industry. In orange, the estimates from the use of Tier 1 Equation 4.4 with a linear increase in abatement are shown. In grey we are presenting the estimates produced using the Tier 2a equation are presented (Equation 4.5) and

in yellow the estimates produced using the Tier 2b (Equation 4.6). The averaged emissions estimates are demonstrated in black (as shown in Figure 4.4). In green the top-down estimates presented in Kim et al. (2014) are shown and in blue the bottom-up estimates presented in the same work (Kim et al., 2014) All values used in Figure 4.6 are presented in Table 4.3.

Comparing the hypothetical, Tier 1 without abatement scenario with the Tier 1 with abatement but also with T2a and T2b it is obvious that abatement has played a significant role in reducing C_2F_6 emissions from the SCI. In the event that no abatement was rolled out by the industry the emissions from C_2F_6 would be ~6 Gg/yr in 2016 while with abatement only an estimated 0.6 Gg/yr were emitted in 2016.

The bottom-up estimates from Kim et al. (2014) are presented in the Figure (4.7) by a blue line. Compared with the newly developed bottom-up inventory these estimates seem to be in good agreement especially between the period 1993 to 2003.

In this instance, and unlike the comparison between the top-down estimates on CF_4, the top-down estimates presented in Kim et al. (2004) the top-down estimates on C_2F_6 produced in the same work appear to be in better agreement with the Tier 1 with abatement scenario (orange line, Figure 4.7).

	C_2F_6 emissions (Gg/yr)				
Year	**Tier 1 (no abatement)**	**Tier 1 (with abatement**	**Tier 2a**	**Tier 2b**	**Averaged total**
1980	0.45	0.45	0.13	0.12	0.18
1981	0.53	0.53	0.15	0.14	0.22
1982	0.61	0.61	0.17	0.17	0.25
1983	0.62	0.62	0.19	0.18	0.26
1984	0.77	0.77	0.21	0.20	0.31
1985	0.78	0.78	0.23	0.25	0.33
1986	0.62	0.62	0.26	0.13	0.30
1987	0.67	0.67	0.28	0.20	0.32
1988	0.75	0.75	0.30	0.19	0.35
1989	0.92	0.92	0.32	0.30	0.41
1990	1.04	1.04	0.34	0.32	0.45
1991	1.11	1.11	0.36	0.34	0.48
1992	1.12	1.12	0.39	0.36	0.50

1993	1.30	1.30	0.41	0.37	0.55
1994	1.60	1.60	0.43	0.40	0.65
1995	2.00	1.89	0.43	0.41	0.73
1996	2.12	1.88	0.43	0.40	0.73
1997	2.29	1.91	0.43	0.42	0.74
1998	2.07	1.61	0.43	0.45	0.66
1999	2.57	1.84	0.43	0.44	0.72
2000	3.19	2.11	0.43	0.41	0.80
2001	2.26	1.37	0.42	0.40	0.59
2002	2.69	1.48	0.41	0.41	0.62
2003	2.96	1.46	0.40	0.40	0.61
2004	3.60	1.57	0.39	0.38	0.64
2005	3.69	1.41	0.38	0.35	0.59
2006	4.45	1.44	0.36	0.32	0.59
2007	4.83	1.30	0.35	0.33	0.54
2008	4.53	0.96	0.33	0.30	0.44
2009	3.76	0.59	0.31	0.30	0.32
2010	5.24	0.52	0.29	0.26	0.29
2011	5.06	0.51	0.29	0.26	0.29
2012	5.06	0.51	0.30	0.30	0.30
2013	5.07	0.51	0.31	0.30	0.30
2014	5.64	0.56	0.32	0.32	0.32
2015	5.89	0.59	0.33	0.32	0.34
2016	6.07	0.61	0.33	0.34	0.34

Table 4.3: This table summarizes the values used in figure 4.6 presenting the bottom-up estimates for C_2F_6 emissions from the SCI derived from the scenarios described in section 4.3 and Tier 1 scenario without abatement (hypothetical scenario), Tier 1 with abatement , Tier 2A, Tier 2B and the averaged emissions scenario. The values for the top-down and bottom-up estimates from Kim et al., 2014 are not presented here as they can be found in the supplementary material of that work (Kim et al., 2014).

4.4.2 Estimating global and per domain PFC emissions using the FSM

As discussed in section 4.3.2, a confidential database was used in order to estimate domain (and country) specific PFC emissions. Below estimates for different years are presented; (a) 1980-1990, (b) 1990-2000, (c) 2000-2010 and (d) 2010-2017. While Equations 4.4 – 4.8 and the method described in section 4.3 (FSM) were used to estimate wafer area production (in m^2) per year and emissions for CF_4 and C_2F_6 (in Gg/yr) this section presents only the results related to Tier 2b method (Equations 4.7 and 4.8). For completion, the remaining results are presented at the end of this section (Table 4.12).

a) 1980 - 1990

As shown in Table 4.4, PFC estimates demonstrate that between 1980 and 1990 the USA produced approximately 8.7 million wafers amounting to an approximately 140,150 wafer area (m^2) while Asia and Europe produced a total of 590,569 m^2 and 157,468 m^2 of wafer area respectively. The full breakdown of production of wafer area per domain and fab type is shown in Table 4.4. Also presented are the same numbers for specific countries in Asia (namely Taiwan, Japan, South Korea and China). Out of the 590,569 m^2 wafer area that was produced in Asia, 486,363 m^2 were produced in Japan, approximately 82% of the Asian production and 32% of the global production.

Wafer Area (m^2) for the period 1980-1990								
Domain	**50mm**	**75mm**	**100mm**	**125mm**	**150mm**	**200mm**	**300mm**	**Total**
USA	565	1,647	14,475	20,617	52,888	49,951	0	140,143
Asia	0	1,590	87,651	155,582	259,866	85,879	0	590,569
Europe	0	0	18,017	0	100,621	38,830	0	157,468
China	0	1,590	19,792	0	18,025	0	0	39,407
Taiwan	0	0	0	3,534	20,389	0	0	23,924
Japan	0	0	67,859	116,263	216,362	85,879	0	486,363
South Korea	0	0	0	3,387	0	0	0	3,387
Other	0	0	0	32,398	5,089	0	0	37,487
Global total	565	4,827	207,793	331,782	673,142	260,539	0	1,478,748

Table 4.4: Presenting estimates of wafer area produced (m^2) per domain for the period between 1980 and 1990 as well as global totals for the different types of fabs (50mm, 75mm, 100mm,125mm.150mm.200mm and 300mm). Domains are Asia, Europe and the USA. Separately presented are the values for the countries belonging to the Asian domain, namely China, Japan, Taiwan, South Korea.

Examining the year 1990, ~0.46 Gg/yr of CF_4 was estimated to be emitted. Examining the domains (USA, Europe and Asia) it was estimated that the USA contributed 29% (approximately 0.12 Gg/yr), Asia contributed 53% (approximately 0.23 Gg/yr) and Europe contributed 17% (approximately 0.07 Gg/yr). Out of the 0.23 Gg/yr of Asian emissions, 3% are attributed to Taiwan, South Korea (approximately 0.007 Gg/yr) while Japan and China are estimated to contribute 84% (approximately 0.19 Gg/yr) and 8% (approximately 0.018 Gg/yr) respectively (Figures 4.8, 4.9 and Table 4.4).

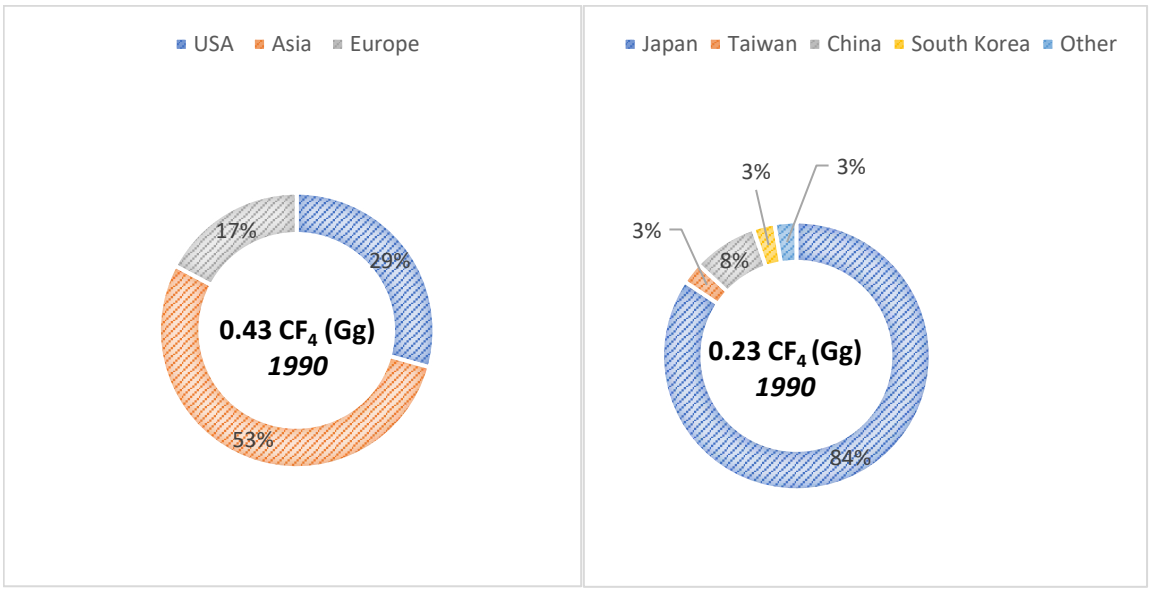

Figure 4.8: Distribution of CF_4 emissions for the year 1990 calculated using Equation 4.6 and the FSM. Left: Distribution per domain (namely USA, Asia and Europe). Right: Distribution between the different Asian countries within the Asian domain.

Comparing the wafer area produced per domain (and per country) to their respective emissions (Table 4.3 and Figures 4.7 and 4.8) a linear correlation between wafer area production and PFC emissions is observed. This was expected for the period between 1980 to

1990 as, as discussed in 4.1, abatement was not rolled out in the majority of the fabs during this period (1980 – 1990) the newer generation fabs were not yet established (Worth, Duffin and Modrey, 1998; Modrey, 2005; Illuzzi and Thewissen, 2010c; Michalopoulou, 2018).

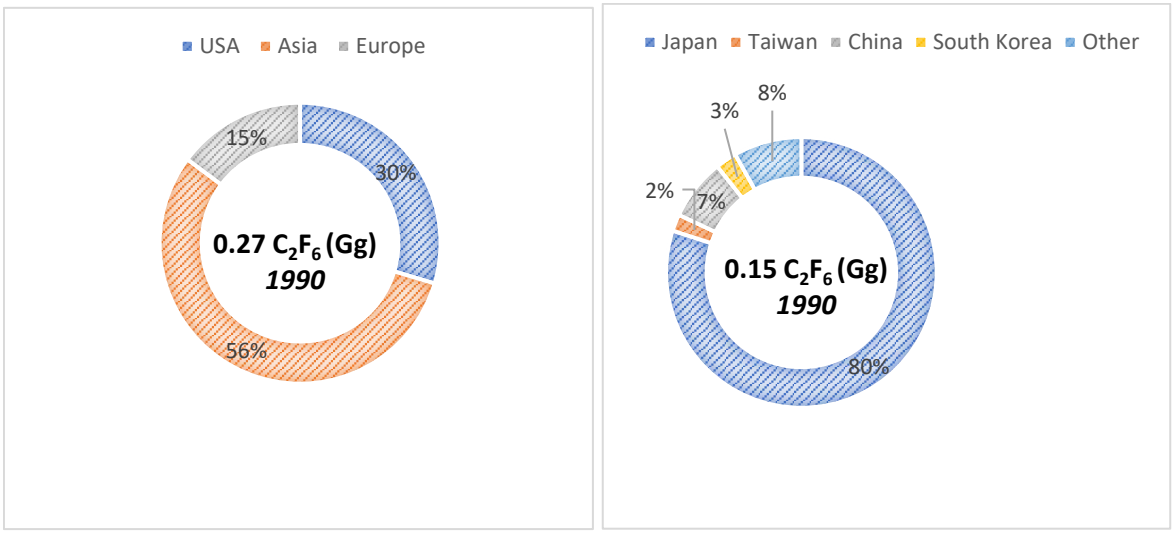

Figure 4.9: Distribution of C_2F_6 emissions for the year 1990 calculated using Equation 4.6 and the FSM. Left: Distribution per domain (namely USA, Asia and Europe). Right: Distribution between the different Asian countries within the Asian domain.

1990					
	CF_4 emissions (Gg/yr and %)			**C_2F_6 emissions (Gg/yr and %)**	
Domain	**Gg/yr**	**%**	**Domain**	**Gg/yr**	**%**
USA	0.12	29%	**USA**	0.08	30%
Asia	0.23	53%	**Asia**	0.15	56%
Europe	0.07	17%	**Europe**	0.04	15%
Global	0.43	100%	**Global**	0.27	100%
Japan	0.19	84%	**Japan**	0.12	80%
Taiwan	0.006	3%	**Taiwan**	0.003	2%
China	0.018	8%	**China**	0.011	7%
South Korea	0.006	3%	**South Korea**	0.003	3%
Other	0.006	3%	**Other**	0.003	8%

Table 4.5: Summary of CF_4 and C_2F_6 (in Gg/yr) emissions per domain (Asia, USA, Europe) and per country included in the Asian domain (China, Taiwan, Japan, South Korea) with their respective percentages for the year 2000.

For the same year (1990), emissions of ~0.27 Gg/yr of C_2F_6 were estimated (Figure 4.9 and Table 4.5). Examining the domains (USA, Europe and Asia) it was estimated that the USA contributed 30% (approximately 0.13 Gg/yr), Asia contributed 53% (approximately 0.23 Gg/yr) and Europe contributed 17% (approximately 0.07 Gg/yr). Out of the 0.23 Gg/yr of Asian emissions, 3% are attributed to Taiwan, South Korea (approximately 0.007 Gg/yr) while Japan and China are estimated to contribute 84% (approximately 0.19 Gg/yr) and 8% (approximately 0.018 Gg/yr) respectively.

b) 1990 – 2000

Shown in Table 4.5 are the wafer area (in m^2) estimates for the time period between 1990 and 2000. During this time, in the USA, approximately 18 million wafer starts per month were estimated amounting to an approximately 402,000 wafer area (m^2) while Asia and Europe produced a total of approximately 1,79 million m^2 and 340,000 m^2 of wafer area respectively. The full breakdown of production of wafer area per domain and fab type is shown in Table 4.6. Also presented are the same numbers for specific countries in Asia (namely Taiwan, Japan, South Korea and China). Out of the 1,79 million m^2 wafer area that was produced in Asia, 831,104 m^2 were produced in Japan, approximately 46% of the Asian production.

Wafer Area (m^2) for the period 1990-2000								
Domain	**50mm**	**75mm**	**100mm**	**125mm**	**150mm**	**200mm**	**300mm**	**Total**
USA	565	1,737	15,747	31,220	114,655	182,539	56,407	402,871
Asia	0	2,354	97,207	187,833	522,616	975,898	0	1,785,908
Europe	0	0	18,130	12,075	132,006	177,374	0	339,586
China	0	1,590	26,672	13,695	51,000	21,488	0	114,446

Taiwan	0	0	0	5,743	79,797	292,847	0	378,387
Japan	0	763	70,535	132,610	319,062	308,134	0	831,104
South Korea	0	0	0	3,387	22,711	257,862	0	283,960
Other	0	0	0	32,398	50,046	95,567	0	178,010
Global total	565	6,444	228,292	418,961	1,291,893	2,311,71	56,407	4,314,273

Table 4.6: Presenting estimates of wafer area produced (m^2) per domain for the period between 1990 and 2000 as well as global totals for the different types of fabs (50mm, 75mm, 100mm, 125mm, 150mm, 200mm and 300mm). Domains are Asia, Europe and the USA. Separately presented are the values for the countries belonging to the Asian domain, namely China, Japan, Taiwan, South Korea.

Examining the year 2000, emissions ~0.56 Gg/yr of CF_4 were estimated. Examining the domains (USA, Europe and Asia) it was estimated that the USA contributed 25% (approximately 0.13 Gg/yr), Asia contributed 58% (approximately 0.33 Gg/yr) and Europe contributed 17% (approximately 0.095 Gg/yr). Out of the 0.33 Gg/yr of Asian emissions, 12% are now attributed to Taiwan (approximately 0.02 Gg/yr), 7% to South Korea (approximately 0.023 Gg/yr) while Japan and China are estimated to contribute 67% (approximately 0.22 Gg/yr) and 9% (approximately 0.03 Gg/yr) respectively (Figures 4.10, 4.11 and Table 4.7).

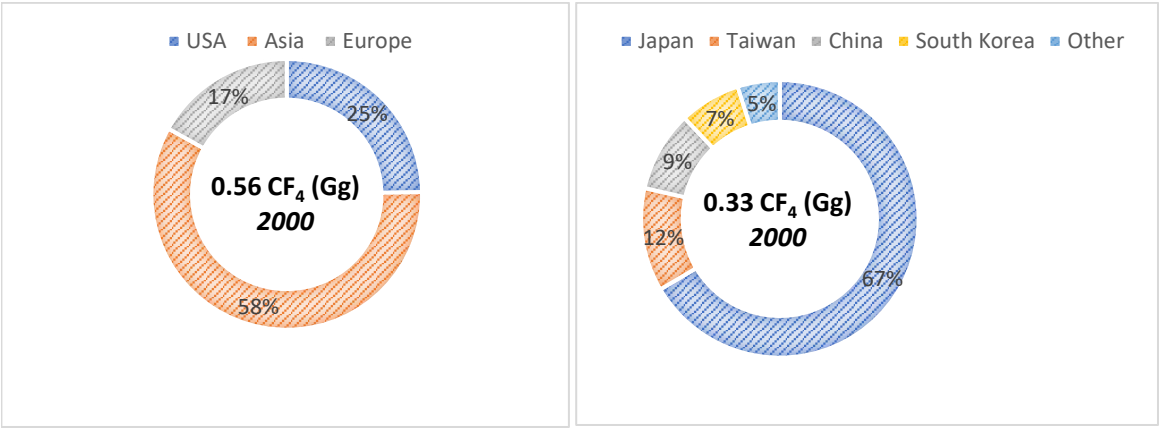

Figure 4.10: Distribution of CF_4 emissions for the year 1990 calculated using Equation 4.6 and the FSM. Left: Distribution per domain (namely USA, Asia and Europe). Right: Distribution between the different Asian countries within the Asian domain.

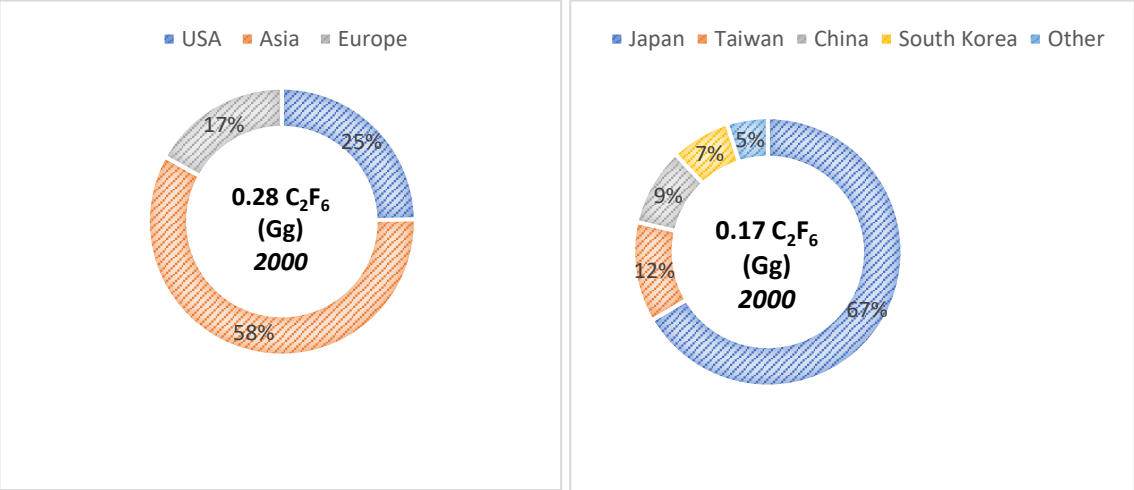

Figure 4.11: Distribution of C_2F_6 emissions for the year 2000 calculated using Equation 4.6 and the FSM. Left: Distribution per domain (namely USA, Asia and Europe). Right: Distribution between the different Asian countries within the Asian domain.

2000					
	CF_4 emissions (Gg/yr and %)			**C_2F_6 emissions (Gg/yr and %)**	
Domain	**Gg/yr**	**%**	**Domain**	**Gg/yr**	**%**
USA	0.1354	24%	**USA**	0.0716	25%
Asia	0.3254	59%	**Asia**	0.1689	58%
Europe	0.0944	17%	**Europe**	0.0490	17%
Global	0.5552	100%	**Global**	0.2896	100%
Japan	0.2164	67%	**Japan**	0.1124	67%
Taiwan	0.0204	6%	**Taiwan**	0.0204	12%
China	0.0305	9%	**China**	0.0158	9%
South Korea	0.0232	7%	**South Korea**	0.0121	7%
Other	0.016	11%	**Other**	0.0083	5%

Table 4.7: Summary of CF_4 and C_2F_6 (in Gg/yr) emissions per domain (Asia, USA, Europe) and per country included in the Asian domain (China, Taiwan, Japan, South Korea) with their respective percentages for the year 2000.

For the same year (2000), emissions ~0.28 Gg/yr of C_2F_6 were estimated (Figure 4.11 and Table 4.7). Examining the domains (USA, Europe and Asia) it was estimated that the USA contributed 25% (approximately 0.07 Gg/yr), Asia contributed 58% (approximately 0.16 Gg/yr) and Europe contributed 17% (approximately 0.04 Gg/yr). Out of the 0.17 Gg/yr of Asian emissions, 12% are attributed to Taiwan (approximately 0.02 Gg/yr), 7% to South Korea (approximately 0.012 Gg/yr) while Japan and China are estimated to contribute 67% (approximately 0.11 Gg/yr) and 9% (approximately 0.015 Gg/yr) respectively.

c) 2000 - 2010

Shown in Table 4.7 are the wafer area (in m^2) estimates for the time period between 2000 and 2010. During this time, in the USA, approximately 25,2 million wafer starts per month were estimated amounting to an approximately 787,000 wafer area (m^2) while Asia and Europe produced a total of approximately 4,9 million m^2 and 510,000 m^2 of wafer area respectively. The full breakdown of production of wafer area per domain and fab type is shown in Table 4.8. Also presented are the same numbers for specific countries in Asia (namely Taiwan, Japan, South Korea and China). Out of the 4,9 million m^2 wafer area that was produced in Asia, 1,4 million m^2 were produced in Japan, approximately 29% of the Asian production.

Wafer Area (m^2) for the period 2000-2010								
Domain	**50mm**	**75mm**	**100mm**	**125mm**	**150mm**	**200mm**	**300mm**	**Total**
USA	565	1,869	16,350	31,220	128,047	229,852	378,820	786,723
Asia	0	25,150	100,977	223,912	580,190	1,290,121	2,728,332	4,948,682
Europe	0	0	18,319	14,432	156,445	220,427	99,667	509,290
China	0	24,387	28,557	42,412	96,168	171,154	247,683	610,360
Taiwan	0	0	1,885	8,688	79,797	292,847	944,928	1,328,146
Japan	0	763	70,535	137,028	320,123	355,446	566,618	1,450,513
South Korea	0	0	0	3,387	24,302	316,296	829,145	1,173,129
Other	0	0	0	32,398	59,800	154,378	139,958	386,534
Global total	**565**	**52,169**	**236,624**	**493,476**	**1,444,872**	**3,030,520**	**5,935,150**	**11,193,376**

Table 4.8: Presenting estimates of wafer area produced (m^2) per domain for the period between 2000 and 2010 as well as global totals for the different types of fabs (50mm, 75mm, 100mm, 125mm, 150mm, 200mm and 300mm). Domains are Asia, Europe and the USA. Separately presented are the values for the countries belonging to the Asian domain, namely China, Japan, Taiwan, South Korea.

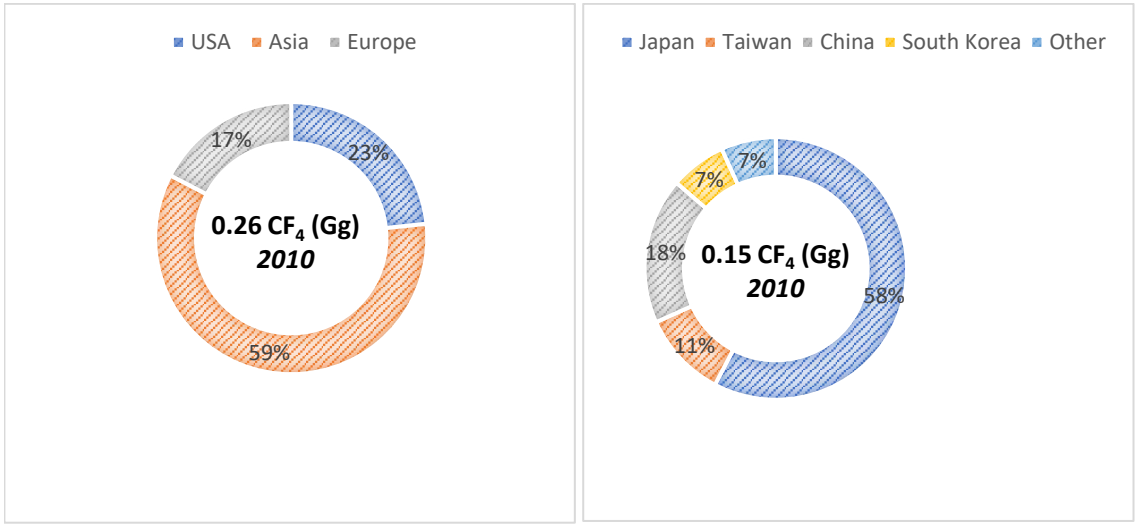

Figure 4.12: Distribution of CF_4 emissions for the year 2010 calculated using Equation 4.6 and the FSM. Left: Distribution per domain (namely USA, Asia and Europe). Right: Distribution between the different Asian countries within the Asian domain.

Examining the year 2010, emissions ~0.26 Gg/yr of CF_4 were estimated. Examining the domains (USA, Europe and Asia) it was estimated that the USA contributed 23% (approximately 0.06 Gg/yr), Asia contributed 59% (approximately 0.15 Gg/yr) and Europe contributed 17% (approximately 0.04 Gg/yr). Out of the 0.15 Gg/yr of Asian emissions, 12% are now attributed to Taiwan (approximately 0.02 Gg/yr), 8% to South Korea (approximately 0.01 Gg/yr) while Japan and China are estimated to contribute 56% (approximately 0.08 Gg/yr) and 18% (approximately 0.03 Gg/yr) respectively (Figures 4.10, 4.11 and Table 4.6).

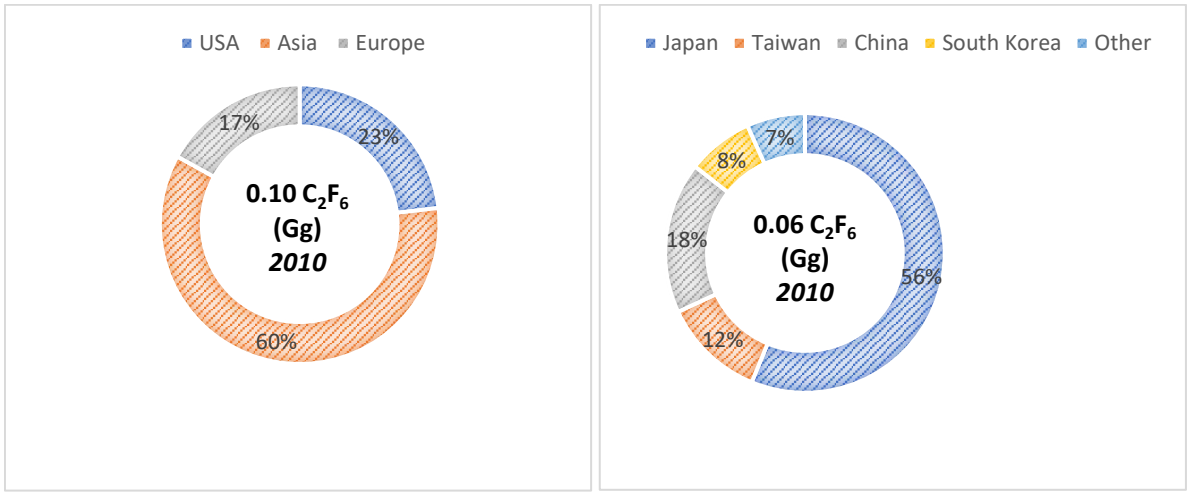

Figure 4.13: Distribution of C_2F_6 emissions for the year 2010 calculated using Equation 4.6 and the FSM. Left: Distribution per domain (namely USA, Asia and Europe). Right: Distribution between different Asian countries within the Asian domain.

2010					
	CF_4 Emissions			**C_2F_6 Emissions**	
Domain	**Gg**	**%**	**Domain**	**Gg**	**%**
USA	0.06	23%	**USA**	0.023	23%
Asia	0.15	59%	**Asia**	0.060	60%
Europe	0.04	17%	**Europe**	0.017	17%
Global	0.25	100%	**Global**	0.101	100%
Japan	0.08	58%	**Japan**	0.034	56%
Taiwan	0.01	11%	**Taiwan**	0.007	12%
China	0.02	18%	**China**	0.010	18%
South Korea	0.01	7%	**South Korea**	0.004	8%
Other	0.01	7%	**Other**	0.004	7%

Table 4.9: Summary of CF_4 and C_2F_6 (in Gg/yr) emissions per domain (Asia, USA, Europe) and per country included in the Asian domain (China, Taiwan, Japan, South Korea) with their respective percentages for the year 2010.

For the same year (2000), emissions ~0.1 Gg/yr of C_2F_6 were estimated (Figure 4.11 and Table 4.9). Examining the domains (USA, Europe and Asia) it was estimated that the USA contributed 25% (approximately 0.07 Gg/yr), Asia contributed 58% (approximately 0.16 Gg/yr) and Europe contributed 17% (approximately 0.04 Gg/yr). Out of the 0.17 Gg/yr of Asian emissions, 12% are attributed to Taiwan (approximately 0.02 Gg/yr), 7% to South Korea (approximately 0.012 Gg/yr) while Japan and China are estimated to contribute 67% (approximately 0.11 Gg/yr) and 9% (approximately 0.015 Gg/yr) respectively.

d) 2010 -2017

Shown in Table 4.10 are the wafer area (in m^2) estimates for the time period between 2010 and 2017. During this time, in the USA, approximately 26 million wafer starts per month were estimated amounting to an approximately 876,000 wafer area (m^2) while Asia and Europe produced a total of approximately 6,4 million m^2 and 557,000 m^2 of wafer area respectively. The full breakdown of production of wafer area per domain and fab type is shown in Table

4.10. Also presented are the same numbers for specific countries in Asia (namely Taiwan, Japan, South Korea and China). Out of the 6,4 million m^2 wafer area that was produced in Asia, 1,4 million m^2 were produced in Japan, approximately 27% of the Asian production.

Wafer Area (m^2) for the period 2010-2017								
Domain	**50mm**	**75mm**	**100mm**	**125mm**	**150mm**	**200mm**	**300mm**	**Total**
USA	565	1,869	16,350	31,220	128,047	229,852	467,884	875,787
Asia	0	25,150	100,977	223,912	592,913	1,346,669	4,144,028	6,433,650
Europe	0	0	18,319	14,432	156,445	220,427	147,168	556,790
China	0	24,387	28,557	42,412	108,892	212,623	625,994	1,042,863
Taiwan	0	0	1,885	8,688	79,797	292,847	1,123,057	1,506,274
Japan	0	763	70,535	137,028	320,123	355,446	925,419	1,809,314
South Korea	0	0	0	3,387	24,302	331,375	1,261,742	1,620,806
Other	0	0	0	32,398	59,800	154,378	207,816	454,392
Global total	565	52,169	236,624	493,476	1,470,319	3,143,617	8,903,107	14,299,877

Table 4.10: Presenting estimates of wafer area produced (m^2) per domain for the period between 2010 and 2017 as well as global totals for the different types of fabs (50mm, 75mm, 100mm, 125mm, 150mm, 200mm and 300mm). Domains are Asia, Europe and the USA. Separately presented are the values for the countries belonging to the Asian domain, namely China, Japan, Taiwan, South Korea.

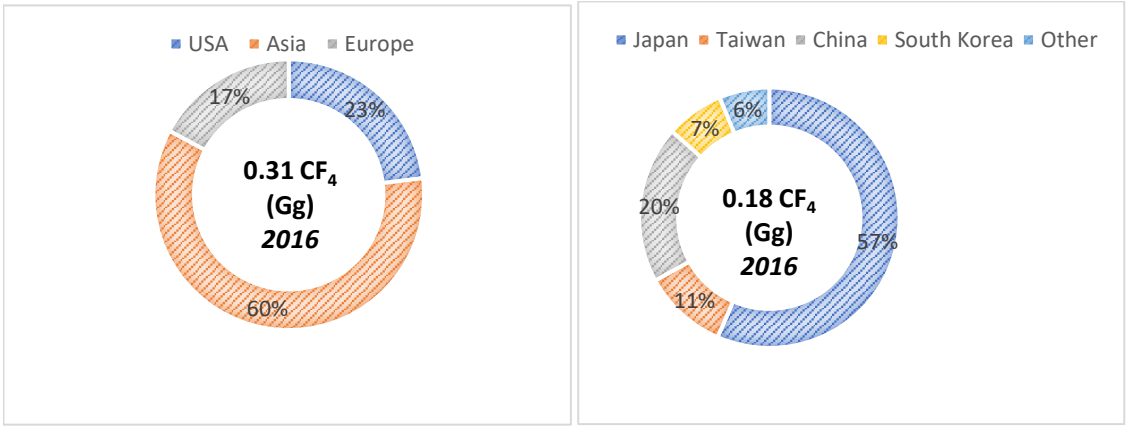

Figure 4.14: Distribution of CF_4 emissions for the year 2017 calculated using Equation 4.6 and the FSM. Left: Distribution per domain (namely USA, Asia and Europe). Right: Distribution between the different Asian countries within the Asian domain.

Examining the year 2017, emissions ~0.31 Gg/yr of CF_4 were estimated Examining the domains (USA, Europe and Asia) it was estimated that the USA contributed 23% (approximately 0.07 Gg/yr), Asia contributed 60% (approximately 0.18 Gg/yr) and Europe contributed 17% (approximately 0.05 Gg/yr). Out of the 0.18 Gg/yr of Asian emissions, 11% are now attributed to Taiwan (approximately 0.01 Gg/yr), 7% to South Korea (approximately 0.01 Gg/yr) while Japan and China are estimated to contribute 57% (approximately 0.1 Gg/yr) and 20% (approximately 0.03 Gg/yr) respectively (Figure 4.10 and Table 4.6).

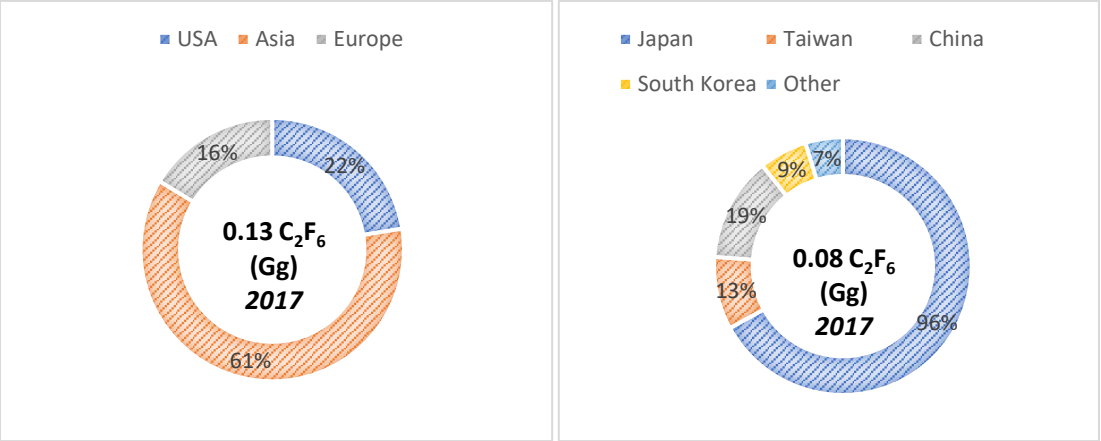

Figure 4.15: Distribution of C_2F_6 emissions for the year 2017 calculated using Equation 4.6 and the FSM. Left: Distribution per domain (namely USA, Asia and Europe). Right: Distribution between the different Asian countries within the Asian domain.

2017					
	CF_4 Emissions (Gg/yr and %)			C_2F_6 Emissions (Gg/yr and %)	
Domain	**Gg/yr**	**%**	**Domain**	**Gg/yr**	**%**
USA	0.07	23%	**USA**	0.03	22%
Asia	0.18	60%	**Asia**	0.08	61%
Europe	0.05	17%	**Europe**	0.02	16%
Global	0.30	100%	**Global**	0.13	100%
Japan	0.10	57%	**Japan**	0.08	96%
Taiwan	0.019	11%	**Taiwan**	0.01	13%
China	0.03	20%	**China**	0.01	19%
South Korea	0.01	7%	**South Korea**	0.007	9%
Other		6%	**Other**	0.005	7%

Table 4.11: Summary of CF_4 and C_2F_6 (in Gg/yr) emissions per domain (Asia, USA, Europe) and per country included in the Asian domain (China, Taiwan, Japan, South Korea) with their respective percentages for the year 2017.

For the same year (2017), emissions ~0.14 Gg/yr of C_2F_6 were estimated (Figure 4.15 and Table 4.11). Examining the domains (USA, Europe and Asia) it was estimated that the USA contributed 22% (approximately 0.03 Gg/yr), Asia contributed 61% (approximately 0.08 Gg/yr) and Europe contributed 16% (approximately 0.02 Gg/yr). Out of the 0.08 Gg/yr of Asian emissions, 13% are attributed to Taiwan (approximately 0.01 Gg/yr), 9% to South Korea (approximately 0.007 Gg/yr) while Japan and China are estimated to contribute 96% (approximately 0.08 Gg/yr) and 19% (approximately 0.015 Gg/yr) respectively.

Finally, for completion, all the estimates produced using Equations 4.1 – 4.7 for the FSM are presented in Table 4.12.

	CF_4 emissions (Gg/y) using the FSM			**C_2F_6 emissions (Gg/y) using the FSM**		
Year	**Tier 1 (no abatement)**	**Tier 2a**	**Tier 2b**	**Tier 1 (no abatement)**	**Tier 2a**	**Tier 2b**
1980	0.16	0.09	0.08	0.35	0.15	0.18
1981	0.22	0.12	0.12	0.40	0.17	0.16
1982	0.23	0.16	0.15	0.43	0.20	0.17
1983	0.27	0.19	0.19	0.47	0.17	0.18
1984	0.34	0.23	0.22	0.51	0.21	0.22
1985	0.37	0.26	0.26	0.54	0.20	0.19
1986	0.44	0.30	0.29	0.54	0.17	0.16
1987	0.47	0.33	0.33	0.60	0.21	0.22
1988	0.54	0.37	0.36	0.78	0.24	0.20
1989	0.56	0.40	0.39	0.86	0.25	0.23
1990	0.64	0.44	0.43	0.98	0.25	0.27
1991	0.71	0.47	0.46	1.12	0.26	0.28
1992	0.75	0.51	0.50	1.36	0.28	0.28
1993	0.84	0.54	0.53	1.36	0.22	0.24
1994	0.92	0.58	0.57	1.58	0.25	0.21
1995	1.11	0.59	0.57	1.83	0.25	0.20
1996	1.31	0.58	0.57	1.99	0.26	0.22
1997	1.40	0.60	0.57	2.27	0.28	0.25
1998	1.61	0.60	0.57	2.76	0.28	0.27
1999	1.70	0.60	0.56	2.91	0.30	0.28
2000	1.87	0.60	0.55	3.02	0.31	0.28
2001	2.15	0.59	0.54	3.12	0.29	0.28

2002	2.38	0.58	0.52	3.49	0.26	0.27
2003	2.61	0.57	0.50	3.48	0.24	0.25
2004	2.91	0.56	0.47	3.69	0.20	0.21
2005	3.50	0.54	0.44	3.72	0.20	0.20
2006	3.88	0.52	0.41	3.83	0.18	0.16
2007	4.34	0.50	0.38	4.19	0.15	0.12
2008	4.44	0.48	0.34	4.35	0.1	0.12
2009	4.57	0.45	0.30	4.74	0.1	0.08
2010	4.81	0.42	0.25	4.98	0.09	0.06
2011	5.21	0.43	0.26	5.20	0.09	0.06
2012	5.50	0.44	0.27	5.25	0.08	0.08
2013	5.52	0.46	0.28	5.27	0.09	0.1
2014	5.75	0.47	0.28	5.36	0.1	0.06
2015	5.96	0.48	0.29	5.48	0.12	0.08
2016	6.11	0.49	0.30	5.57	0.11	0.07

Table 4.12: Estimates for CF_4 and C_2F_6 (in Gg/yr) using the FSM and equations 4.4 – 4.8.

4.4.3 Comparing the results of the two methods

Comparing results derived from using the CF method versus the results from the FS method for Equations 4.1 – 4.8 and both gases CF_4 and C_2F_6 it is shown that both methods produced comparable results, for all the equations and both gases (Figures 4.16 and 4.17). Figures 4.16 and 4.17 illustrate two examples of this comparison between the CF method and the FS method using the Tier 1 with abatement equations and Tier 2 methods for CF_4.

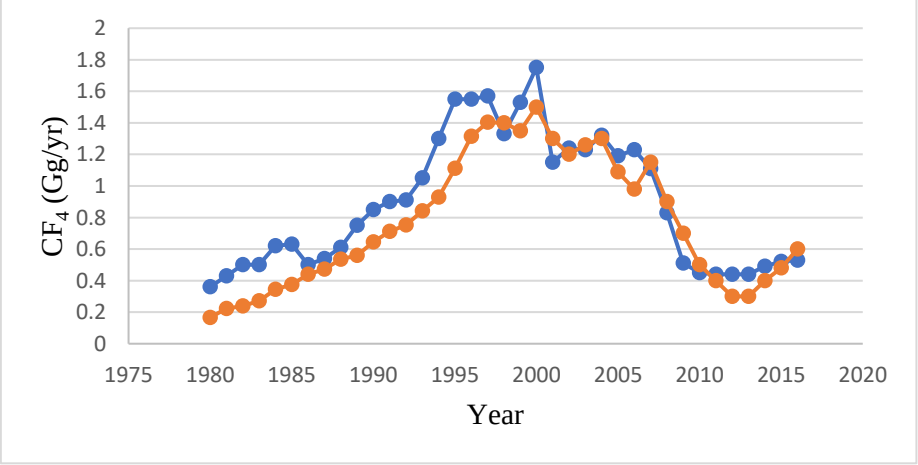

Figure 4.16: Comparison of the CF_4 estimates produced using the CF method and Tier 1 with abatement equations (blue line) versus results produced using the FS method and Tier 1 with abatement (orange line).

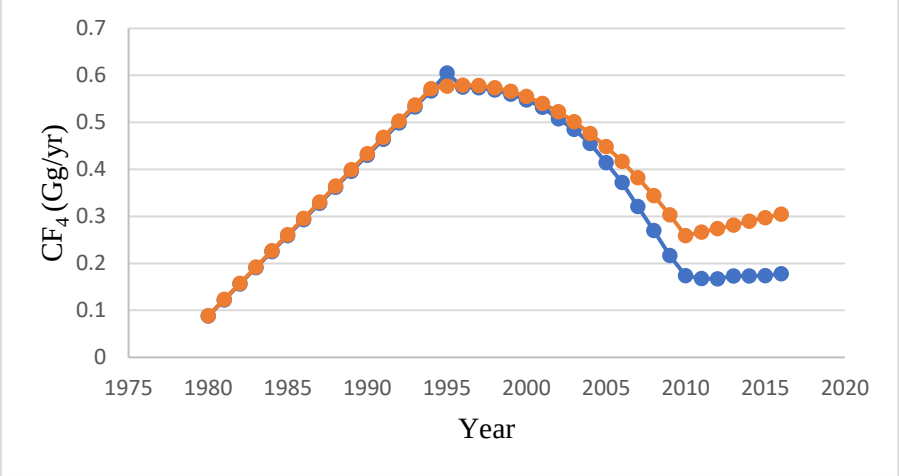

Figure 4.17: Comparison of the CF_4 estimates produced using the CF method and Tier 2 equations (blue line) versus results produced using the FS method and Tier 2 (orange line).

4.4.4 Spatial Distribution

As discussed in section 4.3, using the coordinates included in the database that was acquired, Figure 4.17 shows the locations of fabs globally (Figure 4.17) (Mühle et al., 2019). The semiconductor fabs locations are presented in dark blue while the aluminium smelters are also shown in light blue for comparison.

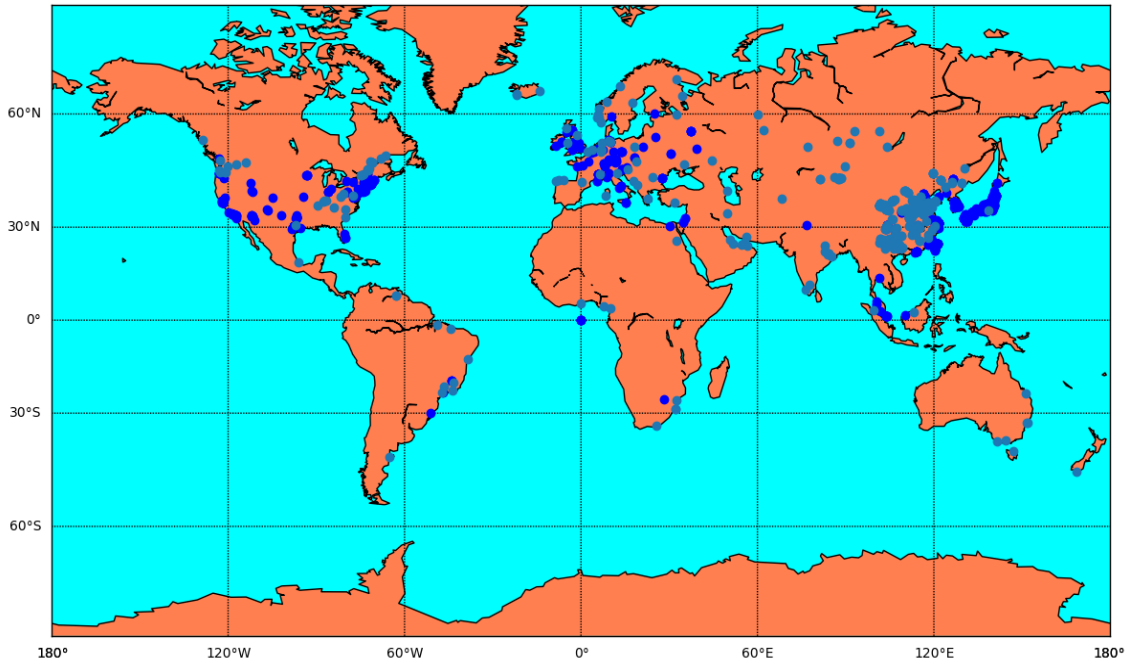

Figure 4.18: Locations of semiconductor fabs (blue dots) and aluminium smelters (light blue dots) globally.

Figure 4.18 shows the sum of the locations of all the aluminium smelters and all the SC fabs. This map (with the added locations of the RESI smelters) will be used, with the emissions estimates from each industrial activity as a prior field for the inverse modelling discussed in chapter 6.

4.5 Conclusion

CF_4 and C_2F_6 estimates were produced using two different methods that were developed as part of this work: the CFM and the FSM. These methods were developed in order to produce an independent bottom-up inventory of SCI specific PFC emissions that will be added to the global bottom-up inventory (discussed in Chapter 7). Both these methods produced results of comparable magnitude. The reason why the existence of an independent bottom-up inventory is essential because prior to this work (and particularly prior to the inclusion of PFC emissions from the RESI that will be discussed in chapter 5) the assumption was that PFC emissions from this industry were greatly underestimated (Kim et al., 2014). It was suggested that PFC emissions from the SCI were the dominant source of discrepancy in the global PFC budget (Kim et al., 2014). This work and the results of this chapter contest this assumption.

Based on these estimates, this chapter concludes that the SCI has always been and remains to be a minor contributor of PFC emissions especially when compared with the aluminium industry. Abatement has played a significant and important role in drastically decreasing PFC emissions from this industry ever since it was introduced (early 2005).

Chapter 4 has used several assumptions, mainly associated with the annual quantity of CF_4 and C_2F_6 consumed by the SCI. However, these results appear to show good agreement with estimates produced independently by the WSC (WSC, 2010, 2011, 2012, 2013, 2014, 2015).

This chapter set out to answer the following questions:

- Can an industry specific, updated bottom-up inventory be produced?
- How does the inventory deveoped in this work compare to previous work?
- Could an updated method for estimating PFC emissions from this industry brigde persisting discrepancies?

In conclusion, despite the assumptions that went into the newly developed methods this

work used (CFM and the FSM) the compilation of an industry specific bottom-up inventory was successful. Furthermore, this work reinforces and confirms previous estimates that described the SCI as a minor contributor of PFC emissions. Overall, the SCI appears to have been successful in substantially reducing PFC emissions for both CF_4 and C_2F_6 gases and keeping them at pre-1995 levels, however, a small decrease in PFC emissions is shown for both gases and the years after 2012 that should be monitored and re-examined in future work.

Chapter 5

PFC emissions from Rare Earth Smelting (RES)

5.1 Aims

The aims of this chapter are to quantify and discuss PFC emissions from the rare earth smelting industry, discuss limitations and challenges in estimating the PFC emissions. As discussed in chapter 1, section 1.1 this chapter will address the following research questions:

- Are there electrolytical processes used in rare earth smelting have the potential to produce PFC emissions?
- Can PFC emissions from this industry using existing emission factors be quantified?
- What are the implications, related to sustainable development, if rare earth smelting is a significant contributor of PFCs?
- Can an industry specific bottom-up inventory be produced?

Parts of this chapter appear in the paper 'Challenges in estimating CF_4 and C_2F_6 emissions' written by the author of this thesis, Michalopoulou Eleni (Michalopoulou, 2018) and Chapter 4 Volume 3 section 4.8 PFC emissions from the metal industry where the author of this work is a contributing author (IPCC - Task Force on National Greenhouse Gas Inventories, 2019).

5.2 Introduction

5.2.1 Discovery and uses of Rare Earths

Rare earths were discovered in 1788 in Ytterby, Sweden and it was only identified in 1794 as a new type of 'earth', however they are neither rare nor are they 'earth' (Abraham, 2011; Rowlatt, 2014; Klinger, 2015). The term 'rare earths' (RE) or 'rare earth elements' (REE) is used to describe the group of the 17 metallic elements of scandium (Sc) , yttrium (Y) and the lanthanides, i.e.: lanthanum (La), cerium (Ce), praseodymium (Pr), neodymium (Nd), promethium (Pm), samarium (Sm), europium (Eu), gadolinium (Gd), terbium (Tb), dysprosium (Dy), holmium (Ho), erbium (Er), thulium (Tm), ytterbium (Yb) and lutetium (Lu), that are chemically similar. The raw materials and trading goods are referred to as 'rare earth oxides'

(REO) (Beaudry and Gschneidner Jr, 1978; Liu, 1978; Cardarelli, 2008; Vogel and Friedrich, 2018).

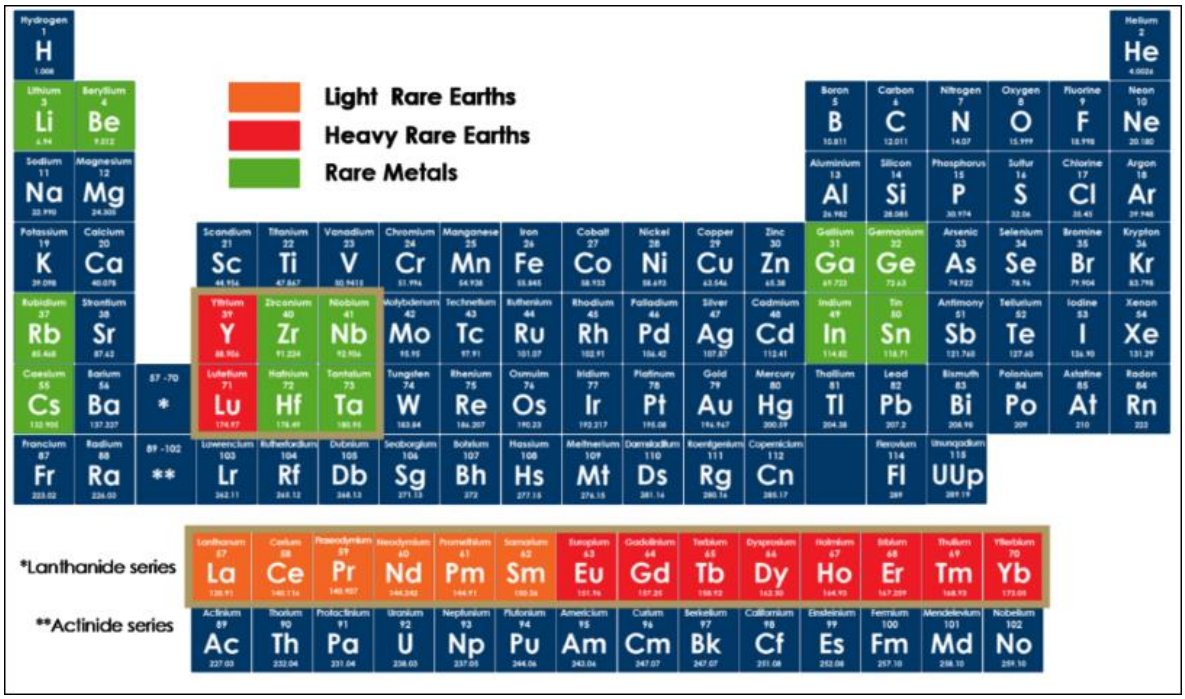

Figure 5.1: Rare Metals (RM) , Light Rare Metals (LRM) and Heavy Rare Metals (LRM) (Australian Rare Earths - Rare Earth Elements Are - Overview).

5.2.2 Production and Uses of Rare Earths

Rare earth elements are used widely in rechargeable batteries, hybrid vehicles, renewable energy (such as wind turbines), mobile phones, flat screen display panels, laptops, glass staining, conductors and amplifiers and the car industry (Becker, Olsson and Simpson, 1999; Hammond, 2000; DePaolo, 2012; Zepf, 2013). Because they are used so widely, in so many different applications there is no ‘single rare earth market’ as there is in the case of aluminium and/or semiconductors (Klinger, 2015). Approximately 60% is converted to metal mainly for the use in permanent magnets used for power generators in wind turbines, that are increasingly becoming an important source of renewable energy, and electric motors (Goodenough, Wall and Merriman, 2018). Other uses include flint for lighters, added to glass to remove the green colour caused by iron contaminants.

Figure 5.2 shows a non-exhaustive list of uses of REE is presented (Applications - Rare Earth Elements - DANTEK Global Sourcing Solutions).

Magnets	**Catalysts**
• Motors • Disc drives & disk drive motors • Power generation • Actuators • Microphones & speakers • MRI • Anti-lock brake system • Automotive parts • Communication systems • Electric drive & propulsion • Frictionless bearings • Microwave power tubes • Magnetic refrigeration • Magnetic storage disk	• Petroleum refining • Chemical processing • Catalytic converter
	Electronics • Display phosphors • CRT • PDP • LCD • Medical imaging phosphors • Lasers • Fiber optics • Optical temperature sensors

Figure 5.2: List of non-exhaustive rare earth uses.

Production of rare earth oxides (REOs) begun in early 1965 in the USA and until 1985 the USA was the major producer of rare earth element oxides. After 1990, the global production is dominated by China. In 2015, about 130 kt of REOs were produced globally with a high uncertainty due to illegal mining and black-market trading (Zepf, 2013; Castilloux, 2014; Kingsnorth, 2015; Vogel and Friedrich, 2018) with China accounting for more than 80% of global production (Rare Earths Statistics and Information, USGS, 2015).

Primary production of rare earth metals and alloys is carried out using a process very similar to the electrolytical process used in primary aluminium production (the Hall-Heroult process). Both the rare earth electrolytical process as well as the aluminium process produce metal from electrolysis of metal oxides in molten fluoride salts using consumable carbon anodes (Vogel and Friedrich, 2017, 2018; Zhang, Wang and Gong, 2018). Metals and alloys produced through these process are Pr, Pr-Nd, La, Dy-Fe, Gd-Fe, Ho-Fe, Ce, La-Ce, Y-Mg, and most commonly, neodymium (Nd) (Vogel and Friedrich, 2018).

The overall production estimate of the most commonly used element, neodymium, is about 30 kt in 2014 with a high uncertainty due to an estimated 40% of illegal mining and black-market trading (Kingsnorth, 2015; Vogel and Friedrich, 2018).

The reasons why it is very challenging to get accurate information on the production numbers of each REO individually is because there exists very little published information, some sources are citing each other and there is large uncertainty related to some of the available estimates (Zepf, 2013; European Union, 2014; Kingsnorth, 2015; Zhou, Li and Chen, 2017; USGS, 2018; Vogel and Friedrich, 2018). Vogel and Friedrich (2018) produced a comprehensive estimate of global, annual production numbers of the basket REOs.

5.2.3 PFC emissions from the rare earth smelting industry

When this work started there was, to knowledge, no bottom-up inventory or any emissions estimates for PFC emissions from the RESI and these emissions had not been taken into account in climate change research and/or policy making (Vogel and Friedrich, 2018). PFC emissions from this industry were absent in the literature.

Laboratory experiments showed however, that the process of rare earth electrolysis is likely to produce continuous CF_4 and C_2F_6 emissions that are formed from the reaction of the carbon anode with the fluoride melt (Vogel et al., 2017; Vogel and Friedrich, 2018) following Equations 5.1 to 5.4.

$$4NdF_3 + 3C = 4NdF + 3CF_4 \quad (5.1)$$

$$4LiF + C = 4Li + 3CF_4 \quad (5.2)$$

$$2NdF_3 + 2C = 2Nd + C_2F_6 \quad (5.3)$$

$$6LiF + 2C = 6Li + C_2F_6 \quad (5.4)$$

As described in Vogel et al., (2016) when laboratory experiments were conducted PFC emissions were measured during the production of Nd metal and Dy-Fe alloy in China (Zhang, Wang and Gong, 2018), Pr-Nd alloy, Dy-Fe alloy and La metal in China (Cai et al., 2018).

5.3 Methods

As discussed in section 5.1 most of the current knowledge regarding RE production, PFC emissions and emission factors comes from extremely limited published work (Cai et al., 2018; Vogel and Friedrich, 2018; Zhang, Wang and Gong, 2018). The Cai et al. (2018) and Zhang, Wang and Gong (2018) papers are basing their emission factors estimates on measured PFC emissions in different smelters while the Vogel and Friedrich (2018) paper is basing its estimates in laboratory simulation of the operation of a rare earth smelting cell making these emission factors very different in terms of magnitude (that will be discussed further in section 5.3).

Additionally, these different studies are measuring or estimating emissions from different metals and/or alloys. There are currently more than 10 types of rare earth metals and alloys being produced by electrolysis per year (Cai et al., 2018). That means that for every REO produced the equivalent activity data (MP) of the specific metal is needed in order to apply the emission factors presented in Table 5.1 and estimate PFC emissions. This was not possible to be found for every rare earth element produced due to lack of published activity information and/or the equivalent emission factors. What is used instead is the total metal production of all REO produced. The average emission factor is calculated based on the results shown in Zhang et al. (2018), Cai et al. (2018) and Vogel et al. (2018).

		Emission Factor (g PFC / t RE metal)		
	RE Metal	**CF_4**	**C_2F_6**	
Zhang et al., 2018	Nd	16.4	n/a	Measured
	Nd	46.4	n/a	
	Dy-Fe	182.9	n/a	
Cai et al., 2018	Pr-Nd	26.66	2.98	
	Dy-Fe	109.43	10.95	
	La	36.16	0.26	Measured
	Pr-Nd	33.96	10.83	
Vogel & Friedrich., 2018	Nd	739,000	116,000	Worst case modelled scenario
	Nd	30,000	3,000	Medium case modelled scenario
	Nd	n/a	n/a	Best case modelled scenario

Table 5.1: Emission factors for CF_4 and C_2F_6 that have been published as part of the work by Zhang et al. (2018); Cai et al. (2018) and Vogel et al. (2018).

The choice of the emission factor when calculating emissions is hugely important but there are currently only two rounds of measurements publicly available (Cai et al., 2018; Zhang, Wang and Gong, 2018) from which an emission factor can be estimated. Uncertainties related to the PFC emission factors alone are significant and, depending on whether or not there are grounds to exclude what is referred to as 'the worst case scenario' in Vogel and Friedrich (2018), can be of the order of +40,000% / - 60% for both CF_4 and C_2F_6.

Finally, it should be highlighted that previous versions of the IPCC good practice guides (IPCC, 2019a) regarding GHG emissions did not have a chapter on emissions coming from rare earths. This will be for the first time included in the 2019 refinement to the IPCC good practice guide chapter 4 volume 3 section 4.8 where the author of this work appears as a contributing author (IPCC - Task Force on National Greenhouse Gas Inventories, 2019).

5.3.1 Estimating PFC emissions from the RESI

In this work production number estimates and emission factors from recently published work (Cai et al., 2018; Vogel and Friedrich, 2018; Zhang, Wang and Gong, 2018) were used to estimate CF_4 and C_2F_6 emissions from rare earth smelting

To calculate PFC emissions from rare earth smelting, a method comparable with the Tier 1 method used for the aluminium industry was used. This method multiplies estimates of production numbers of rare earth metals (Vogel et al., 2018) by the averaged emission factor that was calculated based on available published information (Cai et al., 2018; Vogel and Friedrich, 2018; Zhang, Wang and Gong, 2018). The electrolytical process used in the electrolysis of rare earth elements is very similar to that used in the primary aluminium smelting process, therefore the use of this methodology is assumed to be a good approximation and is shown in Equation 5.5.

$$E_{PFC} = MP \times EF_{PFC} \quad (5.5)$$

In Equation 5.5, MP is the estimated metal production of rare earth metals (in t), and EFPFC is the averaged emission factor (48.1 kg/t for CF4 and 19.4 kg/t for C_2F_6).

As discussed in section 5.2 there are several challenges related to the estimates of CF_4 emissions from the rare earth smelting industry most of which cannot be overcome without more measurements and facility specific information. It was decided to estimate PFC emissions on the basis of ‘scenarios’ per emission factor and produce an averaged emissions estimate scenario. The uncertainties are therefore in this case the deviation of the averaged emissions estimate from the worst-case and best-case scenarios.

5.4 Results and discussion

PFC emissions estimates from the rare earth smelting industry are presented in Figures 5.3 and 5.4. Their relative errors are calculated based on the four different emission factors that are described in limitations and methods.

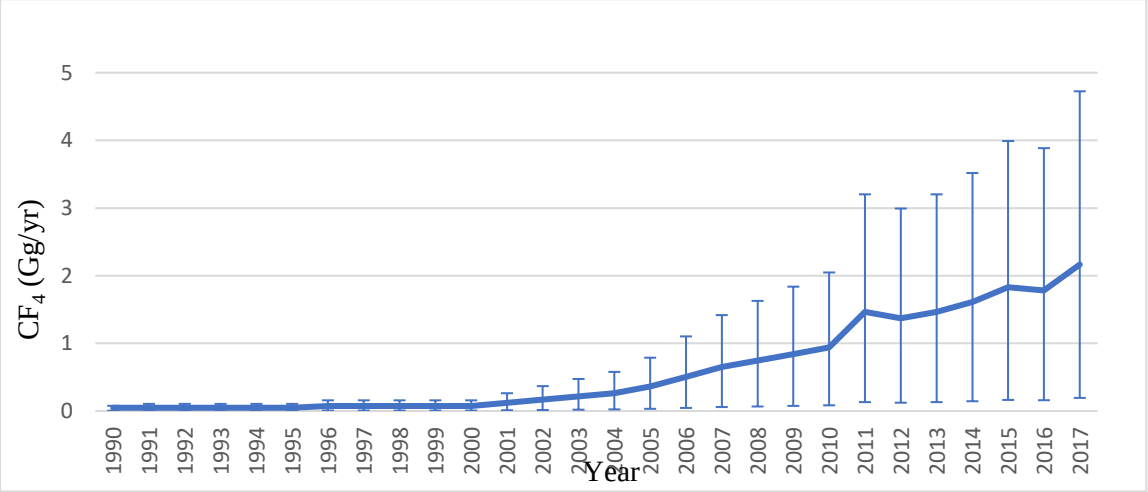

Figure 5.3: Global CF_4 emissions estimates from the rare earth smelting industry and their associated uncertainties.

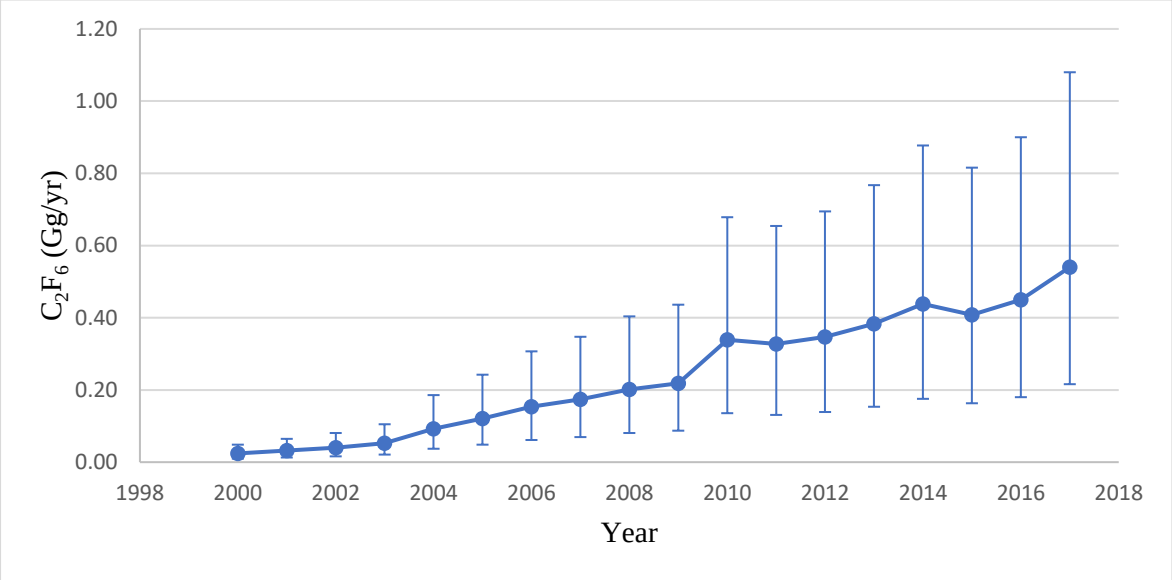

Figure 5.4: Global C_2F_6 emissions estimates from the rare earth smelting industry and their associated uncertainties.

As shown in Figures 5.3 and 5.4 PFC emissions from RES could be significant with an estimate of 2.1 (+2.7/-1.8) Gg/yr for CF_4 in 2017 and approximately 0.5 (+0.5/-0.3) Gg/yr for C_2F_6 for 2017. Based on these estimates, PFC emissions from the RES appear to be comparable with PFC emissions from the aluminium industry. These results will be discussed further as part of the analysis of chapter 7.

While the uncertainties related to these estimates are very large however, given the information available at the moment it is impossible to produce more accurate estimates using the bottom-up approach until more accurate and consistent measurements take place and until information related to the metal and alloy specific production information becomes available.

5.5 Conclusion

When this work started investigating PFC emissions from the RESI there was already a part of the literature that was investigating missing emissions of PFCs that could help bridge the gap in the PFC budgets. However, PFC emissions from rare earth smelting were, at the time, dismissed as not significant (Mühle et al., 2010a; Kim et al., 2014; Wong et al., 2015). This works presents an estimate of the PFC emissions from the RESI using estimates of the REOs production numbers and all the emission factors that have been previously published as part of peer reviewed work (Vogel and Friedrich, 2017, 2018; Cai et al., 2018; USGS, 2018; Zhang, Wang and Gong, 2018). However, large uncertainties still remain.

Despite the large uncertainties associated with estimates produced from this work because REOs are widely in renewable energy production, and electric cars (among other uses) it is critical that estimates of PFC emissions are presented and, in future work, re-estimated with improved uncertainties.

There is ample discussion in the literature targeting geopolitical, financial, social and environmental issues regarding the extraction, mining, and smelting processes of rare earths from the deposits to the end product. This discussion ranges from debunking rare earths as conflict materials to discussing recycling issues and their associated GHG emissions (Ali, Ali and H., 2014; Baldi, Peri and Vandone, 2014; Mclellan et al., 2014; Charalampides et al., 2015; Klinger, 2015, 2018; Smith Stegen, 2015; Apergis and Apergis, 2017).

However, despite this discussion around rare earths gaining more and more momentum there is still very little published work regarding specifically the contribution of PFC emissions from rare earth smelting to the carbon footprint of renewable energies such as wind power (T E Norgate, Jahanshahi and Rankin, 2007; Ghenai, 2012; Haapala and Prempreeda, 2014;

Andersen, Eriksson and Hillman, 2015; Razdan and Garrett, 2015; Thomson and Harrison, 2015; Irving, 2019). It should be highlighted that while the concern regarding PFC emissions does exist in the literature however, it is not made specific, and to my knowledge it is not explicitly quantified apart from a preliminary attempt in the work of Venås and Arvesen (2015) (Venås and Arvesen, 2015).

Equally, similar discussions are taking place in the literature regarding electric vehicles, however the focus still lays on availability and dependency of the electric vehicles on rare earths and the environmental impact of mining and extraction processes rather than the environmental impact from PFC emissions during the electrolytical process described in section 5.1 and Equations 5.1 – 5.4 (Leuenberger and Frischknecht, 2010; Alonso et al., 2012; Hawkins et al., 2013; Koltun and Tharumarajah, 2014; Messagie et al., 2014; Nordelöf et al., 2014; Ellingsen et al., 2014; Speirs, 2015; Egede et al., 2015; Tagliaferri et al., 2016; Dominish and Florin, 2017; Goldman, 2017; Helmers and Weiss, 2017; Hernandez et al., 2017; Kukreja, 2018; EEA, 2018; Asaithambi, Treiber and Kanagaraj, 2019).

As briefly discussed in section 5.1, demand for rare earth metal is increasing and it is expected to continue to increase for at least the next ten years as transition to more renewable energies is made and as there are plans for entire nations and cities to replace their entire fleets with electric vehicles (Alonso et al., 2012; Hatch, 2012; Zhou, Li and Chen, 2017; Desai, 2018; Egbaria, 2018; Fishman and Graedel, 2019).

It is beyond the scope of this work to look into how the life cycle analyses and inventories of both electric vehicles and wind turbines would change if the contribution of PFC emissions from the rare earth smelting was added to the existing information. However, this is a critical area where further investigation is required especially regarding transport where the UK seeks to lead ‘the world in the design, development and manufacture of electric batteries through investments of up to £246 million in the Faraday Challenge’ (BEIS 2017).

At no point does either the Clean Growth Strategy or the Industrial Policy document mention electric motors and their rare-earth dependent supply chains. Instead, great emphasis is placed on the smooth integration of EVs into energy systems. This work demonstrates that it is absolutely critical for more accurate and extensive measurements of PFC emissions from rare earth smelters to happen soon so that better and less uncertain estimates can be produced and included to the contribution of these emissions to the carbon footprint of wind turbines and electric cars (among other end products).

Chapter 6

Modelling PFC emissions

6.1 Aims

The purpose of this chapter is to explore the updated bottom-up inventory, developed in chapters 3 to 5, as prior information in an atmospheric inversion study of CF_4. It was decided to only perform this exercise for CF_4 as its inventory included all the key new elements compared to previous inventories (e.g. LVAE emissions) while the inventory for C_2F_6 did not. Two methods are used throughout this chapter; an analytical Bayesian method and a hierarchical Bayesian method. The analytical Bayesian method was conducted in collaboration with Dr. Alistair Manning and Dr. Alisson Redford from the UK MetOffice, the top-down estimates presented in section 6.4.1 were provided through personal communication by another Atmospheric Chemistry Research Group (ACRG) member, Dr. Matt Rigby.

There are little published works that examine the allocation of PFC emissions to their original sources through the use of inverse modelling (Arnold et al. 2018; Kim et al. 2014). Arnold et al. (2018) used an analytical Bayesian framework (described in section 6.1.2.6) to run inversions specific to the domain of East Asia (Arnold et al. 2018). In this work, Arnold et al., (2018) tried to minimise the reliance of the prior information on the Bayesian-based posterior emission estimates and they also discussed how poor availability of good prior information was forcing their emission estimates to be largely influenced by the atmospheric measurements (Arnold et al. 2018).

However, prior distributions can play a significant role in inverse Bayesian methods. Using this works prior emission field, this chapter explores the use of two modelling approaches, the hierarchical and analytical approach, that are widely used in conjunction with the Bayesian framework. The goal of this chapter is to model emissions in the domain of East Asia; in the case of the hierarchical method this is work has not been attempted before and in the case of the analytical method results produced will be compared to previous work which used a different prior. Given the complexity of the bottom-up emissions in the East Asian domain, a simpler domain was chosen as a test case study, the Australia case study. Finally, posterior emissions from South Korea will be discussed as part of the East Asia case study.

While every effort has been made to reduce uncertainties as much as possible,

significant uncertainties remain. Additionally, as some of these results are new and cannot be compared against previous work, it is best if they are not considered conclusive but rather a preliminary attempt to investigate the behavior of inverse modelling when coupled with a well-defined prior distribution.

6.2 Introduction

Having produced an updated bottom-up inventory of CF_4 emissions, this inventory will now be used as a prior estimate for a set of modelling methods referred to as Bayesian inversions. These inverse methods are widely used in order to allocate GHG emissions to their sources. This method has been successfully used in the case of CFC-11 (Rigby et al., 2019). However, little exists in the literature regarding the use of these inverse methods specifically in relation to PFC gases.

A domain that is of interest is the East Asia domain. This domain contains the following countries: China, Japan, South Korea, North Korea and Taiwan. The reason why this domain is so interesting is because in the case of some countries (e.g. China) all three PFC emitting industries are present. Therefore, attempting to allocate PFC emissions to their original sources in this domain is a tool that can be used as a supplement to the bottom-up inventory produced in previous chapter in order improve even further the understanding of the geospatial distribution of the emissions.

Arnold et al. (2018) used an analytical Bayesian framework (described in section 6.2.3) to run inversions specific to the domain of East Asia (Arnold et al. 2018). In their work, Arnold et al., (2018) tried to minimise the reliance of the prior information on the Bayesian-based posterior emission estimates and they also discussed how poor availability of good prior information was forcing their emission estimates to be largely influenced by the atmospheric measurements (Arnold et al. 2018).

Using the updated bottom-up inventory, this goal of this chapter is to model emissions from the East Asia domain in order to produce domain and country specific estimates and uncertainties. Two inversion methods were used to model this domain:

a) The hierarchical inversion method: This is an inversion method that has not been used before to model CF_4 emissions in this domain.

b) The analytical inversion method: This is an inversion method that has been used before (Arnold et al., 2018). The reason why this method is used is so that the results of this work can

be compared to results of previous work.

The East Asia domain is a very complex domain both in terms of the distribution of the industries and the variation of this distribution over time as well as having a very complex meteorology and topography. In the case of the hierarchical method that has never been used to model these gases before, it was deemed appropriate to first model a simpler area. For this purpose, the Australia was chosen as a test case.

Australia has a very small amount of CF_4 emitting facilities. Specifically, only five smelters exist in Australia and none of the other two industries are present. All other PFC emitting sources are very far from these locations. So, overall, Australia is a good approximation of a closed system where any CF_4 emissions detected should be, in principle, coming from the five existing smelters. To run the inversions a prior emissions field specific to the Australian AI emissions was constructed and atmospheric observations from the AGAGE station Cape Grim are used (discussed in section 6.3.3). The year examined was 2014 and monthly estimates are produced. This temporal analysis was chosen to examine whether HVAE would be detected by the inversion and whether any seasonality could be detected in the estimates. As the Australian inversions would only serve as a test case this inversion was only run for a small period of time. Results are presented for those months were atmospheric data was available.

East Asia has a very large number of CF_4 emitting facilities. In total, more than 300 facilities are spread across this domain. The industry specific distribution of these facilities has been discussed in previous chapters (3,4 and 5). A prior emissions field specific to East Asia was constructed and atmospheric observations are taken from the AGAGE station Gosan on the Jeju island (discussed in section 6.3.3). Both the analytical and hierarchical methods are run using the same prior and the same atmospheric observations. The period examined in this case are the years 2008-2016. This was deemed an adequate period of study in order to reach conclusions regarding the distribution of the industries and the magnitude of these emissions. Annual estimates and their uncertainties were produced for the domain and each country. Results from the hierarchical inversion method are presented for three years (2008, 2012, 2016) averaged over a year while the results from the analytical inversion are presented for the same years (2008, 2012,2016) but are presented averaged over two months.

South Korea is distinctive within the East Asia domain as it only has one industry emitting CF_4, which is the SCI, with no other sources of CF_4 emissions. Therefore, as for Australia, it was decided to produce another test case, this time focusing on South Korea. Estimates specific to South Korea are presented in two-monthly averages.

6.2.1 Atmospheric Dispersion Models

An atmospheric dispersion model attempts to simulate of the atmospheric dispersion of a gas. For this simulation to be achieved, mathematical and algorithms that replicate atmospheric processes are used. As part of the inversion a chemical transport model (CTM) is used to determine the sensitivity between atmospheric mole fractions taken at discrete locations and estimates of emissions over an entire region over a period of time. Figure 6.1 shows an example of CF_4 mole fractions measured (ppt) in four different locations of the AGAGE network: the Gosan station in South Korea (in red), the Cape Grim station in Australia (in grey), the Mace Head station in Ireland (in green) and Trinidad Head in California (in yellow) (AGAGE, MIT Center for Global Change Science).

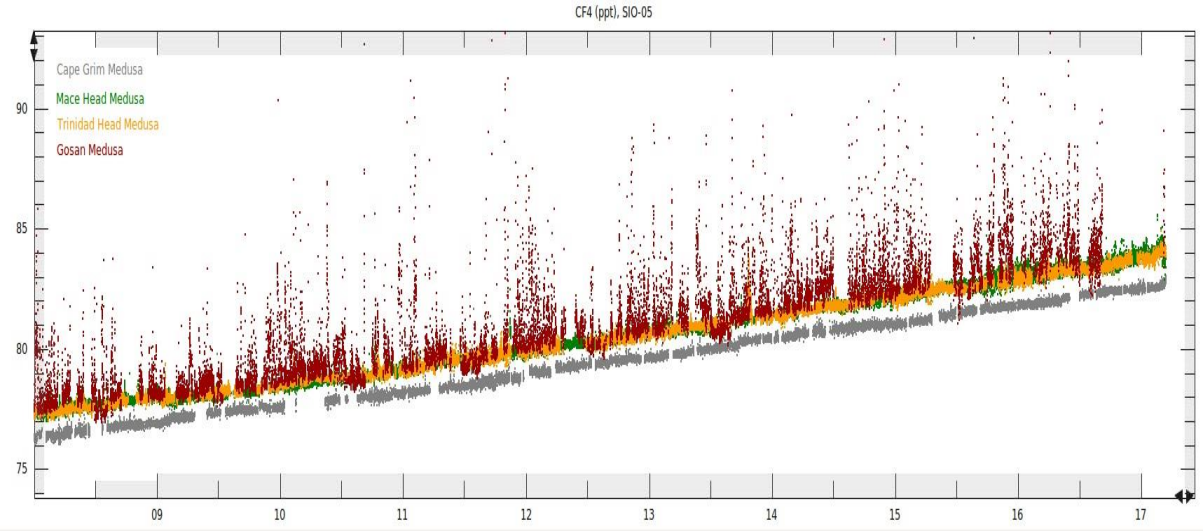

Figure 6.1: CF_4 mole fractions (in ppt) from four different stations; Gosan (South Korea) in red, Cape Grim (Australia) in grey, Mace Head (Ireland) in green and Trinidad Head (California) in yellow (AGAGE, MIT Center for Global Change Science).

While there are many kinds of dispersion models with resolutions ranging from the global scale to very well-defined regional scales, they are broadly categorized in two types: a) Eulerian and b) Lagrangian. The Eulerian model uses a set of boxes (grids) through which a gas is advected and/or can undergo chemical reactions. A Lagrangian Particle Dispersion Model (LPDM) is a CTM that releases several particles into the atmosphere; these particles are

then transported, governed by the meteorology with additional random sideways movements that account for turbulence. Lagrangian models are usually used for regional scale inversions (as opposed to global inversions). This work uses a Lagrangian particle dispersion model, NAME, for atmospheric transport within the inversion domain, and a Eulerian model, MOZART, for producing concentrations at the boundary.

6.2.2.1 The Numerical Atmospheric Dispersion Modelling Environment (NAME)

NAME (Numerical Atmospheric dispersion Modelling Environment) is a regional Lagrangian atmospheric dispersion model that has been developed by the UK Met – Office (Jones et al., 2007; Manning et al., 2011). While it was originally developed in the aftermath of the Chernobyl disaster, it is now used as tool to investigate the atmospheric and chemical behaviour of a large range of gases.

This LPDM works by releasing a number of particles from a specific location and then tracing their dispersion over a given time. The information on the particle advection comes from Numerical Weather Prediction (NWP) meteorological fields from the Met Office's Unified Model (UM). Information contained in these fields include wind speed, temperature, pressure, surface heat flux, precipitation and boundary layer height. The model is run back in time, tracking the particles for 30 days and giving an air history map (usually referred to as a 'footprint') (Jones et al., 2007; Manning et al., 2011). Examples of footprints are shown in Figures 6.4 – 6.7. The 30-day period is chosen because it gives the majority of particles enough time to leave the domain of interest, if particles are still in the domain it means that there is still a possibility that they could contribute to the footprint. The model is run with a spatial resolution of 0.25^{o} x 0.25^{o} and a 2-hour temporal resolution.

6.2.2.2 The Model for OZone And Related chemical Tracers (MOZART)

Unlike NAME, the Model for OZone And Related chemical Tracers (MOZART,) is a global Eulerian model (Emmons et al., 2010). GHG emissions are not distributed evenly across the lower levels of the atmosphere. The emissions in the northern hemisphere are mostly greater than those in the southern hemisphere and because of the multi-year time scale when mixing between the two hemisphere occurs, a notable gradient can be observed for long lived GHGs (shown in Figure 6.1).

NAME is a regional LPDM and as such, in order to estimate GHG concentrations

within a studied domain, it requires a set of boundary conditions which are produced by MOZART. This model is driven by a meteorological dataset and an emissions inventory. For each domain presented in this work (Australia, South East Asia) the MOZART model was used in order to produce this prior boundary conditions. The dynamics used to drive each simulation were taken from the Modern-Era Retrospective analysis for Research and Application (MERRA, (Rienecker et al., 2011). This is a reanalysis product that combines climate model fields and irregularly spaced observations in a gridded meteorological dataset (Rienecker et al., 2011). Resolution of MERRA's field is 2.5º x 1.875º with 72 levels out of which, only 56 are used by MOZART. Those levels extend from the surface up to a pressure of approximately 2hPa.

6.2.3 Inverse Modelling and Bayesian Inversions

An inversion is a method that can be used to estimate emissions of a gas at the surface of a domain from atmospheric measurements of these gases (Figure 6.1), usually in mole fractions. This term describes a statistical approach of using data to estimate parameter values. The most common inverse method is the Bayesian approach that uses a prior estimate of the parameters, updated by incorporating new information from atmospheric data. The reason this Bayesian approach is favoured over other approaches is because, when there is a lack of data it allows for the estimate of the parameter to be constrained by a prior estimate of the parameter. Bayesian inversions are widely used across a variety of disciplines and subjects (especially for environmental challenges) within the literature and so is the use of prior information to solve these inverse problems (Winkler, 1967; Greenland, 2000; Tenorio, 2001; Gelman, El-shaarawi and Piegorsch, 2002; Uusitalo, 2007; Aguilera et al., 2011; Chen and Pollino, 2012; Weber et al., 2012; Yao and Eddy, 2014; Franco et al., 2016; Phan et al., 2016; Consonni et al., 2018). The benefits and limitations of the presence of absence of a prior to run the inversions are one of the key topics of discussion. This section describes the principles of Bayesian inversions, the hierarchical and analytical method.

6.2.3.1 Bayesian inversions

The Bayesian approach is based on Bayes' probability theorem whose principle is based on the following: 'given some prior knowledge on the probability of parameter A taking a particular value, what is the probability of that parameter taking the same value, given that we

have information on the value of B?'. Mathematically this is expressed through the common form of Bayes' theorem as shown in Equation 6.1:

$$p\,(A|B) = \frac{p\,(B|A) \cdot\ p(A)}{p(B)} \qquad (6.1)$$

Where p is defined as a probability density function (PDF) that describes the probability of A or B taking a particular value. P (A|B) is referred to as the 'posterior PDF' since the value of A is depended on the value of B. The term p(A) is referred to as the 'prior PDF of A' with is value being independent of B. P(B|A) is referred to as the conditional pdf of B when A has a given value. P(B) is referred to as 'evidence'. P(B) is the probability of B taking on a particular value in the absence of any information on A. It acts simply as a normalising constant.

What Bayesian statistics allows is for prior beliefs (or prior values) to be informed by evidence (Figure 6.2) in order to produce the posterior belief.

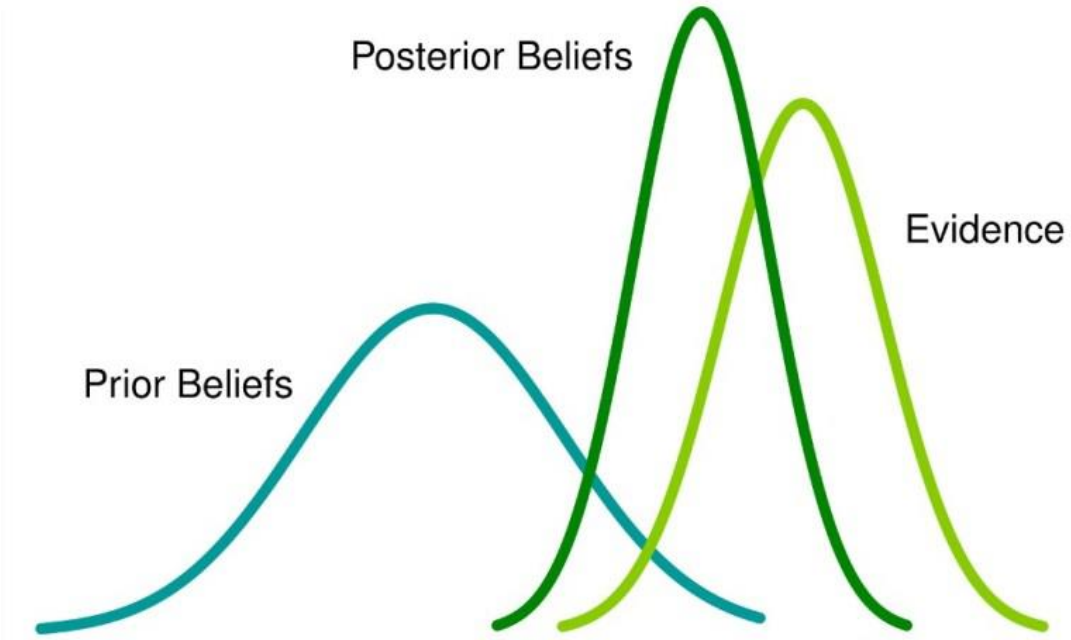

Figure 6.2: Schematic representation of a prior belief distribution, an 'evidence' distribution and a posterior belief distribution (NSS, 2016).

In atmospheric inverse modelling, the term B represents the observed data, in this instance, data collected from one or more of the AGAGE stations. The term A represents the

set of parameters that will be updated from the prior to the posterior using information from B (the observations). The parameters related to A for this work represent source terms.

The common form of Bayes' theorem represents single values for A and B but in the atmospheric inverse problems there are usually tens or hundreds of values. Therefore, Equation 7.1 can be rewritten to reflect this by replacing A with a vector **x** and B with the vector **y** as shown in Equation 6.2:

$$\mathrm{p}\,(\mathbf{x}|\mathbf{y}) = \frac{\mathrm{p}\,(\mathbf{y}|\mathbf{x}) \cdot \mathrm{p}(\mathbf{x})}{\mathrm{p}(\mathbf{y})} \qquad (6.2)$$

The relationship between the parameters **x** and the data **y** can be described by a simple, forward model (Equation 6.3):

$$\mathbf{y} = \mathbf{H}\mathbf{x} + \varepsilon \qquad (6.3)$$

Where ε represents errors in the model and measurements and **H** (Equation 6.4) is referred to as a 'sensitivity matrix' that maps the change in **y** given a change in **x**.

$$\mathrm{H}_{ij} = \frac{\Delta \mathrm{y}_i}{\Delta \chi_j} \qquad (6.4)$$

The prior distribution (p(**x**)) and the likelihood function (p(**y**|**x**)) are represented using multivariate Gaussian distributions of the generic form shown in Equation 6.5:

$$\mathrm{f}(\mathrm{x}) = \frac{1}{\sqrt{|\Sigma|2\pi}} \exp\left[-\frac{1}{2}\,(\mathrm{x}-\mu)^{\mathrm{T}}\Sigma^{-1}\,(\chi-\mu) \right] \qquad (6.5)$$

Where Σ is a covariance matrix describing the variance of the parameters and the covariance between them and μ is the man of the distribution. For **y** (the data), the term **Σ** is given by a covariance matrix **R**. This matrix includes the variances of the individual data points and the covariance between them. Vector x (the prior parameters) has an associated covariance matrix

P. With the mean of the Gaussian distributions being the value of the data, **y**, and the prior emissions value, $\mathbf{x_{ap}}$ Equation 6.2 is expanded to Equation 6.6:

$$p(\mathbf{x}|\mathbf{y}) = \frac{1}{\sqrt{|\mathbf{R}||\mathbf{P}|2\pi}} \exp\left[-\frac{1}{2}(\mathbf{y}-\mathbf{H}\mathbf{x})^{\mathrm{T}}\mathrm{R}^{-1}(\mathbf{y}-\mathbf{H}\mathbf{x})\right]\exp\left[-\frac{1}{2}\left(\mathbf{x_{ap}}-\mathbf{x}\right)^{\mathrm{T}}\mathrm{P}^{-1}\left(\mathbf{x_{ap}}-\mathbf{x}\right)\right] \quad (6.6)$$

To solution to the inverse problem can be found by minimizing the cost function (Equation 6.7)

$$\mathbf{J} = (\mathbf{y}-\mathbf{H}\mathbf{x})^{\mathrm{T}}\mathrm{R}^{-1}(\mathbf{y}-\mathbf{H}\mathbf{x}) + \left(\mathbf{x_{ap}}-\mathbf{x}\right)^{\mathrm{T}}\mathrm{P}^{-1}\left(\mathbf{x_{ap}}-\mathbf{x}\right) \quad (6.7)$$

This cost function can be minimised using different techniques. To apply this problem to source attribution, surface fluxes are broken down into a set of regions (basis functions) to represent the elements of the parameters vector **x**. For less complex problems, this approach (Bayesian synthesis) can be used as it reduces the size of the problem and it allows for this function to be solved analytically (e.g. Enting at al, 1995; Kaminski et al., 2001). This method will henceforth be referred to as the analytical method.

While there are clear advantages to this relatively simple approach (e.g. minimizing computational time) there are also several challenges. One challenge related to this approach is the choice of a Gaussian PDF for the prior emissions distribution is not appropriate as it assumes that the probability distribution is symmetric about a mean value allowing for the possibility of values in negative parameter space. This assumption is unrealistic for parameters such as emissions for gasses with no sinks which are always, only positive.

A method that allows for such problems to be solved without the use of a of Gaussian PDFs is the application of the Markov-chain Monte-Carlo (MCMC) method (Rigby et al., 2011) which demonstrated the use of exponential PDFs in order to describe prior emissions and posterior distributions were explored using the Metropolis-Hastings algorithm (Metropolis et al., 1953; Green, 1995; Tarantola, 2005; Lunt et al., 2016). The Metropolis – Hastings algorithm generates states from a proposal distribution and selectively accepts transitions so that the stationary distribution of the resulting chain represents the posterior distribution.

Another known challenge is the so called 'aggregation error'. In order to minimise the computational expense that comes with the multi-dimensional fields of fluxes derived within the inverse modelling framework, they are broken down into a set of basis functions. And while this partitioning is often based on the expert's choice, the derived fluxes and their uncertainties are greatly depended on the choices made. To avoid issues related to this error (the aggregation

error) a transdimensional type of inversion developed by Lunt et al., (2016) is used. This approach allows for this partitioning to be determined by the data itself eliminating the need for expert choice of the basis functions.

A key principle of Bayesian inversion methods is that the prior estimate of the emissions and the data (observations) are independent. This principle is used across this chapter, the methods and results presented in this.

6.2.3.2 The Hierarchical Bayesian Method

Another known issue with the traditional Bayesian inversions is the difficulty to assign uncertainties that form the variances of the diagonals for both the prior estimates of the fluxes (**P**) and the model-representation error (**R**), uncertainties which can significantly impact the posterior emissions (Ganesan et al., 2014). The introduction of a set of hyper-parameters (θ), that describe the prior uncertainties and the structure of the R matrix is referred to as the 'Hierarchical Bayesian Inversion Framework'. This method introduced by Ganesan et al., (2014) addresses the concern regarding the uncertainties by allowing for propagation of 'uncertainties of the uncertainties' to the posterior distribution while using at the same time the data in order to solve for those uncertainties.

Equation 6.8 is Equation 6.2 with the denominator omitted for simplicity.

$$\mathrm{p}\,(\mathbf{x}|\mathbf{y}) = \mathrm{p}\,(\mathbf{y}|\mathbf{x}) \cdot \mathrm{p}(\mathbf{x}) \qquad (6.8)$$

Equation 6.8 is now modified to include the hyper-parameters (Equation 6.9):

$$\mathrm{p}\,(\mathbf{x}, \theta|\mathbf{y}) = \mathrm{p}\,(\mathbf{y}|\mathbf{x}, \theta) \cdot \mathrm{p}(\mathbf{x}, \theta) \qquad (6.9)$$

Equation 6.9 according to the probability chain rule (p(A,B) = p (A|B) x p(B)) becomes (Equation 6.10):

$$\mathrm{p}\,(\mathbf{x}, \theta|\mathbf{y}) = \mathrm{p}\,(\mathbf{y}|\mathbf{x}, \theta) \cdot \mathrm{p}(\mathbf{x}|\theta) \cdot \mathrm{p}(\theta) \qquad (6.10)$$

Where Equation 6.10 is Bayes rule for the hierarchical case. The hierarchical framework allows solving not only for the parameters, **x**, but also for the set of hyper-parameters, θ, thus allowing for exploration of the space of the 'uncertainties of the uncertainties'. Ganesan et al. (2014)

and Lunt et al. (2018), demonstrated how this approach can minimize the effect of errors in assumptions about uncertainties in the model-measurements (R).

The hyper-parameters include, the parameter τ (a timescale correlation parameter), μ_x which describes the log mean and σ_x which describes the log standard deviation of a lognormal a priori emissions PDF. The parameter σ_y, describes the standard deviation of a Gaussian model-measurement uncertainty PDF. The hierarchical model where $\mathbf{x}$ and the hyper parameters are informed by the data ($\mathbf{y}$) is expressed through Equation 6.11.

$$p\left(\mathbf{x}, \mu_{\boldsymbol{\chi}}, \sigma_{\boldsymbol{\chi}}, \sigma_y \middle| \mathbf{y}\right) \propto p\left(\mathbf{y} \middle| \mathbf{x}, \sigma y\right) \cdot p\left(\mathbf{x}, \mu_{\boldsymbol{\chi}}, \sigma_y\right) \cdot p\left(\mu_{\boldsymbol{\chi}}, \sigma_{\boldsymbol{\chi}}, \sigma_y\right) \quad (6.11)$$

A lognormal distribution was used for emissions and PDF parameters while model-measurement uncertainties were assumed to be Gaussian because random errors in the instrument are assumed. The posterior distribution, $p\left(\mathbf{x}, \mu_{\boldsymbol{\chi}}, \sigma_{\boldsymbol{\chi}}, \sigma_y \middle| \mathbf{y}\right)$ is explored using the MCMC method with a Metropolis–Hastings algorithm (Rigby et al., 2011; Tarantola, 2005). A "burn-in" period of 25,000 iterations was discarded to remove any memory of the initial state. A further 25,000 iterations were run to sample the parameter PDFs and to form the posterior PDFs.

Overall, there are two main activities that need to be modelled, atmospheric dynamics and chemistry. An overview of the atmospheric dynamics was presented in chapter 1 including the boundary layer and will therefore not be replicated in this chapter. Key processes that need to be modelled include the loss processes of gases in the atmosphere, processes that determine a species atmospheric lifetime. However, in the case of the PFCs studied here no such loss processes have been identified in the troposphere (as described in chapter 1). Additionally, while in most cases chemistry is needed in order to describe the atmospheric behavior of a gas and how it interacts with other gases, both PFCs are completely inert and do not react with any other atmospheric species.

6.3 Methods

A top-down approach ideally requires widespread and continuous measurements of greenhouse gases from a variety of polluted and non-polluted areas. For the Australia, East Asia and South Korea high frequency observations from two AGAGE stations were used, namely the Cape Grim station in Australia and the Gosan station in South Korea. The Cape Grim station (from here on termed CPO) is located on the southern tip of Cape Grim (40° S, 144° E). The Gosan station (from here on termed GSN) is located on the south-western tip of Jeju Island in South Korea (33° N, 126° E)

The aim of these inversions is to estimate the spatial distribution of emissions across a defined geographical area. For this work and both case studies, it was assumed the prior emissions estimates to be constant in time over the inversion time period, which in this case was a year. Assuming the emissions are invariant over long periods of time is a simplification but is necessary given the limited number of observations available. The methods described here were used to derive annual regional emissions for CF_4, annual country emissions and uncertainties.

6.3.2 Regional inversions using Bayesian frameworks

6.3.2.1 The Australian case study

As discussed, the reason why Australia was chosen as a case study to test these prior estimates is because it is a good approximation of a closed system. The only sources of CF_4 present in this domain are the five aluminium smelters operating in different locations. The locations of the aluminium smelters are shown in Figure 6.3.

Figure 6.3: The locations of the five different aluminium smelters in Australia, namely the Boyne, Tomago, Point Henry, Portland and Bell Bay smelters.

To construct the Australia specific prior, two types of bottom-up data were used. Aluminium production data that came from the IAI surveys (IAI, 2014), HVAE median emission factors as calculated by the IAI (IAI, 2014). The PFC emission rates were estimated as described in chapter 3 (IPCC, Guidelines for National Greenhouse Gas Inventories, 2006). This prior did not include the newly discovered LVAE emissions. This prior field was then regridded on a 0.25º x 25º grid across the domain to match the NAME gridding. For the year studied (2014) prior emissions were estimated to be 0.5 Gg/yr. Uncertainty estimates on this prior field are well defined (discussed in chapter 3) so an a priori uncertainty equal to 20% of the median emissions was assumed; this uncertainty was then itself allowed to vary within the hierarchical method by +/-50%.

The LPDM NAME used in this work is introduced in section 6.2.5. The domain used to calculate atmospheric transport that covers Australia expands from a longitude 70º to -145º and a latitude of -65º to 5º. At each two-hourly measurement time step, the model releases 20,000 particles, which are tracked back in time for 30 days, so that by the end of this period

the majority of particles will have left the model domain.

NAME uses air history maps called footprints. Figures 6.4 and 6.5 show Australia specific footprints. Depending on the direction of the wind, the areas of land or sea it has passed within the ABL can be seen and locations of where possible pollution events can be identified. This is a means to observe when and where non-polluted or polluted air is coming from.

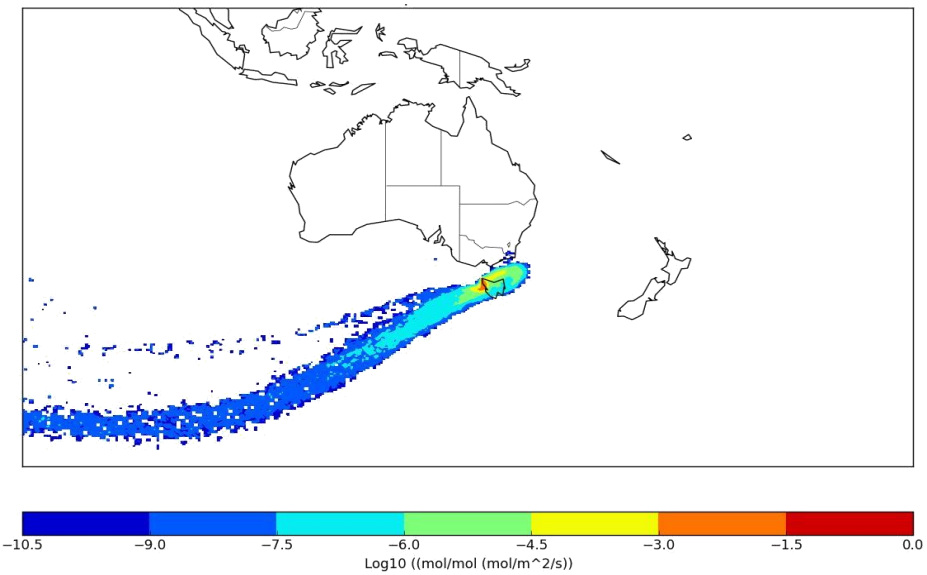

Figure 6.4: NAME output for the site at Cape Grim. For this footprint, the wind was South – Eastern and was coming from a location with no sources, so it is mostly clean.

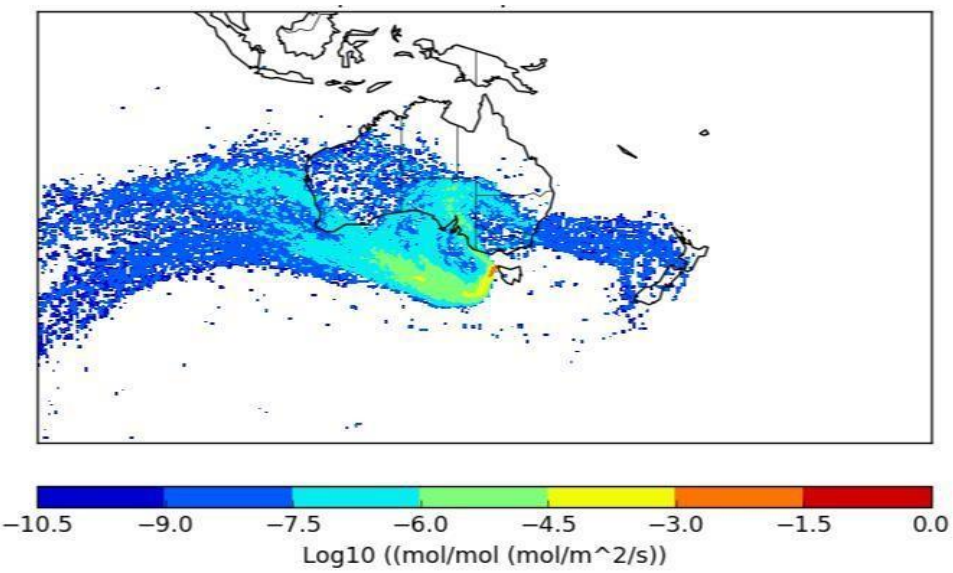

Figure 6.5: NAME output for the site at Cape Grim. For this footprint, the wind is Eastern, North-Eastern and is detecting influences from the Australian mainland and the factories that are located there.

6.3.2.2 The East Asia case study

This domain (East Asia) is far more complex than the Australian domain as all three CF_4 are present within the boundaries of the domain. The East Asia domain expands from 54º to -168º longitude and -5º to 74º latitude. The East Asia domain contains (among others) the following countries: China, Japan, Taiwan, South Korea and North. These are the countries for which annual country totals will be estimated. The two Bayesian approaches used are:

a) **Hierarchical:** A hierarchical Bayesian method that uses the MCMC transdimensional approach described in section 6.2.3.1 was used to estimate CF_4 emissions on a domain and country scale and their uncertainties. The prior $\mathbf{x_{ap}}$ estimate used in this method is the domain specific bottom-up inventory for CF_4. The atmospheric observations (**y**) are data from the AGAGE GSN station.
b) **Analytical:** An analytical Bayesian method described in Arnold et al., (2018). The main difference between the hierarchical approach described in (a) and this approach, is that it does not use the MCMC transdimensional and solves the cost function described in section 6.2.3 analytically.

The prior used for this case study was constructed similarly to the Australian case study. Annual emission totals from every industry were estimated for this domain. The industry specific emission totals were summed for each year studied and regridded on a 0.25º x 0.25º grid. For the years studied (2008 – 2010) the prior estimate used was 4.79 Gg/yr. Uncertainty estimates for this domain are less well defined than those related to the Australian domain as it occurs from the uncertainties discussed in chapters 3, 4 and 5. Therefore, an a priory uncertainty of 50% was assumed for this domain and when then allowed to vary using the hierarchical scheme by +/- 50%.

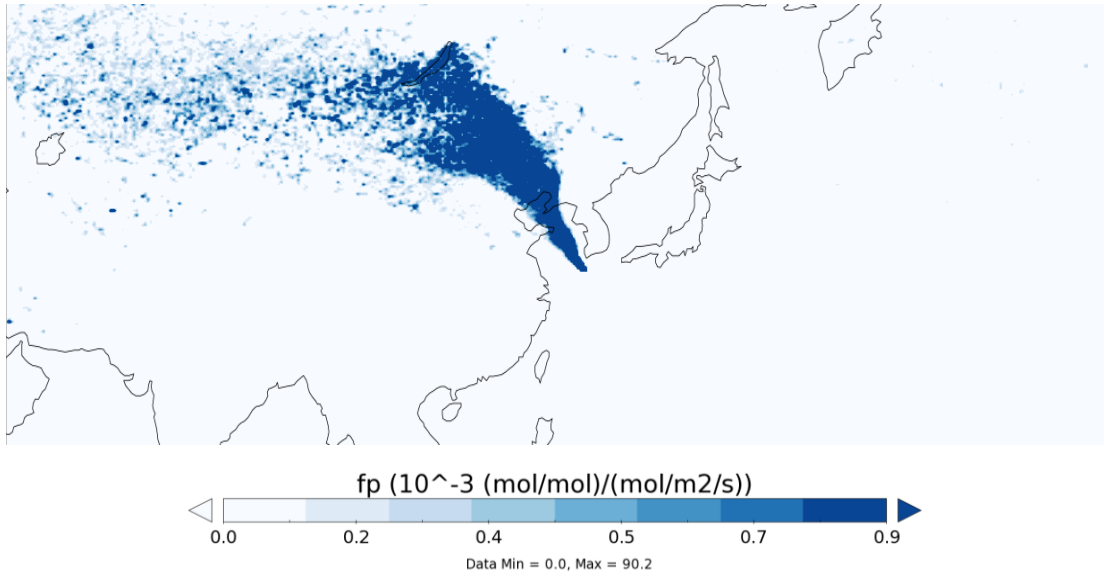

Figure 6.6: Example of the NAME output for the site at GSN station. For this footprint, the wind was coming from the North –East. (note the difference in scale compared to the CPO footprints).

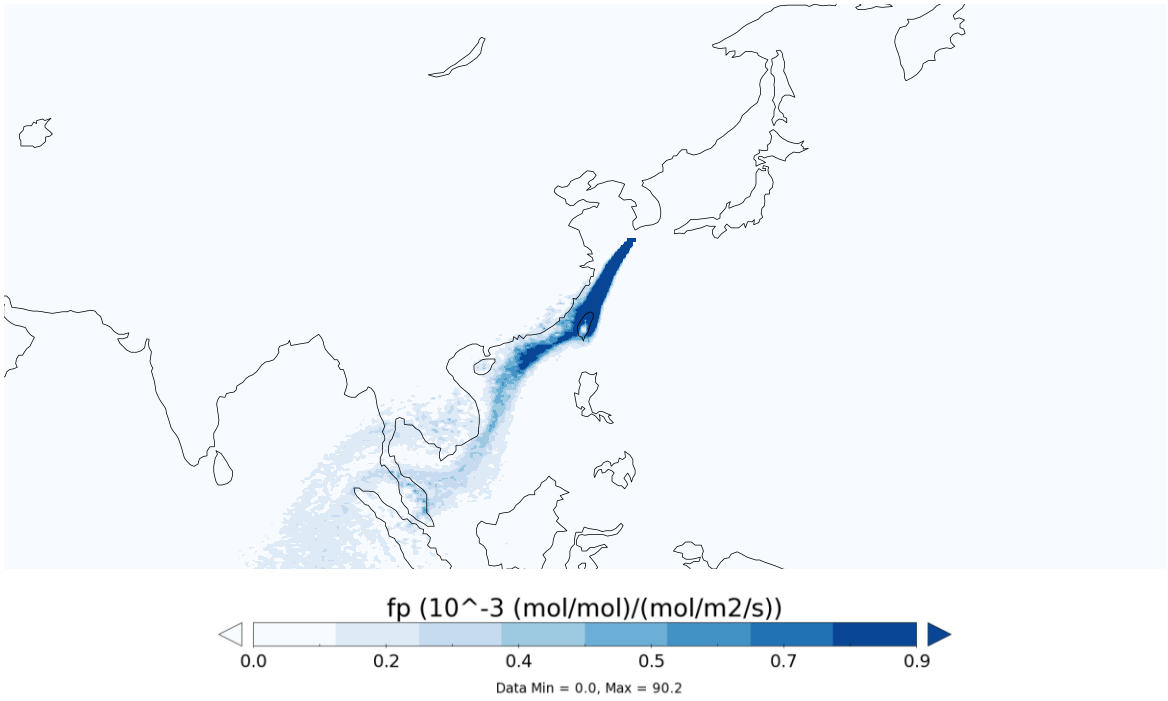

Figure 6.7: Example of NAME output for the site at GSN station. For this footprint, the wind was coming from the South – East (note the difference in scale compared to the CPO footprints).

6.3.1 Top-down PFC emissions estimates

As part of its many functions, the Atmospheric Chemistry Research Group (ACRG) in the Chemistry department of the University of Bristol, it also provides the AGAGE network with top-down estimates of the global total of GHG emissions.

Estimates of global total emissions of PFCs are made using long-term measurements of atmospheric mole fractions in the background atmosphere. In this chapter, an update to these PFC estimates is provided. The author of this work was provided these estimates through personal communication with Dr. Matt Rigby; both the author and Dr. Matt Rigby are members of the ACRG group.

Data from five AGAGE stations are used to estimate the monthly mean CF_4 and C_2F_6 mole fraction in the atmosphere far from any major sources. This data is compared with simulated mole fractions of CF_4 and C_2F_6 using a two-dimensional atmospheric transport and chemistry model (2-D 12-box AGAGE model) (Cunnold et al., 1983; Rigby et al., 2013). Emissions were derived using the model and the data and a Bayesian inverse framework that assumed a priori that the rate of growth in emissions from one year to the next was zero +/- 20% of the maximum emissions in EDGAR v4.2 (Vollmer et al., 2018).

This top-down approach provides an estimate of total global emissions that is independent of the inventory presented here. It must be noted however, that this method using remote monitoring stations cannot separate the contribution of different sources of CF_4 and C_2F_6 to the global total.

6.4 Results and discussion

6.4.2 Inverse modelling and the Australian case study

For the Australian case study, only the hierarchical Bayesian method described in section 6.2 was used. In this case the inversions were run monthly for every month for the year 2014 but results are shown for the months February, March, July, August and September; where no results are shown large parts of atmospheric observations were missing and/or had significant gaps. The purpose of this test case study is to examine the response of the hierarchical Bayesian method when supplied with well-defined prior. It was assumed that because Australia hosts only one of the CF_4 emitting industries (and thus prior knowledge of this closed system is well defined) it would be easier to observe the behavior of the posterior. For each month the

inversion was run Figure 6.14 shows (to the left) the scaling of the prior and the timeseries comparison plots of the measured CF_4 mole fractions (red dots) and (to the right) the modelled mole fractions (blue line). The posterior baseline is shown as a black line. The pale blue shading represents the estimated model uncertainty.

- **February (2014)**

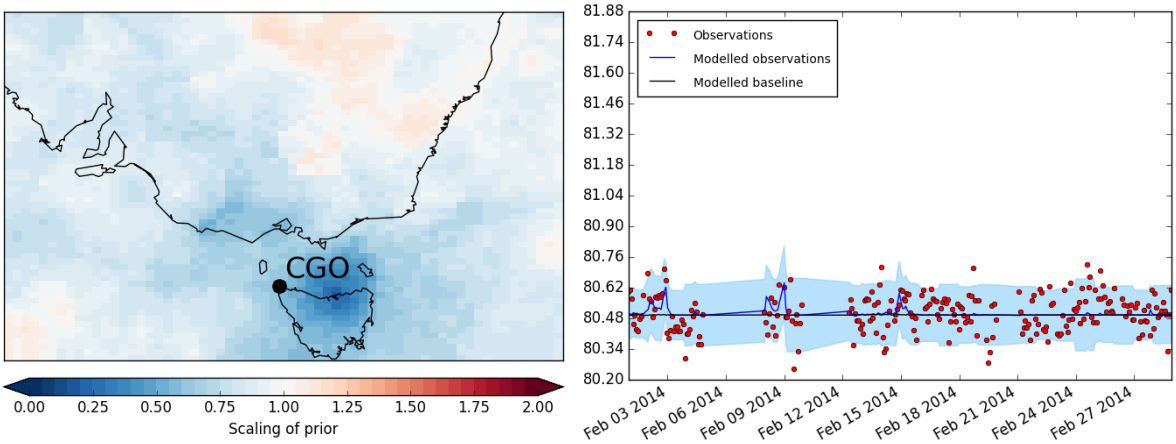

- **March (2014)**

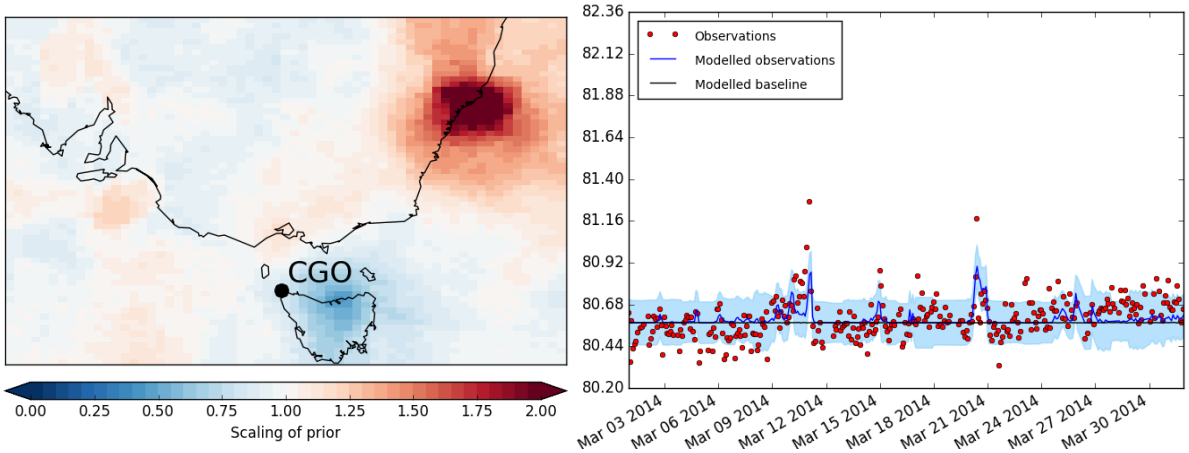

- **July (2014)**

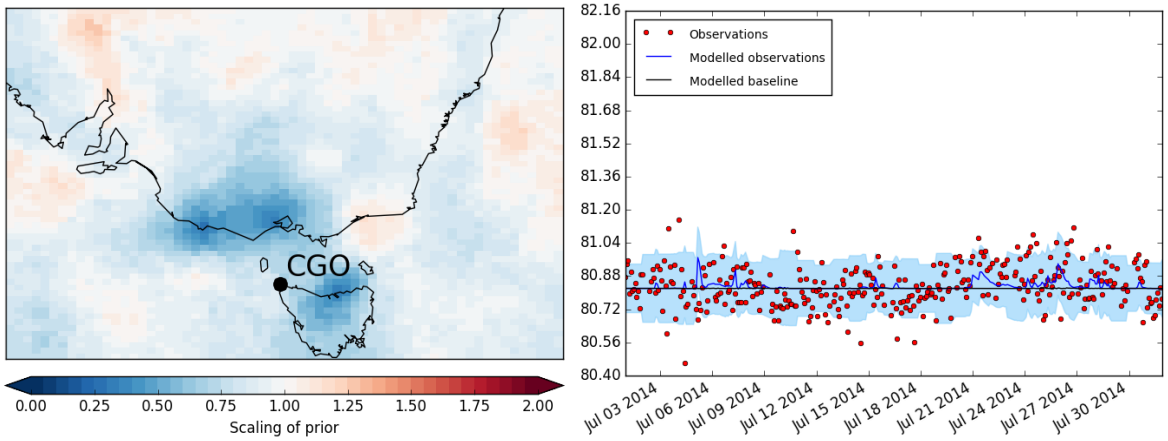

- **August (2014)**

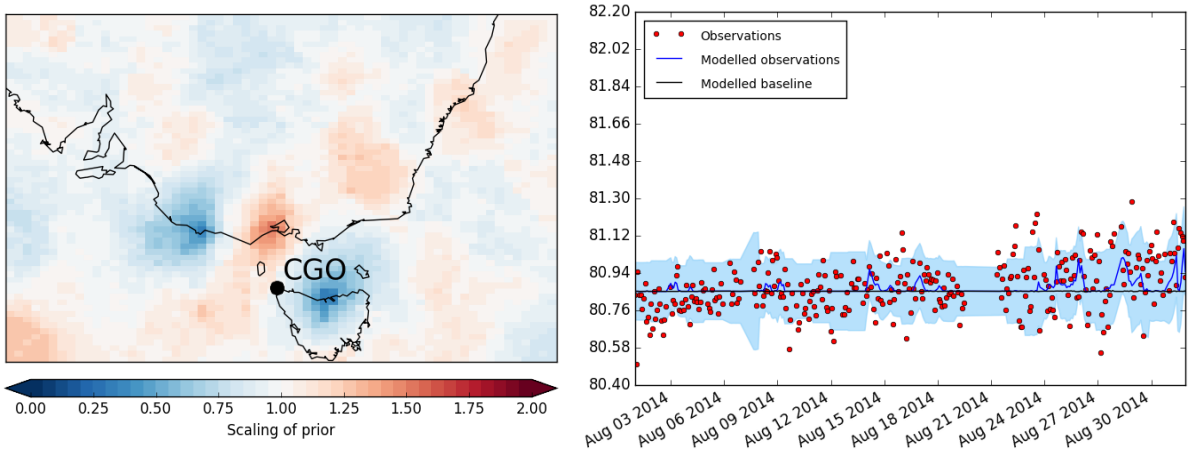

- **September (2014)**

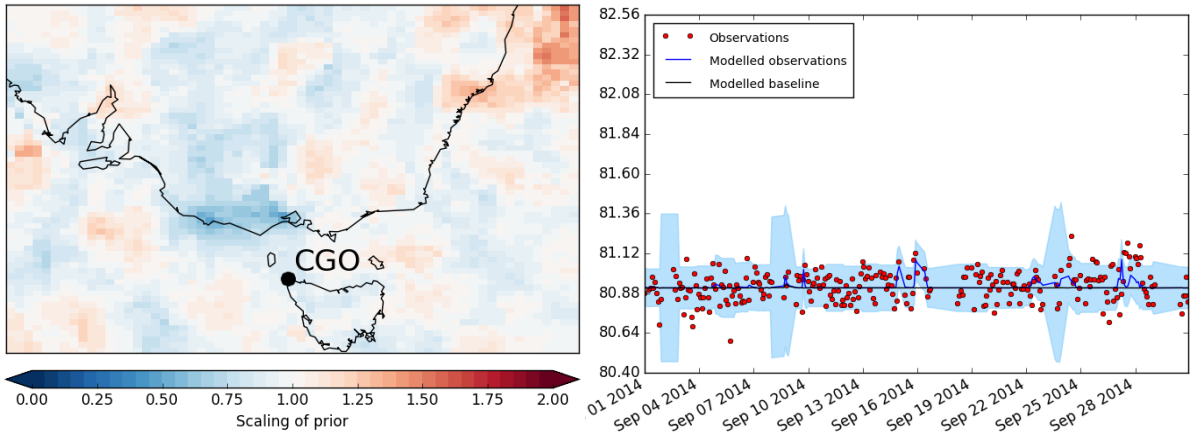

Figure 6.8: To the left – Monthly maps showing the scaling of prior. The location of CGO is also shown. To the right – timeseries comparison plots of the measured CF4 mole fractions (red dots) and modelled mole fractions (blue line). The posterior baseline is shown as a black line. The pale blue shading represents the estimated model uncertainty.

For 2014 the following results and conclusions could be observed. Very little variation was observed in the atmospheric data measured by CGO. As discussed, aluminium smelters are known to emit CF_4 during the duration of HVAE. However, very few pollution events (spikes in the data) seem to have been detected from the station. It should be highlighted that the primary function of the CGO was to measure background (therefore mostly clean) air. However, it could be the case that HVAE were very infrequent and of small magnitude for the duration of 2014. This assumption is reinforced by the variance of the scaling maps. The function of a scaling map is to provide information on whether is prior has overestimated or

underestimated the emissions in a specific area over a given period. For most of the months presented here, the prior seems to be quite consistently overestimating emissions coming from Boyne Island. An interesting find occurred for March when the scaling map shows a significant underestimate of the prior emissions near the location of the Tomago smelter. Looking at the timeseries produced for the same month, there are two notable pollution events in the atmospheric observations (the 2nd and 3rd week of March) which could indicate the presence of a HVAE. The magnitude of this spike is ~81.5 ppt other observations for this month are ~80 ppt and this was the biggest recorded spike for the whole of 2014. And while a difference of ~1.5 ppt from the baseline is in general a small difference, the scaling map for this month shows that even small changes in the observed data could result in significant variations of the scaling of the prior estimates. Another interesting find which is consistent for all the months presented here is the behavior of the posterior baseline. All the posterior baselines are flat and there is no variation of this baseline for any month; it would be expected that the posterior baseline variates in order to account for significant variations in the emission fluxes. The fact that the posterior baselines in this case do not fluctuate could be explained by the fact that a flat, fixed prior baseline estimate was used. With the boundary conditions surrounding the Australian domain not allowed to variate and the CF_4 concentrations within the domain being small, the posterior baseline was almost exclusively informed by the prior baseline estimate. This shows the importance of choosing appropriate baseline and boundary conditions. The modelled observations are a good fit to the observations for most of the months examined. Interestingly the modelled observations are a better fit to the data for the summer months than in the winter months. This could be explained predominantly by the small and synoptic and large-scale meteorology of the area. During the winter months the prevailing wind in the area is North-Northeast and, in the summer, South-Southeast.

Overall, the Australian test case study was deemed successful as it was able to provide us with information regarding key aspects (e.g. boundary conditions) of the inverse modelling methods that needed.

6.4.3 Inverse modelling and the East Asia case study

6.4.3.1 Results from the hierarchical Bayesian framework.

For the East Asia case study, both the hierarchical and the analytical Bayesian methods described in section 6.2 were used. In this case, the inversions were run annually for every year between 2008 and 2016. The purpose of this case study was to produce country and domain specific emission totals and uncertainties. The East Asia domain hosts all three PFC emitting industries AI, SCI and RESI. That the more PFC emitting facilities are present in a specific geographical area, the harder it could be to allocate emissions to their equivalent sources. As the models are run at a 0.25^o x 0.25^o spatial resolution it could be the case that sources that are approximately in the same area cannot be distinguished in the model.

Hierarchical inversions were run annual for each year during the period 2008-2016. Here only the years 2010, 2012, 2014, 2016 are shown. Figures 6.9A-6.16A show maps of the posterior, **x,** in $g/m^2/s$. Figures 6.9B-6.10B show timeseries comparison plots of the measured CF_4 mole fractions in ppt (red dots) and modelled mole fractions (blue line). The posterior baseline is shown as a black line. The pale blue shading represents the estimated model uncertainty. Figures 6.0C-6.10C show maps of the difference between the prior, $\mathbf{x_{ap}}$ and posterior, **x**, (prior-posterior) in $g/m^2/s$. Figures 6.9D-6. 10D show the scaling map of posterior (**x**). This is the degree of scaling which has been applied to prior emissions ($\mathbf{x_{ap}}$). Domain and country total emissions will be shown and discussed separately in section 6.5. The domain (East Asia) and country (China, Taiwan, Japan, South Korea, North Korea) posterior emissions estimates produced using the hierarchical Bayesian method for every year between 2008-2018 will be presented in section 6.5. Table 6.1 will present the domain and country numbers per year while and Figures 6.15 and 6.16 will focus on the Chinese and South Korean posterior emissions estimates.

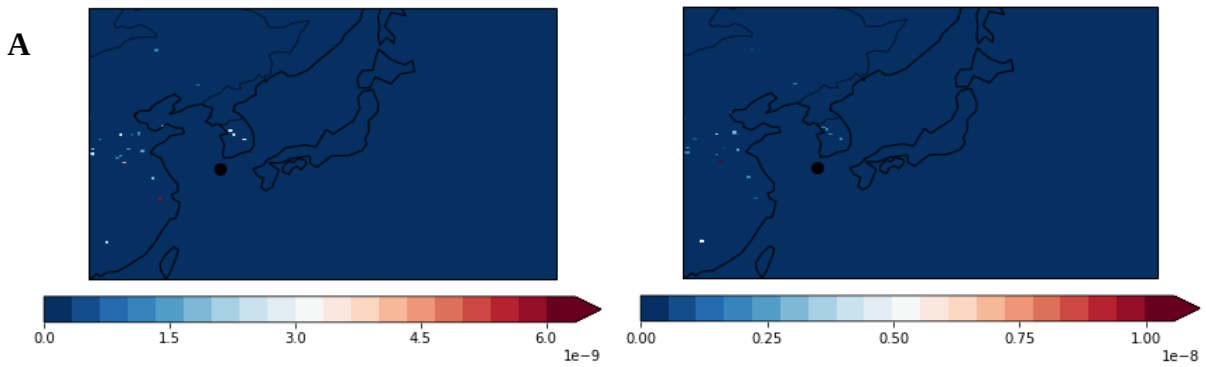
A
0.0
1.5
3.0
4.5
6.0
1e−9
0.00
0.25
0.50
0.75
1.00
1e−8

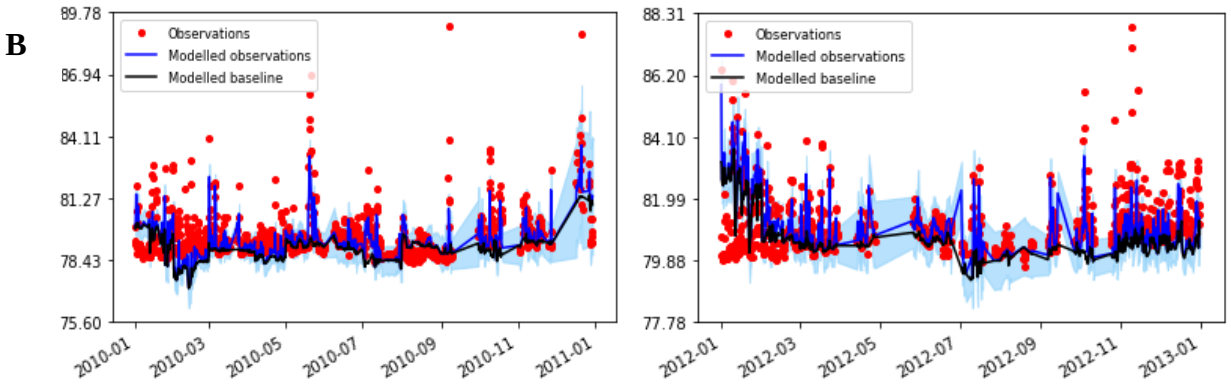
B
89.78
86.94
84.11
81.27
78.43
75.60
Observations
Modelled observations
Modelled baseline
2010-01
2010-03
2010-05
2010-07
2010-09
2010-11
2011-01
88.31
86.20
84.10
81.99
79.88
77.78
Observations
Modelled observations
Modelled baseline
2012-01
2012-03
2012-05
2012-07
2012-09
2012-11
2013-01

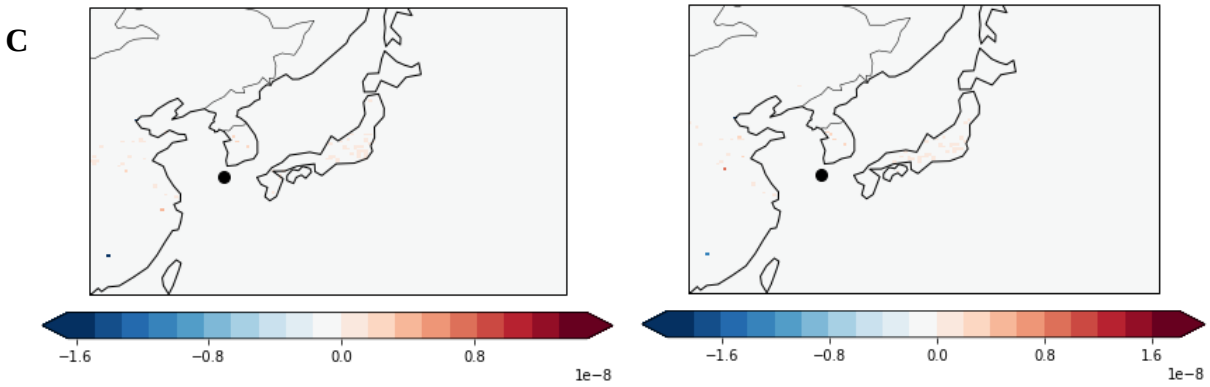
C
−1.6
−0.8
0.0
0.8
1e−8
−1.6
−0.8
0.0
0.8
1.6
1e−8

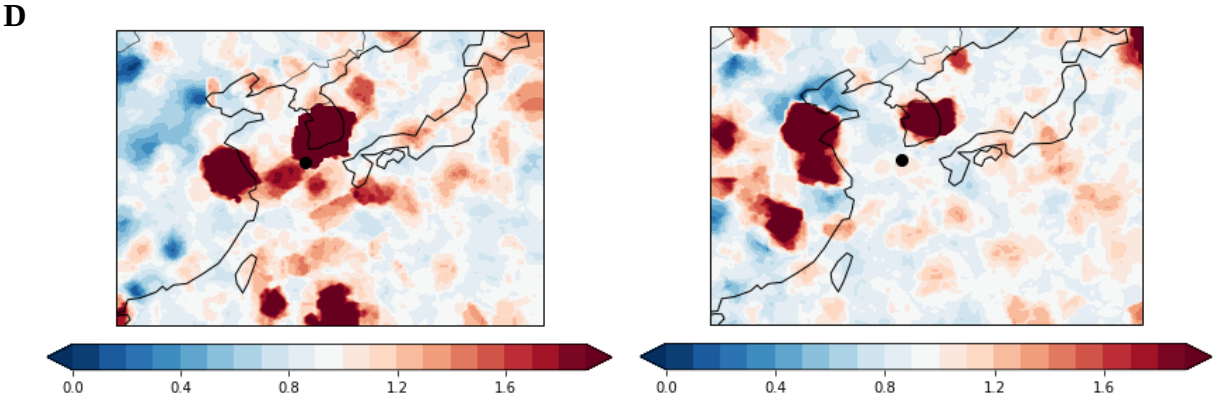
D
0.0
0.4
0.8
1.2
1.6
0.0
0.4
0.8
1.2
1.6

Figure 6.9: To the left are the estimates for 2010 and to the right are the estimates for 2012. Figures 6.19A shows the map of the posterior, x, in g/m2/s. Figures 6.9B shows a timeseries comparison of the measured CF_4 mole fractions in ppt (red dots) and modelled mole fractions (blue line). The posterior baseline is shown as a black line. The pale blue shading represents the estimated model uncertainty. Figures 6.19B show the map of the difference between the prior, $\mathbf{x_{ap}}$ and posterior, **x**, (prior-posterior) in $g/m^2/s$. Figures 6.19D show the scaling map of posterior (**x**) The location of GSN is also shown.

Figures 6.9A show the posterior distribution of the emissions according to the hierarchical Bayesian approach. For 2010, this posterior distribution matches a lot of the locations that were identified as PFC emitting locations in the prior. Areas of interest are the North East coast of China where there is known activity of the AI and the South Korean peninsula where there is known SCI activity. In 2012 the posterior distribution still matches some of the locations identified in the prior, but PFC emissions appeared reduced in comparison to 2010. This disagrees with the prior estimates, especially in the case of the North-East coast of China. However, Chinese smelters are known to either cut down on aluminium production, or altogether stop production if they have reached their annual quota. This can be observed in Figure 3.1 (chapter 3) that shows annual aluminium production per country. PFC emissions from the South Korean peninsula are still detected by the inversion but their magnitude is smaller compared to 2010. An interesting find is that the posterior emissions could not detect emissions from Japan. This is best explained by looking at the timeseries plots.

Figures 6.9B show timeseries of the atmospheric observations (red dots), the modelled data (blue line) and the posterior baseline (black line). The GSN station is in the center of an area where PFCs concentrations are high. While the annual average of these concentrations is ~82 ppt, pollution spikes detected by GSN station are ~88 ppt. However, even though the data collected by this station are very frequent, the meteorology of the area must also be considered in order to interpret the results of the posterior emissions. The prevailing wind in the East Asia domain is Northeastern and, in the summer, it is Southeastern as the atmospheric circulation is reversed. This means that while the GSN station is in an area of high emissions activity, the wind almost never comes from Japan's location. The assumption that the reason why the posterior does not show any emissions from Japan is because the wind from Japan almost never reaches the GSN station is reinforced by the prior-posterior difference maps (Figures 6.19C).

These maps show that while the prior does allocate emissions to Japan, those emissions could not be resolved in the inversion.

For both years, 2010 and 2012, the modelled observations are a good fit to the data, with notable exceptions being instances of large pollution events. Another interesting observation for the results is that, unlike the Australia test case study, the posterior baseline for both 2010 and 2012 appears to fluctuate more and follows the trend of the atmospheric data. It is thought that this is the result of using an improved prior baseline and improved boundary conditions.

The scaling maps for both years give valuable insight (Figures 6.9D). For both years, it appears that the prior has underestimated emissions occurring in the North-East coast of China as well as the South Korean peninsula. It could be the case, that the prior estimates for both those locations were too conservative. This was discussed in chapter 3 where the uncertainty of emissions from the AI were presented so these results were expected. The underestimation of the South Korean prior emissions was however, not expected. This works prior estimates for South Korea was adequately accurate based on industrial knowledge and existing information. One factor that was not included in those prior estimates was, however, PFC emissions as a result of by-product activity. One assumption, therefore, is that in the case of South Korea, by-product PFC emissions could be important. However, another assumption is that, because of the local meteorology (especially synoptic scale phenomena) the GSN station is detecting emissions which have originated in another location, but the inversion is trying to allocate to the South Korean peninsula. The South Korean emissions are explored using the analytical inversion method (section 6.4.1), however, at this stage, no conclusion can be reached on either of these assumptions and it is suggested that future work explores this further.

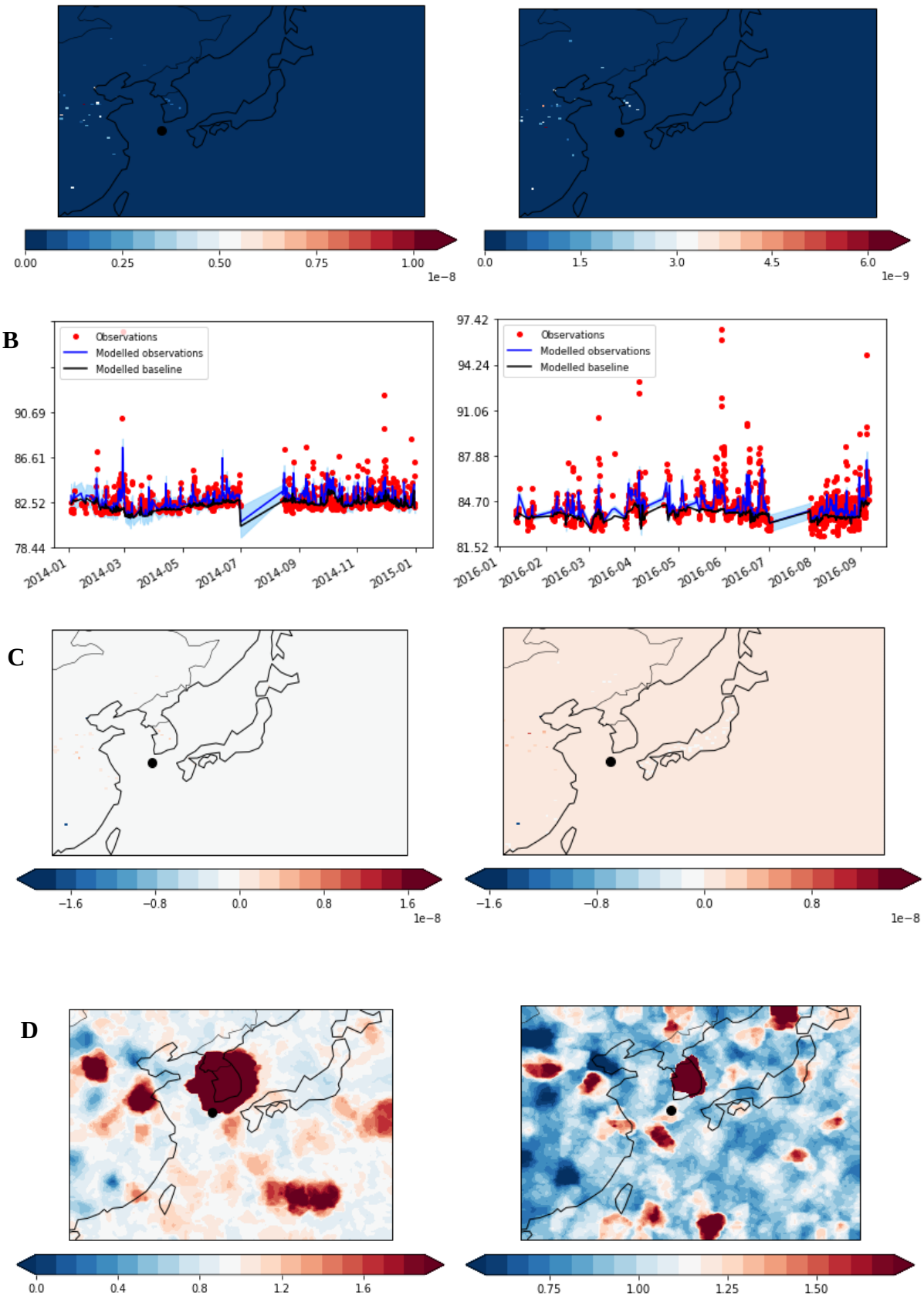
B
C
D
Observations
Modelled observations
Modelled baseline
0.00
0.25
0.50
0.75
1.00
1e−8
0.0
1.5
3.0
4.5
6.0
1e−9
90.69
86.61
82.52
78.44
97.42
94.24
91.06
87.88
84.70
81.52
2014-01
2014-03
2014-05
2014-07
2014-09
2014-11
2015-01
2016-01
2016-02
2016-03
2016-04
2016-05
2016-06
2016-07
2016-08
2016-09
−1.6
−0.8
0.0
0.8
1.6
1e−8
0.4
1.2
0.75
1.00
1.25
1.50

Figure 6.10(A-D): To the left, results for the year 2012 and to the right, results for the year 2016. Figures 6.10A show the map of the posterior, x, in g/m2/s. Figures 6.10C show a timeseries comparison of the measured CF_4 mole fractions in ppt (red dots) and modelled mole fractions (blue line). The posterior baseline is shown as a black line. The pale blue shading represents the estimated model uncertainty. Figures 6.9B show the maps of the difference between the prior, xap and posterior, x, (prior-posterior) in g/m2/s. Figure 6.10D shows the scaling map of posterior (**x**).

Results for the years 2014 and 2016 are quite similar to the results for the years 2010 and 2012. The posterior distributions (Figures 6.9A) still show PFC emissions coming from the Noth-East coast of China and the South Korean peninsula while, the Japanese emissions are again not resolved in the inversion. For four years shown here, an interesting and concistant observation is that the posterior appears to detect emissions of varying magnitude from the Northeast provinces of China.

In terms of atmospheric observations (Figures 6.10B), the years 2014 and 2016 had less frequent pollution events than those recorded for 2010 and 2012. However, more spikes were recorded by GSN station in 2016 than in 2014. This is reflected in the modelled data that are a better fit for 2014 than for 2016 when they could not account for the pollution events. The posterior baseline fluctuates following the atmospheric data trend.

The prior-posterior differences (Figures 6.9C) are very small (~0.2 Gg/yr). For 2014, the scaling of the prior shows that this works prior estimates continued to underestimate emissions coming from the Noth-Easth coast of China but mainly, emissions from South Korea where again understimated. The scaling map for 2016 is different than the maps for previous years. While the South Korean emissions are again underestimated by the prior, this map shows an overrestimate of the prior emissions from the Chinese mainland and parts of the Northeastern coast. While estimates related to the IAI do not show a decrease in the Chinese aluminium production for 2016, there is no information regarding the per smelter aluminium production that could potentially explain the overestimate of the prior emissions for this year. This should be further investigated in the future.

6.4.3.2 Results from the analytical Bayesian approach

Inversions run for the years 2008 to 2017 used the setup described in section 6.3.2. Results from 2010, 2012,2014 and 2016 and those months where data was available will be shown in this section for East Asia and South Korea (Figures 6.11 and 6.12 respectively); domain and country annual emission totals will be shown and discussed in section 6.5.

Two types of results are presented: a) two-month domain (East Asia) averages b) two-month country specific averages. Prior estimates and the footprints used in this inverse method are the same as those used in the hierarchical method. For this reason, only the posterior maps and maps demonstrating the aggregation of the dilution matrices for each year, illustrating the relative sensitivity of measurements at GSN to emissions in the region, will be shown.

The function of the dilution matrices is to provide information regarding how sensitive the GSN station is to emissions coming from different locations and directions. As seen in Figure 6.11 (to the right) there is have reasonable confidence up to the 0.01 contour (the boundary between the palest yellow shown and the next shade). It should be noted how this region (>0.01) varies throughout the year. For example, as discussed for the case of Japan, Taiwan is also, often, not seen at all by GSN station and large areas of China are very uncertain. As discussed in relation to the results from the hierarchical inversion, it is also the case in this instance that uncertainty increases as distance from GSN increases which means that some country totals are very uncertain. There is however much more confidence closer to GSN (e.g.) and therefore, in the South Korean estimates. The domain (East Asia) and country (China, Taiwan, Japan, South Korea, North Korea) posterior emissions estimates produced using the analytical Bayesian method for every year between 2008-2018 will be presented in section 6.5. Table 6.1 will present the domain and country numbers per year while and Figures 6.15 and 6.16 will focus on the Chinese and South Korean posterior emissions estimates.

a) Two-month East Asia averages

- **2010**

GS_G_201001_cf4_2mth_H_avg_032

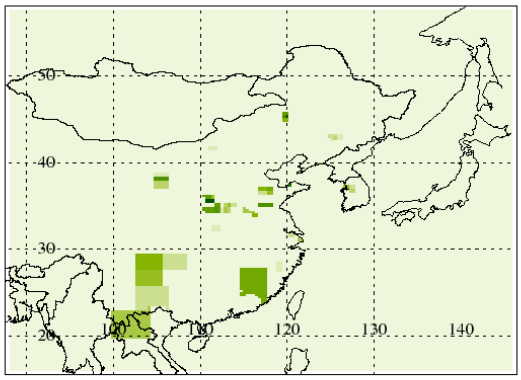

Maximum value = 4317. pg/m^2/s

0. 143. 451. 1424. 4500.

janfeb

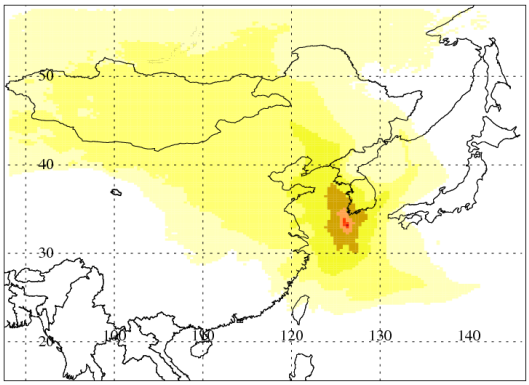

Maximum value = 7.387 s/m

0.003 0.030 0.300 3.000 30.000

GS_G_201005_cf4_2mth_H_avg_032

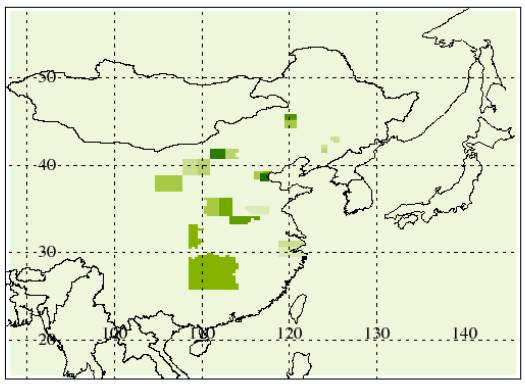

Maximum value = 1782. pg/m^2/s

0. 143. 451. 1424. 4500.

mayjun

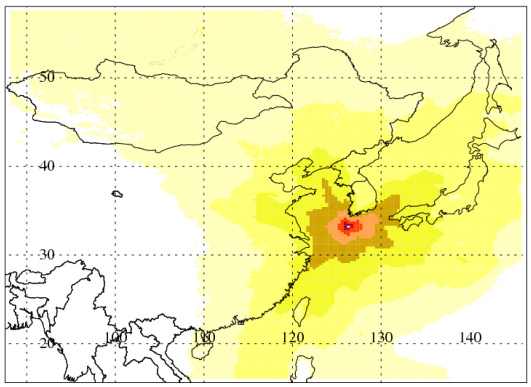

Maximum value = 38.902 s/m

0.003 0.030 0.300 3.000 30.000

GS_G_201009_cf4_2mth_H_avg_032

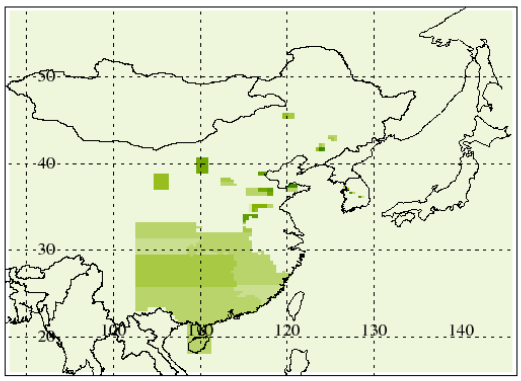

Maximum value = 1039. pg/m^2/s

0. 143. 451. 1424. 4500.

sepoct

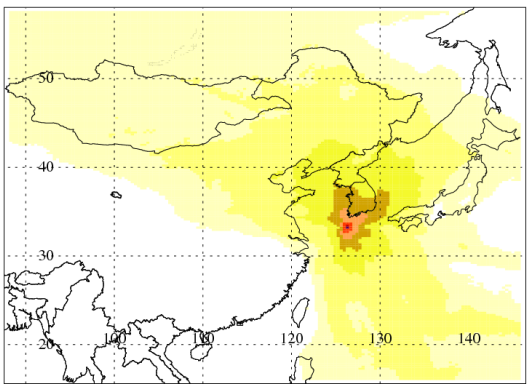

Maximum value = 16.254 s/m

0.003 0.030 0.300 3.000 30.000

- **2012**

GS_G_201201_cf4_2mth_H_avg_032

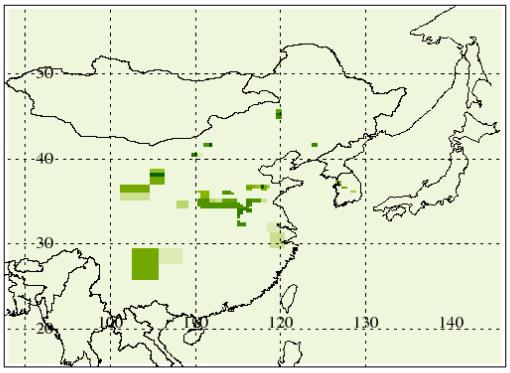

Maximum value = 3679. pg/m^2/s

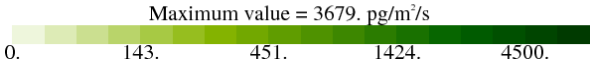

janfeb

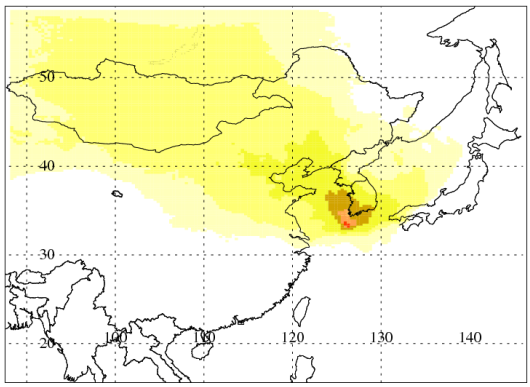

Maximum value = 2.685 s/m

GS_G_201209_cf4_2mth_H_avg_032

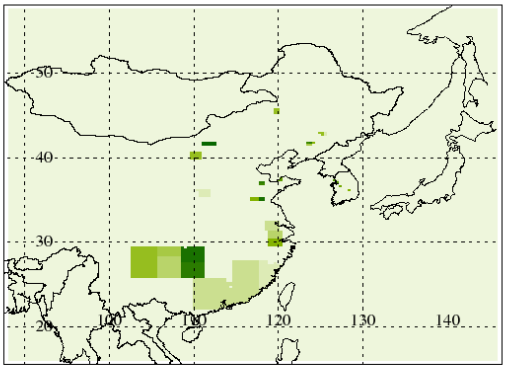

Maximum value = 2219. pg/m^2/s

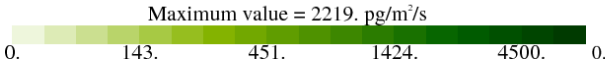

sepoct

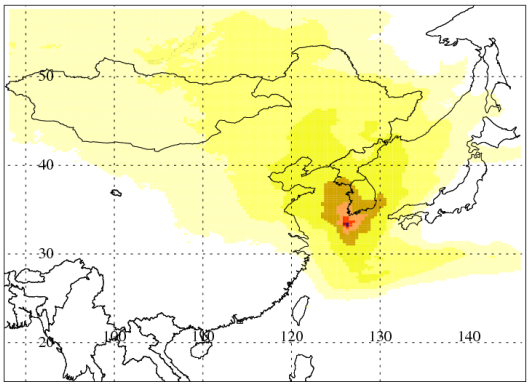

Maximum value = 12.765 s/m

- **2014**

GS_G_201401_cf4_2mth_H_avg_032

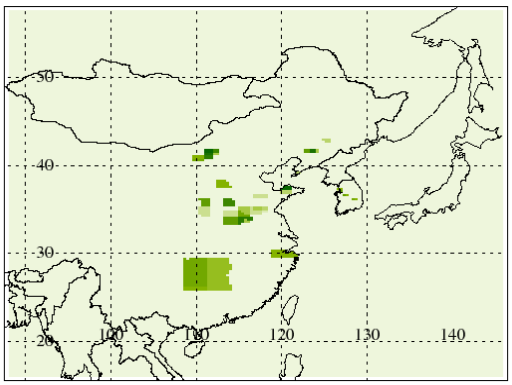

Maximum value = 2445. pg/m^2/s

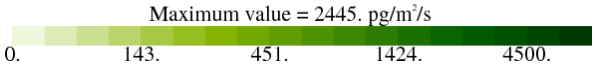

janfeb

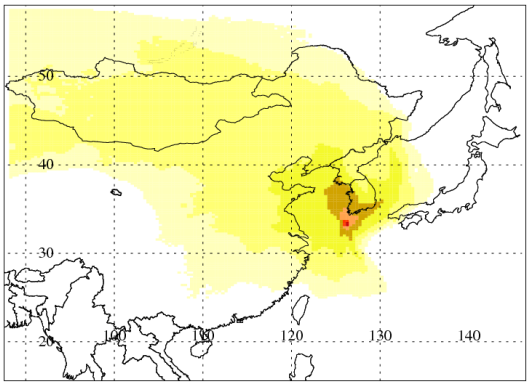

Maximum value = 3.738 s/m

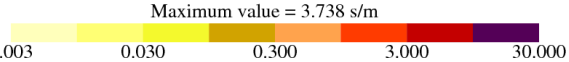

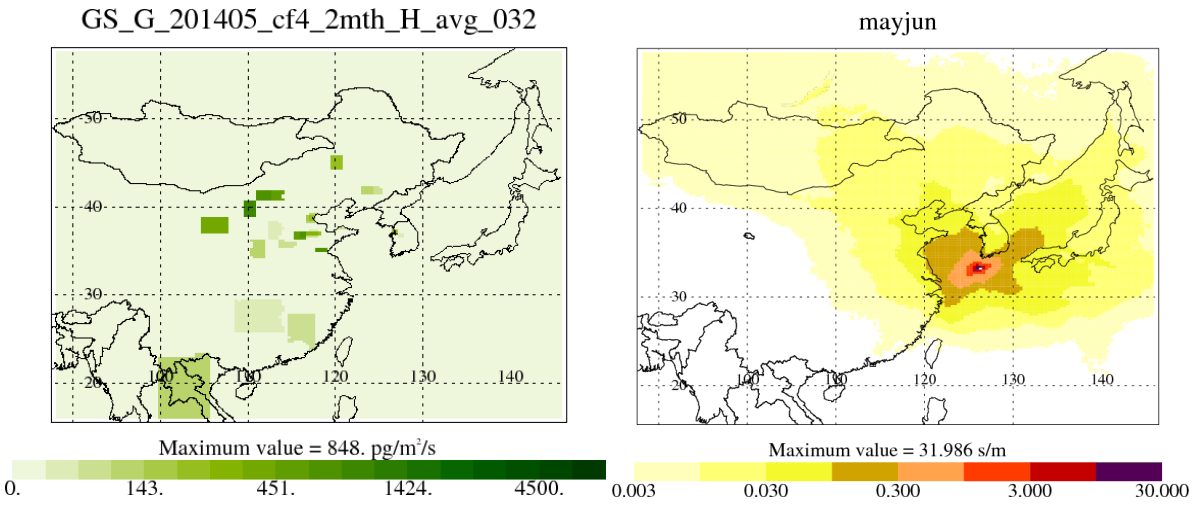

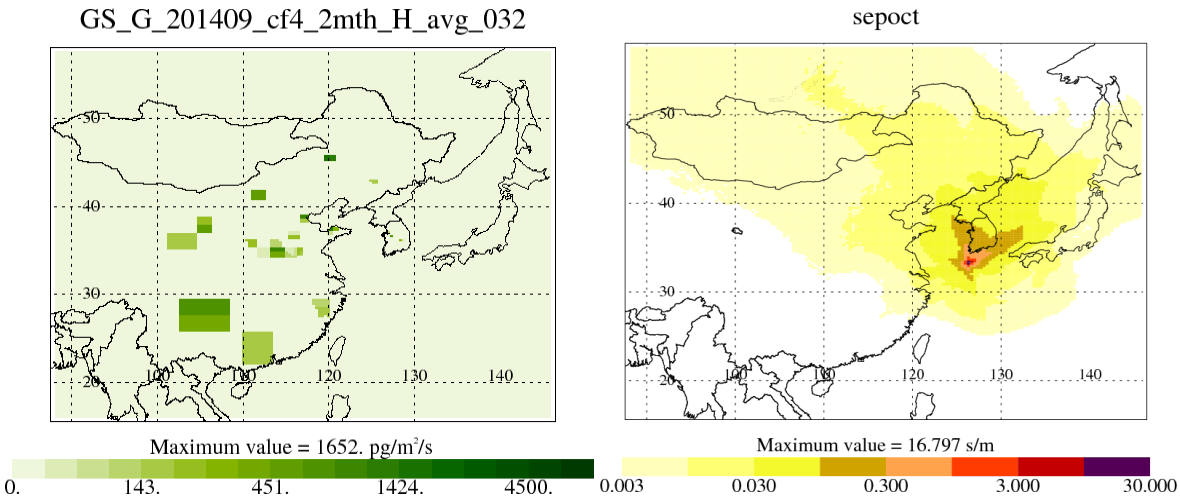

- **2016**

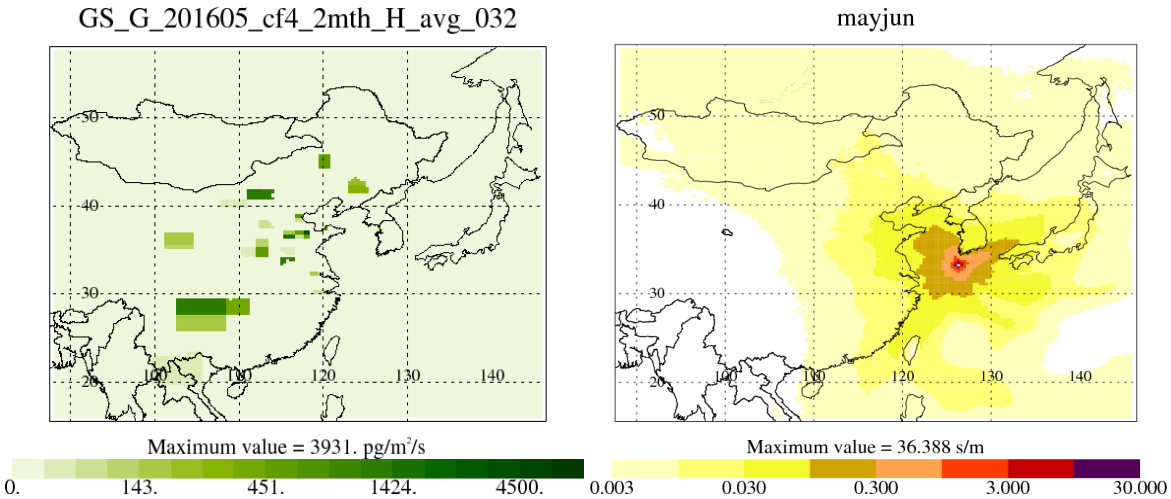

Figure 6.11: To the left – two month averaged posterior emissions maps for CF_4 over the East Asia Domain using the analytical method described in section 6.3.4. (note units are in pg/m^2/s). To the right – the dilution matrix map for the same period studied.

There are significant similarities in the posterior distributions from the hierarchical and analytical methods. The North-East coast of China remains an area of interest as posterior emissions are allocated in this area consistently throughout the years 2010-2016. The same applies for the North Eastern provinces of China and South Korea.

What is of interest in these results is the behavior of the sensitivity in the areas surrounding the GSN station. As briefly mentioned, the further an area is from the station, the less sensitive the station is to emissions coming from this area, making emission estimates from these areas very uncertain.

Throughout the 2010-2016 period, and for all seasons presented here, GSN station is adequately sensitive to emissions coming from South Korea, the North-East coast of China and parts of the North East provinces; these are the areas of the highest confidence. Japan, as discussed, is almost never seen by the station and this is demonstrated in Figure 6.15 for all the months studied apart from May-June. According to the dilution matrices for every year, May-June is the only occasion when wind from Japan could arrive to the GSN. Observing these results was the reason why for this case, a higher temporal resolution was chosen (two-month averages), compared to the coarser (annual averages) resolution chosen for the hierarchical method.

The domain and country totals and their uncertainties produced by this method will be further investigated in section 6.5 and compared to the results of the hierarchical inversion and the results of previous work using the same analytical method.

b) A focus on South Korea

Much like the case study of Australia, that was chosen because only one CF_4 emitting source was present (the five aluminium smelters present in the country), similarly, in South Korea the only CF_4 emitting industry present is the SCI.

Figures 6.12 shows the two-month averaged posterior emission maps for CF_4 focusing on South Korea. From left to right the months shown when data was available are: January-February, May-June and November-December.

- **2010**

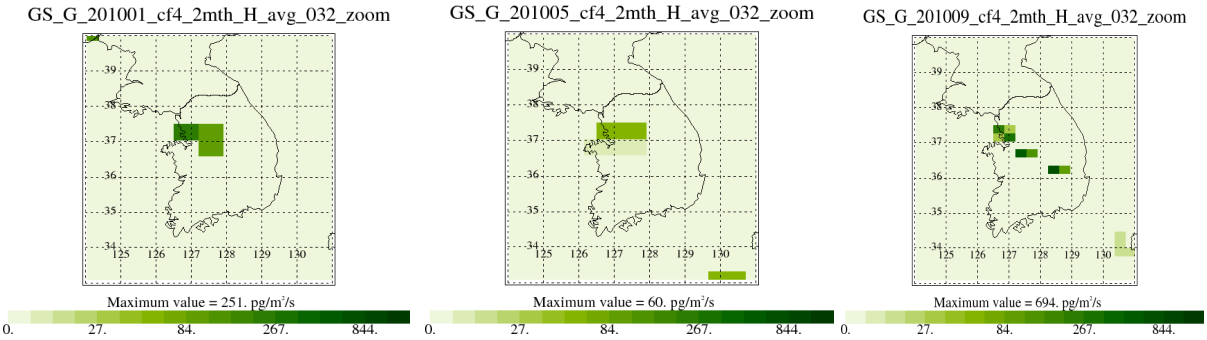

- **2012**

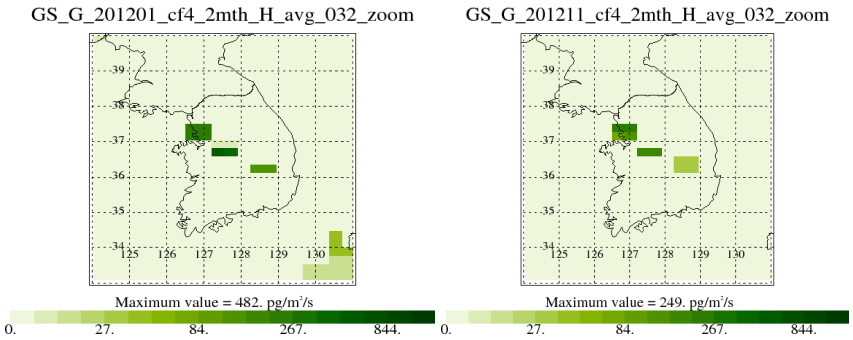

- **2014**

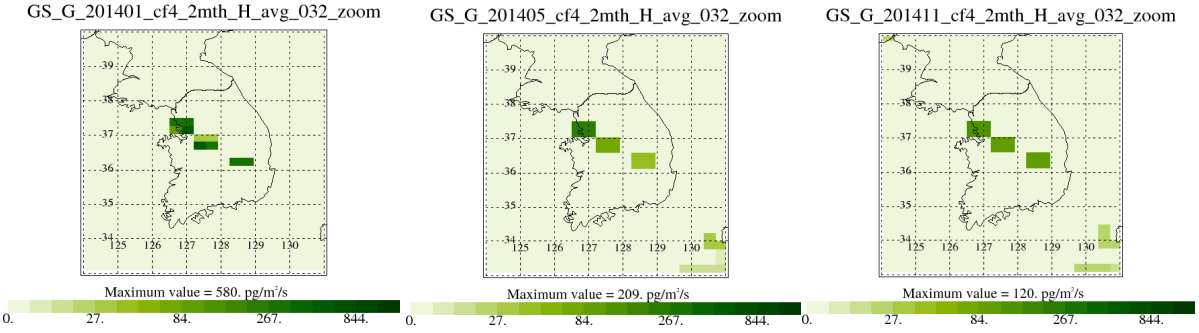

- **2016**

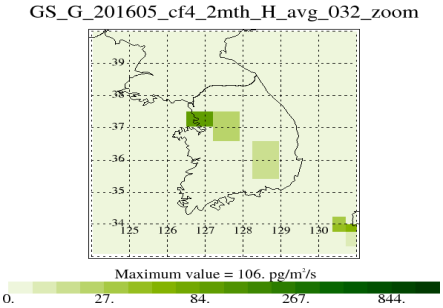

Figure 6.12: Averaged (two-month) posterior emission maps for CF_4 focusing on South Korea for the years 2010-2016 and the months January-February, May-June and November-December when data was available.

Posterior estimates for the period 2010-2016, are consistently allocating emissions in the locations shown in the maps presented in Figure 6.12. The magnitude of these emissions appears to variate throught the same year but also between years. From the results occuring from the dilution matrix, this is an area of high confidence regarding both the magnitude but also the spatial distribution of the emissions.

Overall, the analytical method was in good agreement with the hierarchical method both in terms of the distribution of the posterior emissions and the magnitude of the posterior emissions (shown in Table 6.1 and Figure 6.13). While the GSN station provides the inversion with a lot of high frequency observations for areas close to the station (e.g. Northeast coast of China and South Korea), the sensitivity of the station is limiting when it comes to detecting emissions coming from Japan and Taiwan. This limitation, when combined with a well-defined prior emissions field could potentially result in the inversion trying to allocate posterior emissions in areas of higher confidence rather than in areas of low confidence. This assumption could provide another explanation for the results of the scaling maps that showed a consistent underestimation of the emissions in the Northeast coast of China and South Korea.

6.4.1 Top-down estimates for CF_4 and C_2F_6

Using the high frequency atmospheric measurements from AGAGE stations in conjunction to the 2-D 12-box AGAGE model Dr. Matt Rigby provided the following top-down estimates for CF_4 and C_2F_6 (in Gg/yr) for the years 1979 – 2017 presented in Figures 6.13-6.14.

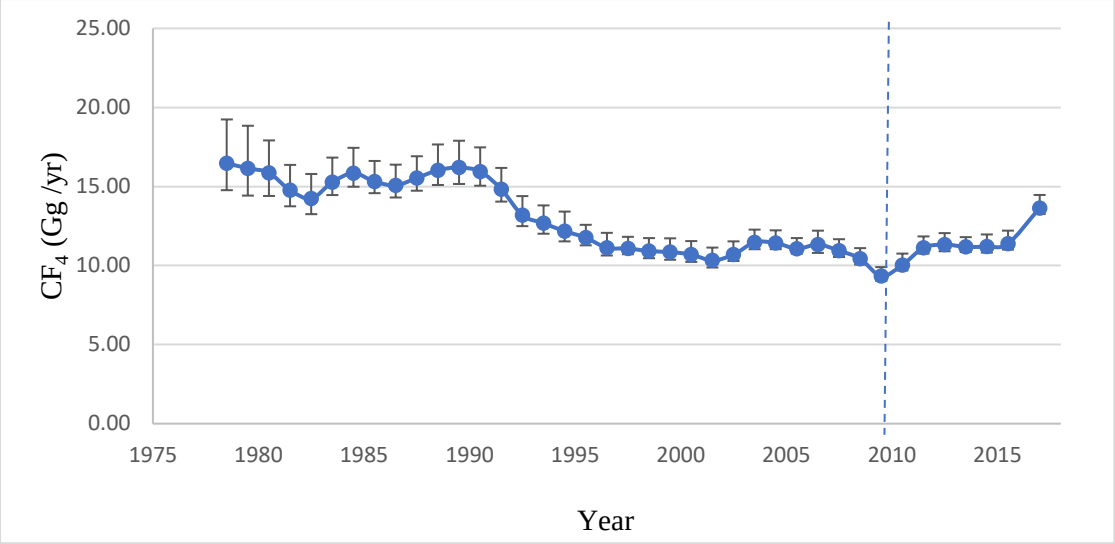

Figure 6.13: Global CF_4 emissions from the inversion of AGAGE atmospheric data and the AGAGE 2-D 12-box model. The dotted line represents those years for which new data is presented.

Figure 6.13 shows global CF_4 emissions from the inversion of AGAGE atmospheric data and the AGAGE 2-D 12-box model. Top-down CF_4 emissions shown in this Figure were ~16 Gg/yr in 1979, ~15 Gg/yr around 1985, declining to ~11 Gg/yr in 2000, and stabilizing at ~11 Gg/yr until they reached a notable low ~9 Gg/yr in 2010. From 2010 and onward CF_4 emissions appear to be steadily increasing reaching ~13Gg/yr in 2010, an emissions' estimate similar to the pre-1993 estimates (~13 Gg/yr).

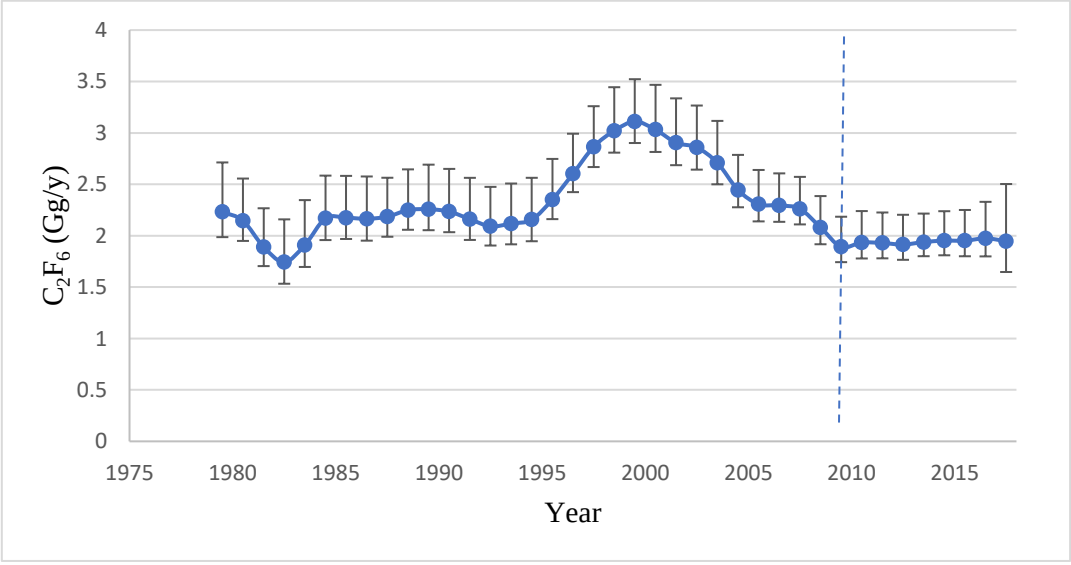

Figure 6.14: Global C_2F_6 emissions (Gg/yr) from the inversion of AGAGE atmospheric data with the AGAGE 2-D 12-box model. The dotted line represents those years for which new data is presented.

Figure 6.14 shows global C_2F_6 emissions from the inversion of AGAGE atmospheric data and the AGAGE 2-D 12-box model. Top-down C_2F_6 emissions shown in this Figure (6.9) were ~2 Gg/yr from 1979 to 1995 apart from a notable decline to ~1.5 Gg/yr in 1982, then steadily increased to ~3 Gg/yr in 1999, following a decline to ~1.8 Gg/yr in 2010 where they remained thereafter.

These top-down estimates are presented in continuation to the work published by Mühle et al., (2010) (Mühle et al., 2010a) and are showing seven years of top-down estimates never presented before. These top-down estimates will be used in chapter 7 where the discrepancies between the top-down and bottom-up estimates will be discussed in detail.

6.5 Conclusions

Table 6.1 and Figures 6.15-6.16 present the country and domain total posterior emissions for the years studied (2008 – 2016). The results of the two methods used in this work are compared to each other and to previously published work by Arnold et al., (2018).

Table 6.1 presents summary of this chapter's estimates of emissions from the five major emitting countries (China, South Korea, North Korea, Japan, Taiwan) within the East Asian domain. The values marked with an asterisk (*) are also taken from the paper by Arnold at al., (2018) with the footnote: "Kim et al. (2010) estimated CF_4 emissions from China in the range 1.7–3.1 Gg/yr and Li et al. (2011) in the range 1.4–2.9 Gg/yr. For South and North Korea (combined), Li et al. (2011) estimated emissions of CF_4 at 0.19–0.26 Gg/yr and from Japan at 0.2–0.3 Gg/yr" (Kim et al., 2010; Li et al., 2011; Arnold et al., 2018). While the three inversions produced comparable results in terms of posterior emissions estimates there are significant uncertainties that remain. Particularly for the domain of China, uncertainties in both the analytical and hierarchical methods are very high.

		CF_4 posterior emissions in Gg/yr					
Year		**China**	**South Korea**	**North Korea**	**Japan**	**Taiwan**	**Domain Total**
2008	Arnold et al., (2018)	4.66	0.31	0.05	0.57	0.01	5.60
		(1.82)*	(0.05)*	(0.12)*	(0.36)*	(0.01)*	(2.36)*
	This work (analytical)	3.40	0.10	0.00	0.13	0.0009	3.63
	This work (hierarchical)	3.11	0.25	0.05	0.17	0.00	3.58
2009	Arnold et al., (2018)	4.01	0.15	0.02	0.23	0.32	4.73
		(1.80)	(0.05)	(0.10)	(0.33)	(0.17)	(2.45)
	This work (analytical)	2.76	0.09	0.00	0.06	0.0026	2.90
	This work (hierarchical)	3.35	0.04	0.00	0.10	0.10	3.59
2010	Arnold et al., (2018)	4.42	0.29	0.00	0.10	0.06	4.87
		(2.06)	(0.05)	(0.16)	(0.48)	(0.13)	(2.88)
	This work (analytical)	3.75	0.20	0.00	0.10	0.0015	4.05
	This work (hierarchical)	2.89	0.05	0.00	0.20	0.01	3.83
2011	Arnold et al., (2018)	4.12	0.32	0.06	0.18	0.00	4.68
		(2.37)	(0.05)	(0.15)	(0.67)	(0.26)	(3.50)
	This work (analytical)	4.35	0.19	0.00	0.08	0.0007	4.62
	This work (hierarchical)	4.89	0.27	0.00	0.20	0.10	4.64
2012	Arnold et al., (2018)	8.25	0.29	0.00	0.16	0.04	8.74
		(2.59)	(0.05)	(0.13)	(0.60)	(0.40)	(3.77)
	This work (analytical)	5.31	0.11	0.00	0.09	0.0012	5.51
	This work (hierarchical)	3.67	0.17	0.00	0.20	0.08	5.34
2013	Arnold et al., (2018)	2.82	0.26	0.08	0.11	0.09	3.36
		(2.49)	(0.04)	(0.13)	(0.48)	(0.26)	(3.40)
	This work (analytical)	3.14	0.15	0.00	0.07	0.0021	3.36

	This work (hierarchical)	4.09	0.30	0.08	0.10	0.01	3.60
2014	Arnold et al., (2018)	5.35	0.21	0.07	0.21	0.00	5.84
		(2.61)	(0.05)	(0.15)	(0.50)	(0.30)	(3.61)
	This work (analytical)	5.19	0.17	0.00	0.08	0.0014	5.44
	This work (hierarchical)	4.09	0.17	0.00	0.15	0.01	5.42
2015	Arnold et al., (2018)	4.33	0.36	0.00	0.36	0.00	5.05
		(2.65)	(0.11)	(0.26)	(0.57)	(0.44)	(4.03)
	This work (analytical)	5.45	0.19	0.00	0.06	0.0008	5.70
	This work (hierarchical)	3.9	0.20	0.00	0.20	0.00	5.45
2016	Arnold et al., (2018)	n/a	n/a	n/a	n/a	n/a	n/a
		n/a	n/a	n/a	n/a	n/a	n/a
	This work (analytical)	4.71	0.29	0.00	0.09	0.0025	5.09
	This work (hierarchical)	3.1	0	0	0.1	0.008	4.00

Table 6.1: A summary of this works' CF_4 posterior estimates (Gg/yr) from the five major emitting countries (China, South Korea, North Korea, Japan, Taiwan) within the East Asian domain and comparison of these posterior estimates with previous work by Arnold et al., (2018), Kim et al., (2010) and Li et al., (2011).

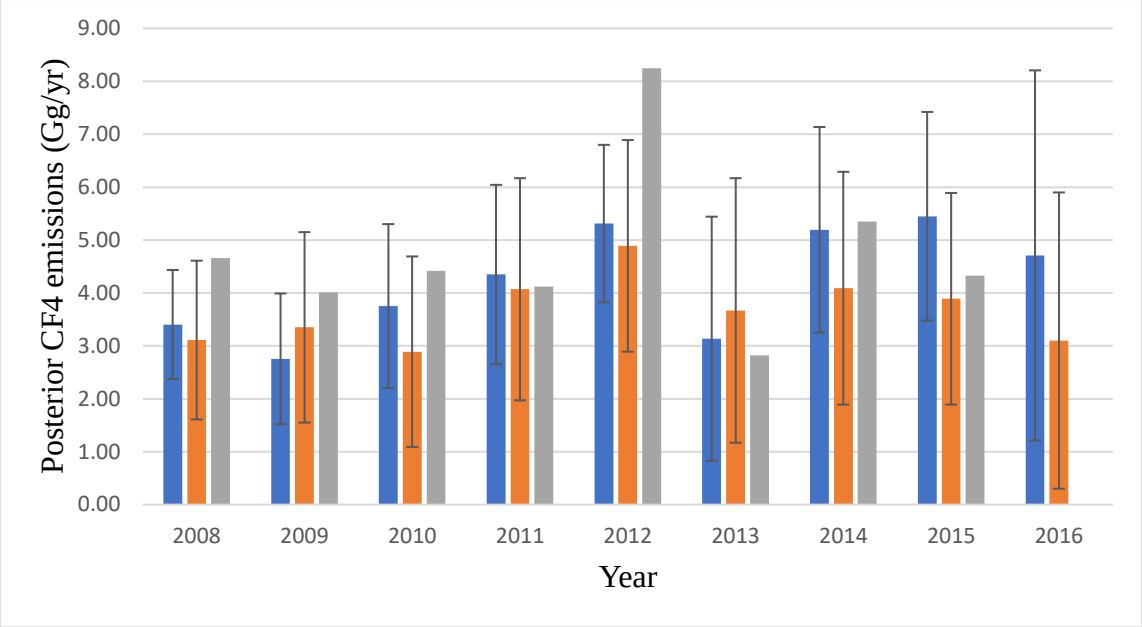

Figure 6.15: Comparison of the posterior CF_4 emissions (Gg/yr) of this works analytical and hierarchical method (in blue and orange respectively) against previously published work by Arnold et al., (2018) (in grey) for China and the years 2008-2016.

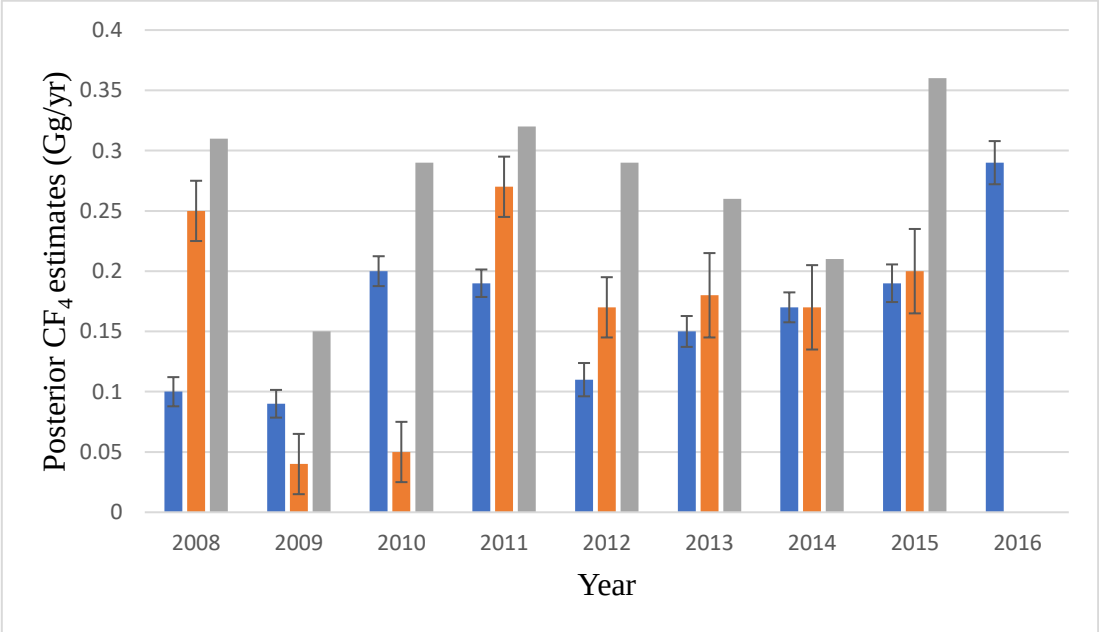

Figure 6.16: Comparison of the posterior CF_4 emissions (Gg/yr) of this works analytical and hierarchical method (in blue and orange respectively) against previously published work by Arnold et al., (2018) (in grey) for South Korea and the period 2008-2016.

As discussed in Arnold et al., (2018) posterior estimates of CF_4 were produced using a prior with uncertainty 100 times the emissions at each grid square (Arnold et al. 2018)

In their work, Arnold et al., discuss the poor understanding of CF_4, the lack of appropriate prior estimates and the need for improved and updated prior estimates (Arnold et al. 2018). This chapter presents the first comparison of posterior emissions produced used highly uncertain prior estimates and posterior emissions produced using well-defined prior estimates (4.79 (3.60 – 5.89) Gg/yr).

Figures 6.15 and 6.16 present a graphical comparison between the three different posterior estimates; the posterior estimates using the analytical methods (blue), the posterior estimates using the hierarchical method (in orange) using this works prior estimates and the posterior estimates from previously published work (in grey). These figures are focusing on the areas of greatest interest, namely China (Figure 6.15) and South Korea (Figure 6.16). The remaining countries of the domain will not be discussed further. In the case of North Korea, zero or negligible emissions were estimated from all three methods. In the case of Japan and Taiwan, as discussed there is little confidence in the emissions as these are areas almost never seen by the GSN station.

For China, where there is not much variation between the three posterior estimates compared in Figure 6.15, significant uncertainties in these estimates remain. This uncertainty is most likely linked with uncertainty related to poor sensitivity of the GSN station observations to these sources.

For South Korea, while uncertainties are much smaller, it seems the posterior estimates from the different methods variate a lot. For instance, in 2008, while both the analytical and the hierarchical methods had small uncertainties associated with their respective posterior estimates, when compared to each other there is a discrepancy of ~0.15 Gg/yr. The years 2011-2015 appear to be in better agreement for all three methods while each method's uncertainty remains small.

It is very difficult at this stage to conclude whether one method was better or more accurate than the other methods. However, having tested these inversions using a well-defined prior emissions field, it is suggested that future work repeats the inversions described above using the well-defined emission field with additional atmospheric observations (e.g. from the AGAGE station Shangdianzi, located in mainland China).

Chapter 7

Conclusions and recommendations for further work

7.1 Aims

The purpose of this chapter is to give an overview of the research questions answered in this work and the conclusions reached.

- Combining the updated inventories estimated in this work, what happens to the discrepancies for both PFC gases?
- How does this updated inventory compare to previous work?

This work set out to explore historic and existing discrepancies between top-down and bottom-up estimates of the PFC gases CF_4 and C_2F_6. Previous bottom-up studies were flawed in various ways and this will be discussed in section 7.2. To improve the bottom-up estimates this work explored each of the PFC emitting industries AI (in chapter 3), SCI (in chapter 4) and RESI (in chapter 5) and updated each, industry specific bottom-up estimate. In this chapter the new bottom-up estimates are compared with previous bottom-up work and top-down estimates. This chapter will examine how the gap looks now after these significant improvements to the bottom-up estimates have been made. It will also present top-down estimates to 2017, adding 7 years from the last time the emissions gap was assessed.

Overall, it is concluded that for the AI, the recent findings that revealed the significant contribution of LVAEs have significantly contributed to bridging the gap (chapter 3). Emissions from the SCI appear to remain of minor important and while have always been uncertain, this works presents a better way of estimated thing (chapter 4). RESI were not considered in previous studies, but this work provided a way of estimating them, albeit with high uncertainties (chapter 5).

7.2 Bridging the gap between top-down and bottom up discrepancies

7.2.1 CF_4

Figure 7.1 presents the bottom-up inventory developed through this work and the three bottom-up estimates derived for the different industries; emissions from the AI (described in

chapter 3), emissions from the SCI (described in chapter 4) and emissions from the RESI (described in chapter 5).

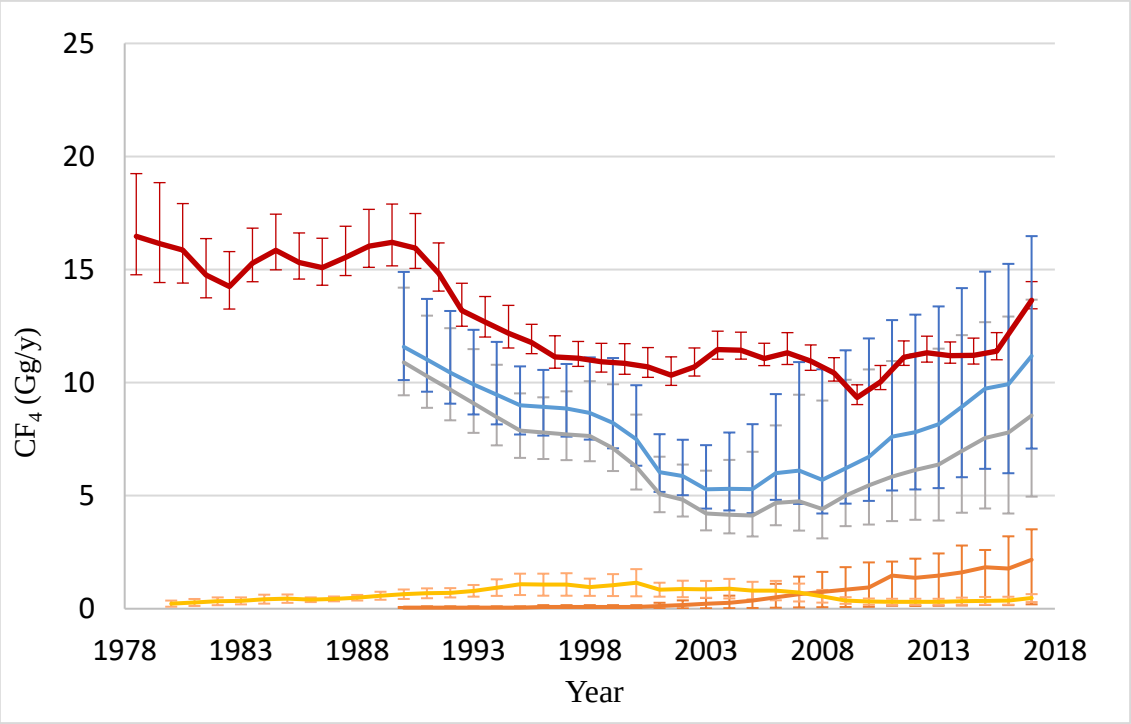

Figure 7.1: Global CF_4 emissions inferred from atmospheric data in conjunction with the AGAGE 2-D 12-box model (red line). The figure also shows estimates of CF_4 emissions from aluminium (grey line), rare earth metal (orange line) and semiconductor (yellow line) industries as well as the sum of those estimates which is the bottom-up inventory developed in this work (blue).

The AGAGE global top-down CF_4 emissions shown in this Figure (7.1) were ~16 Gg/yr in 1979, reaching another peak in 1990 of ~16 Gg/yr, declining until 2002 where they remained relatively stable within uncertainty and reached their lowest point in 2009 of ~ 9 Gg/yr. This decline in emissions could also be in part attributed to the economic crisis of 2008 which resulted in significant decrease in the AI and SCI production numbers significantly. However, the most likely explanation of this decrease in the emissions is the implementation of the Kyoto protocol and industry specific targets for PFC emissions. Post-2010 CF_4 emissions appear to be increasing again reaching ~13.6 Gg/yr in 2017. This increase in emissions is quite alarming as the last time as it is comparable with the pre-Kyoto protocol emission levels (e.g. ~12.5Gg/yr in 1995). CF_4 emission estimates from the AI were ~ 11Gg/yr in 1990 and declined steadily until 2009 when they reached their lowest point of ~3 Gg/yr. Post-2009 CF_4 are increasing with ~8.5 Gg/yr of CF_4 emitted in 2017. Two major drivers of this increase can be identified: a)

contribution from the LVAE and b) contribution from the Chinese emissions. LVAE contribution is significant but only after 2007. The percentage of LVAE contribution, however, is increasing over time and is currently (2017) more than 1/3 of the industry totals. There is significant uncertainty associated with CF_4 emissions from the AI (discussed in section 3.1). This uncertainty is attributed to those smelters who do not report their emissions to the AES, and thus, emission factors with significant uncertainties must be applied to their emissions. CF_4 emission estimates related to the RESI are also shown. Between 1990 to 2001, emissions from this industry appear to be negligible due to small production quantity. Emissions after 2001 are increasing reaching ~2 Gg/yr in 2017. There is significant uncertainty related to this source of CF_4 as few published papers on PFC emissions from RESI exist. However, CF_4 emissions from this industry could become a major source of CF_4 especially as REO production increases and this source needs further investigation.

Finally, emissions from SCI are also shown here. The SCI appears to have been and still is only a minor source of CF_4. Emissions from this industry were ~0.2 Gg/yr in 1980 and increased to ~1 Gg/yr in 1995. After the industry underwent efforts to apply gas abatement systems (post-1995) CF_4 emissions related to this industry decreased reaching ~0.5 Gg/yr in 2017.

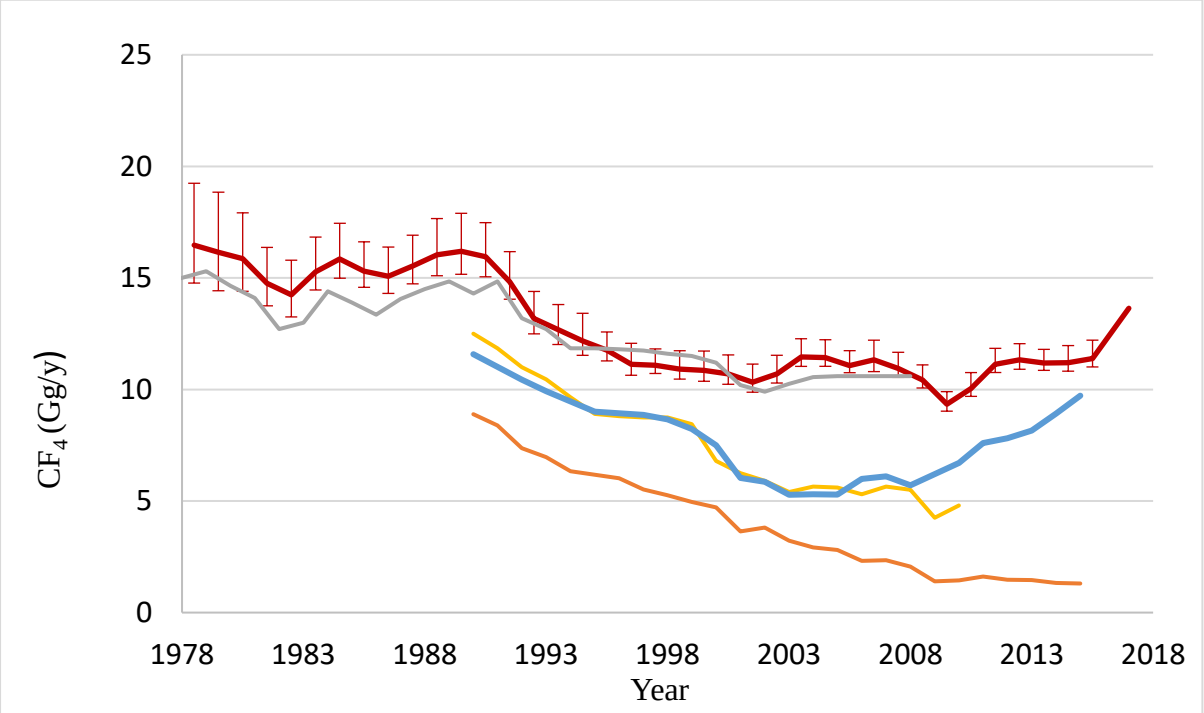

Figure 7.2: Comparison of this works CF_4 bottom-up inventory (blue line) with top-down estimates from AGAGE (red line) and previous bottom-up inventories from UNFCCC (orange line), EDGAR v4 (grey line) and Kim et al. (2014) (yellow line).

Figure 7.2 shows AGAGE global top-down emissions estimates (red line) for CF_4 at ~16 Gg/y in 1979 which decreased to ~11 Gg/yr in 2000 and onwards until 2017 when they surpassed 13 Gg/y. The EDGAR v4 bottom-up estimates appear to be in good agreement with the top-down estimates from AGAGE. However, this inventory has been contested in the literature as the way it is compiled is very unclear and it most likely uses emissions derived from mole fraction data and therefore is not a pure bottom-up inventory (Mühle et al. 2010a; Kim et al. 2014).

The inventory developed through this work is in significant agreement with the work of Kim et al. (2014) for the years 1990 to 2009. This agreement for this time period was expected as between the years 1990 and 2009, the additional sources considered in this inventory (LVAE, Chinese specific AI emissions and RESI emissions) were, at the time, not major contributors of CF_4.

CF_4 emission estimates by UNFCCC are based on emission data collected from the NIRs (UNFCCC 2015). It was expected that emissions included in this works inventory would be substantially larger than emissions produced by the NIRs as Annex I countries account for a very small percentage of the emissions. Additionally, among the non- Annex I countries that emit PFCs are China and India that have increased GHG emissions in comparison to the Annex I countries. Finally, the UNFCCC inventory does not include any estimate of the emissions from RESI emissions. The bottom-up inventory of this work shows significant agreement with the top-down AGAGE estimates for the time period 1990-2000. However, between 2000 and 2010, this inventory and the top-down estimates appear to diverge with discrepancies increasing between them (maximum discrepancy ~5 Gg/yr in 2005). After 2010, this works bottom-up estimates and the top-down estimates appear to be in better agreement.

The combined LVAE, RESI emissions (and CFM to a smaller degree) are significant considerations for understanding the top-down vs bottom-up gap, especially in more recent years, as presented here for the first time. There are large uncertainties related to this updated inventory (see Figure 7.1), as this is an inclusive and comprehensive bottom-up inventory, it can be updated easily as more information becomes available. These uncertainties and the persisting gap in the early 2000's that are not addressed by this updated bottom-up inventory should be addressed in future studies, for example through regional emissions estimates.

7.2.2 C_2F_6

Figure 7.3 presents the bottom-up inventory developed through this work and the three bottom-up estimates derived for the different industries; emissions from the AI (described in chapter 3), emissions from the SCI (described in chapter 4) and emissions from the RESI (described in chapter 5).

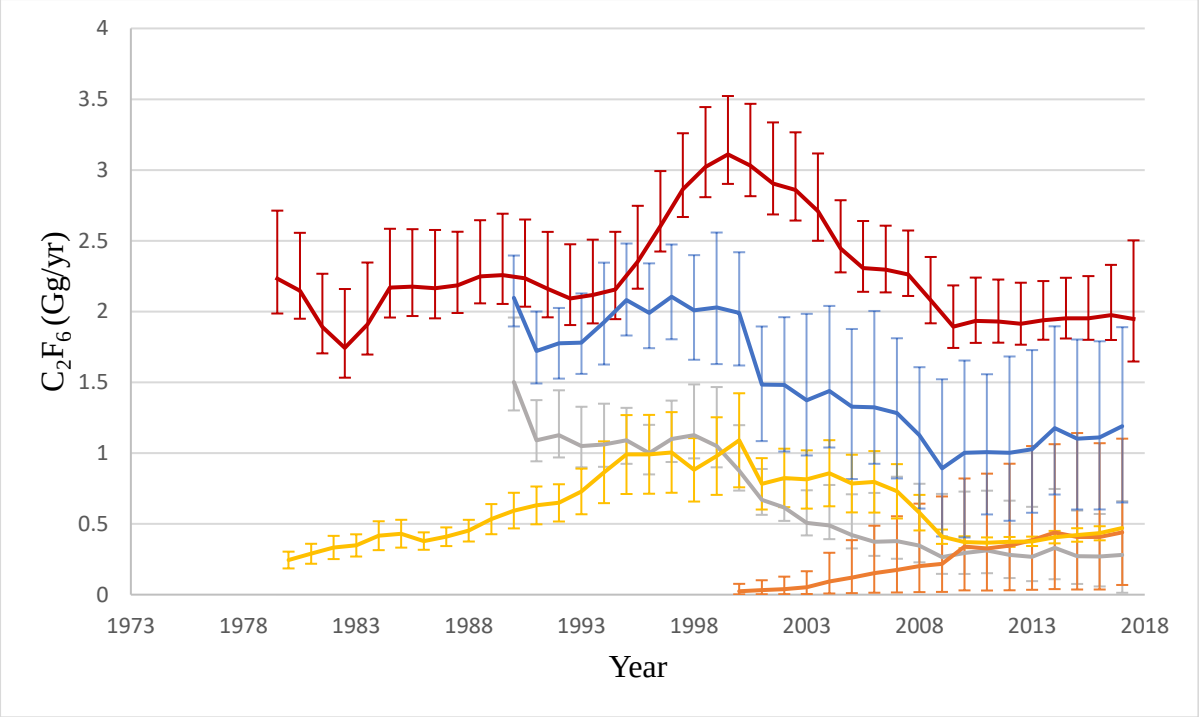

Figure 7.3: Global C_2F_6 emissions inferred from atmospheric data in conjunction with the AGAGE 2-D 12-box model (red line). The figure also shows estimates of C_2F_6 emissions from the AI (grey line), the RESI (orange line) and semiconductor (yellow line) industries as well as the sum of those estimates which is the bottom-up inventory developed in this work (blue line).

The AGAGE global top-down C_2F_6 emissions shown in this Figure (7.3) were ~2.2 Gg/yr in 1979, reached a peak of ~3.1 Gg/yr in 1999 and then declined to ~1.8 Gg/yr in 2009 where they have remained since (~1.9 Gg/yr in 2017). Unlike CF_4, C_2F_6 does not demonstrate the same increase in emissions after 2010.

C_2F_6 emission estimates from the AI were ~ 1.5 Gg/yr in 1990 and declined steadily until 2017 when they reached their lowest point of ~0.2 Gg/yr. Unlike CF_4, it is reported that C_2F_6 is not detected during LVAE (Marks and Nunez 2018; IPCC 2019). In the case of C_2F_6 emissions from the AI, it appears that two major drivers that increased CF_4 emissions (Chinese emissions and LVAE) are not contributing to an increase in C_2F_6 emissions. Uncertainties

remain as this are driven by the same non-reporting entities that are driving CF_4 related uncertainties.

C_2F_6 emission estimates related to the RESI are also shown. Between 1990 to 2001, emissions from this industry appear to be negligible due to small production quantity (e.g. ~0.02 Gg/yr of C_2F_6 were emitted in 2001). Emissions after 2001 are increasing reaching ~0.5 Gg/yr in 2017. There is significant uncertainty related to this source of C_2F_6 as few published papers on PFC emissions from RESI exist. However, as discussed for CF_4, C_2F_6 emissions from this industry could become a major source of PFCs and they require further investigation.

Finally, emissions from SCI are also shown here. The SCI appears to have been and still is only a minor source of CF_4. Emissions from this industry were ~0.2 Gg/yr in 1980 and increased to ~1 Gg/yr in 2000. After the industry underwent efforts to apply gas abatement systems (post-1995) C_2F_6 emissions related to this industry decreased reaching ~0.5 Gg/yr in 2017.

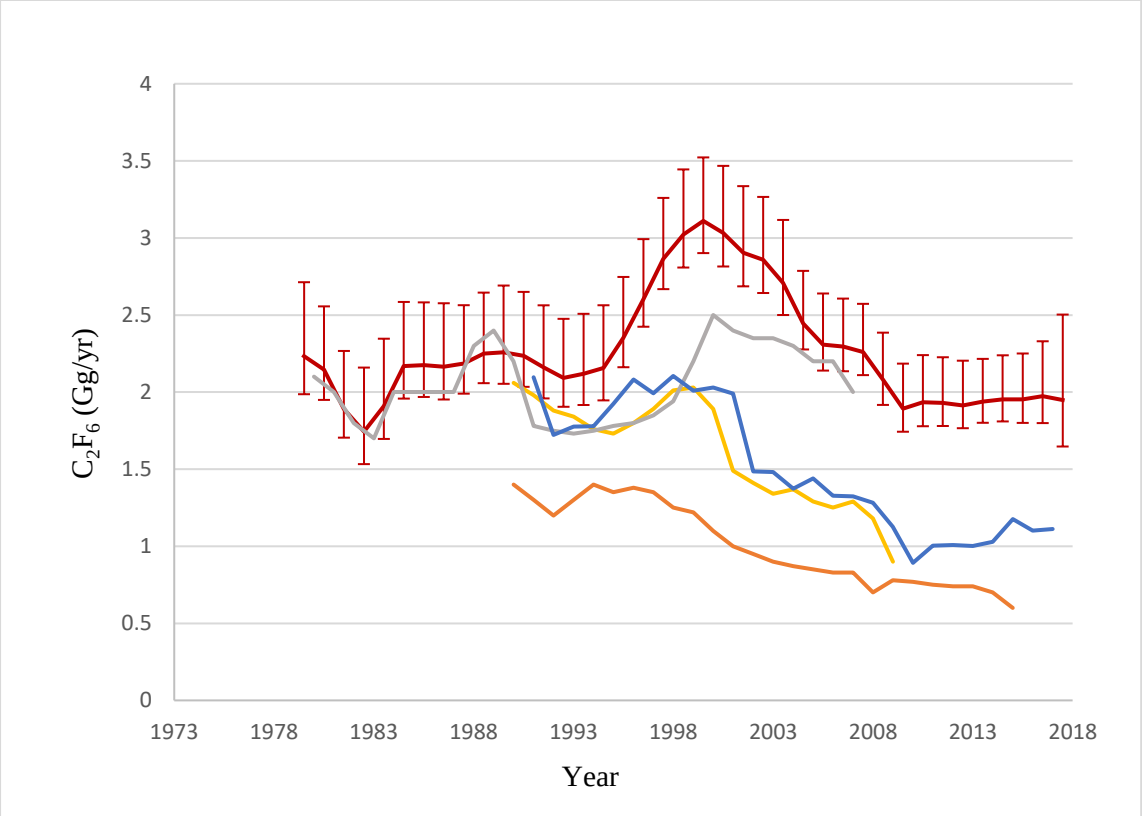

Figure 7.4: Comparison of this works C_2F_6 bottom-up inventory (blue line) with top-down estimates from AGAGE (red line) and previous bottom-up inventories from UNFCCC (orange line), EDGAR (grey line) and Kim et al. (2014) (yellow line).

Figure 7.4 shows AGAGE global top-down emissions estimates (red line) for C_2F_6 at ~2.2 Gg/y in 1979 which decreased to ~3.1 Gg/y in 2000, decreased to ~1.8 Gg/yr in 210 where and remained until 2017 w. The EDGAR v4 bottom-up estimates appear to be in good agreement with the top-down estimates from AGAGE, much like in the CF_4 case. The same limitations apply for the C_2F_6 emissions and this inventory as discussed in section 7.2.1.

The inventory developed through this work is in significant agreement with the work of Kim et al. (2014) for the years 1990 to 2009. This agreement for this time period was expected as between the years 1990 and 2009, the additional sources considered in this inventory (Chinese specific AI emissions and RESI emissions) were, at the time, not major contributors of C_2F_6 emissions.

C_2F_6 emission estimates by UNFCCC are based on emission data collected from the NIRs (UNFCCC 2015). It was expected that emissions included in this works inventory would be substantially larger than emissions produced by the NIRs as Annex I countries account for a very small percentage of the emissions. Additionally, among the non- Annex I countries that emit PFCs are China and India that have increased GHG emissions in comparison to the Annex I countries.

The bottom-up inventory of this work is in good agreement with the top-down AGAGE estimates for the time period 1990-2000. However, between 2000 and 2010, our inventory and the top-down estimates diverge with discrepancies increasing between them (maximum discrepancy ~1.3 Gg/yr in 2004). Unlike CF_4, discrepancies between top-down and bottom-up for the case of C_2F_6 persist even after 2010 (discrepancy of ~0.9 Gg/yr in 2017).

The combined RESI emissions (and CFM to a smaller degree) are significant considerations for understanding the top-down vs bottom-up gap, especially in more recent years, as presented here for the first time. There are large uncertainties related to this updated inventory (see Figure 7.3), as this is an inclusive and comprehensive bottom-up inventory, it can be updated easily as more information becomes available. These uncertainties and the persisting gap (mostly after the year 2000) that are not addressed by this updated bottom-up inventory should be addressed in future studies, for example through regional emissions estimates.

7.3 Future work

Overall, it is suggested that this updated inventory must be revised as more emission factors become available from the PFC emitting industries; at that point the uncertainties associated with the inventory should be re-examined. Furthermore, it is suggested that future analysis is done using the inverse modelling methods described in Chapter 6. The results produced in Chapter 6 form the basis of preliminary posterior estimates using an analytical and a hierarchical Bayesian approach, further analysis is required in order to examine which method is best suited not just for CF_4 but for the majority of F-gases monitored under the Kyoto protocol.

Finally, one more CTM was used during this work. STOCHEM, a global 3-dimensional chemistry transport model, originally developed at the UK Met Office. In STOCHEM, the troposphere is divided into 50,000 constant mass air parcels, which are advected through the model domain every 3 hours via a Lagrangian approach, allowing the transport and chemical processes within the model to be uncoupled. The model works offline and incorporates archived meteorological data from the UK Met Office UM to drive the transport of the air parcels. The archived data from the model have a grid resolution of 1.25° longitude by 0.83° latitude by 12 unevenly spaced vertical levels, with an upper boundary of 100 hPa. STOCHEM is a computationally efficient model which allows the implementation of a detailed chemistry mechanism (Common Representative Intermediates mechanism, CRI v2-R5) for the study of ozone, odd-H, and related species within the troposphere. The most current version of this mechanism describes the degradation of methane and 26 non-methane hydrocarbons, using 229 species in 627 photochemical reactions.

Figures 7.5 – 7.6 show the correlation between modelled data for a winter and a summer month in the same year (2017) for both PFCs, CF_4 and C_2F_6 for six zonal bands What was expected from producing these correlation maps, was a strong positive correlation for all the six zonal bands, both months and both gases. The reason this was expected is the long lifetime of both PFCs and the fact that there are no known sinks in the lower troposphere. However, a strong correlation was observed between measured and modelled data for both gases in the zonal bands of 20N-40N, 40N-60N and 60N-90N, no correlation in the zonal band of 20S-20N and a strong anti-correlation in the zonal bands of 20S-40S and 40S-90S.

a) CF_4

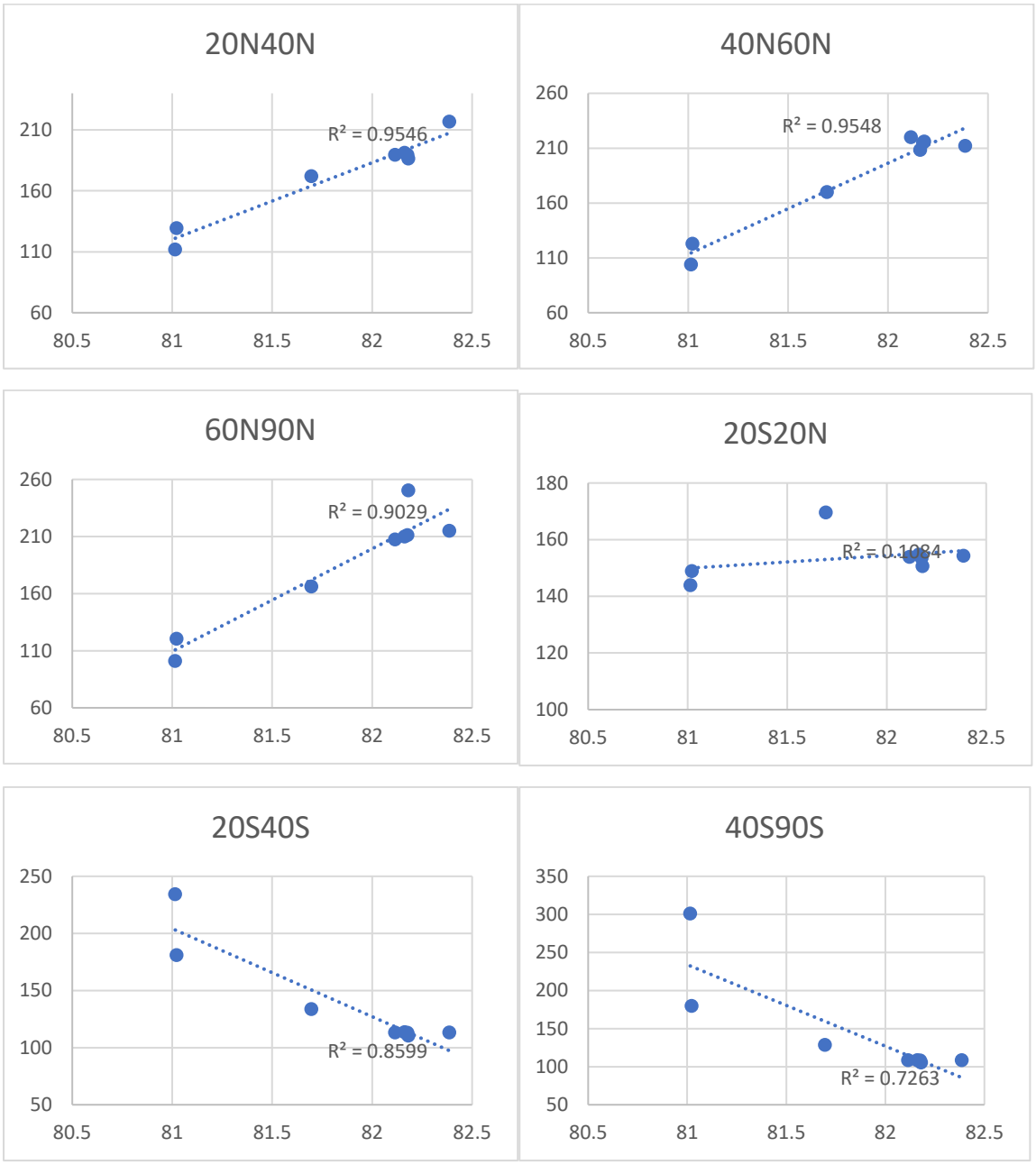

Figure 7.5: Correlation between measured vs modelled data for CF_4 for December 2017.

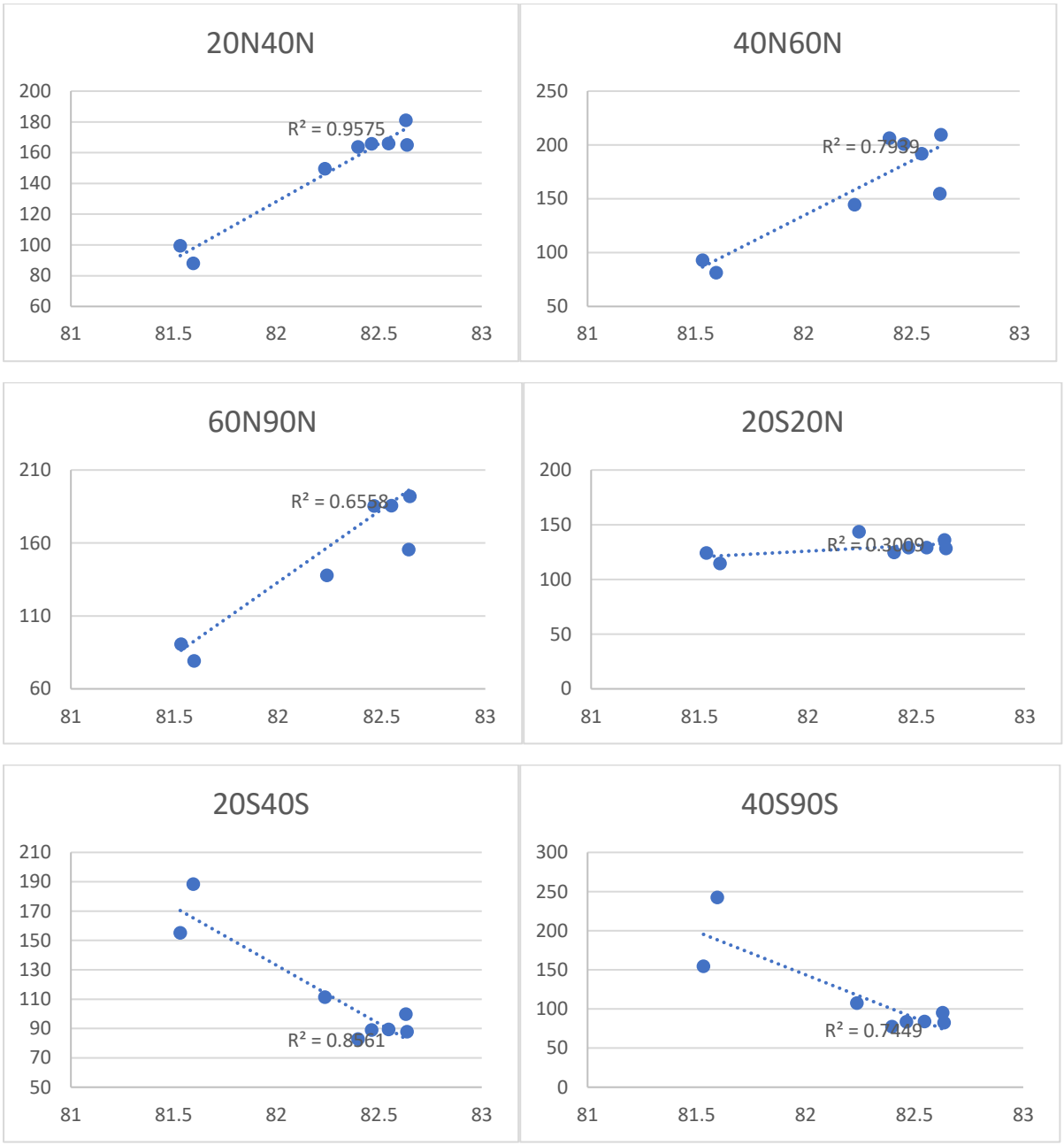

Figure 7.6: Correlation between measured vs modelled data for CF_4 for August 2017.

b) C_2F_6

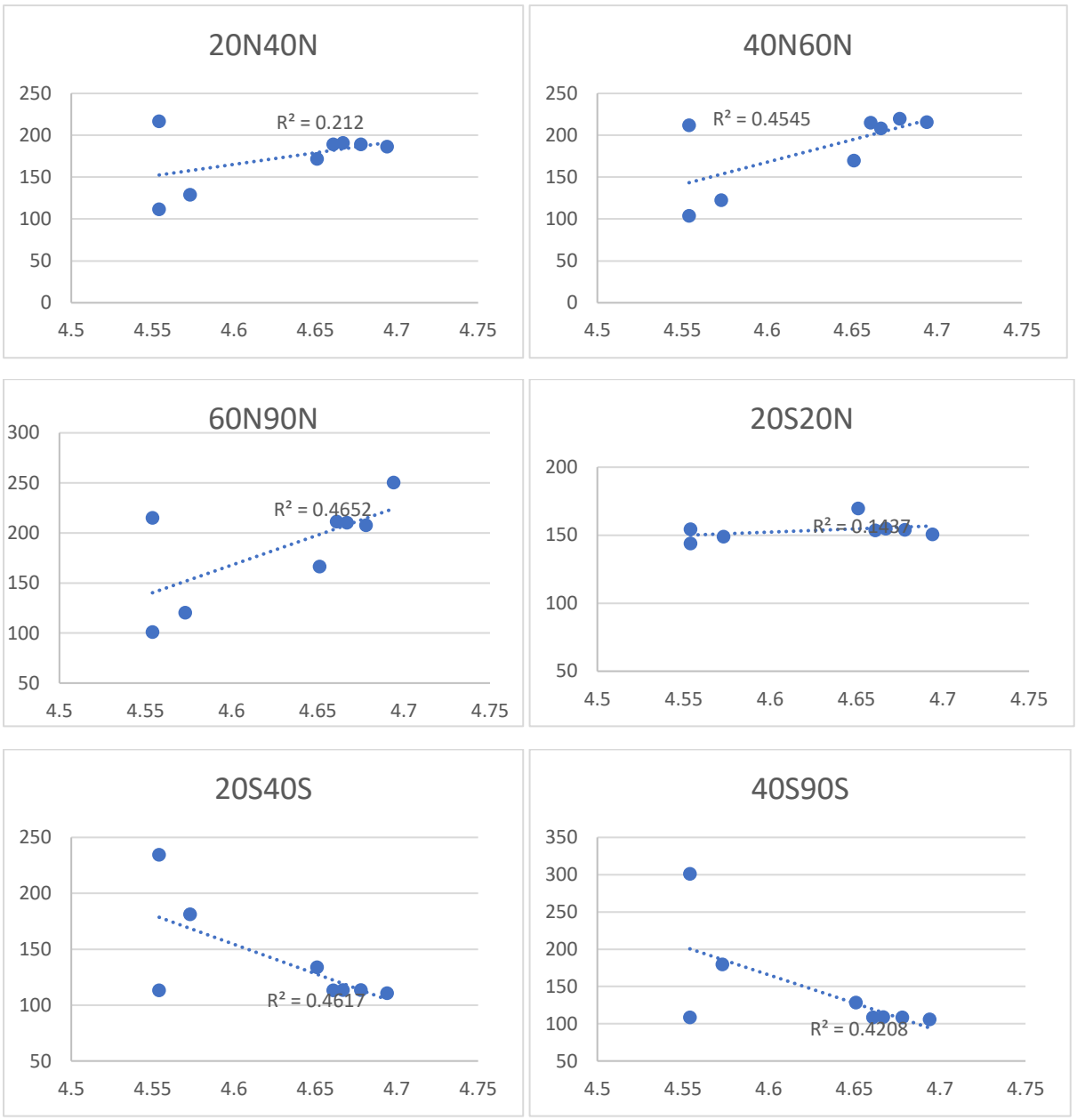

Figure 7.7: Correlation between measured vs modelled data for C_2F_6 for December 2017.

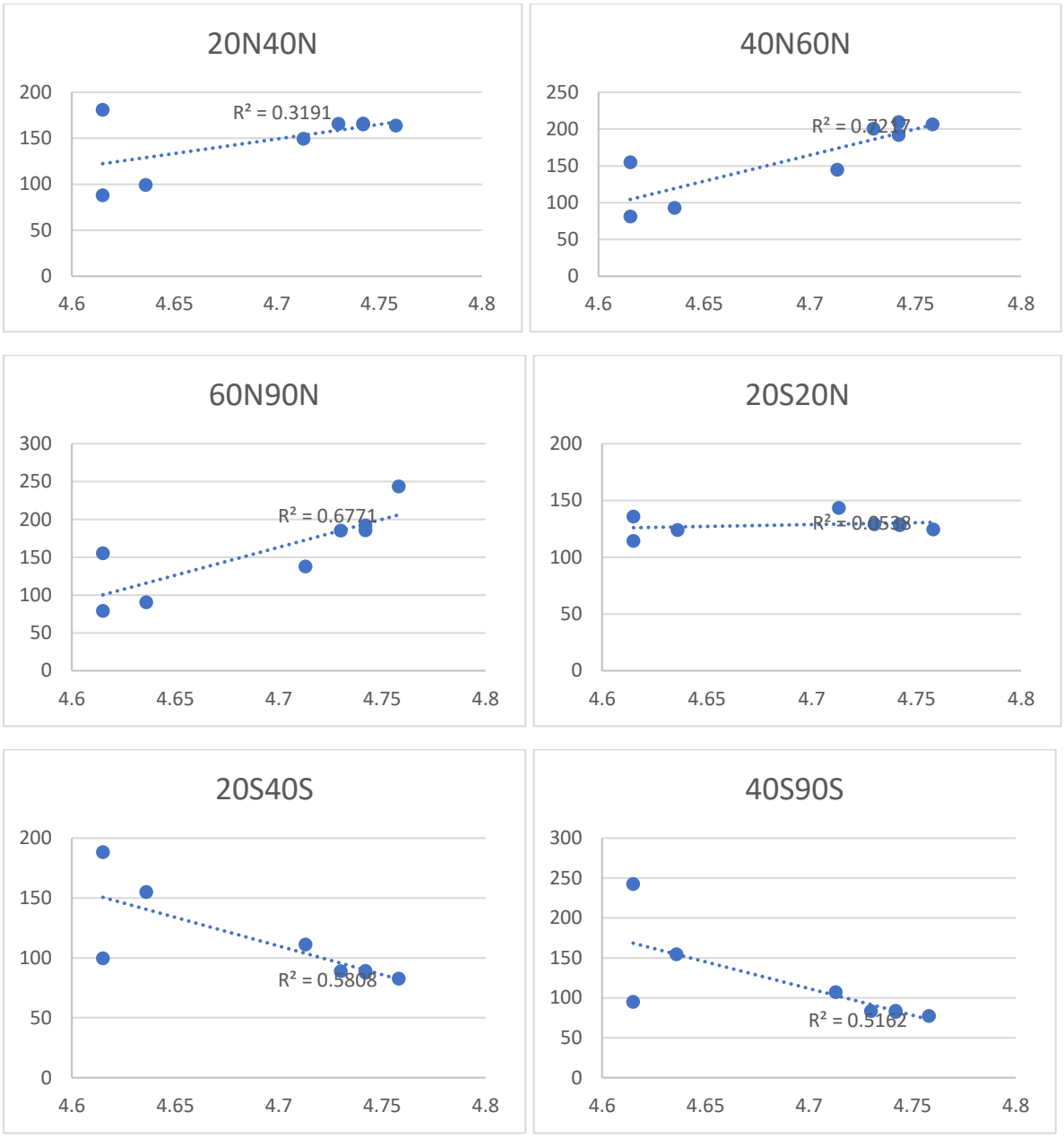

Figure 7.8: Correlation between measured vs modelled for C_2F_6 for August 2017.

It is thought that the reason for this negative correlation could be synoptic scale meteorological phenomena not properly resolved within STOCHEM. While it is considered unlikely that this negative correlation could potentially indicate the presence of a sink in those zonal bands, it is deemed that this requires further investigation.

7.4 Concluding summary

Overall, the most important contributions of this work are a) the quantification and analysis of PFC emissions from the three different industries that emit them; the aluminium, semiconductor and rare earth smelting industries b) closing the gap between bottom-up and top-down estimates.

However, there is also a qualitative aspect of this work that should be highlighted. This work demonstrates that appropriate industrial governance can lead to significant success in reducing greenhouse gas emissions, in this particular case, PFC emissions. The aluminium industry, through decades of effort have managed a significant reduction of their PFC gases. After the International Aluminium Institute was established, the aluminium industry took proactive measures in order to reduce their emissions. Through voluntary industry wide surveys, pledges and measurement campaigns, technological innovation and development the aluminium industry demonstrates the importance of governance in relation to PFC reduction.

Equally, the semiconductor industry has taken industry-wide, voluntary action in order to achieve GHG emissions reductions. Unlike the AI where PFCs are emitted "accidentally" during the smelting process, the SC actively uses PFCs for etching and chamber cleaning purposes. In 1999 the World Semiconductor Council (WSC) pledged to reduce its CF4 emissions using gas abatement equipment. Gas abatement systems were rolled out in 1995 and were gradually introduced throughout the entire SI. This resulted in a reduction of CF4 emissions from approximately 1 Gg/y in 1990 to 0.3 Gg/y in 2018.

These success stories of both the AI and the SC industry demonstrate is that the early identification of a problem, combined with the application of existing best practices and improved technologies could be the key to solving a climate change related challenge at its roots. The technological dependence on REs proves that this is not a commodity that we can do without so early quantification of these emissions combined with a re-examination of the carbon footprint of both the wind turbines and electric vehicles is paramount in order to meet the 1.5 degree target set by the IPCC.

Finally, this section will briefly summarise the contribution of every chapter and will give an overall summary of what this work has achieved.

Chapter 2 interpreted PFC emissions as part of the global challenges' narrative has to my knowledge not been attempted before. Additionally, it considered the challenge of PFC emissions through the lens of systems thinking and sustainable development using methods and approaches from a wide range of disciplines. This allowed to produce a new impact factor,

the De Minimis Scaling Impact Factor (DMSIF). This factor uses principles from law, economics, social sciences, atmospheric chemistry and physics, in order to consider the impact of PFC emissions from a different perspective. This perspective allowed for quantification of socioeconomic parameters associated with the industries that produce PFCs on a per country (over time) basis. Finally, the introduction of the DMSIF is an extremely innovative approach on how both the environmental impact of PFC emissions but also consider the socio-economic parameters (e.g. the UNs Human development Index (HDI) can be considered when estimating the impact of a GHG.

A new bottom-up inventory of PFC emissions was produced. Chapter 3, 4 and 5 quantified historic and current PFC emissions from the AI, SCI and RESI respectively. To quantify emissions from the AI existing information on HVAE from the IAI was used as well as newly updated information regarding LVAE. To quantify emissions from the SCI two new methods to estimate PFC emissions were developed, the CFM and FSM. Both these methods produced results comparable to those reported by the WSC. Finally, to quantify emissions from the RESI and consider them as part of an inventory for the first time, newly published information was used.

Chapter 6 presented how this inventory was tested as a prior field for different inverse methods. Some of the results presented in the work have not been presented before. This chapter showed that posterior emissions, can be estimated using a well-defined prior field which was tested in simple (Australia, South Korea) and complex (East Asia) domains. Posterior emissions distributions and their magnitudes are in good agreement both with this works prior estimates but also with posterior estimates of previously published work.

Chapter 7 showed how the combined LVAE, rare earth and SCI contribution are significant considerations for understanding the top-down vs bottom-up gap. Our new bottom-up estimates, while in some agreement with the top-down estimates, still come with significant uncertainties that should be addressed in the future.

These new approaches, methods and frameworks resulted in significant, industry-specific impact of this work, as well as impact related to policy making. Part of this work is included in the International Panel on Climate Change (IPCC) 2019 refinement to the 2006 guidelines, Chapter 4, Metal Industry Emissions: Rare Earth Smelting. I am extremely grateful to have engaged in a productive and continuous dialogue with the aluminium industry, the semiconductor industry and the gas abatement industry. Much of the inspiration of this work was drawn from those discussions and I am really proud to have established an excellent working relationship with these industries. Several limitations were encountered during this

work, but as they are limitations specific to each industry these will be expanded upon under the respective chapters. Some limitations could not be overcome (e.g. data being publicly available or confidential), however because of the working relationship developed with these industries it is hoped that in the near future these limitations will be resolved by having (e.g.) access to better, more detailed, industry specific data.

I am extremely grateful to have been part of the excellent community of researchers within the University of Bristol's research institutes, namely the Cabot Institute, the Centre of Innovation and Enterprise and the City Futures Institute for providing me if not with answers, but always with the right questions.

Appendix A:

This appendix provides some additional material related to Chapter 2 where a preliminary socioeconomic analysis of PFCs was attempted.

A.1 The role of atmospheric chemistry in the Anthropocene

The point highlighted in the extract from the work of MacKinnon, Hine & Barnard (2013) (Mackinnon, Hine and Barnard, 2013) is very important: it is the problem (challenge or question) the scientist is trying to address that will define the appropriate approach(es) (or the appropriate science tools) (Michalopoulou et al. 2019).

This leads to the next question: What are the current problems, or as they are also called, global challenges? We now live in the era of the Anthropocene (Crutzen, 2002) where humans are a globally significant force capable of reshaping the face of the planet. In the case of the human-environment interaction system, the myriad ways that humans have been changing the planet are a side-effect of our 'learning about global change by doing global change' (Clark, Crutzen, and Schellnhuber 2005; Michalopoulou et al. 2019).

Atmospheric chemistry is an interdisciplinary branch of the atmospheric sciences that studies the composition of the atmosphere. It is obvious, by looking at the SDGs that atmospheric chemistry is directly linked to goal 13 (climate action) and indirectly to goals 14 and 15 (life below water and life on land). There are of course, more indirect links with other goals but for the purpose of this discussion only a limited number of examples for the indirect links are given.

In 'The End of Simple Problems: Re-positioning Chemistry in Higher Education and Society Using a Systems Thinking Approach and the United Nations' Sustainable Development Goals as a Framework' Michalopoulou et al., (2019) attempted to map the direct and indirect role Chemistry has to play in addressing the SDGs. Equally, atmospheric chemistry and atmospheric chemists have a bigger role to play than studying and monitoring the composition of the atmosphere. They inform policy, communicate science, engage with different stakeholders (the industries being one of those stakeholders) and participate in intergovernmental bodies such as the IPCC.

Specifically, in the case of PFCs, it will be shown in section 2.3.3, that by combining atmospheric chemistry with systems thinking and the post-disciplinary approach the discussion

regarding PFCs and their impact broadens and the challenge of PFCs is presented as more than a climate and/or environment specific challenge.

A.2 Problem solving and wicked problems

Albert Einstein is often quoted to have said: "If I were given one hour to save the planet, I would spend 59 minutes defining the problem and one minute resolving it" and whether Einstein did say this or not, problem solving theory suggests that the way one understands, and therefore structures or phrases ones problem plays a big role in how they will set out to solve the problem (Jonassen, 2000; Dostál, 2015). The term 'wicked problem' was coined by Rittel and Weber in 1973 (Rittel and Webber, 1973) and it was used to describe a set of problems with very specific characteristics (Climate change and development as 'wicked', complex problems; Australian Public Service Commission, 2007; Rittel and Webber, 1973):

1. Wicked problems are difficult to define clearly. They have many interdependencies and often have multiple causes, and these can be defined at different levels in hierarchies of causes.
2. There is no definitive formulation of a wicked problem. The information needed to understand the problem depends upon initial ideas for solving it (and thus depends upon the backgrounds, training and experience of those looking for solutions).
3. There is no test of a solution. Any solution, when implemented, will generate intended and unintended consequences over an extended period of time, and hence change the problem.
4. Similarly, solutions are not true-or-false, correct-or-incorrect, but good-or-bad, and thus their evaluation and acceptance depend upon judgments that are likely to differ widely between individuals and groups with different interests, values, and backgrounds.
5. Every solution is unique, as every problem is unique, but there is also no opportunity to learn by trial-and-error as attempts at solutions themselves change the problem.
6. Solutions are socially and organisationally complex, and require co-ordinated action by a range of stakeholders, including government agencies at national and subsidiary levels, non-profit organisations, private businesses, civil society groups, and individuals, and do not fit neatly within the responsibility of any one agency.
7. Solutions tend to involve changing behaviour.
8. Some wicked problems are characterised by chronic policy failure.

9. There is no definitive solution or resolution to the problem, at the end of which the problem is solved - rather the problem and measures to address it continually evolve

Climate change is already treated as a wicked problem in the literature (Australian Public Service Commission, 2007; FitzGibbon and O.Mensah, 2012; Incropera, 2016; UNDP, 2018c; Walls, 2018) because it fulfils the criteria just stated. However, before these criteria in relation to PFC emissions can be considered, three different levels of understanding and framing of the problem of PFC emissions must be created.

A.3 Wicked PFCs

Having mapped the SDGs and targets that this analysis helps address, PFCs will now be discussed as part of the wicked problems narrative.

Do PFCs fall under the category of wicked problems?

1. Wicked problems are difficult to define clearly. They have many interdependencies and often have multiple causes, and these can be defined at different levels in hierarchies of causes.
2. There is no definitive formulation of a wicked problem. The information needed to understand the problem depends upon initial ideas for solving it (and thus depends upon the backgrounds, training and experience of those looking for solutions).

Atmospheric concentrations of PFCs result from industrial emissions of PFCs. However, PFC emissions are not a simple problem. Each industry emitting PFCs does so in an industry unique way. Therefore, three different types of processes need to be considered when attempting to define the PFC challenge holistically. At the same time, these processes, as described above are supporting the economic activity, which in turn supports social (and other) structures. Whether this issue can be confined to the industry specific processes that emit those gases (meso-system) or whether this issue will be addressed using a bigger system (the macro-system), there are many interdependencies and multiple causes and different levels of the problem on different scales.

As discussed in section 1.8 and as it will be demonstrated in detail in chapter 3 and 4, the combined efforts of the AI and the SI and the implementation of the Kyoto protocol resulted in a decrease in PFC emissions for these industries. However, another source of PFCs was recently discovered (the RESI) and, previously unknown emissions the AI have also been

identified (Marks and Nunez, 2018; IPCC, 2019a). Currently, despite the AI and SCI putting huge efforts into reducing their PFC emissions as they did in the past, global PFC emissions appear to be increasing. This will be discussed in detail in chapter 7. Any industrial effort and strategy to reduce PFC emissions, often translates into costs; and whether that cost is financial or related to a resource (e.g. human, energy) these resources are finite and have footprints and handprints of their own.

3. There is no test of a solution. Any solution, when implemented, will generate intended and unintended consequences over an extended period of time, and hence change the problem.
4. Similarly, solutions are not true-or-false, correct-or-incorrect, but good-or-bad, and thus their evaluation and acceptance depend upon judgments that are likely to differ widely between individuals and groups with different interests, values, and backgrounds.
5. Every solution is unique, as every problem is unique, but there is also no opportunity to learn by trial-and-error as attempts at solutions themselves change the problem.
6. Solutions are socially and organisationally complex, and require co-ordinated action by a range of stakeholders, including government agencies at national and subsidiary levels, non-profit organisations, private businesses, civil society groups, and individuals, and do not fit neatly within the responsibility of any one agency.
7. Solutions tend to involve changing behaviour.

Any, and all the solutions that have been applied to the AI and SCI in order to reduce PFC emissions have intended and unintended consequences themselves. For instance, the SCI applies gas abatement in order to reduce PFC emissions. Gas abatement is, broadly speaking, a series of methods that prevent potent GHGs like PFCs from being emitted back into the atmosphere after they have been used by the industry; this will be discussed in greater detail in chapter 4. Gas abatement instruments have, of course, to be built and consequently have emissions of their own and are depleting other (if not the same) resources in order to be built in the first place.

As the industries that emit PFCs are different, industry specific solutions must be unique, much like the problems and limitations they face are unique. Similarly, and because of the widely different geospatial distribution of the aforementioned industries, each industry will have a different understanding and prioritisation of the problem, a different culture when it comes to dealing with this problem. Equally, the country hosting each industry will have different priorities, different development and environmental targets, which will of course fluctuate through time. Different industries are comprised of different stakeholders,

government agencies, structures priorities. This spatiotemporal differentiation of the industries and therefore the PFC emissions is the heart of this challenge.

8. Some wicked problems are characterised by chronic policy failure.

It is difficult to assess whether the problem of PFCs has been characterised by chronic policy failure. In principle, at least for the cases of the AI and SCI, there are governing bodies in place that monitor and report their PFC emissions as per their commitments to the Kyoto protocol. As we be discussed in chapter 7, between the years 1990 and 2008 global PFC emissions were in fact decreasing. PFC emissions started to increase again at the end of 2010, and they are currently still increasing (2019).

9. There is no definitive solution or resolution to the problem, at the end of which the problem is solved - rather the problem and measures to address it continually evolve.

The problem of PFCs will, in all probability and as described by the handprint principles, not reach a definitive solution or resolution. In the case of the AI and the RESI it is unlikely that the events producing PFCs will be completely eradicated and in the case of the SCI, even if the specific PFCs are replaced from the etch and chamber cleaning processes, other gases will replace them that may carry a significant GWP. And while the industries should and are striving to reduce their environmental footprint, in the case of PFCs it may be that the discussion in terms of impact and solutions needs to shift to an entirely new direction. This direction should hold the principles of sustainable development, those of needs vs limitations and this is what section 2.4.3 will attempt to discuss and quantify.

References

2005, W. (2005) ‘WSC Indexed PFC Emissions’, *WSC Reports*, p. 1.

3.2 Climate change and development as ‘wicked’, complex problems (no date). Available at: https://www.soas.ac.uk/cedep-demos/000_P524_CCD_K3736-Demo/unit1/page_18.htm (Accessed: 6 August 2019).

Abraham, I. (2011) ‘Rare earths: the cold war in the annals of travancore’, *Entangled Geographies: Empire and Technopolitics in the Global Cold War*. MIT Press Cambridge, MA, pp. 101–124.

Aggarwal, C. C. and Zhai, C. (2012) *Mining text data*. Springer Science & Business Media.

Aguilera, P. A. *et al.* (2011) ‘Bayesian networks in environmental modelling’, *Environmental Modelling and Software*. Elsevier Ltd, 26(12), pp. 1376–1388. doi: 10.1016/j.envsoft.2011.06.004.

Akkermans, H. A. and Van Wassenhove, L. N. (2013) ‘Searching for the grey swans: the next 50 years of production research’, *International Journal of Production Research*. Taylor & Francis, 51(23–24), pp. 6746–6755.

Ali, S., Ali and H., S. (2014) ‘Social and Environmental Impact of the Rare Earth Industries’, *Resources*. Multidisciplinary Digital Publishing Institute, 3(1), pp. 123–134. doi: 10.3390/resources3010123.

Alonso, E. *et al.* (2012) ‘An Assessment of the Rare Earth Element Content of Conventional and Electric Vehicles’, *SAE International Journal of Materials and Manufacturing*, 5(2), pp. 2012-01–1061. doi: 10.4271/2012-01-1061.

Analysis of Semiconductor Market Data (no date). Available at: https://www.semiconductors.org/wp-content/uploads/2018/05/20th-WSC-Joint-Statement-May-2016-Seoul-FINAL.pdf (Accessed: 5 June 2019).

Andersen, N., Eriksson, O. and Hillman, K. (2015) *Wind turbine end-of-life: Characterisation of waste material*. Available at: https://www.diva-portal.org/smash/get/diva2:873368/FULLTEXT01.pdf (Accessed: 17 July 2019).

Annex III: Revision of 2013 World Semiconductor Council (WSC) PFC data (2014). Available at: http://www.semiconductorcouncil.org/wp-content/uploads/2016/04/WSC-JS-Annex-lll-5-November-2014.pdf (Accessed: 14 June 2019).

Apergis, E. and Apergis, N. (2017) ‘The role of rare earth prices in renewable energy consumption: The actual driver for a renewable energy world’, *Energy Economics*. Elsevier, 62, pp. 33–42. doi: 10.1016/j.eneco.2016.12.015.

Applications - Rare Earth Elements - DANTEK Global Sourcing Solutions (no date). Available at: https://www.dantek-minerals.com/application/ (Accessed: 4 July 2019).

Arnold, R. D. and Wade, J. P. (2015) ‘A Definition of Systems Thinking : A Systems Approach’, *Procedia - Procedia Computer Science*. Elsevier Masson SAS, 44, pp. 669–678. doi: 10.1016/j.procs.2015.03.050.

Arnold, T. *et al.* (2018) ‘Inverse modelling of CF<inf>4</inf> and NF<inf>3</inf> emissions in East Asia’, *Atmospheric Chemistry and Physics*, 18(18), pp. 13305–13320. doi: 10.5194/acp-18-13305-2018.

Asaithambi, G., Treiber, M. and Kanagaraj, V. (2019) ‘International Climate Protection’, *International Climate Protection*, (October). doi: 10.1007/978-3-030-03816-8.

Åsheim, H. *et al.* (2014) ‘Monitoring of continuous PFC formation in small to moderate size aluminium electrolysis cells’, in *Light Metals 2014*. Springer, pp. 535–539.

Asian Metalpedia (2012) *REE: industry associations and famous companies*. Available at: http://metalpedia.asianmetal.com/metal/rare_earth/organization.shtml (Accessed: 25 September 2019).

Australian Public Service Commission (2007) *Tackling wicked problems : A public policy perspective | Australian Public Service Commission*. Available at: https://www.apsc.gov.au/tackling-wicked-problems-public-policy-perspective (Accessed: 7 August 2019).

Baird, C. (1998) *Environmental chemistry*. New York: W.H. Freeman.

Baldi, L., Peri, M. and Vandone, D. (2014) ‘Clean energy industries and rare earth materials: Economic and financial issues’, *Energy Policy*. Elsevier, 66, pp. 53–61. doi: 10.1016/J.ENPOL.2013.10.067.

Barbier, E. B. (1987) ‘The Concept of Sustainable Economic Development’, *Environmental Conservation*. 2009/08/24. Cambridge University Press, 14(2), pp. 101–110. doi: DOI: 10.1017/S0376892900011449.

Bazzaz, F. *et al.* (1998) ‘No Title’.

Beaudry, B. J. and Gschneidner Jr, K. A. (1978) ‘Preparation and basic properties of the rare earth metals’, *Handbook on the physics and chemistry of rare earths*. Elsevier, 1, pp. 173–232.

Becker, P. M., Olsson, A. A. and Simpson, J. R. (1999) *Erbium-doped fiber amplifiers:*

fundamentals and technology. Elsevier.

Biagioli, M. (2009) *Postdisciplinary Liaisons: Science Studies and the Humanities*. Available at: http://www.journals.uchicago.edu/t-and-c.

Biemer, J., Dixon, W. and Blackburn, N. (2013) 'Our environmental handprint: The good we do', in *2013 1st IEEE Conference on Technologies for Sustainability (SusTech)*, pp. 146–153. doi: 10.1109/SusTech.2013.6617312.

Brundtland, G. H. *et al.* (1987) 'Our common future', *New York*.

C J. T. Houghton 1994, 1997, 2004 (2002) 'Global Warming on Climate Change , Chairman of the UK ' s Royal Commission on'.

Cai, B. *et al.* (2018) 'Estimating perfluorocarbon emission factors for industrial rare earth metal electrolysis', *Resources, Conservation and Recycling*. Elsevier, 136, pp. 315–323.

Cardarelli, F. (2008) *Materials handbook: a concise desktop reference*. Springer Science & Business Media.

Carson, R. (2002) *Silent spring*. Houghton Mifflin Harcourt.

Castilloux, R. (2014) 'Rare earth market outlook: supply, demand, and pricing from 2014–2020', *Adamas Intelligence, Ontario, Canada*.

Central Bank, E. (2017) *What is driving metal prices?* doi: 10.2866/81373.

Centre for Climate and Energy Solutions (2015) *Greenhouse Gas Emissions, 2015*. Available at: https://www.c2es.org/content/international-emissions/.

Ceric, H. (2010) *1.3 IC Fabrication Process Steps*. Available at: http://www.iue.tuwien.ac.at/phd/ceric/node8.html (Accessed: 27 June 2019).

Chapter 4: Metal Industry Emissions METAL INDUSTRY EMISSIONS (2006). Available at: https://www.ipcc-nggip.iges.or.jp/public/2006gl/pdf/3_Volume3/V3_4_Ch4_Metal_Industry.pdf (Accessed: 5 June 2019).

Charalampides, G. *et al.* (2015) 'Rare Earth Elements: Industrial Applications and Economic Dependency of Europe', *Procedia Economics and Finance*. Elsevier, 24, pp. 126–135. doi: 10.1016/S2212-5671(15)00630-9.

Chen, S. H. and Pollino, C. A. (2012) 'Good practice in Bayesian network modelling', *Environmental Modelling and Software*. Elsevier Ltd, 37, pp. 134–145. doi: 10.1016/j.envsoft.2012.03.012.

Chitkara, R. and Pausa, E. (2016) *China's impact on the semiconductor industry: 2016 update*. Available at: www.pwc.com/chinasemicon.

Cicerone, R J (1979) 'Atmospheric carbon tetrafluoride: a nearly inert gas.', *Science (New York, N.Y.)*, 206(12), pp. 59–61. doi: 10.1126/science.206.4414.59.

Cicerone, Ralph J (1979) 'Atmospheric carbon tetrafluoride: A nearly inert gas', *Science*. American Association for the Advancement of Science, 206(4414), pp. 59–61.

Clark, W. C., Crutzen, P. J. and Schellnhuber, H. J. (2005) *Science for Global Sustainability: Toward a New Paradigm*, *SSRN*. doi: 10.2139/ssrn.702501.

Consonni, G. *et al.* (2018) 'Prior distributions for objective Bayesian analysis', *Bayesian Analysis*, 13(2), pp. 627–679. doi: 10.1214/18-BA1103.

Cook, E. (1995) *Lifetime commitments: Why climate policy-makers can't afford to overlook fully fluorinated compounds*. World Resources Institute.

Creech, H. (2012) *Sustainable Development Timeline - 2012*. Available at: www.iisd.org.

Crutzen, P. J. (2002) 'Crutzen 2002 Geology of mankind NATURE', 415(January), p. 2002. doi: 10.1038/415023a.

Czerniak, M. R., Tang, K. and Li, S. (2010) 'Has the Challenge of PFCs Really Been Solved ? In the semiconductor industry , chemical vapor deposition (CVD) chambers were traditionally cleaned using perfluorocarbon (PFC) gases such', (Cvd).

Deeds, D. A. *et al.* (2008) 'Evidence for crustal degassing of CF4and SF6in Mojave Desert groundwaters', *Geochimica et Cosmochimica Acta*, 72(4), pp. 999–1013. doi: 10.1016/j.gca.2007.11.027.

Deeds, D. A., Mühle, J. and Weiss, R. F. (2008) 'Tetrafluoromethane in the deep North Pacific Ocean', *Geophysical Research Letters*, 35(14), pp. 1–5. doi: 10.1029/2008GL034355.

Delmas, R. J. (2013) *Ice core studies of global biogeochemical cycles*. Springer Science & Business Media.

DePaolo, D. J. (2012) *Neodymium isotope geochemistry: an introduction*. Springer Science &

Business Media.

Derwent, R. G., Powlson, D. S. and Conrad, R. (1995) 'Air Chemistry and Terrestrial Gas Emissions: A Global Perspective [and Discussion]', *Philosophical Transactions: Physical Sciences and Engineering*. The Royal Society, 351(1696), pp. 205–217. Available at: http://www.jstor.org/stable/54411.

Desai, P. (2018) *Tesla's electric motor shift to spur demand for rare earth neodymium - Reuters*, *Reuters*. Available at: https://www.reuters.com/article/us-metals-autos-neodymium-analysis/teslas-electric-motor-shift-to-spur-demand-for-rare-earth-neodymium-idUSKCN1GO28I (Accessed: 17 July 2019).

Dion, L. *et al.* (2016) 'Prediction of low-voltage tetrafluoromethane emissions based on the operating conditions of an aluminium electrolysis cell', *JOM*. Springer, 68(9), pp. 2472–2482.

Dion, L., Nunez, P., *et al.* (2018) 'Evaluation of time consistency when quantifying emissions of perfluorocarbons resulting from low voltage anode effects', in *TMS Annual Meeting & Exhibition*. Springer, pp. 1457–1462.

Dion, L., Gaboury, S., *et al.* (2018) 'Universal Approach to Estimate Perfluorocarbons Emissions During Individual High-Voltage Anode Effect for Prebaked Cell Technologies', *JOM*. Springer, 70(9), pp. 1887–1892.

Dixon, D. A. *et al.* (1995) 'Bond energies in organofluorine systems: applications to Teflon® and fullerenes', *Journal of Fluorine Chemistry*. Elsevier, 72(2), pp. 209–214. doi: 10.1016/0022-1139(94)00409-9.

Dominish, E. and Florin, N. (2017) *Electric cars can clean up the mining industry – here's how*. Available at: https://theconversation.com/electric-cars-can-clean-up-the-mining-industry-heres-how-115369 (Accessed: 17 July 2019).

Dostál, J. (2015) 'Theory of Problem Solving', *Procedia - Social and Behavioral Sciences*, 174(July), pp. 2798–2805. doi: 10.1016/j.sbspro.2015.01.970.

Dufour, C. (2019) *Strategic Management: Industry Characteristics*. Available at: https://pitt.libguides.com/strategicmanagement/industrycharacteristics.

EEA (2018) *Electric vehicles from life cycle and circular economy perspectives*.

Egbaria, F. (2018) *Rare Earths MMI: Metals Prices Move Up, Demand for Neodymium Grows - Steel, Aluminum, Copper, Stainless, Rare Earth, Metal Prices, Forecasting | MetalMiner*. Available at: https://agmetalminer.com/2018/04/04/rare-earths-mmi-metals-prices-move-up-demand-for-neodymium-grows/ (Accessed: 17 July 2019).

Egede, P. *et al.* (2015) 'Life cycle assessment of electric vehicles - A framework to consider influencing factors', *Procedia CIRP*. Elsevier B.V., 29, pp. 233–238. doi: 10.1016/j.procir.2015.02.185.

Ellingsen, L. A. W. *et al.* (2014) 'Life Cycle Assessment of a Lithium-Ion Battery Vehicle Pack', *Journal of Industrial Ecology*, 18(1), pp. 113–124. doi: 10.1111/jiec.12072.

Emmons, L. K. *et al.* (2010) 'Description and evaluation of the Model for Ozone and Related chemical Tracers, version 4 (MOZART-4)'.

Enting, I. G., Trudinger, C. M. and Francey, R. J. (1995) 'A synthesis inversion of the concentration and δ13 C of atmospheric CO2', *Tellus B*. Wiley Online Library, 47(1-2), pp. 35–52.

EPA (2013) *Greenhouse Gas Reporting Rule (40 CFR Part 98) Training Presentation*.

European Union (2014) 'EU critical raw materials profiles', pp. 77–85. doi: Ref. Ares(2015)1819595 - 29/04/2015.

European Union (2018) *Fluorinated greenhouse gases 2018*.

Fabian, P. *et al.* (1987) 'CF4 and C2F6 in the Atmopshere', *Journal of Geophysical Research*, 92, pp. 9831–9835.

Fabian, P. and Gomer, D. (1984) 'The Vertical Distribution of Halocarbons in the Stratosphere', *Fresenius' Journal of Analytical Chemistry*, 319(8), pp. 890–897.

Facing new crisis, can aluminum industry learn from past crisis? Andy Home - Reuters (no date). Available at: https://www.reuters.com/article/us-aluminium-market-ahome/facing-new-crisis-can-aluminum-industry-learn-from-past-crisis-andy-home-idUSKCN0VK1ZU (Accessed: 26 June 2019).

Feldman, R. and Sanger, J. (2007) *The text mining handbook: advanced approaches in analyzing unstructured data*. Cambridge university press.

Fishman, T. and Graedel, T. E. (2019) 'Impact of the establishment of US offshore wind

power on neodymium flows', *Nature Sustainability*. Nature Publishing Group, 2(4), pp. 332–338. doi: 10.1038/s41893-019-0252-z.

FitzGibbon, J. and O.Mensah, K. (2012) 'Climate Change as a Wicked Problem: An Evaluation of the Institutional Context for Rural Water Management in Ghana', *SAGE open*. doi: 10.1177/2158244012448487.

Forster, P. *et al.* (2007) 'Changes in atmospheric constituents and in radiative forcing. Chapter 2', in *Climate Change 2007. The Physical Science Basis*.

Franco, C. *et al.* (2016) 'A Bayesian Belief Network to assess rate of changes in coral reef ecosystems', *Environmental Modelling and Software*. Elsevier Ltd, 80, pp. 132–142. doi: 10.1016/j.envsoft.2016.02.029.

Fthenakis, V. (2001) 'Options for Abating Greenhouse Gases From Exhaust Streams', p. 31.

Ganesan, A. L. *et al.* (2014) 'Characterization of uncertainties in atmospheric trace gas inversions using hierarchical Bayesian methods', *Atmospheric Chemistry and Physics*. Copernicus GmbH, 14(8), pp. 3855–3864.

Garratt, J. R. (1994) 'The atmospheric boundary layer', *Earth-Science Reviews*. Elsevier, 37(1–2), pp. 89–134.

Gases, P. and Reduction, E. (2013) 'Results of the 2013 Anode Effect Survey', (February 2009).

Gassmann, M (1974) 'Freon-14 in pure Krypton and in Atmosphere', *Naturwissenschaften*. SPRINGER VERLAG 175 FIFTH AVE, NEW YORK, NY 10010, p. 127.

Gassmann, M. (1974) 'Freon 14 in the "ultra clean" krypton and in the atmosphere', *Naturwissenschaften*, 61, p. 127.

Gelman, A., El-shaarawi, A. H. and Piegorsch, W. W. (2002) 'Prior distribution Prior distribution', *Environmetrics*, 3, pp. 1634–1637.

Ghenai, C. (2012) *2 Life Cycle Analysis of Wind Turbine*. Available at: www.intechopen.com (Accessed: 17 July 2019).

Global Semiconductor Market Trends Innovative Technologies Provide the Platforms for Industry Growth (2018). Available at: http://theconfab.com/wp-content/uploads/P-18-Len-Jelinek.pdf (Accessed: 27 June 2019).

Goldman, J. (2017) *Electric Vehicles, Batteries, Cobalt, and Rare Earth Metals - Union of Concerned Scientists*. Available at: https://blog.ucsusa.org/josh-goldman/electric-vehicles-batteries-cobalt-and-rare-earth-metals (Accessed: 17 July 2019).

Green, P. J. (1995) 'Reversible jump Markov chain Monte Carlo computation and Bayesian model determination', *Biometrika*. Oxford University Press, 82(4), pp. 711–732.

Greenhouse Gas Protocol (2019) 'The Greenhouse Gas Protocol Initiative'.

Greenland, S. (2000) 'Principles of multilevel modelling', *International Journal of Epidemiology*, 29(1), pp. 158–167. doi: 10.1093/ije/29.1.158.

Grönman, K. *et al.* (2019) 'Carbon handprint – An approach to assess the positive climate impacts of products demonstrated via renewable diesel case', *Journal of Cleaner Production*, 206, pp. 1059–1072. doi: 10.1016/j.jclepro.2018.09.233.

Gu, S. and Wu, J. (2012) 'Review on the Energy Saving Technologies Applied in Bayer Process in China', (62), pp. 379–384.

Haapala, K. R. and Prempreeda, P. (2014) *''Comparative life cycle assessment of 2.0 MW wind turbines'', Int. J. Sustainable Manufacturing*. Available at: https://www.ourenergypolicy.org/wp-content/uploads/2014/06/turbines.pdf (Accessed: 17 July 2019).

Hammond, C. R. (2000) 'The elements', *Handbook of chemistry and physics*. CRC press Boca Raton, FL, 81.

Handl, G. (2012) *Declaration of the United nations Conference on the Human Environment (Stockholm Declaration), 1972 and the Ria Declaration on Environment and Development, 1992*. Available at: www.un.org/law/avl.

Hardin, G. (1968) 'The tragedy of the commons', *science*. American Association for the Advancement of Science, 162(3859), pp. 1243–1248.

Harnisch, J. *et al.* (1996) 'Tropospheric trends for CF4 and C2F6 since 1982 derived from SF6 dated stratospheric air', *Geophysical research letters*. Wiley Online Library, 23(10), pp. 1099–1102.

Harnisch, J. *et al.* (2000) 'Natural fluorinated organics in fluorite and rocks', *Geophysical Research Letters*. Wiley Online Library, 27(13), pp. 1883–1886.

Harnisch, J. and Eisenhauer, A. (1998a) 'Natural CF4 and on Earth', *Geophysical Research Letters*, 25(13), pp. 2401–2404. doi: 10.1029/98GL01779.

Harnisch, J. and Eisenhauer, A. (1998b) 'Natural CF4 and SF6 on Earth', *Geophysical Research Letters*. Wiley Online Library, 25(13), pp. 2401–2404.

Hartmann, D. *et al.* (2013) *Observations: Atmosphere and Surface. In: Climate Change 2013: The Physical Science Basis. Contribution of Working Group I to the Fifth Assessment Report of the Intergovernmental Panel on Climate Change Coordinating Lead Authors: Lead Authors: Contributin*.

Hatch, G. P. (2012) 'Dynamics in the Global Market for Rare Earths', *Elements*. GeoScienceWorld, 8(5), pp. 341–346. doi: 10.2113/gselements.8.5.341.

Haupin, W. E. (2009) 'Electrochemistry of the Hall-Heroult process for aluminum smelting', *Journal of Chemical Education*, 60(4), p. 279. doi: 10.1021/ed060p279.

Hawkins, T. R. *et al.* (2013) 'Comparative Environmental Life Cycle Assessment of Conventional and Electric Vehicles', *Journal of Industrial Ecology*, 17(1), pp. 53–64. doi: 10.1111/j.1530-9290.2012.00532.x.

Helmers, E. and Weiss, M. (2017) 'Advances and critical aspects in the life-cycle assessment of battery electric cars', *Energy and Emission Control Technologies*. Dove Press, Volume 5, pp. 1–18. doi: 10.2147/EECT.S60408.

Hernandez, M. *et al.* (2017) 'Environmental impact of traction electric motors for electric vehicles applications', *The International Journal of Life Cycle Assessment*, 22(1), pp. 54–65. doi: 10.1007/s11367-015-0973-9.

Herzog, T., Parshing, J. and Baumert, A. K. (2005) *"Navigating the Numbers: Greenhouse gases and international climate change agreements".* Available at: http://pdf.wri.org/navigating_numbers.pdf.

Hess Corporation (2017) 'Environmental, Health and Safety Guideline', p. 200.

Higgins, P. A. T., Chan, K. M. A. and Porder, S. (2006) 'Bridge over a philosophical divide', pp. 249–256.

Hind, A. R., Bhargava, S. K. and Grocott, S. C. (1999) 'The surface chemistry of Bayer process solids: a review', *Colloids and surfaces A: Physicochemical and engineering aspects*.

Elsevier, 146(1–3), pp. 359–374.

History | World Semiconductor Council (no date). Available at: https://www.semiconductorcouncil.org/about-wsc/history/ (Accessed: 27 June 2019).

Holiday, R. D. and Henry, J. L. (1959) 'Anode polarization and fluorocarbon formation in aluminium reduction cells', *Journal of Industrial and Engineering Chemistry*, 51(10), pp. 1289–1292.

Hoornweg, D. (2015) *A Cities Approach to Sustainability*.

Hunt, W. H. (2004) 'The China factor: Aluminum industry impact', *Jom*, 56(9), pp. 21–24. doi: 10.1007/s11837-004-0194-3.

'I nternational A luminium I nstitute THE INTERNATIONAL ALUMINIUM INSTITUTE REPORT ON THE ALUMINIUM INDUSTRY ' S GLOBAL PERFLUOROCARBON GAS EMISSIONS REDUCTION PROGRAMME' (2006) *Analysis*, (June).

'I nternational A luminium I nstitute THE INTERNATIONAL ALUMINIUM INSTITUTE REPORT ON THE ALUMINIUM INDUSTRY ' S GLOBAL PERFLUOROCARBON GAS EMISSIONS REDUCTION PROGRAMME' (2007) *Analysis*, (May).

IAI (2009) 'Aluminium for Future Generations / 2009 update', *International Aluminium Institute*, p. 7.

IAI (2011) 'International Aluminium Institute Historical Statistics', Accessed M. Available at: https://stats.world-aluminium.org/iai/stats_new/index.asp.

Illuzzi, F. and Thewissen, H. (2010a) 'Perfluorocompounds emission reduction by the semiconductor industry', *Journal of Integrative Environmental Sciences*, 7(SUPPL. 1), pp. 201–210. doi: 10.1080/19438151003621417.

Illuzzi, F. and Thewissen, H. (2010b) 'Perfluorocompounds emission reduction by the semiconductor industry', *Journal of Integrative Environmental Sciences*, 7(SUPPL. 1), pp. 201–210. doi: 10.1080/19438151003621417.

Illuzzi, F. and Thewissen, H. (2010c) 'Perfluorocompounds emission reduction by the semiconductor industry', *Journal of Integrative Environmental Sciences*, 7(S1), pp. 201–210. doi: 10.1080/19438151003621417.

Illuzzi, F. and Thewissen, H. (2010d) 'Perfluorocompounds emission reduction by the

semiconductor industry', *Journal of Integrative Environmental Sciences*, 7(S1), pp. 201–210. doi: 10.1080/19438151003621417.

Incropera, F. P. (2016) *Climate change: a wicked problem: complexity and uncertainty at the intersection of science, economics, politics, and human behavior*. Cambridge University Press.

integrated circuit (IC) | JEDEC (no date). Available at: https://www.jedec.org/standards-documents/dictionary/terms/integrated-circuit-ic (Accessed: 27 June 2019).

International Aluminium Institute (2009) 'International Aluminium Institute A voluntary sectoral approach – a case study : Aluminium Sectoral arrangements have momentum within international climate change discussions', (March). doi: 10.21676/23897856.1360.

International Aluminium Institute (2011) 'Results of the 2010 Anode Effect Survey', (July 2010).

Ipcc (2006) 'Chapter 4 Metal Industry EmissionsM', *2006 IPCC Guidelines for National Greenhouse Gas Inventories 6.1*, 3, p. 85. Available at: http://www.ipcc-nggip.iges.or.jp/public/2006gl/pdf/3_Volume3/V3_4_Ch4_Metal_Industry.pdf.

IPCC (2006) 'ELECTRONICS INDUSTRY EMISSIONS', *IPCC*, 3. doi: 10.1186/s13617-018-0079-8.

IPCC (2015) *Global warming of 1.5°C An IPCC Special Report on the impacts of global warming of 1.5°C above pre-industrial levels and related global greenhouse gas emission pathways, in the context of strengthening the global response to the threat of climate change, , 2015*. Available at: https://www.ipcc.ch/sr15/ (Accessed: 9 July 2019).

IPCC (2019a) 'Chapter 4:Metal Industry Emissions', p. 85. Available at: http://www.ipcc-nggip.iges.or.jp/public/2006gl/pdf/3_Volume3/V3_4_Ch4_Metal_Industry.pdf.

IPCC (2019b) 'CHAPTER 6 ELECTRONICS INDUSTRY EMISSIONS', 3, pp. 1–72.

IPCC - Task Force on National Greenhouse Gas Inventories (no date). Available at: https://www.ipcc-nggip.iges.or.jp/public/2019rf/index.html (Accessed: 8 July 2019).

Irving, S. (2019) 'General rights Life cycle assessment of onshore and offshore wind energy-from theory to application', *Downloaded from orbit.dtu.dk on*. doi: 10.1016/j.apenergy.2016.07.058.

Jonassen, D. H. (2000) *Toward a Design Theory of Problem Solving*. Available at: https://link.springer.com/content/pdf/10.1007%2FBF02300500.pdf (Accessed: 6 August 2019).

Jones, A. *et al.* (2007) 'The UK Met Office's next-generation atmospheric dispersion model, NAME III', in *Air pollution modeling and its application XVII*. Springer, pp. 580–589.

Kaminski, T. *et al.* (2001) 'On aggregation errors in atmospheric transport inversions', *Journal of Geophysical Research: Atmospheres*. Wiley Online Library, 106(D5), pp. 4703–4715.

Khalil, M Aslam K *et al.* (2003) 'Atmospheric perfluorocarbons', *Environmental science & technology*. ACS Publications, 37(19), pp. 4358–4361.

Khalil, M. A K *et al.* (2003) 'Atmospheric perfluorocarbons', *Environmental Science and Technology*, 37(19), pp. 4358–4361. doi: 10.1021/es030327a.

Kim, J. *et al.* (2010) 'Regional atmospheric emissions determined from measurements at Jeju Island, Korea: Halogenated compounds from China', *Geophysical Research Letters*, 37(12). doi: 10.1029/2010GL043263.

Kim, J. *et al.* (2014) 'From Atmospheric Measurements', pp. 4787–4794. doi: 10.1002/2014GL059783.Received.

Kim, J., Allenby, G. M. and Rossi, P. E. (2005) *Product Attributes and Models of Multiple Discreteness*.

King, J. R. (2001) *The aluminium industry*. Elsevier.

Kingsnorth, D. (2015) 'The Global Rare Earth Industry Today-Plagued by Illegal Production in China', in *11th Rare Earth Conference, Metal Events Ltd., Singapore*.

Kjos, O. S. *et al.* (2012) 'Studies of perfluorocarbon formation on anodes in cryolite melts', in *Light Metals 2012*. Springer, pp. 623–626.

Klinger, J. M. (2015) 'A historical geography of rare earth elements: From discovery to the atomic age', *The Extractive Industries and Society*, 2(3), pp. 572–580. doi: 10.1016/j.exis.2015.05.006.

Klinger, J. M. (2018) 'Rare earth elements: Development, sustainability and policy issues', *Extractive Industries and Society*. doi: 10.1016/j.exis.2017.12.016.

Koltun, P. and Tharumarajah, A. (2014) ‘Life Cycle Impact of Rare Earth Elements’, *ISRN Metallurgy*, 2014(April), pp. 1–10. doi: 10.1155/2014/907536.

Kranz, R. (1966) ‘No Title’, *Naturwissenschaften*, 53, pp. 593–599.

Kriegler, E. *et al.* (2012) ‘The need for and use of socio-economic scenarios for climate change analysis: a new approach based on shared socio-economic pathways’, *Global Environmental Change*. Elsevier, 22(4), pp. 807–822.

Kriegler, Elmar *et al.* (2014) ‘A new scenario framework for climate change research: the concept of shared climate policy assumptions’, *Climatic Change*, 122, pp. 401–414. doi: 10.1007/s10584-013-0971-5.

Kuhn, T. S. (no date) *The Structure of Scientific Revolutions*.

Kukreja, B. (2018) *Life Cycle Analysis of Electric Vehicles Quantifying the Impact*. Available at: https://sustain.ubc.ca/sites/default/files/2018-63 Lifecycle Analysis of Electric Vehicles_Kukreja.pdf (Accessed: 17 July 2019).

KyotoProtocol - Toward Climate Stability (no date). Available at: http://www.kyotoprotocol.com/ (Accessed: 27 June 2019).

Lauritzen, P. H. *et al.* (2011) *Numerical techniques for global atmospheric models*. Springer Science & Business Media.

Leber, B. P. *et al.* (1998) ‘Perfluorocarbon (PFC) Generation at Primary Alulminum Smelters’, pp. 277–285.

Lecture, T. H. E. R. (1959) ‘C.P. Snow THE REDE LECTURE, 1959 ©’.

Lee, Y. H. and Chen, M.-M. (1983) ‘Silicon etching mechanism and anisotropy in CF4+O2 plasma’, *Journal of Applied Physics*, 54, pp. 5966–5973. doi: 10.1063/1.331774.

Leedham Elvidge, E. *et al.* (2018) ‘Evaluation of stratospheric age of air from CF 4 , C 2 F 6 , C 3 F 8 , CHF 3 , HFC-125, HFC-227ea and SF 6 ; Implications for the calculations of halocarbon lifetimes, fractional release factors and ozone depletion potentials’, *Atmospheric Chemistry and Physics*, 18(5), pp. 3369–3385. doi: 10.5194/acp-18-3369-2018.

Leuenberger, M. and Frischknecht, R. (2010) ‘Life cycle assessment of battery electric vehicles and concept cars’, *Report, ESU-Services Ltd*, 2. Available at: http://www.esu-services.ch/fileadmin/download/leuenberger-2010-BatteryElectricVehicles.pdf.

Li, W. *et al.* (2011) ‘On continuous PFC emission unrelated to anode effects’, in *Light Metals 2011*. Springer, pp. 309–314.

Lindley, J. (2016) ‘What on Earth is Post Disciplinary Ethnography?’, *Ethnography Matters*.

Liu, S. H. (1978) ‘Electronic structure of rare earth metals. Chapter 3’, in *Handbook on the physics and chemistry of rare earths. Volume 1*.

Lunt, M. F. *et al.* (2016) ‘Estimation of trace gas fluxes with objectively determined basis functions using reversible-jump Markov chain Monte Carlo’, *Geoscientific Model Development*. Copernicus GmbH, 9(9), pp. 3213–3229.

Mackinnon, P. J., Hine, D. and Barnard, R. T. (2013) ‘Interdisciplinary science research and education’, 4360. doi: 10.1080/07294360.2012.686482.

Macwilliams, J. (2014) ‘Semiconductors Drive the Electronics Industry.’, pp. 2–4.

Madria, S. K. *et al.* (1999) ‘Research issues in web data mining’, in *International Conference on Data Warehousing and Knowledge Discovery*. Springer, pp. 303–312.

Mahieu, E. *et al.* (2014) ‘Spectrometric monitoring of atmospheric carbon tetrafluoride (CF4) above the Jungfraujoch station since 1989: evidence of continued increase but at a slowing rate’, *Atmospheric Measurment Techniques*, 7(1).

Malthus, T. (1798) ‘An essay on the principle of population. Printed for J. Johnson’, *St. Paul’s church-yard, London*, pp. 1–126.

Manahan, S. E. (2005) *Environmental chemistry*. CRC Press. Available at: https://books.google.co.uk/books?id=k01YDY2vQwoC&pg=PA345&lpg=PA345&dq=global+cf4+market+tons&source=bl&ots=IBfkVKxYsO&sig=-2nbwCS6nQVvuDBla3tKFQlcRJw&hl=en&sa=X&ei=FdCTVcajKIPvUKGgnJAD&ved=0CEwQ6AEwBg#v=onepage&q=global cf4 market tons&f=false (Accessed: 28 June 2019).

Manning, A. J. *et al.* (2011) ‘Estimating UK methane and nitrous oxide emissions from 1990 to 2007 using an inversion modeling approach’, *Journal of Geophysical Research: Atmospheres*. Wiley Online Library, 116(D2).

Markandya, A. and Dale, N. (2001) *Measuring environmental degradation: developing pressure indicators for Europe*. Edward Elgar Publishing.

Marks, J. (2006) ‘Methods for calculating PFC emissions from primary alu-minium

production', *Light Metals*, (4), pp. 4–7. Available at: http://my.alacd.com/tms/2006/papers/185.pdf.

Marks, J. and Bayliss, C. (2012) 'GHG measurement and inventory for aluminum production', in *Light Metals 2012*. Springer, pp. 805–808.

Marks, J. and Nunez, P. (2018) 'Updated factors for calculating PFC emissions from primary aluminum production', *Minerals, Metals and Materials Series*, Part F4, pp. 1519–1525. doi: 10.1007/978-3-319-72284-9_198.

Martinelli, L. and Worth, W. (1994) 'Global Warming: A White Paper on the Science, Policies and Control Technologies that Impact the US Semiconductor Industry', *SEMATECH Technology Transfer paper*, 9311207.

Masson-Delmotte, V. *et al.* (no date) *Global warming of 1.5°C An IPCC Special Report on the impacts of global warming of 1.5°C above pre-industrial levels and related global greenhouse gas emission pathways, in the context of strengthening the global response to the threat of climate change, sustainable development, and efforts to eradicate poverty Summary for Policymakers Edited by Science Officer Science Assistant Graphics Officer Working Group I Technical Support Unit*. Available at: https://report.ipcc.ch/sr15/pdf/sr15_spm_final.pdf (Accessed: 6 August 2019).

Matlin, S. A. *et al.* (2016) 'One-world chemistry and systems thinking', *Nature Publishing Group*. Nature Publishing Group, 8(5), pp. 393–398. doi: 10.1038/nchem.2498.

Mattrey, J. F., Sherer, J. M. and Miller, J. D. (2000) 'Minimize emissions from semiconductor facilities', *Chemical engineering progress*. American Institute of Chemical Engineers (AIChE), 96(5), pp. 35–41.

McGraw Hill Education (2017) *Chemistry Concepts and Applictions, 2017*. Available at: http://novella.mhhe.com/sites/0078807239/student_view0/chapter17/standardized_test_practice.html.

Mclellan, B. C. *et al.* (2014) 'ScienceDirect 4th International Conference on Sustainable Future for Human Security, SustaiN 2013 Sustainability of the Rare Earths Industry', *Procedia Environmental Sciences*, 20, pp. 280–287. doi: 10.1016/j.proenv.2014.03.035.

Messagie, M. *et al.* (2014) 'The hourly life cycle carbon footprint of electricity generation in Belgium, bringing a temporal resolution in life cycle assessment', *Applied Energy*, 134, pp.

469–476. doi: 10.1016/j.apenergy.2014.08.071.

Metropolis, N. *et al.* (1953) ‘Equation of state calculations by fast computing machines’, *The journal of chemical physics*. AIP, 21(6), pp. 1087–1092.

Michalopoulou, E. (2018) *Challenges in estimating global CF<inf>4</inf>and C<inf>2</inf>F<inf>6</inf>Emissions, Minerals, Metals and Materials Series*. doi: 10.1007/978-3-319-72284-9_196.

Michalopoulou, Eleni (2018) ‘Challenges in Estimating Global CF 4 and C 2 F 6 Emissions’, in *TMS Annual Meeting & Exhibition*. Springer, pp. 1499–1506.

Michalopoulou, E. *et al.* (2019) ‘The End of Simple Problems: Repositioning Chemistry in Higher Education and Society Using a Systems Thinking Approach and the United Nations’ Sustainable Development Goals as a Framework’, *Journal of Chemical Education*. American Chemical Society. doi: 10.1021/acs.jchemed.9b00270.

MIT Center for Global Change Science (2019) *AGAGE*. Available at: http://cgcs.mit.edu/research/agage (Accessed: 5 June 2019).

Mitchell, John F., B. (1989) ‘The “Greenhouse” effect and climate change’, *Reviews of Geophysics*, 27(1), pp. 115–139.

Mitchell, J. F. B. *et al.* (1990) ‘Equilibrium climate change and its implications for the future’, *Climate change: The IPCC scientific assessment*. Cambridge University Press Cambridge, 131, p. 172.

Modrey, L. (2005) *Reduction of Perfluorocompound (PFC) Emissions: 2005 State-of-the-Technology Report International SEMATECH Manufacturing Initiative Technology Transfer #05104693A-ENG*. Available at: https://www.epa.gov/sites/production/files/2016-02/documents/final_tt_report.pdf (Accessed: 14 June 2019).

Moss, R. (2008) *Towards New Scenarios for Analysis of Emissions, Climate Change, Impacts, and Response Strategies*.

Moss, R. H. *et al.* (2010) ‘The next generation of scenarios for climate change research and assessment’. doi: 10.1038/nature08823.

Mühle, J. *et al.* (2010a) ‘Perfluorocarbons in the global atmosphere: Tetrafluoromethane, hexafluoroethane, and octafluoropropane’, *Atmospheric Chemistry and Physics*, 10(11), pp.

5145–5164. doi: 10.5194/acp-10-5145-2010.

Mühle, J. *et al.* (2010b) 'Perfluorocarbons in the global atmosphere: Tetrafluoromethane, hexafluoroethane, and octafluoropropane', *Atmospheric Chemistry and Physics*, 10(11), pp. 5145–5164. doi: 10.5194/acp-10-5145-2010.

Mühle, J. *et al.* (2019) 'Perfluorocyclobutane (PFC-318, c-C4F8) in the global atmosphere', *Atmos. Chem. Phys. Discuss.* Copernicus Publications, 2019, pp. 1–44. doi: 10.5194/acp-2019-267.

Mulder, I. *et al.* (2013) 'A new purge and trap headspace technique to analyze low volatile compounds from fluid inclusions of rocks and minerals', *Chemical Geology*. The Authors, 358, pp. 148–155. doi: 10.1016/j.chemgeo.2013.09.003.

Mulder, M. (2012) 'The Journal of Agricultural Education Interdisciplinarity and education : towards principles of pedagogical practice Interdisciplinarity and education : towards principles of pedagogical practice', (October), pp. 37–41.

Myhre, G. *et al.* (1998) 'New estimates of radiative forcing due to well mixed greenhouse gases', *Geophysical Research Letters*, 25(14), pp. 2715–2718. doi: 10.1029/98GL01908.

Myhre, G. *et al.* (2013) 'IPCC AR5 (2013) Chapter 8: Anthropogenic and Natural Radiative Forcing', *Climate Change 2013: The Physical Science Basis. Contribution of Working Group I to the Fifth Assessment Report of the Intergovernmental Panel on Climate Change*, pp. 659–740. doi: 10.1017/ CBO9781107415324.018.

Nakicenovic, N. *et al.* (2000) 'N Victor and Z'. Dadi.

Nappi, C. (2013) *The Global Aluminium Industry 40 years from 1972*. Available at: www.world-aluminium.orgwww.thealuminiumstory.com (Accessed: 6 June 2019).

Nations, U. (2014) 'International Implementation Scheme'.

Nations, U. (2015) *The Sustainable Development Goals*. Available at: https://www.un.org/sustainabledevelopment/sustainable-development-goals/ (Accessed: 29 March 2019).

NDRC (2008) 'Review Sustainable Development in China (2008)', *16th Session of the Commission on Sustainable Development of the United Nations*.

Nordelöf, A. *et al.* (2014) 'Environmental impacts of hybrid, plug-in hybrid, and battery

electric vehicles—what can we learn from life cycle assessment?', *The International Journal of Life Cycle Assessment*, 19(11), pp. 1866–1890. doi: 10.1007/s11367-014-0788-0.

Norgate, T. E., Jahanshahi, S. and Rankin, W. J. (2007) 'Assessing the environmental impact of metal production processes', *Journal of Cleaner Production*, 15(8–9), pp. 838–848. doi: 10.1016/j.jclepro.2006.06.018.

Norgate, T E, Jahanshahi, S. and Rankin, W. J. (2007) 'Assessing the environmental impact of metal production processes', *Journal of Cleaner Production*. Elsevier, 15(8–9), pp. 838–848.

Norris, G. (2015) *Handprint-Based NetPositive Assessment*. Available at: http://energy.gov/energysaver/reduce-hot-water-use-energy-savings.

Nyström, P. (2007) *Disciplinarity, Inter-disciplinarity and Post-disciplinarity: Changing Disciplinary Patterns in the History Discipline*.

O'neill, B. C. *et al.* (2014) 'A new scenario framework for climate change research: the concept of shared socioeconomic pathways', *Climatic Change*, 122, pp. 387–400. doi: 10.1007/s10584-013-0905-2.

O'Neill, B. C. *et al.* (2012) 'Workshop on The Nature and Use of New Socioeconomic Pathways for Climate Change Research Core Writing Team Acknowledgments', *Meeting Report of the Workshop on The Nature and Use of New Socioeconomic Pathways for Climate Change Research*, (January), pp. 1–37. Available at: http://www.isp.ucar.edu/socio-economic-pathways.

O'Neill, B. C. *et al.* (2017) 'The roads ahead: Narratives for shared socioeconomic pathways describing world futures in the 21st century', *Global Environmental Change*. Elsevier Ltd, 42, pp. 169–180. doi: 10.1016/j.gloenvcha.2015.01.004.

Overview, E. (2010) 'reducing PFC emissions'.

Pandey, D., Agrawal, M. and Pandey, J. S. (2011) 'Carbon footprint: Current methods of estimation', *Environmental Monitoring and Assessment*, 178(1–4), pp. 135–160. doi: 10.1007/s10661-010-1678-y.

Peacor, D. R. *et al.* (no date) 'The Clay Minerals Society Glossary for Clay Science Project'. Citeseer.

Penkett, S A *et al.* (1981) ‘Atmospheric measurements of CF4 and other fluorocarbons containing the CF3 grouping’, *Journal of Geophysical Research: Oceans*. Wiley Online Library, 86(C6), pp. 5172–5178.

Penkett, S. A. *et al.* (1981) ‘Atmospheric Measurements of CF4 and other Fluorocarbons Containing the CF3 Grouping’, *Journal of Geophysical Research*, 86(C6), pp. 5172–5178.

‘Perfluorocarbon emissions reduction programme 1990-2000’ (2000).

Phan, T. D. *et al.* (2016) ‘Applications of Bayesian belief networks in water resource management: A systematic review’, *Environmental Modelling and Software*. Elsevier Ltd, 85, pp. 98–111. doi: 10.1016/j.envsoft.2016.08.006.

Phillips, N. A. (2000) ‘An explication of the coriolis effect’, *Bulletin of the American Meteorological Society*. American Meteorological Society, 81(2), pp. 299–303. doi: 10.1175/1520-0477(2000)081<0299:AEOTCE>2.3.CO;2.

Prinn, R. G. *et al.* (2000) ‘A history of chemically and radiatively important gases in air deduced from ALE/GAGE/AGAGE’, *Journal of Geophysical Research: Atmospheres*. Wiley Online Library, 105(D14), pp. 17751–17792.

Raich, G. (no date) *GONZALES, ATTORNEY GENERAL, ET AL. v. RAICH ET AL., 2004*. Available at: https://scholar.google.ca/scholar_case?case=15647611274064109718&q=545+U.S.+1&hl=en&as_sdt=2,5# (Accessed: 7 August 2019).

Rare Earths Statistics and Information (no date). Available at: https://www.usgs.gov/centers/nmic/rare-earths-statistics-and-information (Accessed: 13 June 2019).

Rasmussen, R A, Penkett, S. A. and Prosser, N. (1979) ‘Measurement of carbon tetrafluoride in the atmosphere’, *Nature*. Nature Publishing Group, 277(5697), p. 549.

Rasmussen, R. A., Penkett, S. A. and Prosser, N. J. D. (1979) ‘Measurements of carbontetrafluoride in the atmosphere’, *Nature*, 277, pp. 549–550.

Ravishankara, A. R. *et al.* (1993) ‘Atmospheric lifetimes of long-lived halogenated species’, *Science*. American Association for the Advancement of Science, 259(5092), pp. 194–199.

Razdan, P. and Garrett, P. (2015) *LIFE CYCLE ASSESSMENT OF ELECTRICITY*

PRODUCTION FROM AN ONSHORE V112-3.3 MW WIND PLANT. Available at: https://www.vestas.com/~/media/vestas/about/sustainability/pdfs/lcav11020mw181215.pdf (Accessed: 17 July 2019).

Rees, W. E. (1992) 'Ecological footprints and appropriated carrying capacity: what urban economics leaves out', *Environment and Urbanization*. SAGE Publications Ltd, 4(2), pp. 121–130. doi: 10.1177/095624789200400212.

Reis-Filho, J. S., Soares, R. and Schmitt, F. C. (2014) *5th Assesment report*. doi: 10.1046/j.1365-2559.2002.1340a.x.

Research and technological development (no date). Available at: https://sr.rusal.com/upload/iblock/635/07_RD.pdf (Accessed: 26 June 2019).

Results of the 2012 Anode Effect Survey Report on the Aluminium Industry's Global Perfluorocarbon Gases Emissions Reduction Programme (no date). Available at: www.world-aluminium.org (Accessed: 5 June 2019).

Results of the 2016 Anode Effect Survey Report on the Aluminium Industry's Global Perfluorocarbon Gases Emissions (2017). Available at: http://www.world-aluminium.org/media/filer_public/2017/07/26/2016_anode_effect_survey_result_2017.pdf (Accessed: 5 June 2019).

Results of the 2017 Anode Effect Survey Report on the Aluminium Industry's Global Perfluorocarbon Gases Emissions (2018). Available at: http://www.world-aluminium.org/media/filer_public/2018/07/31/2017_anode_effect_survey_result_2018.pdf (Accessed: 14 June 2019).

Richmond, B. (1993) 'Systems thinking : critical thinking skills for the 1990s and beyond', 9(2), pp. 113–133.

Rienecker, M. M. *et al.* (2011) 'MERRA: NASA's modern-era retrospective analysis for research and applications', *Journal of climate*, 24(14), pp. 3624–3648.

Rigby, M., Manning, A. J. and Prinn, R. G. (2011) 'Inversion of long-lived trace gas emissions using combined Eulerian and Lagrangian chemical transport models', *Atmospheric Chemistry and Physics*. Copernicus GmbH, 11(18), pp. 9887–9898.

Rittel, H. W. J. and Webber, M. M. (1973) 'Dilemmas in a general theory of planning', *Policy sciences*. Springer, 4(2), pp. 155–169.

Rowlatt, J. (2014) ‘Rare earths: Neither rare, nor earths’, *BBC News Magazine*.

Rusal targets 2021 to roll out carbon-free aluminium | Financial Times (no date). Available at: https://www.ft.com/content/e4a0f8f6-5252-11e9-b401-8d9ef1626294 (Accessed: 26 June 2019).

Sachs, J. D. (2012) ‘From Millennium Development Goals to Sustainable Development Goals’, *The Lancet*, 379(9832), pp. 2206–2211. doi: 10.1016/s0140-6736(12)60685-0.

Schellnhuber, H. J. *et al.* (2005) ‘Earth system analysis for sustainability’, *Environment*, 47(8), pp. 10–25. doi: 10.3200/ENVT.47.8.10-25.

Schmitt, J. *et al.* (2013) ‘Atmospheric CF4 trapped in polar ice - A new proxy for granite weathering’, *in: Goldschmidt Conference, Mineralogical Magazine*, p. 77(5) 2160.

Seinfeld, J. H., Pandis, S. N. and Noone, K. (1998) ‘Atmospheric chemistry and physics: from air pollution to climate change’, *Physics Today*, 51, p. 88.

Semiconductor Capacity Utilization Rising – Semiwiki (2014). Available at: https://semiwiki.com/design-services/semiconductor-intelligence/4118-semiconductor-capacity-utilization-rising/ (Accessed: 12 June 2019).

Senge, P. M. and Sterman, J. D. (1992) ‘Systems thinking and organizational learning: Acting locally and thinking globally in the organization of the future’, *European Journal of Operational Research*, 59(1), pp. 137–150. Available at: https://econpapers.repec.org/RePEc:eee:ejores:v:59:y:1992:i:1:p:137-150.

Smith Stegen, K. (2015) ‘Heavy rare earths, permanent magnets, and renewable energies: An imminent crisis’, *Energy Policy*. Elsevier, 79, pp. 1–8. doi: 10.1016/J.ENPOL.2014.12.015.

Society, R. E. and Journal, T. E. (2019) ‘Review Reviewed Work (s): The Social Function of Science . by J . D . Bernal Review by : Barbara Wootton Published by : Wiley on behalf of the Royal Economic Society Stable URL : https://www.jstor.org/stable/2225099’, 49(194), pp. 319–321.

Speirs, J. (2015) *Electric vehicles and critical metals - Jamie Speirs, Imperial College Centre for Energy Policy and Technology | SETIS - European Commission, Electric vehicles and critical metals*. Available at: https://setis.ec.europa.eu/setis-reports/setis-magazine/materials-energy/electric-vehicles-and-critical-metals-jamie-speirs (Accessed: 17 July 2019).

Statista (2019) ‘Semiconductor Industry Sale worldwide 1987-2020’.

Sterman, J. D. and Sweeney, L. B. (2000) ‘Bathtub dynamics: initial results of a systems thinking inventory’, *System Dynamics Review*, 16(4), pp. 249–286.

Summary for Policymakers of IPCC Special Report on Global Warming of 1.5°C approved by governments (2018). Available at: www.ipcc.ch.

Symonds, R. B., Rose, W. I. and Reed, M. H. (1988) ‘Contribution of Cl- and F-bearing gases to the atmosphere by volcanoes’, *Nature*, 334, pp. 415–418. doi: 10.1038/332141a0.

Tabereaux, A. (2004) ‘Anode effects and PFC emission rates’, in *8th Australasia Aluminium Smelting Technology Conference and Workshops*.

Tabereaux, Alton T. (1994) ‘Anode effects, PFCs, global warming, and the aluminum industry’, *Jom*, 46(11), pp. 30–34. doi: 10.1007/BF03222629.

Tabereaux, Alton T (1994) ‘Anode effects, PFCs, global warming, and the aluminum industry’, *JOM*. Springer, 46(11), pp. 30–34.

Tagliaferri, C. *et al.* (2016) ‘Life cycle assessment of future electric and hybrid vehicles: A cradle-to-grave systems engineering approach’, *Chemical Engineering Research and Design*. Elsevier, 112, pp. 298–309.

Taipei, C., Manufacturing, S. and Corporation, I. (2014) ‘[FINAL] JOINT STATEMENT OF THE 18 th MEETING OF THE WORLD SEMICONDUCTOR COUNCIL (WSC)’, pp. 1–30.

Taipei, C., Manufacturing, S. and Corporation, I. (2015) ‘JOINT STATEMENT OF THE 19th MEETING OF WORLD SEMICONDUCTOR COUNCIL (WSC) MAY 21, 2015’, *WSC Reports*, pp. 1–30.

Tarantola, A. (2005) *Inverse problem theory and methods for model parameter estimation*. siam.

Taylor, K. E., Stouffer, R. J. and Meehl, G. A. (2012) ‘An overview of CMIP5 and the experiment design’, *Bulletin of the American Meteorological Society*. American Meteorological Society, 93(4), pp. 485–498.

Teach, R. D. (1990) *Demand Equations which include product attributes*.

Tenorio, L. (2001) ‘Statistical regularization of inverse problems’, *SIAM review*. SIAM,

43(2), pp. 347–366.

Terborgh, J. (2004) ‘Reflections of a Scientist on the World Parks Congress’, *Conservation Biology*, 18(3), pp. 619–620. doi: 10.1111/j.1523-1739.2004.01837.x.

The Aluminium Association (2019) *Recycling*. Available at: https://www.aluminum.org/industries/production/recycling#targetText=Nearly 75 percent of all,and retains its properties indefinitely.

The Anode Effect - The Aluminum Smelting Process (no date). Available at: http://www.aluminum-production.com/anode_effect.html (Accessed: 6 June 2019).

The Atmospheric Boundary Layer - Met Office (no date). Available at: https://www.metoffice.gov.uk/research/foundation/parametrizations/boundary-layer (Accessed: 5 June 2019).

The Chinese Society of Rare Earths (2019) *No Title*. Available at: http://www.cs-re.org.cn/ (Accessed: 25 September 2019).

‘The Credit Hour and Faculty Instructional Workload’ (no date), (122), pp. 45–55.

The history of aluminium industry (no date). Available at: https://www.aluminiumleader.com/history/industry_history/ (Accessed: 6 June 2019).

‘the International Aluminium Institute Report on the Aluminium Industry ’ S Global’ (2008) *Analysis*, (July).

The, S. *et al.* (2019) ‘Author (s): Tamara Swora and James L . Morrison Stable URL : https://www.jstor.org/stable/27796409 Linked references are available on JSTOR for this article : INTERDISCIPLINARI ^ AND HIGHER EDUCATION’, 26(1), pp. 45–52.

Thomson, C. and Harrison, G. P. (2015) *Life Cycle Costs and Carbon Emissions of Offshore Wind Power*. Available at: www.climatexchange.org.uk (Accessed: 17 July 2019).

Thonstad, J. *et al.* (2001) ‘Aluminium Electrolysis: Fundamentals of the Hall-Herault Process’.

Thonstad, J. and Rolseth, S. (2017) ‘Low Voltage PFC Emission from Aluminium Cells’, 10(1). doi: 10.17516/1998-2836-0003.

Trudinger, Cathy M., Fraser, P. J., Etheridge, D. M., Sturges, W. T., Vollmer, M. K., Rigby, M., Martinerie, P., Mühle, J., *et al.* (2016) ‘Atmospheric abundance and global emissions of

perfluorocarbons CF₄, C₂F₆ and C₃F₈ since 1800 inferred from ice core, firn, air archive and i', *Atmospheric Chemistry and Physics*, 16(18), pp. 11733–11754. doi: 10.5194/acp-16-11733-2016.

Trudinger, Cathy M *et al*. (2016) 'Atmospheric abundance and global emissions of perfluorocarbons CF 4, C 2 F 6 and C 3 F 8 since 1800 inferred from ice core, firn, air archive and in situ measurements', *Atmospheric chemistry and physics*. Copernicus GmbH, 16(18), pp. 11733–11754.

Trudinger, Cathy M., Fraser, P. J., Etheridge, D. M., Sturges, W. T., Vollmer, M. K., Rigby, M., Martinerie, P., M??hle, J., *et al.* (2016) 'Atmospheric abundance and global emissions of perfluorocarbons CF4, C2F6 and C3F8 since 1800 inferred from ice core, firn, air archive and in situ measurements', *Atmospheric Chemistry and Physics*, 16(18), pp. 11733–11754. doi: 10.5194/acp-16-11733-2016.

Tsai, W.-T., Chen, H.-P. and Hsien, W.-Y. (2002) 'A review of uses, environmental hazards and recovery/recycle technologies of perfluorocarbons (PFCs) emissions from the semiconductor manufacturing processes', *Journal of Loss Prevention in the Process Industries*. Elsevier, 15(2), pp. 65–75.

UN (2014) *Country classification*. Available at: http://data.worldbank.org/about/country-classifications.

UN (2015a) *Imbalances in paid and unpaid work. Chapter 4 Human Development Report 2015 Work for Human Development*. Available at: www.undp.org.

UN (2015b) *SDG 1*. Available at: https://sustainabledevelopment.un.org/sdg1.

UN (2015c) *SDG 12*. Available at: https://sustainabledevelopment.un.org/sdg12.

UN (2015d) *SDG 5*. Available at: https://sustainabledevelopment.un.org/sdg5.

UN (2015e) *SDG 9*. Available at: https://sustainabledevelopment.un.org/sdg9.

UN (2015f) *The 2030 Agenda For Sustainable Development*.

UN (2019) *Voluntary National Reviews, Sustainable Development Knowledge Platform*. Available at: https://sustainabledevelopment.un.org/vnrs/.

UNDP (2018a) ‘Human Development Indices and Indicators. 2018 Statistical Update’, *United Nations Development Programme*, 27(4), p. 123. Available at: http://hdr.undp.org/sites/default/files/2018_human_development_statistical_update.pdf%0Ahttp://www.hdr.undp.org/sites/default/files/2018_human_development_statistical_update.pdf%0Ahttp://hdr.undp.org/en/2018-update.

UNDP (2018b) ‘Technical notes: Human Development Indices and Indicators’, pp. 1–16. Available at: http://hdr.undp.org/sites/default/files/hdr2018_technical_notes.pdf.

UNDP (2018c) *Wicked solutions for wicked problems*. Available at: https://www.adaptation-undp.org/wicked-solutions-wicked-problems (Accessed: 6 August 2019).

UNDP (2019) *Human Development Reports*. Available at: http://hdr.undp.org/en.

UNFCCC (2006) *HANDBOOK UNITED NATIONS FRAMEWORK CONVENTION ON CLIMATE CHANGE*.

UNFCCC (2007) *United Nations Framework Convention on Climate Change*.

UNFCCC (2008) *Kyoto Protocol Reference Manual*.

UNFCCC (2013a) *National Inventory Submissions 2013, 2013*. Available at: https://unfccc.int/process/transparency-and-reporting/reporting-and-review-under-the-convention/greenhouse-gas-inventories/submissions-of-annual-greenhouse-gas-inventories-for-2017/submissions-of-annual-ghg-inventories-2013 (Accessed: 5 June 2019).

UNFCCC (2013b) ‘Revision of the UNFCCC reporting guidelines on annual inventories for Parties included in Annex I to the Convention.’, (January), pp. 1–54. Available at: https://unfccc.int/resource/docs/2013/cop19/eng/10a03.pdf#page=2.

UNFCCC (2019) *Common metrics*. Available at: https://unfccc.int/process-and-meetings/transparency-and-reporting/methods-for-climate-change-transparency/common-metrics.

UNFCCC (no date) *Kyoto Protocol - Targets for the first commitment period, 2012*. Available at: https://unfccc.int/process/the-kyoto-protocol (Accessed: 5 June 2019).

United Nations (2019) *Conference of the Parties (COP)*. Available at: https://unfccc.int/process/bodies/supreme-bodies/conference-of-the-parties-cop.

US EPA, O. (2017) ‘Semiconductor Industry’. Available at: https://www.epa.gov/f-gas-

partnership-programs/semiconductor-industry (Accessed: 12 July 2019).

USGS (2018) ‘Global Rare Earth Oxide Mine Production’, *USGS*.

Uusitalo, L. (2007) ‘Advantages and challenges of Bayesian networks in environmental modelling’, *Ecological Modelling*, 203(3–4), pp. 312–318. doi: 10.1016/j.ecolmodel.2006.11.033.

Venås, C. and Arvesen, A. (no date) *Life cycle assessment of electric power generation by wind turbines containing rare earth magnets*. Available at: https://pdfs.semanticscholar.org/0cd5/2fa142e110bf4d3588d16e14a94fd6fdc252.pdf (Accessed: 17 July 2019).

Vogel, H. *et al.* (2017) ‘Reducing Greenhouse Gas Emission from the Neodymium Oxide Electrolysis. Part I: Analysis of the Anodic Gas Formation’, *Journal of Sustainable Metallurgy*. Springer International Publishing, 3(1), pp. 99–107. doi: 10.1007/s40831-016-0086-0.

Vogel, H. and Friedrich, B. (2017) ‘Reducing Greenhouse Gas Emission from the Neodymium Oxide Electrolysis. Part II: Basics of a Process Control Avoiding PFC Emission’, *International Journal of Nonferrous Metallurgy*, 06(03), pp. 27–46. doi: 10.4236/ijnm.2017.63003.

Vogel, H. and Friedrich, B. (2018) ‘An Estimation of PFC Emission by Rare Earth Electrolysis’, in Martin, O. (ed.) *Light Metals 2018*. 1st edn. Cham: Springer International Publishing, pp. 1507–1517. doi: 10.1007/978-3-319-72284-9.

van Vuuren, Detlef P *et al.* (2011) ‘The representative concentration pathways: an overview’, *Climatic Change*, 109, pp. 5–31. doi: 10.1007/s10584-011-0148-z.

van Vuuren, Detlef P *et al.* (2014) ‘A new scenario framework for Climate Change Research: scenario matrix architecture’, *Climatic Change*, 122, pp. 373–386. doi: 10.1007/s10584-013-0906-1.

Walkey, D. J. (2018) *Basic Integrated Circuit Processing ELEC 3908, Physical Electronics, Lecture 4*. Available at: http://www.doe.carleton.ca/~tjs/4705Slides.pdf (Accessed: 27 June 2019).

Wallace, J. M. and Hobbs, P. V (1977) ‘Atmosphere science-an introductory survey.’, *Atmospheric Science*.

Walls, H. L. (2018) ‘Wicked problems and a “wicked” solution’. doi: 10.1186/s12992-018-0353-x.

Wangxing, L. *et al.* (2012) ‘Latest results from PFC investigation in China’, in *Light Metals 2012*. Springer, pp. 619–622.

Warneck, P. (1999) *Chemistry of the natural atmosphere*. Elsevier.

Weber, P. *et al.* (2012) ‘Overview on Bayesian networks applications for dependability, risk analysis and maintenance areas’, *Engineering Applications of Artificial Intelligence*. Elsevier, 25(4), pp. 671–682. doi: 10.1016/j.engappai.2010.06.002.

West’s Encyclopedia of American Law (2008) *De minimis, Edition 2*.

What Caused the Aluminum Industry’s Crisis? (no date). Available at: https://www.bcg.com/publications/2013/metals-mining-corporate-strategy-what-caused-aluminum-crisis.aspx (Accessed: 26 June 2019).

Wiedmann, T. and Minx, J. (2007) ‘A Definition of ‘ Carbon Footprint’, *Science*, 1(01), pp. 1–11. doi: 10.1088/978-0-750-31040-6.

Winkler, R. L. (1967) ‘The Assessment of Prior Distributions in Bayesian Analysis’, *Journal of the American Statistical Association*. Taylor & Francis, 62(319), pp. 776–800. doi: 10.1080/01621459.1967.10500894.

Wolmark, J. and Gates-Stuart, E. (2004) *Cultural hybrids, post-disciplinary digital practices and new research frameworks: Testing the limits*.

Wong, D. S. *et al.* (2014) ‘PFCs from Low Voltage Propagating AEs & Non-Propagating AEs’, *11th AustralAsian Aluminium Smelting Technology Conference*, pp. 1–20.

Wong, D. S. *et al.* (2015) ‘PFC emissions from detected versus nondetected anode effects in the aluminum industry’, *JOM*. Springer, 67(2), pp. 342–353.

World Aluminium — The Institute (no date). Available at: http://www.world-aluminium.org/about/institute/ (Accessed: 6 June 2019).

World Semiconductor Council Best Practice Guidance for Semiconductor PFC Emission Reduction (2017). Available at: http://www.semiconductorcouncil.org/wp-content/uploads/2017/07/Best-Practice-Guidance-of-PFC-Emission-Reduction.pdf (Accessed: 27 June 2019).

Worth, W., Duffin, B. and Modrey, L. (1998) ‘Current State of Technology: Perfluorocompound (PFC) Emissions Reduction’. Available at: http://www.sematech.org/docubase/document/3508atr.pdf.

Worton, David R. *et al.* (2007) ‘Atmospheric trends and radiative forcings of CF4and C2F6inferred from firn air’, *Environmental Science and Technology*, 41(7), pp. 2184–2189. doi: 10.1021/es061710t.

Worton, D R *et al.* (2007) ‘Protocol for Measurement of CF4 and C2F6 from Primary Aluminum Production’, 41(7), pp. 2184–2189. doi: 10.1021/es061710t.

WSC (2005) ‘JOINT STATEMENT ON THE NINTH MEETING OF THE WORLD SEMICONDUCTOR COUNCIL (WSC) May 19, 2005’, *WSC Reports*, 48(9), pp. 800–809.

WSC (2008) ‘JOINT STATEMENT OF THE 12TH MEETING OF THE WORLD SEMICONDUCTOR COUNCIL (WSC) MAY’, *WSC Reports*, pp. 1–20.

WSC (2009) ‘JOINT STATEMENT OF THE 13 MEETING OF THE WORLD SEMICONDUCTOR COUNCIL (WSC) MAY 21, 2009’, *WSC Reports*, pp. 1–8.

WSC (2010) ‘JOINT STATEMENT OFTHE 14TH MEETINGOFTHE WORLD SEMICONDUCTOR COUNCIL (WSC)’, *WSC Reports*, pp. 6–8.

WSC (2011) ‘JOINT STATEMENT OF THE 15TH MEETING OF THE WORLD SEMICONDUCTOR COUNCIL (WSC) MAY 26, 2011’, *WSC Reports*, (1), pp. 1–23.

WSC (2012) ‘JOINT STATEMENT OF THE 16TH MEETING OF THE WORLD SEMICONDUCTOR COUNCIL (WSC) MAY 24, 2012’, *WSC Reports*, pp. 1–15. Available at: http://www.semiconductorcouncil.org/wp-content/uploads/2016/07/Public-WSC-2012-Joint-Statement-FINAL.pdf.

WSC (2013) ‘JOINT STATEMENT OF THE 17TH MEETING OF THE WORLD SEMICONDUCTOR COUNCIL (WSC) 23 MAY, 2013’, *WSC Reports*, (1), pp. 1–23.

Yao, Z. and Eddy, W. F. (2014) ‘A statistical approach to the inverse problem in magnetoencephalography’, *The Annals of Applied Statistics*. Institute of Mathematical Statistics, 8(2), pp. 1119–1144.

Zander, R. *et al.* (1996) ‘Increase of stratospheric carbon tetrafluoride (CF4) based on ATMOS observations from space’, *Geophysical Research Letters*, 23(17), pp. 2353–2356.

doi: 10.1029/96GL00957.

Al Zarouni, Abdalla and Al Zarouni, Ali (2011) ‘DUBAL’s Experience of Low Voltage PFC Emissions’, in *10th Aust. Aluminium Smelting Technology Conference*.

Zepf, V. (2013) *Rare earth elements: a new approach to the nexus of supply, demand and use: exemplified along the use of neodymium in permanent magnets*. Springer Science & Business Media.

Zhang, L., Wang, X. and Gong, B. (2018) ‘Perfluorocarbon emissions from electrolytic reduction of rare earth metals in fluoride/oxide system’, *Atmospheric Pollution Research*. Elsevier Ltd, 9(1), pp. 61–65. doi: 10.1016/j.apr.2017.06.006.

Zhou, B., Li, Z. and Chen, C. (2017) ‘Global Potential of Rare Earth Resources and Rare Earth Demand from Clean Technologies’, *Minerals*, 7(11), p. 203. doi: 10.3390/min7110203.

Zion Market Research (2019) *Global Rare Earth Metals Market Will Reach USD 14.43 Billion By 2025*. Available at: https://www.globenewswire.com/news-release/2019/04/16/1804623/0/en/Global-Rare-Earth-Metals-Market-Will-Reach-USD-14-43-Billion-By-2025-Zion-Market-Research.html (Accessed: 25 September 2019).